THE ROLE OF DENDRITIC CELLS AND MACROPHAGES IN *HELICOBACTER PYLORI* INDUCED IMMUNITY AND TOLERANCE

DISSERTATION

ZUR

ERLANGUNG DER NATURWISSENACHFTLICHEN DOKTORWÜRDE
(DR. SC. NAT.)

VORGELEGT DER

MATHEMATISCH-NATURWISSENSCHAFTLICHEN FAKULÄT

DER

UNIVERSITÄT ZÜRICH

VON

SABINE URBAN

AUS

DEUTSCHLAND

PROMOTIONSKOMMISSION:

PROF. DR. ANNE MÜLLER (VORSITZ UND LEITUNG DER DISSERTATION)

PROF. DR. MARIES VAN DEN BROEK

PROF. DR. MELANIE GRETER

PROF. DR. MANFRED KOPF

ZÜRICH, 2017

TABLE OF CONTENT

SUMMARY

Helicobacter pylori is a gram-negative bacterium colonizing the stomach mucosa of half of the world`s population. Persistent infections with *H. pylori* are linked to gastritis and carriers are predisposed to an elevated gastric cancer risk. However, the host is not able to clear the infection leading to a persistence of *H. pylori* and a concomitant chronic inflammation. These persistent effects of *H. pylori* have likely developed as a by-product of more than 60.000 years of co-evolution with the human host. *H. pylori* has evolved both innate and adaptive immune evasion strategies that allow it to overcome host defenses. Besides its well known negative consequences, chronic *H. pylori* infections also exert beneficial effects. Epidemiological and animal studies inversely link *H. pylori* infection to the risk of developing allergic asthma and inflammatory bowel diseases, especially when infection occurs early in life. In previous studies, we have shown that the tolerogenic activity of DCs and the IL-18-dependent expansion of T_{reg} cells are essential for asthma protection driven by *H. pylori*. However, little was known about the molecular mechanisms promoting tolerogenic responses of dendritic cells and the different contribution of the various myeloid resident populations in the stomach mucosa to tolerance and immunity to *H. pylori*.

We observed that CX3CR1^{hi} macrophages, monocytes and CD11b^{+} DCs take up *H. pylori* and NLRP3 expression is required for the differentiation of CD11b^{+} DCs. In addition, CD11b^{+} DCs seem to have a tolerogenic phenotype as the deficiency in these cells leads to an overshooting T_H1 response. In contrast, BATF3-dependent CD103^{+} DCs are necessary for an *H. pylori*-specific T_H1 response in the stomach lamina propria. We could further show that CD103^{+} DCs and IL-10 expression of CD11c^{+} cells are essential for allergic asthma protection by regulating allergen-specific T_H2 responses. We identified β-catenin signaling in CD11c^{+} DCs to be required for allergen specific asthma protection. Focusing on the role of bacterial factors, we found the two immunoregulatory factors, GGT and VacA, to be sufficient for asthma protection. The protection conferred by purified VacA from *H. pylori* culture supernatant is dependent on IL-18, IL-10 and CD103^{+} DCs. The activation of IL-18 was dependent on *H. pylori* urease inducing TLR2 to upregulate NLRP3 transcription and the subsequent activation of the NLRP3 inflammasome. Urease-expressing *H. pylori*, TLR2 and NLRP3 are all essential for asthma protection with live bacteria. Further, we could identify TLR2 and NLRP3 expression to be upregulated in macrophages and CD11b^{+} DCs take

up *H. pylori* in the stomach lamina propria. This finding supports their importance as immunosuppressive mediators during *H. pylori* infection.

Overall, our results show a division of labor among different gastric phagocytosing cell subsets. We identified $CD103^+$ DCs, IL-10 production and β-catenin signaling in $CD11c^+$ cells, as well as the urease/TLR2/IL-18 axis as essential mediators of *H. pylori*-induced immune tolerance. With these findings, we contribute to a better understanding of tolerance induction by this important human pathogen.

ZUSAMMENFASSUNG

Helicobacter pylori (*H.pylori*) ist ein gram-negatives Bakterium, das den menschlichen Magen besiedelt und zu einer chronischen Infektion führen kann. Solche persistenten Infektionen stehen im engen Zusammenhang mit chronischer Gastritis und einem erhöhten Magenkrebsrisiko. Diese Persistenz ist die Folge verschiedener Mechanismen der Anpassung von *H. pylori,* entwickelt um die angeborene und auch adaptive Immunantwort des menschlichen Wirtes zu umgehen. Neben den negativen Effekten zeigen epidemiologische und experimentelle Studien aber auch, dass eine *H. pylori* Infektion zusätzliche positive Effekte für das menschliche Immunsystem hat. Dies wird durch eine inverse Korrelation zwischen *H. pylori* Infektionen und der Erkrankung an Allergien wie Asthma und chronisch-entzündlichen Darmerkrankungen deutlich. In vorhergehenden Studien konnten wir zeigen, dass tolerogene Dendritische Zellen (DCs) und die daraus folgende IL-18 abhängige Differenzierung von regulatorischen T-Zellen (T_{reg}) essentiell für einen *H. pylori* gesteuerten Asthmaschutz ist.

Ziel dieser Arbeit war die Aufklärung der molekularen Mechanismen, die der Umprogrammierung der Dendritischen Zellen zu tolerogenen Zellen während einer *H. pylori* Infektion zu Grund liegen. Zusätzlich sollte die Funktion verschiedener myeloider Zellen in der Entwicklung von inflammatorischen und tolerogenen Immunantworten im Verlauf einer *H. pylori* Infektion in der Lamina propria des Magens untersucht werden.

Hierbei konnten wir CX3CR1^{hi} Makrophagen, Monozyten und CD11b^{+} DCs als *H. pylori* internalisierende Zelltypen identifizieren. Zusätzlich konnten wir zeigen, dass die NLRP3 Genexpression essenziel für die Differenzierung von CD11b^{+} DCs ist und diese Zellen während einer *H. pylori* Infektion einen tolerogenen Phänotyp aufweisen. Im Gegensatz dazu sind BATF3-abhängige CD103^{+} DCs für die *H. pylori* spezifische T_H1 Antwort in der Lamina propria des Magens verantwortlich. In der Lunge sind wiederum CD103^{+} DCs essentiell für die Regulierung der allergen-spezifischen T_H2 Antwort. Als weitere Regulatoren der T_H2 Antwort während einer *H. pylori* Infektion konnten wir die IL-10 Produktion sowie den β-Catenin Signalweg in CD11c^{+} DCs identifizieren. Als bakterielle Faktoren sind zwei immunoregulatorische Proteine, VacA und GGT, für den Asthmaschutz verantwortlich. Hierbei war der Schutz durch aufgereinigtes VacA abhängig von einer IL-18 und IL-10 Produktion sowie von CD103^{+} DCs. Die Aktivierung von IL-18 ist wiederum abhängig von der *H. pylori* Urease, die den TLR2 Signalweg induziert und damit das NLRP3 Inflammasoms aktiviert. Des Weiteren konn-

ten wir eine erhöhte Expression von TLR2 und NLRP3 in Makrophagen und DCs nach *H. pylori* Aufnahme beobachten. Dies unterstreicht die immunosuppressive Bedeutung der beiden Faktoren während einer *H. pylori* Infektion.

Zusammenfassend zeigen unsere Ergebnisse die diversen Wirkungsweisen der unterschiedlichen phagozytierenden Zelltypen im Magen während einer *H. pylori* Infektion. Des Weitern konnten wir die IL-10 Produktion und β–Catenin Aktivierung in $CD11c^+$ Zellen sowie den Urease/TLR2/IL18- Signalweg als wichtige Mechanismen im Asthmaschutz identifizieren. Diese Arbeit trägt somit dazu bei, die Regulation der Immunantwort durch dieses wichtige humane Pathogen besser zu verstehen.

INTRODUCTION

1. THE MONONUCLEAR PHAGOCYTE SYSTEM

1892 Metchnikoff detected that particle engulfment by cells, the so-called phagocytosis, plays an important role in host resistance against infection and named these phagocytic cells macrophages [1]. In 1969, a new concept, valid until now, groups only highly phagocytic cells and their precursors into the so-called "mononuclear phagocyte system" (MPS) [2]. Since Steinman's discovery of dendritic cells (DCs) in 1970, we can further differentiate the pool of cells in the MPS into macrophages and dendritic cells. These cells are not only able to phagocytose pathogens and commensals, they also represent the missing link between antigen recognition and T and B cell activation [3]. For this discovery, Ralph Steinman and colleagues were awarded the Nobel Prize in 2011.

1.1 Development of dendritic cells and macrophages

The ontogeny of DCs and macrophages is a matter of ongoing research; nevertheless I will try to sum up the latest insight in this chapter. Common myeloid progenitors (CMP) and lymphoid progenitors arise from hematopoietic stem cells in the bone marrow [4]. These CMPs develop into macrophage-dendritic cell progenitors (MDP) if the core-binding factor subunit β (Cbfβ) is expressed, or into granulocyte monocyte progenitors (GMP) in the absence of Cbfβ (Figure 1). However, the origin of MDPs is still under debate [5]. The MDPs further differentiate into dendritic cells and monocytes/macrophages. The two lineages diverge when the MDPs give rise to common monocyte progenitors (cMoP) and conventional dendritic cell precursors (CDPs), which differentiate in an FLT3-dependent manner [6,7]. CDPs give rise to pre-DCs or plasmacytoid DCs (pDC), which enter the bloodstream and migrate to lymphoid and non-lymphoid tissues. pDCs depend on E2-2 expression whereas pre-DCs ($CD8^+$ and $CD4^+$) require zbtb46 [8,9]. Pre-DCs can be further differentiated into Basic Leucine Zipper ATF-Like Transcription Factor 3 (BATF3)/ Interferon regulatory factor 8 (IRF8)-dependent DCs and Interferon regulatory factor 4 (IRF4)-dependent DCs [10].

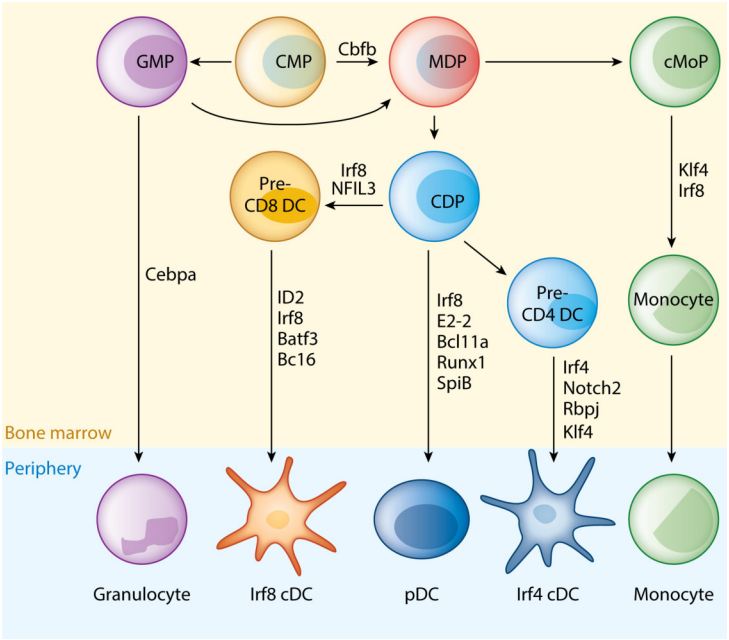

Figure 1: Ontogeny of DCs and monocytes

A scheme showing myeloid lineage development from the CMP, indicating transcription factors required for particular transitions between stages. Although unresolved, we show a scheme with GMP and MDP divergence from the CMP. Commitment to Irf8 and Irf4 branches of cDCs can occur in the bone marrow [10].

The development, and also the maintenance, of preDCs and pDCs in non lymph node (NLN) tissue and lymph nodes (LN) is dependent on the protein FLT3 [11,12]. Consequently, FLT3 receptor- and FLT3 ligand-deficient mice show a strong reduction of all DC subsets.

In the following chapter, I will discuss the function of preDCs and macrophages focusing on the gastrointestinal tract in general, as nothing yet is known about the gastric lamina propria (LP), the sight of *H. pylori* colonization. From previous studies in our lab we know that especially DCs are essential in regulating the immune response against *H. pylori*, which will be introduced later. The topic of this work will be to study the gastric LP and the role of DCs and macrophages in more detail.

1.2 Dendritic cells

1.2.1 The role of dendritic cells in adaptive immunity

Dendritic cells represent the link between the innate and the adaptive immune system. They are the sentinels detecting, taking up and sampling foreign antigens and microorganisms. DCs are thought to direct and regulate local innate immune responses, as well as determine the balance between tolerogenic and inflammatory adaptive responses [13]. Particularly at mucosal sites, DCs are constantly active to balance the immune response and establish homeostasis by inducing peripheral tolerance. Upon pathogen recognition, DCs undergo a program of maturation. They reduce their phagocytotic activity and downregulate toll like receptor (TLR) expression at the surface. Instead, they gain T cell stimulatory capacity by upregulating MHCII/I and the co-stimulatory factors CD80, CD86, and CD40. Activated DCs further upregulate CCR7, which guides them to the draining lymph nodes [14,15]. In the lymph nodes, DCs activate and differentiate naive T cells towards a T helper cell (T_H) 1, T_H2, T_H17 or a regulatory T cell (T_{reg}) phenotype, depending on the cytokines they secrete (Figure 2). IL-12 is the main inducer of T_H1 immune responses and is produced by DCs activated by intracellular pathogens. A T_H2 response is induced by IL-4 upon detection of allergens [16]. Both T helper cell types suppress T_H17 responses. T_H17 cells are activated by IL-23 and IL-6, which in turn inhibits the regulatory immune response [17]. Beside this, T_H9 and follicular T helper (TfH) cells were more recently described subsets. T_H9 cells are known to secrete IL-9 upon IL-2 and TGFβ secretion of DCs and might favor pulmonary inflammation in asthmatic mice, however this needs to be further studied [18]. DCs can also induce memory B cell activation via the secretion of IL-6 and by this favor the development of TfH cells. In addition, DC can also induce a tolerogenic immune response that counteracts the other T_H cell responses [19,20]. Such tolerogenic DCs do not mature completely but reside in a semi-mature state characterized by low surface levels of MHC class II and costimulatory molecules [21]. This leads to a differentiation of T_{reg}, which release anti-inflammatory cytokines such as IL-10 and TGF-β1 and thereby maintain peripheral tolerance. Furthermore, DCs are able to respond to virus infections by cross-presenting antigens via MHCI and thereby inducing $CD8^+$ cytotoxic T cells [22]. All this underlines that DCs are a very heterogeneous leukocyte population [23]. In the next chapter, the role of different DC subsets in tissue homeostasis and inflammation will be discussed.

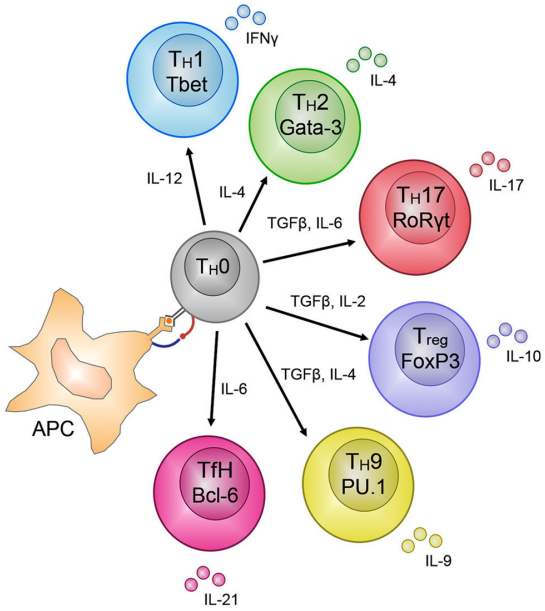

Figure 2: T helper cell differentiation depends on the cytokine stimuli the naive cell receives from activated DCs

$CD4^+$T cells show remarkable plasticity and are able to differentiate into many different subsets based on the soluble molecules secreted during priming of the subsets by antigen presenting cells (APC), e.g., IL-12 for T_H1 cells. The different subsets can be distinguished by the transcription factors that regulate and maintain their lineage-specific effector functions, e.g. T-bet for T_H1 cells. The molecules secreted by these subsets, e.g. IFN-γ for T_H1 cells, are finely tuned to control the pathogen that mediated the release of the specific molecules by the APC during activation of theT_H0 cells into the various subsets [24].

1.2.2 Classification of dendritic cells

Classical DCs can be divided into two lineages depending on the lineage-defining transcription factors [25]. In non-lymphoid tissues the first branch of IRF8-dependent DC subsets expresses $CD103^+$ and the second IRF4-dependent DC subset expresses $CD11b^+$. Both have resident counterparts in the lymph nodes: IRF8-dependent $CD8a^+$ DCs and IRF4-dependent $CD11b^+$ DCs. In addition, lymph nodes comprise migratory $CD103^+$ and $CD11b^+$ DCs, which originate from the drained tissue [11]. The two branches can be distinguished by mutually exclusive expression of CXCR1 on $IRF8^+$ cDCs and the expression of signal regulatory protein α (SIRPa) on $IRF4^+$ cDCs, which is independent of their activation stage (Figure 3) [26,27].

IRF8-dependent DCs require the transcription factors IRF8 and BATF3 [10]. In steady state, BATF3 supports IRF8 expression and thereby stabilizes the DC population [28]. Irf4-dependent DC development is dependent on RelB and GM-CSF and their survival and differentiation depend on IRF4. IRF4-dependent $CD11b^+$ DCs are restricted to the lung, intestine, and spleen, and only the NLT DCs require IRF4 for survival. In organs

such as dermis, kidney or liver, IFR4-dependent DCs could not be detected. This leads to the hypothesis of a mucosal CD11b$^+$ DC population [29]. Murphy *et al.* go even further to suggest that IRF4 is only required for some minor function and not DC maintenance as IRF4$^{-/-}$ mice do not lack CD11b$^+$CD103$^+$ DCs [23]. IRF4-dependent DCs are subdivided into two populations characterized by the expression of either Neurogenic locus notch homolog protein 2 (Notch2) or Kruppel-like factor 4 (Klf4), which exert different functions as discussed later [30].

In the intestinal mucosa, DCs are distributed diffusely throughout the intestinal lamina propria as well as gut-associated lymphoid tissue and Peyer`s patches. Until recently, the intestine was considered unique as it harbors an IRF4-dependent CD11b$^+$CD103$^+$ population. Only recently this population was also found in the nasal mucosa during homeostasis, however not much is known about it yet [31]. Besides this, the intestine harbors a not well described CD103$^-$CD11b$^+$CX3CR1^{dim} DC population. As I will focus in this thesis on the CD11b$^+$ DC subset, I will summarize shortly the latest knowledge gained of this DC population in the intestine.

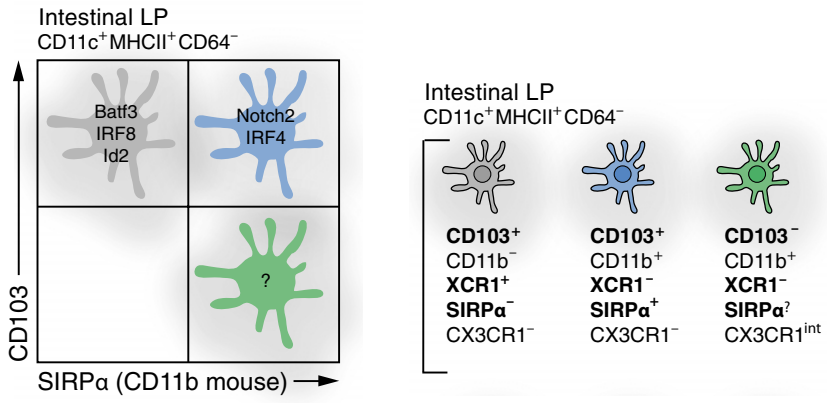

Figure 3: Dendritic cell subsets in the mouse intestinal lamina propria [32]

Intestinal CD11b$^+$CD103$^-$ DCs

Originally, CD11b$^+$CD103$^-$ DCs were classified as inflammatory DCs of monocyte origin. With the help of more defined markers, Scott *et al.* were now able to identify CD11b$^+$CX3CR1^{dim} MNP as a mix of 85% macrophages (CD64$^+$, F4/80$^+$) and 15% being *bona fide* DCs. The DC fraction is similar to *bona fide* DCs as they are FLT3-dependent and express CCR7 and Zbtb46. They differ from CD11b$^+$ macrophages in their phenotype and gene expression. This DC population can be further divided into two populations depending on their ability to express CCR2. Around 80 % are CCR2 negative

and the smaller population expresses CCR2. In addition, Scott *et al.* found functional differences between these populations, which will be discussed later. As the expression of $CD103^+CD11b^+$ DCs is special for the intestine; Scott *et al*. hypothesize that the $CCR2^+$ DCs, which also express IRF4, represent an intermediate state of $CD103^+CD11b^+$ DCs, losing CCR2 and increase CD103 expression upon environmental triggers [33].

1.2.3 Division of labor of DCs subsets

DC subsets mediate homeostasis

Dendritic cells are able to mediate oral and peripheral tolerance by the induction of T_{reg} cells [34]. In this regard, both $CD103^+$ DC subsets are able to induce T_{reg} cells via a mechanism tightly linked to retinoic acid (RA) and TGF-β1 induction [35]. $CD103^+CD11b^-$ DCs express higher amounts of RALDH2 compare to $CD103^+CD11b^+$ DCs, which converts retinol into retinoic acid (RA). RA itself induces IL-10 secretion and the expression of the gut-homing receptors CCR9 and α4β7 on naive T and B cells in the intestine [36,37]. In the lung, the maintenance of tolerance is essential to protect from allergic diseases, such as asthma [38]. In addition, RA negatively regulates T_H17 cells by directly reducing RAR-related orphan receptor gamma (RoRγT) expression and is itself regulated by prostaglandin E2 (PGE2) [39,40]. In the lung, it was shown that $CD103^+$ DCs control T_H17 differentiation via IL-2 and IL-23 secretion [41]. Two additional tolerogenic mediators in $CD103^+$ DCs are β-catenin and Indolamin-2,3-Dioxygenase (IDO), which favor T_{reg} induction in the lung and intestine. IDO catalyzes the metabolism of tryptophan to kynurenine, leading to the starvation of effector T cells (T_{eff}) and also to cell cycle arrest [42,43]. The β-catenin pathway will be discussed later in more detail. However, the idea that $CD103^+$ DCs are the main cell type regulating T_{reg} responses is questioned, as also $CD11b^+$ DCs are able to induce α4β7 and CCR9 on T_{reg} cells. This suggests that DC subsets have a redundant role in establishing tolerance at least in the intestine [32,44]. $CD103^+$ DCs with the greatest tolerogenic potential also have the highest expression of IL-12p40, IL-15 and TLR9 and are essential regulators of T_H1 responses. It becomes clear that depending on the type of stimulus and the antigen load, DC subsets are additionally able to exert inflammatory immune responses. This highlights the plasticity and pleiotropic function of DCs in regulating immune responses.

DC subsets regulate immunity

Beside their tolerogenic role, IRF8$^+$ DCs are specialized in cross-presentation and the defense against intracellular pathogens, whereas IRF4$^+$ cDCs regulate T_H17 responses to extracellular pathogens and T_H2 responses to allergens and parasites (Figure 4) [45]. IRF8-dependent CD8a$^+$ DCs and CD103$^+$ DCs share common functions in regulating T_H1 responses. They are specialized in cross-presentation and the activation of CD8$^+$ effector T cell to cytotoxic T cells (Figure 4) [45]. This ability depends on the XCR1 expression limited to BATF3-dependent DCs, the ligand of which is expressed by T_{eff} cells [46]. As mentioned before, IRF8$^+$ DCs represent an obligate source of IL-12 to mount protective type I immunity. They are potent IL-12 producers during *Leishmania major* infection, driving a T_H1 response in skin-draining lymph nodes [47] and during the parasitic infection with *Toxoplasma gondii* [48]. During colitis, CD103$^+$ DCs can favor an inflammatory T cell response by increasing IFN-γ expression. This might be caused by an increase in inflammatory cytokines in the intestine or the direct recruitment of DCs from the blood and their evasion of tolerogenic gut priming [39,49]. Whereas IRF8$^+$ DCs induce T_H1 cells upon intracellular detection and cytotoxic T cells upon virus infection, IRF4$^+$ DCs are known to promote T_H2 immunity to allergens as well as the T_H17 response to an extracellular pathogen (Figure 4) [29,32,50]. IRF4 expression is necessary for both types of responses. Notch2 expression is essential for T_H17 responses whereas KLF4 expression is important mainly for the T_H2 immune response [30,51]. Schlitzer *et al.* identified IRF4$^+$ DCs in lung and colon to be essential to build up a T_H17 cell response during an *Aspergillus fumigates* infection [29]. Notch2$^+$CD11b$^+$ DCs differentiate naive T cells into T_H17 cells through the secretion of IL-23, IL-6, and TGF-β [52,53]. *In vitro,* IL-6 secretion is induced mostly by TLR2, 5 and 9 activation. This argues that additional inflammatory signals might be necessary to induce T_H17 differentiation. However, the full mechanisms remain unclear [52]. In addition *Scott et al*. found in the intestine that the before mentioned CCR2$^+$ CD11b$^+$ DCs are even better T_H17 producer compared to CD103$^+$IRF4$^+$ DCs [33]. KLF4$^+$ cells were shown to be essential for a proper T_H2 response during *Schistosoma mansoni* infection and house dust mite (HDM) challenge, without affecting other T_{eff} cell responses [51]. CD103$^+$ DCs are known to also regulate T_H2 responses in allergic asthma, indicating that specific functions are not limited to one DC subset [38,50,54]. It rather shows that the DC subsets have a specific function but also fulfill overlapping roles in immune regulation. These overlapping properties might go along with similar transcription factors of these cell types and highlight the plasticity of dendritic cells [55].

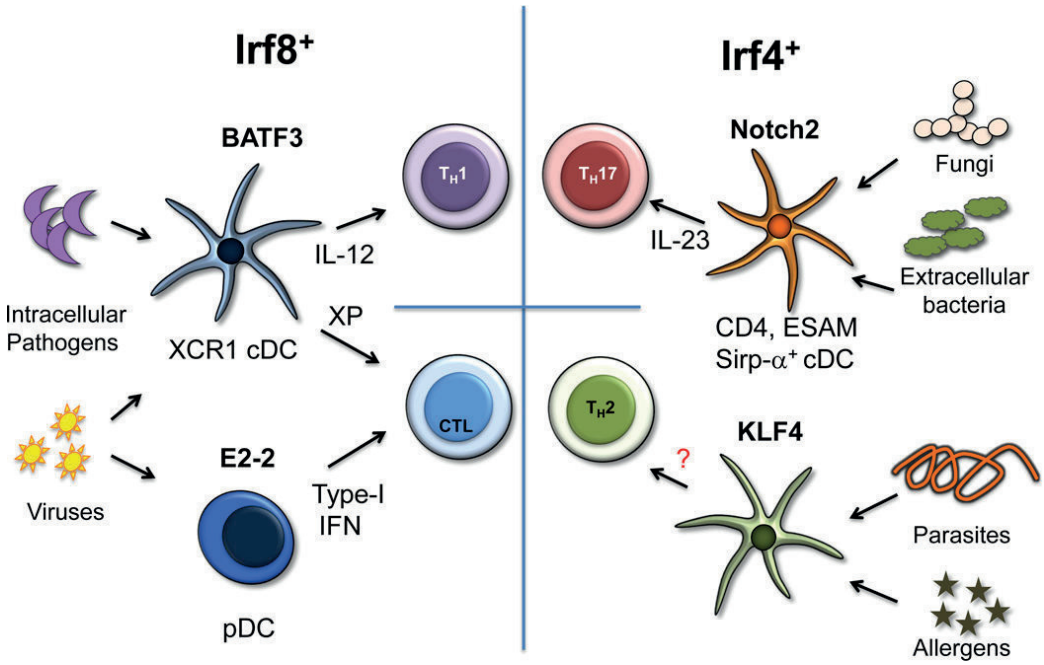

Figure 4: The various DC subsets serve distinct immune responses

Transcription factor dependencies identify four subsets of DC whose actions are directed primarily toward distinct immune effector modules. Irf8$^+$ DCs comprise plasmacytoid DC (pDC) and one branch of classical DC (cDC). Irf4$^+$ DCs are heterogeneous by surface markers but display at least two transcriptional programs directed at different types of immune responses [10].

1.3 Macrophages

1.3.1 Macrophage ontogeny

The second cell type that was classified as part of the mononuclear phagocyte system are macrophages, which were thought to originate from bone marrow derived blood monocytes. Nowadays, we know from fate-mapping experiments, that most tissue macrophages develop prenatally from yolk sac or fetal liver macrophages [56]. These cells are characterized by long-term persistence with self-renewing capacity and are therefore independent of bone marrow hematopoiesis. Organs, which are exposed to microorganisms and thereby show inflammatory conditions, like the intestine and skin, are an exception to this rule. At the time of weaning fetal liver-derived macrophages are replaced out by bone marrow-derived Ly6^{hi} monocytes, mainly driven by the increased microbiota and commensal bacterial colonization of these organs [57]. This replenishment is CCR2 dependent. This observation is further supported by the fact that macrophages are not completely absent in mice deficient for the receptor or ligand of CCR2 but strongly reduced. In addition intestinal monocytes cannot divide in situ in general [58,59]. These macrophages show a unique short half-life of 3 weeks [60]. Therefore, monocytes have emerged as a third, highly plastic and dynamic cellular system that can complement the classical tissue-resident mononuclear phagocyte compartment on demand [61]. They are divided into two subsets, the blood circulating Ly6C^{hi} and the patrolling Ly6C^{lo} monocytes [62]. Beside this it was recently shown, that Ly6C^{hi} monocytes can persist in the steady state and might contribute to an antigen transport to lymph nodes [63,64]. In the intestine, maturing Ly6C^{hi} monocytes differentiate further into macrophages in a process termed monocyte waterfall (Figure 5, left side). Maturing Ly6C^{hi} monocytes gradually lose Ly6C and CCR2 expression and acquire MHCII and CX3CR1 expression via several intermediate steps. This process takes about a week [62,64].

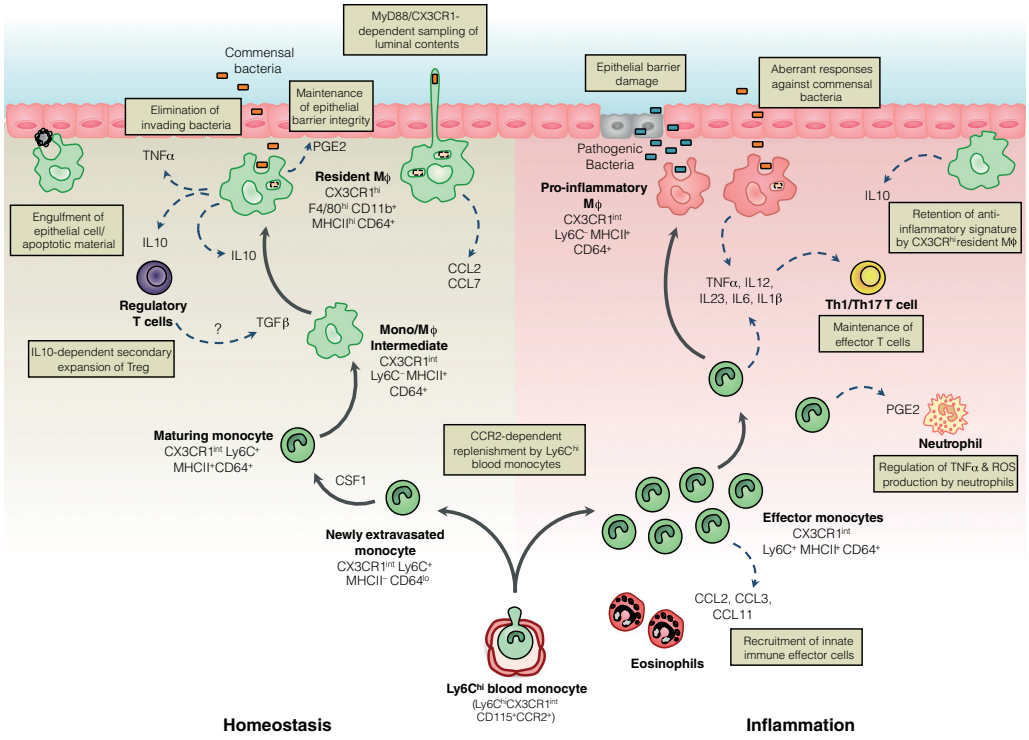

Figure 5: The development of Ly6C^{hi} monocytes into mature CX3CR1^{hi} macrophages

Under steady state conditions, Ly6C^{hi} blood monocytes constitutively enter the intestinal mucosa. They differentiate into mature CX3CR1^{hi} F4/80^{+} macrophages through a series of short-lived CX3CR1^{int} intermediaries. These CX3CR1^{hi} macrophages migrate to the epithelial barrier and contribute to its integrity. First, they secrete PGE2, which favours proliferation of epithelial progenitors. Second, they have a high phagocytic capacity to capture and destroy invading commensals or pathogens and eliminate apoptotic cells. Third, they might also directly sample the luminal contents by extending their dendrites between the cells of the intestinal epithelial barrier. CX3CR1^{hi} macrophages also produce interleukin-10 (IL-10), constitutively supporting T_{reg} differentiation, and may also prime newly arrived monocytes. During inflammation or infection, Ly6C^{hi} monocytes and their CX3CR1^{int} derivatives accumulate in large numbers. They produce pro-inflammatory cytokines, which may support the maintenance of other effector cells such as IFNγ-producing T cells. In addition, they secrete inflammatory chemokines, which lead to the recruitment of innate effector cells. During inflammation, CX3CR1^{hi} macrophages retain their anti-inflammatory signature, e.g. IL-10 production [65].

1.3.2 Homeostatic function of CX3CR1^{hi} macrophages in the intestine

Intestinal macrophages are characterized by high expression of the chemokine receptor CX3CR1 and low CCR2 expression [59]. They are the regulators of intestinal anergy and maintain the symbiotic relationship between the host and microbes. In steady state CX3CR1^{hi} macrophages secrete IL-10 and have a reduced susceptibility towards TLR ligands [66-68]. IL-10 secretion induces T_{reg} cells and indirectly inhibits T_{eff} cells favoring homeostatic conditions [69]. In addition, macrophages are phagocyting

microbial and dead cells, without provoking tissue damage [69]. Beside this, CX3CR1^{hi} macrophages suppress T_H17 responses in the intestine by inhibiting the T_H17 promoting function of CD103$^+$CD11b$^+$ DCs. Thereby CX3CR1^{hi} macrophages are able to initiate a tolerance towards commensal microbiota and maintain homeostasis. This ability of CX3CR1^{hi} cells exists even during inflammation. However, in these circumstances, incoming monocytes do not develop further but rather arrest in a Ly6C^{hi}CX3CR1^{dim} monocyte pro-inflammatory phenotype, secreting TNFα, IL-6, and IL-12 (Figure 5, right sight) [66].

Further studies have revealed, that bacterial sensing is essential for macrophages to build up anergy. Experiments using microbiota depletion or myeloid differentiation primary-response protein 88-deficient (MyD88$^{-/-}$) mice have shown a CCR7-dependent migration of CX3CR1^{hi} macrophages towards the MLNs. Along with this line, MyD88$^{-/-}$ mice in which bacterial sensing is diminished, have a reduced IL-10 expression in macrophages. Consequently, the interplay between microbiota and CX3CR1^{hi} macrophages is essential to keep up anergy [70].

1.3.3 The interplay of intestinal mononuclear phagocytes

The intestinal mucosa contains a diverse number of immune cells, acting together in a tight network (Figure 6). CX3CR1^{hi} macrophages phagocyte antigens via their transepithelial dendrites from the intestinal lumen [71]. However, this pathway is not the only way of antigen uptake, indicated in CX3CR1-dificient mice, which show a comparable load of soluble antigens compared to CX3CR1-expressing mice [72]. CX3CR1^{hi} macrophages further transfer antigen via a Connexin43-dependent direct cell-cell gap junction mechanism to CD103$^+$CD11b$^+$ DCs [73]. These DCs are able to migrate in steady state and inflammation to the MLN in a CCR7-dependent manner. Even though the T_{reg} priming occurs mainly in the MLN, CX3CR1^{hi} macrophages, as well as CD11b$^+$C103$^+$ DC, retain the capacity to promote T_{reg} cell generation in the lamina propria [74,75]. DC primed T cells upregulate $\alpha4\beta7$ and migrate back to the intestine. The T cell response depends thereby on the antigen, detected by the pathogen recognition receptor (PRR), as described in the next chapter [44].

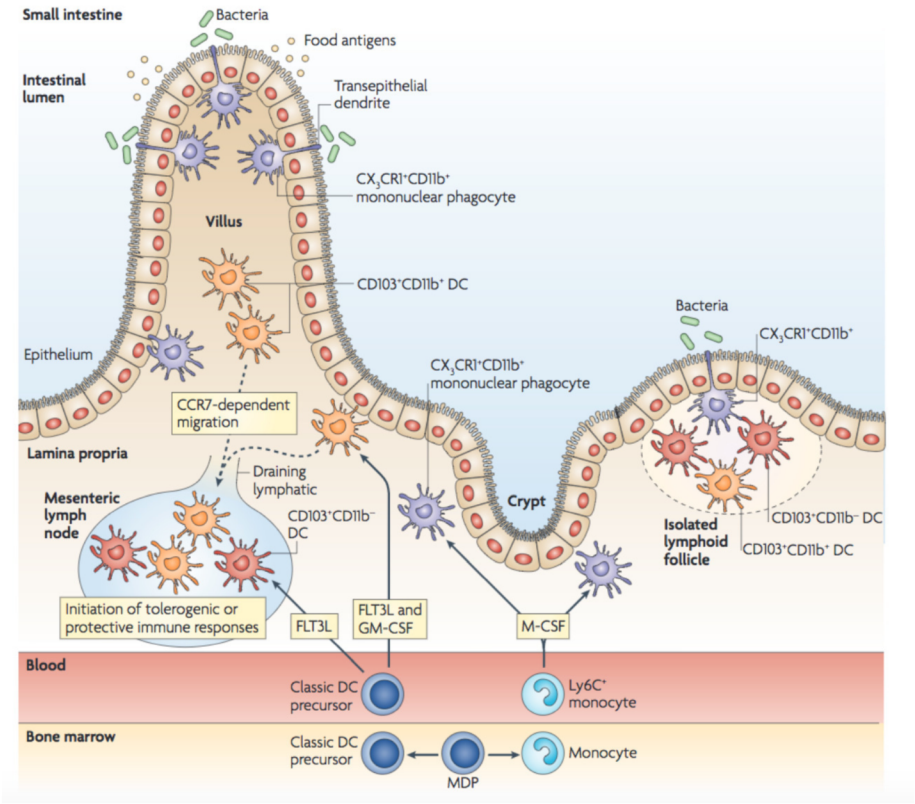

Figure 6.: The network of intestinal lamina propria dendritic cells and the macrophage compartment

In the bone marrow, a common precursor, the macrophage-dendritic cell (DC) precursor (MDP), gives rise to classical DC precursors and monocytes. They enter the circulation and migrate to the gut. Locally, in a GM-CSF and FLT3-dependent process, classical DC precursors give rise to $CD103^{+}CD11b^{+}$ and $CD103^{+}CD11b^{-}$ lamina propria and lymphoid DCs. Following antigen challenge, $CD11b^{+}CD103^{+}$ lamina propria DCs migrate to the mesenteric lymph nodes in a CC-chemokine receptor 7 (CCR7)-dependent manner. Depending on the antigen they sample they either promote a tolerogenic or inflammatory response. As the role of $CD11b^{+}CD103^{-}$ DCs in the gut is still a matter of discussion, they are not presented here. $Ly6C^{+}$ monocytes differentiate locally into CX3C-chemokine receptor 1 $(CX3CR1)^{+}$ lamina propria macrophages. With their transepithelial dendrites $CX3CR1^{+}$ macrophages may sample antigens, however they fail to migrate to lymph nodes, but meanwhile they seem to have a local pro- and also anti-inflammatory function [75].

2 INNATE IMMUNE RECOGNITION

2.1 Pattern recognition receptors

The main task of the immune system is to distinguish between commensal bacteria and potentially harmful pathogens to induce homeostasis or immunity, respectively. One of the main players in this challenge are the dendritic cells. The discovery of toll like receptors (TLR) in human in 1997, showed that the innate immune system is specific and detects conserved structures of the pathogen, so-called pathogen-associated molecular pattern (PAMPs) [76]. Pattern recognition receptors (PRR) are expressed on mononuclear phagocytes, T cells, and epithelial cells. They can be divided into transmembrane Toll like receptors, cytosolic Nod-like receptor, retinoic acid inducible gene I (RIG-I) like receptors and c-type lectin receptors. They are the first line of defense and essential for the induction of adaptive immunity.

2.1.2 TLR receptors

Studies using TLR knockout mice have shown that each TLR has a specific function in PAMP recognition [77]. TLR 1, 2, 4, 5, 6 and 11 are expressed on the cell surface, detecting mostly microbial antigens, whereas TLR 3, 7, 8 and 9 are expressed on intracellular vesicles and detect microbial nucleic acids. TLR2 forms heterodimers either with TLR1 or TLR6, sensing lipopeptides [78,79]. TLR4 binds to lipopolysaccharide (LPS) and TLR5 to flagellin. Upon ligand binding individual TLRs recruit different adaptor molecules and thereby trigger different immune responses. The adaptor molecule MyD88 is universally involved except in TLR3 signaling and activates NF-κB and MAPK to induce inflammatory cytokines. TLR2 and TLR4 use additional MyD88-adaptor-like proteins (MAL) to activate target genes (Figure 7) [80].

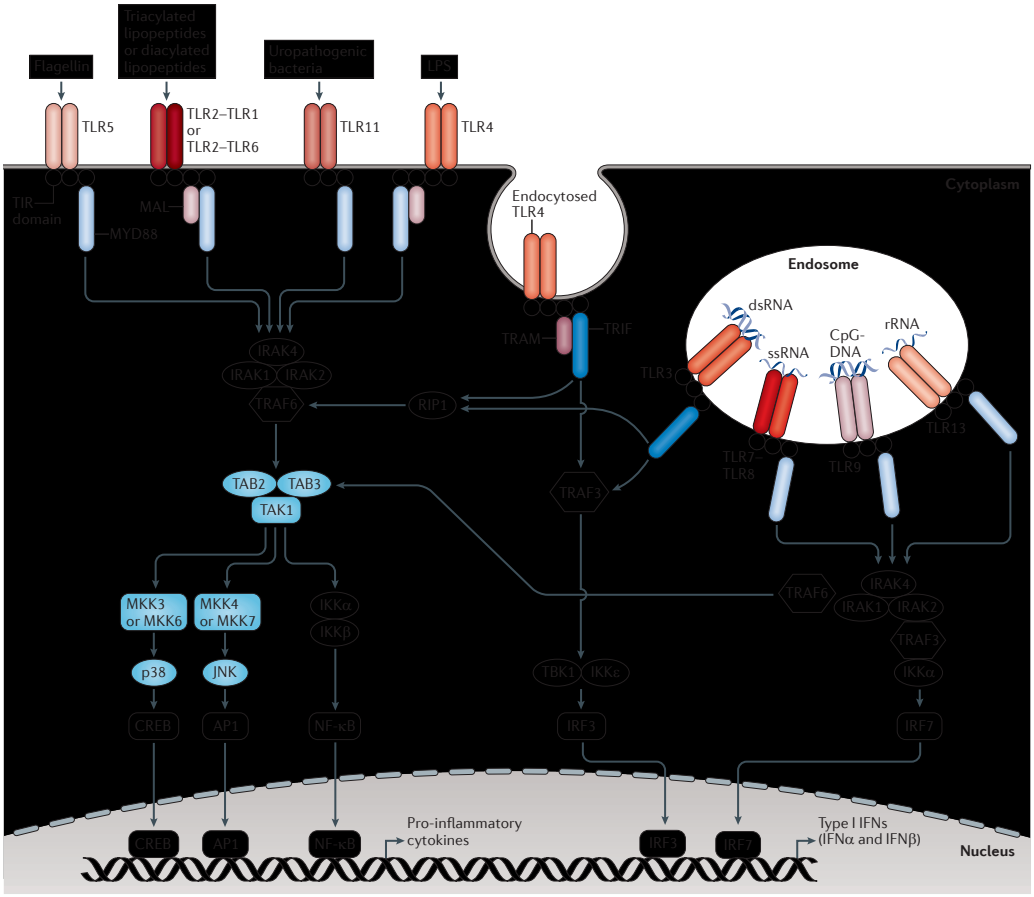

Figure 7: Structure and main signaling pathways of the PRR families

The graph shows a selection of the multiple adaptor molecules and signaling pathways that are activated by the different pattern recognition receptors (PRR). TLRS 3,7-8, 9 and 13 are located to the endosome, where they sense host and microbial-derived nucleoid acids. The others are located at the membrane and TLR4 is localized at both positions. Activation of TLR signaling pathway is induced by a ligand derived dimerization of receptors. This followed by binding of the TIR domain to either myeloid differentiation primary-response protein 88 (MyD88) or TIR domain-containing adaptor protein inducing TFNβ (TRIF) and TRIF-related adaptor molecule (TRAM)) (TLR3 and TLR4). TLR4 is able to migrate to the endosome and signal via TRIF. This favors several downstream targets. These include the interactions between IL-1R-associated kinases (IRAKs) and the adaptor molecules TNF receptor-associated factors (TRAFs), which lead to the activation of the mitogen-activated protein kinases (MAPKs) JUN N-terminal kinase (JNK). It also activates several transcription factors including nuclear factor-κB (NF-κB) and the interferon-regulatory factors (IRFs), A major consequence of TLR signalling is the induction of pro-inflammatory cytokines, and in the case of the endosomal TLRs, the induction of type I interferon (IFN) [81].

2.1.2 NLR receptors

The second family of PRRs are cytosolic proteins, named Nod-like receptors (NLR). After ligand binding, most NLR assembles in an oligomeric structure [82]. NLR can be divided into the NLRP and NLRC subfamily. The most prominent member of the NLRP family is NLRP3. This receptor needs a first priming signal - the NF-κB-dependent transcription of NLRP3. In the second step, NLRP3 forms an oligomer and assembles with a homodimer of caspase-1 and the adaptor protein apoptosis-associated speck-like protein containing c-Terminal CARD (ASC) to form the inflammasome. Activated caspase-1 induces the maturation and secretion of active IL-1β, IL-18, and IL-33 [83,84]. NLRP3 assembly can be caused by many signals including PAMPS of viral RNA or bacterial antigens. However, the ligand leading to the assembly is still under investigation. TLR2 activation has been linked to NLRP3 and IL-1β activation in *Helicobacter pylori (H. pylori)*-infected BMDCs [85].

Although TLR signaling was thought to induce mainly immunity, TLR2 signaling is specifically as it also activates an anti-inflammatory phenotype [86]. Zymosan, a fungal cell wall ligand, which signals through Dectin-1 and the TLR2&6 dimer, induces the expression of IL-10 and RALDH via the extracellular signal-related kinase (ERK) pathway [87,88]. This induces SOCS3, which inhibits p38MAPK and proinflammatory cytokines. A comparable ERK-dependent suppression of IL-12 was observed with TLR2 activation by *Lactobacillus* [16,89]. Moreover, further studies suggest that TLR2 signaling induces β-catenin and its target genes favoring a tolerogenic immune response, and thereby counteracting for instance autoimmune diseases as central nervous system (CNS) pathology in the experimental autoimmune encephalomyelitis (EAE) mouse model [90].

2.2 The role of β-catenin signaling in tolerance and immunity

In recent years several studies have revealed a critical function of β-catenin signaling in regulating DC immune response in various pathological conditions. β-catenin signaling is an evolutionary conserved and important pathway for several biological processes such as embryogenesis, cell growth, survival, and oogenesis. Aberration in these pathways can cause autoimmune diseases and favor cancer [91,92].

The classical ligand of the β-catenin pathway is Wnt, a secreted lipid-modified glycoprotein (Figure 8). Wnt binds to the seven-pass transmembrane Frizzled family receptors (Fzd). This binding can activate the canonical and also the β-catenin independent non-canonical pathway. Here, I will focus on the canonical pathway.

In the absence of Fzd ligands, β-catenin is removed by the destruction complex. This consists of Axin and adenomatous polyposis coli (APC), scaffolding proteins and a Ser/Thr kinase, caseinkinase1a (CK1a) as well as glycogen synthase kinase 3β (GSK3β) (Figure 8) [93]. GSKβ phosphorylates β-catenin and thereby marks it for ubiquitination and proteasomal degradation by β-Trcp and WTX proteins [94]. In contrast, ligand binding increases the β-catenin level in the cytoplasm. It recruits two cofactors LRP5/LRP6 to Wnt/Fzd. This complex attracts disheveled (DVL) which binds at the cytoplasmic tail of the receptor. DVL is able to recruit the destruction complex to the Fzd/Wnt/LRP5/6 complex [95]. Caused by the changed location, GSK3β now phosphorylates the co-receptor instead of β-catenin. In addition, Axin is ubiquitinated by tankyrases (TNKS) in the cytosol and degraded. The destruction complex is destroyed and β-catenin is able to accumulate and to migrate into the nucleus (Figure 8). In the nucleus, β-catenin dislocates Groucho, which was binding to the transcription factors T cell factor and lymphoid enhancer factor (TCF/LEF) and induces β-catenin target gene expression (rev. [96]).

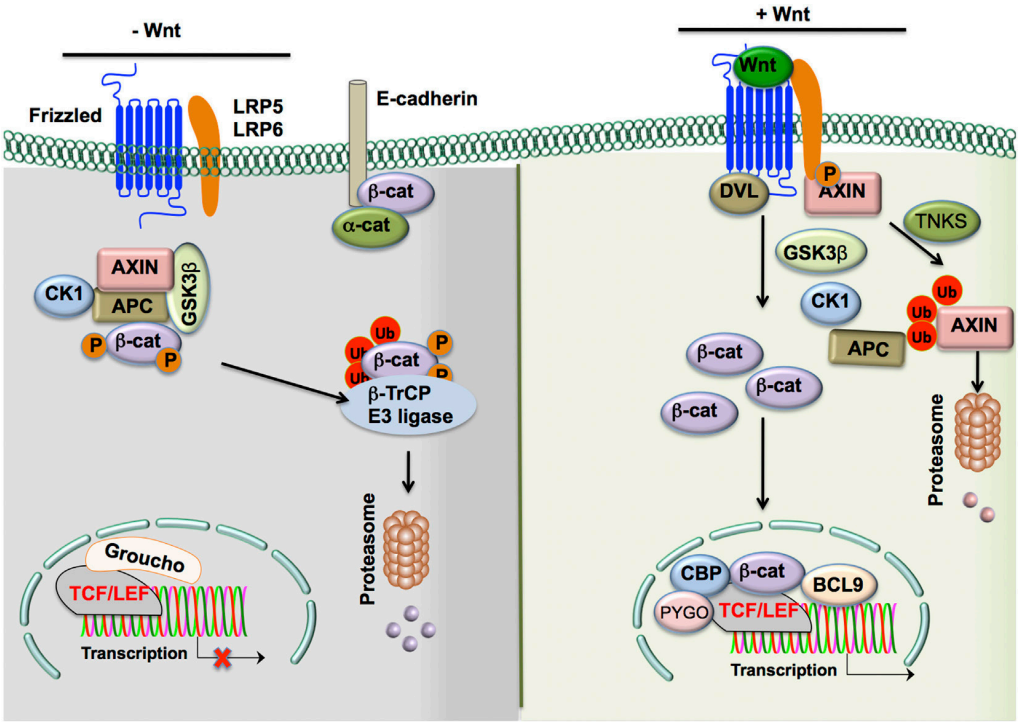

Figure 8: A canonical Wnt/β-catenin signaling pathway

In the absence of Wnt ligands, β-catenin levels are reduced by the following mechanism. A destruction complex consisting of the APC and AXIN, Ser/Thr kinases CK1α and GSK3β, interacts with β-catenin to induce its phospho-inactivation. Phospho-β-catenin is promoted to ubiquitination and proteasomal degradation by β-Trcp and WTX proteins. In the presence of Wnt ligands, β-catenin levels in the cytoplasm are upregulated and regulate cell signaling through the following steps. First, Wnts bind to Frizzled (Fzd) receptors and interact with adjacent LRP5/6 co-receptors. This complex recruits DVL to the cytoplasmic tail of Fzd receptors, which in turn recruits the destruction complex to the Fzd/LRP5/6 complex. The Ser/Thr kinases such as GSK3β phosphorylate the co-receptor instead of β-catenin. Instead, Axin is targeted for proteasomal degradation which supports disruption of the β-catenin destruction complex. The cytosolic β-catenin translocate to the nucleus which leads to a dislocation of the co-repressor Groucho on the TCF/LEF transcription factor by β-catenin. This leads to the recruitment of several co-activators and the transcription of target genes. Beside this activation of β-catenin signaling can be induced by the disruption of epithelial cadherin (E-cadherin)–E-cadherin interactions. This breaks the association of β-catenin to the cytoplasmic domain of E-cadherin and leads to its cytoplasmic accumulation. Abbreviations: APC, adenomatous polyposis coli; CK1α, casein kinase 1α; GSK3β, glycogen synthase kinase 3β; β-Trcp, β-transducin repeat-containing protein; TNKS, tankyrase-1; LRP5/6, low-density lipoprotein receptor-related protein 5/6; DVL, disheveled; TCF/LEF, T-cell factor/lymphoid enhancer factor; BCL9, B-cell CLL/lymphoma 9 protein; CBP, CREB-binding protein; PYGO, Pygopus [97].

Beside this, β-catenin can be activated by several Wnt-independent ligands and receptors in DCs. The disruption of E-cadherin homophilic interaction leads to the activation of β-catenin and a tolerogenic phenotype [98]. As mentioned above, TLR activation is known to induce β-catenin signaling. β-catenin can be induced by TLR2

signaling through the PI3K/AKT pathway. Akt thereby phosphorylates β-catenin at Ser552 and induces its nuclear translocation. In the meantime, AKT phosphorylates GSK3β at Ser9 and inhibits its function to phosphorylate β-catenin and mark it for degradation [99]. Besides TLR2, also other pathways like FAS and TGF-β can activate β-catenin in DCs [100,101]. Some of the β-catenin target genes are the anti-inflammatory cytokines IL-10 and IL-27. This shows that the β-catenin pathway works synergistically with other pathways, as the above mentioned ERK pathway. Thereby they suppress T_H1/T_H17 inflammatory immune responses and favor a tolerogenic DC phenotype (Figure 9) (rev. [102]).

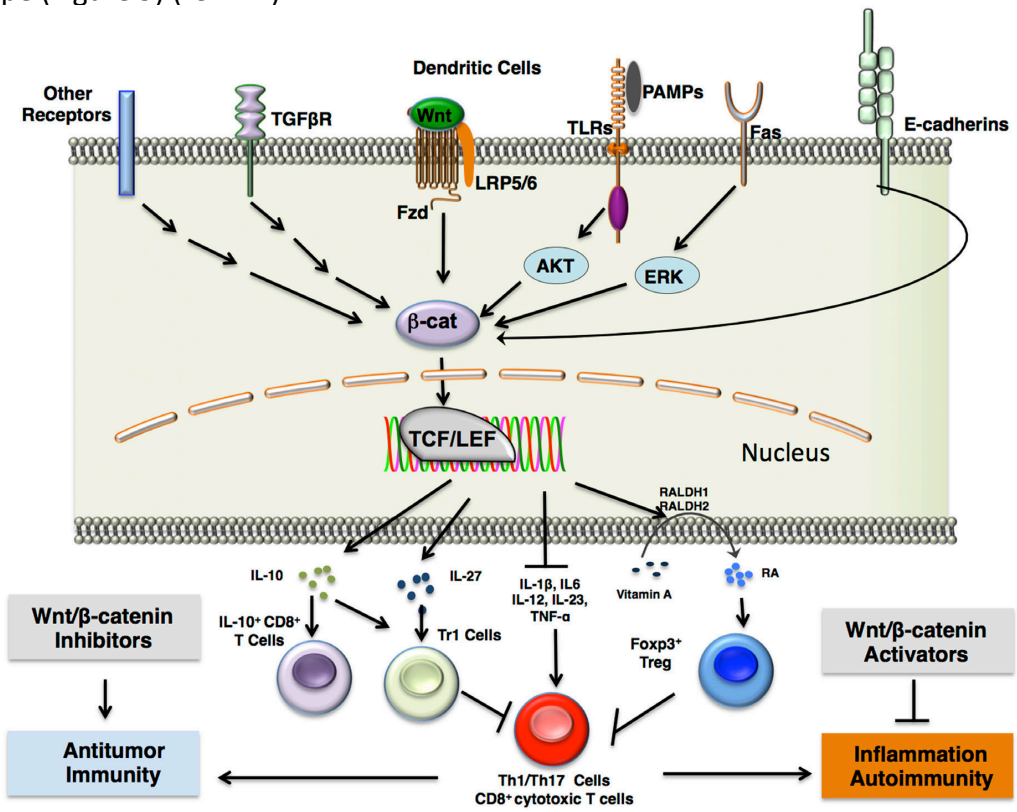

Figure 9: β-catenin signaling in DCs induces immune tolerance

In dendritic cells β-catenin is upregulated via several receptor interactions, including canonical Wnt/Fzd signaling, stimulation of TLRs such as TLR2 with antigen and subsequent ERK signaling and Fas receptor activation. Beside this also the disruption of E-cadherin interactions with β-catenin, or activation of other pattern-recognition receptors can induce nuclear β-catenin translocation. This intersects in β-catenin-mediated association of the TCF/LEF transcription factor with various co-activators that leads finally to the expression of several anti-inflammatory cytokines, such as IL-10 and IL-27, which induce Tr1 cells or $CD8^+IL\text{-}10^+$ T cells. TGF-β and RALDH 1/2 expression in DCs induce T_{reg} cells. Accumulation of T_{regs} in the tissue microenvironment may result in inhibition of Th1/Th17 cells or $CD8^+$ cytotoxic T cells. Abbreviations: Fzd, Frizzled; TLR, Toll-like receptor; ERK, extracellular signal-related kinase; TCF/LEF, T cell factor/lymphoid enhancer factor; IL-10, interleukin 10; IL-27, interleukin 27; FoxP3, forkhead box P3; TGFβ, transforming growth factor β; RALDH 1/2, retinaldehyde dehydrogenase 1/2; Th1/17 cells, T helper 1/17 cells [97].

TLR2 is not the only TLR to induce β-catenin, also TLR3, 5 and 9 are able to induce β-catenin via Akt signaling [103]. However, the full mechanisms and functions are still under investigation. Mucosal DCs are important for regulating peripheral tolerance. Manicassamy *et al.* showed a constant expression of β-catenin in the intestine in DCs and macrophages, which was absent in the spleen. Further, they showed that β-catenin signaling induces T_{reg} cells and thereby suppresses $T_H1/17$ responses in the gut. This strengthens the tolerogenic role of β-catenin in the gut [104]. A second study revealed that MUC2, secreted by goblet cells, induces β-catenin signaling via several receptors as Dectin-1 or FcγRIIB, thereby mediating mucosal tolerance [105].

This highlights the importance of β-catenin signaling for homeostasis and makes clear that aberrant β-catenin signaling may have negative consequences for tissues. β-catenin signaling, for instance, protects from inflammatory diseases, in a dextran sodium sulfate-induced colitis model [104].

This regulatory pathway is predestined and one example of many to be hijacked and activated by pathogens or by cancer cells to consequently evade the immune system. *H. pylori* has developed several mechanisms to evade the immune system which leads to its persistence in the stomach. One of these is the release of β-catenin from E-cadherin, in an *H. pylori* CagA-dependent manner [106]. In addition, further virulence factors like VacA can induce the phosphorylation of AKT, which further phosphorylates GSK3β and marks it for ubiquitin-mediated proteolysis [107]. Increased β-catenin activation in APCs is observed in over 50% of adenocarcinoma compared to healthy gastric mucosa. This indicates that β-catenin is an important regulator in several diseases and an attractive target for further therapies [108].

3. *HELICOBACTER PYLORI*

3.1 Taxonomy

For many years, the human stomach was considered to be free of bacteria because of its acidic environment. This changed with the discovery of *H. pylori* in human gastric biopsies by Marshall and Warren in 1983 [109]. *H. pylori* is a spiral shaped flagellated Gram-negative bacterium. It colonizes the human stomach since over more than 60.000 years [110]. Since then over 32 other bacteria from the same genus were isolated, not restricted to the human stomach. *H. hepaticus* colonizes the liver and colon of mice [111]. Besides these, other *Helicobacter* spp. were isolated from the liver and the pancreas - until then considered to be sterile organs [112].

3.2 Prevalence and transmission

H. pylori is one of the most prevalent global pathogens and colonizes around 50% of the world population. However, there are substantial geographic differences in the prevalence of the infection, with over 50-90% of the infections found in developing countries compared to 3-50% in developed countries [113,114]. Suggested reasons are variation in hygienic standards, family size as well as the use of antibiotic treatment [115]. Thereby the gastro-oral transmission seems to be most likely in reduced hygienic standards and pediatric infections [114,116].

Infection with *H. pylori* is mainly acquired during early childhood and can persist lifelong, in the absence of antimicrobial treatment [117]. *H. pylori* colonization causes gastric inflammation, but most infections stay asymptomatic. However, the presence of *H. pylori* is a risk factor for developing peptic ulcer disease in 10%-, adenocarcinoma in 1-3%- and malt lymphoma in 0.1% of infected individuals and was therefore classified a carcinogen [118]. These findings of a permanent pathogen in the stomach, its connection with chronic disease and cancer as well as the clinical relevance led to the awarding of Marshall and Warren with the Nobel price in 2005. Despite antibiotic treatment, gastric cancer is still the second most common cause of worldwide cancer mortality [119]. Therefore many studies try to elucidate the virulence factors of *H. pylori* that favor disease progression.

3.3 Virulence factors of *Helicobacter pylori*

3.3.1 VacA

Vacuolating cytotoxin A (VacA) is an 88kDa toxin, which induces vacuolization and mitochondrial alteration [120] followed by impaired cell cycle progression and apoptosis [121]. VacA is either secreted into the extracellular space [122] or persists at the surface of *H. pylori* [123]. Once secreted, VacA undergoes proteolytic cleavage into two fragments p33 and p55 [124] [125]. P55 is essential for binding to the host cell, whereas p33 is necessary to form the anion-selective channels and insertion into the host cell. These two fragments show high levels of genetic variation. P33 contains the s region (s1 or s2) and p55 the m region (m1 or m2) [126]. Strains that contain the s1 variant of VacA are associated with increased risk to develop gastric cancer [127]. In addition, VacA m1 strains are linked to increased gastric epithelial damage [128]. Therefore the s1m1 variation is the most cytotoxic VacA variant [129,130].

3.3.2 Gamma glutamyl transpeptidase

Another pathogenic factor of *H. pylori* is gamma glutamyl transpeptidase (GGT) which is highly conserved and expressed in all gastric *H. pylori* species [131]. GGT can be secreted or located in the periplasm. It is important for colonization and inducing apoptosis in the host cell. *H. pylori* is not able to take up extracellular glutamine. GGT converts glutamine and glutathione into glutamate and ammonia respectively. Cysteinylglycine is transported into the bacterium and feeds into the citric acid cycle for glutamine synthesis. In addition, the ammonia produced by *H. pylori* can be used as a nitrogen source, increasing the local pH and thereby favoring the resistance against the acid environment in the stomach. On the host side, glutamine supplementation causes impaired redox balance of the host cell, leading to a higher susceptibility to DNA damage and apoptosis [132]. *H. pylori* lacking GGT lose the ability to colonize, probably caused by the change in mentioned physiological conditions. These changes also induce VacA to internalize in the membrane and together favor toxicity and persistence of the bacterium [133].

3.4 Immune evasion

The host $T_H1/17$ response is necessary to control an *H. pylori* infection, however, it is not strong enough to fully eliminate the pathogen. These conditions lead to the above described chronic inflammation and pathological lesions. But how is the bac-

terium able to evade the immune system? The most efficient adaptation *H. pylori* evolved will be discussed in the following chapter.

One way of adaptation *H. pylori* developed is to evade detection by PRR. TLR4 detects LPS of gram-negative bacteria. *H. pylori* however, expresses a tetra-acylated LPS, which is 1000-fold less active compared to other hexa-acylated forms of gram-negative pathogens such as E-coli LPS (Figure 10). This is due to specific lipid A modifications [134]. Secondly, *H. pylori* contains an N-terminal mutation in flagellin, rendering it a weak TLR5 activator. Even though TLRs are known to induce pro-inflammatory immune responses the binding of *H. pylori* DNA to TLR9 and the binding of an unknown TLR2 ligand (possibly LPS) induce IL-10 signaling and suppress T_H1 response [135]. TLR2 deficient mice show a reduced colonization level and an increased inflammation [136]. Beside this, infected patients reveal an increased receptor expression in DCs, highlighting the importance of this pathway during colonization [137]. Furthermore, DC-SIGN detects the fucose residue of *H. pylori* LPS, which disrupts signaling downstream of DC-SIGN, to induces IL-10 and inhibit IL-12 production, and suppresses T_H1 response (Figure 10) [138]. The failure of the immune system to eliminate *H. pylori* seems to be due to the ability of the bacterium to control T cell responses [139].

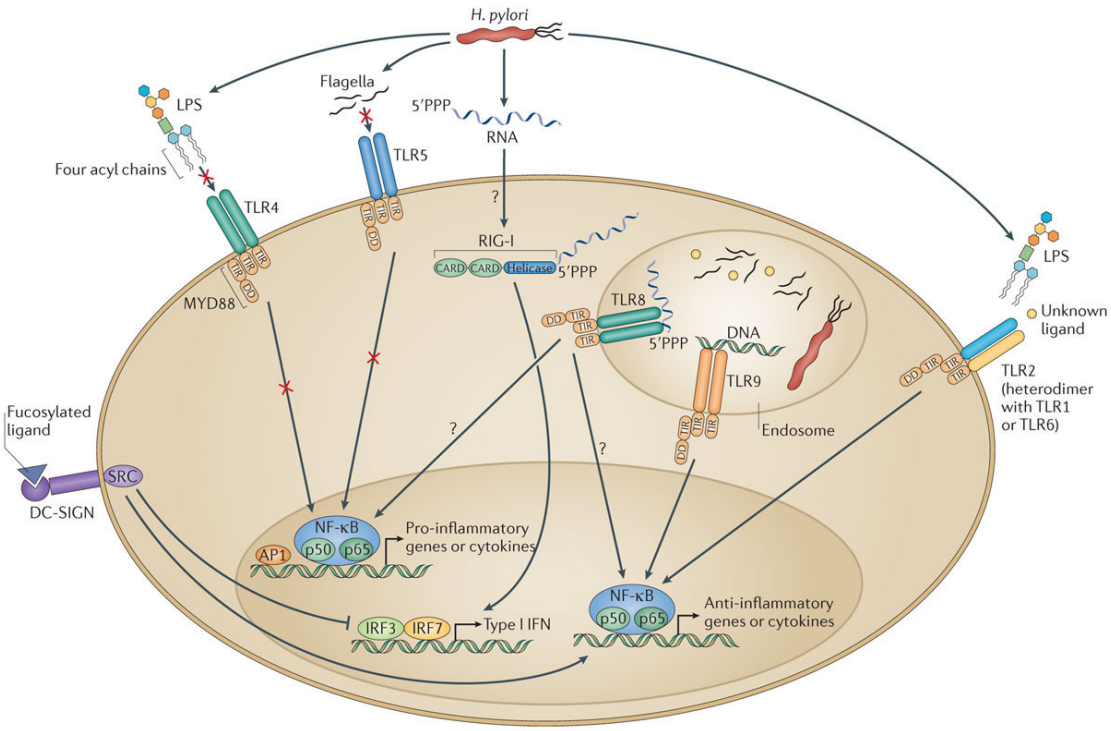

Figure 10: Schematic of *H. pylori* strategies that allow it to evade host immune recognition

H. pylori harbors several PAMPs which allow it to evade detection by pro-inflammatory TLRs. Here they are summarized, even though they are not necessarily expressed on the same cell type. *H. pylori* LPS is less bioactive than the LPS of other gram-negative pathogens due to

specific lipid A modifications that prevent detection by TLR4. *H. pylori* flagella are not detected by TLR5 due to mutations in the TLR5 binding site of flagellin. The bacterium's DNA is detected by TLR9 and *H. pylori* LPS possibly by TLR2. These TLRs predominantly activate anti-inflammatory signaling pathways. 5‘ triphosphorylated RNA is detected by the RLR RIG-I, which activates the transcription factors IRF3 and IRF7 to induce type I IFN expression. *H. pylori* RNA is potentially detected also by TLR8 in endosomes. The fucosylated DC-SIGN ligands suppress activation of the signaling pathways downstream of this CLR and activate anti-inflammatory genes. DD, death domain; TIR, Toll/Interleukin-1 receptor domain; CARD, caspase activation and recruitment domain; MyD88, myeloid differentiation primary response gene 88; DC-SIGN, dendritic cell-specific intercellular adhesion molecule-3 grabbing non-integrin [140].

3.4.1 *Helicobacter pylori* affects effector T cells and regulatory T cells

Several factors are known to allow *H. pylori* to influence T_{eff} cells directly or indirectly and favor *H. pylori* persistence. NLRP3 activation was considered to induce an IL-18 and IL-1β-dependent inflammatory response. However *H. pylori*-activated NLRP3 signaling induces two opposing immune responses. It induces an IL-18-dependent differentiation of T_{reg} cells and in addition an IL-1β-dependent differentiation of T_H1 cells (Figure 11). IL-18 deficient mice have a reduced bacterial burden and increased inflammation, indicating the tolerogenic function, whereas IL-1β deficient mice show the opposite phenotype, underlining a proinflammatory role of IL-1β [141]. Besides the fact that GGT and VacA favor inflammation, they are able to influence T cell response [142]. GGT function disrupts ras signaling which leads to a cell cycle arrest of T-cells in the G1/S phase [143]. In addition, also VacA interferes with T cell proliferation signaling in G1/S phase by inhibiting the activation of the nuclear factor of activated T cells (NFAT) [144]. In addition, Oertli *et al*. showed, that GGT and VacA also affect T effector cells indirectly (Figure 11). Thereby GGT- and VacA-exposed DCs are reprogramed towards a tolerogenic, semi-mature, phenotype. DCs secrete IL-10 and thereby induce T_{reg} cell proliferation and consequently, the inhibition of $T_H1/17$ T_{eff} cells [145]. Beside this, GGT induces COX2 signaling, which is known to inhibit a T_H1 response [146,147]. All this leads to an immune evasion by *H. pylori* and tolerogenic conditions in the host.

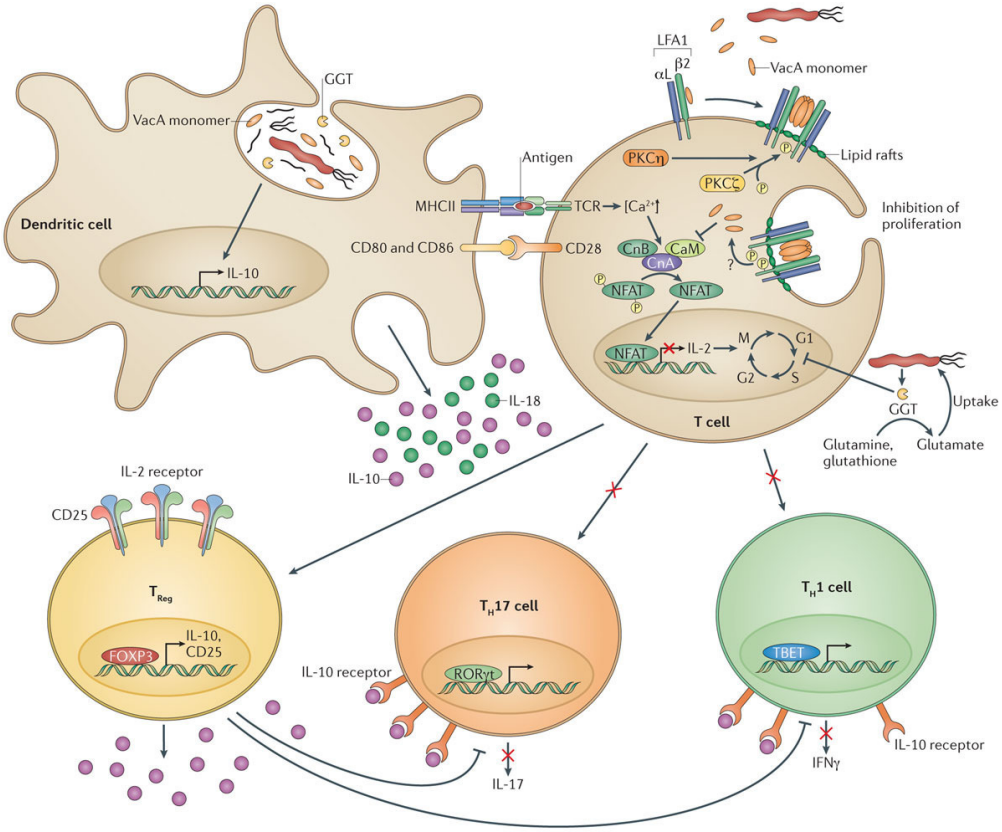

Figure 11: *H. pylori* inhibits T cell-mediated immunity by several mechanisms

All *H. pylori* strains express the secreted virulence factors VacA and GGT. Thereby they directly inhibit T-cell activation, proliferation and effector functions. Hexameric VacA binds to the β2 integrin subunit of the heterodimeric transmembrane receptor LFA-1. Upon phosphorylation by the protein kinase C, the receptor complex is internalized. Cytoplasmic VacA inhibits the Ca^{2+}/calmodulin-dependent phosphatase calcineurin to dephosphorylate NF-AT. It thereby prevents the nuclear translocation of NF-AT and consequently blocks IL-2 production and subsequent T-cell activation and proliferation. GGT arrests T-cells in the G1 phase of the cell cycle preventing their proliferation. Both VacA and GGT also indirectly prevent T cell immunity via re-programming of DCs. VacA/GGT-exposed DCs produce IL-10 and induce the differentiation of T_{reg} cells while preventing T_H1 and T_H17 differentiation. Depicted interactions at the T-cell/DC synapse include MHCII binding to the T-cell receptor, which facilitates Ca^{2+} release in the cell, and binding of costimulatory molecules CD80/CD86 to CD28. The direct interaction of VacA on T cells appears to be human-specific, whereas indirect effects of VacA and GGT on T-cells via DCs have only been documented in the murine system. LFA-1, lymphocyte function-associated antigen-1; NF-AT- nuclear factor of activated T-cells; GGT, γ-glutamyl-transpeptidase; CnA, B, calcineurin A and B subunits; CaM, calmodulin; RORγT, retinoid-related orphan receptor γT; T-bet, T-box transcription factor. [140]

4. *HELICOBACTER PYLORI* AND ALLERGIC ASTHMA

H. pylori is able to evade the immune system and thereby colonize the body permanently in a stage of symbiont/pathobiont. This raises the question of the advantages on the host side. In the second half of the last century, the incidences of *H. pylori* infection decreased while allergic asthma, as well as autoimmune disease in the population, increased. This led to the hypothesis, that *H. pylori* protects from allergies and autoimmune diseases, which will be discussed later in the chapter.

4.1 Pathogenesis of allergic asthma

Asthma is a global health problem with around 300 million affected people and a further increasing number mainly in developing countries (rev. [148,149]). Asthmatic patients have a chronic inflammatory disorder, which is characterized by a bronchial hyperactivity, mucus overproduction, airway wall remodeling in line with airway narrowing. [150]. Environmental risk factors are exposure to allergens, viral respiratory infections, air pollution or cigarette smoke [151-153]. But also obesity, as well as atopic diseases, are risk factors [153]. Even though many people suffer from this disease treatment, methods are non-curative mainly because of the heterogeneity of this disease [154]. For a long time, allergic asthma was thought to be driven by T_H2 cells. But it is now known that asthmatic inflammation can also be neutrophilic and T_H17 driven [155,156]. Allergic antigens are inhaled during sensitization and detected by antigen presenting cells in the lung. Thereby $CD103^-CD11b^+$ DCs are necessary and sufficient to induce allergic sensitization and $CD103^+$ DCs induce tolerance towards inhaled allergens. $CD11b^+$ DCs present the allergen to naive $CD4^+$ T cells in the lung draining lymph node and induce their T_H2 differentiation (Figure 12). Activation of T_H2 cells leads to the release of IL-4 and IL-13 secretion. Thereby, proliferation and class switch of B cells to produce IgE and IgG is induced. IgE and IgG bind with high affinity to the receptor FcεR and FcγR on mast cells. Allergic asthma can be divided in an early and late response. In case of a re-exposure, the allergen directly binds to the mast cell receptor. This leads to a degranulation of mast cells, the release of histamine and granule proteins and an increased vascular cleavage, which characterizes the early phase. T_H2 cell-released IL-13 causes goblet cell metaplasia and bronchial hyperreactivity. In addition, vessels upregulate VCAM-1, which increas their permeability. This favors eosinophil infiltration and causes subsequent progression to the later phase. T_H2 cells and eosinophils secret IL-5, which induces the differentiation

and maturation of eosinophils in the bone marrow. Infiltration of eosinophils, macrophages, neutrophils and lymphocytes induces an inflammatory response and can last for prolonged periods leading to chronic asthma. On the molecular level, asthmatic patients show reduced T_{reg} expression and abrogated tolerogenic signaling pathways such as β-catenin [157].

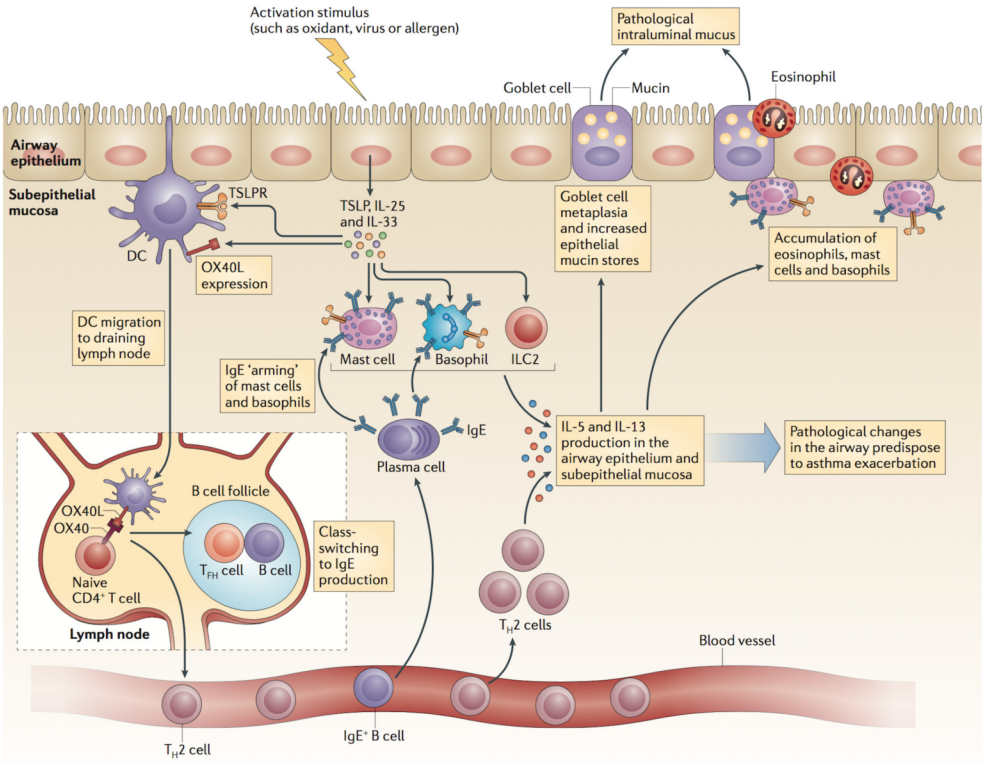

Figure 12: Mechanism of T_H2 mediated allergic asthma upon allergen encounter

Upon antigen encounter epithelial cells release cytokines, particularly IL−33 and thymic stromal lymphopoietin (TSLP). This induces the expression of OX40 ligand (OX40L) on DCs and DC mobilization to local draining lymph nodes where they activate naive $CD4^+$T cells to secret IL−4. These IL−4−competent T cells in the lymph nodes migrate to B cell zones where they differentiate into T follicular helper cells (TFH). TFH cells than move into the circulation and mature to T helper 2 (T_H2) cells. IL−4−secreting TFH cells in parafollicular B cell areas mediate IgE class switching in B cells. T_H2 cells that migrate to the airway epithelium and to the mucosa secrete IL−5 and IL−13. They favor inflammatory and remodeling changes in the airway mucosa that predispose individuals to asthma and to asthma exacerbations. ILC2, group 2 innate lymphoid cell; TSLPR, TSLP receptor [158].

4.2 Treatment of allergic asthma

Today severe asthma treatment relies on a combination therapy of an inhaled corticosteroid, which suppresses the inflammation and a β-adrenergic agonist, which opens the constricted bronchial muscles. However, in 5-10% of patients, this treatment is inefficient, underlining the need for new alternative methods. Alternative treatments are monoclonal antibody therapies against IgE, IL-4, IL-5 and also Il-13 with several ongoing phases 2 and phase 3 trials. Omalizumab, a humanized mAb against the FC portion of IgE on several cells, controls moderate to severe asthma [159,160]. Moreover, clinical trials are done with cytokine inhibitors. Here, a phase III study with dupilumab, an antibody against the α-chain of IL-4, shows effective improvement of the lung function and exacerbation [161]. However further understanding is necessary to gain satisfying treatments against this disease.

4.3 Protective role of *Helicobacter pylori* against allergic asthma

H. pylori infections and allergies are inversely correlated. Basler *et al*. have postulated in the loss of microbiota hypothesis, that a gradual reduction of commensal bacteria such as *H. pylori*, which favors a tolerogenic phenotype, leads to a steady increase in inflammatory disorders causing allergies and autoimmune diseases [115]. These beneficial effects of *H. pylori* infection against asthma but also inflammatory bowel disease (IBD), was linked to the *H. pylori*-induced T_{reg} cells response [162]. Arnold *et al.* showed, that experimentally infected mice are protected against allergic asthma. The protection was most pronounced in neonatally infected mice and driven by T_{reg} cell [163]. Compared to adult infections, showing a pronounced T_{eff} response, these tolerogenic T cells migrate to the lung where they can suppress the inflammatory immune response of asthmatic mice (Figure 13). Transfer of T_{reg} cells from infected mice conferred protection in asthmatic mice arguing that T_{reg} cells are sufficient for this protection [163]. Oertli *et al*. reviled that the infected DCs revile a semi-mature state that renders T_{reg} priming. Further this semi-mature state was dependent on IL-18 secretion; consequently IL-18 deficient mice are not protected from allergic symptoms [164]. Besides this, the two virulence factors of *H. pylori*, GGT and VacA, promote tolerogenic DCs. In addition, isogenic mutants fail to promote T_{reg} induction and neonatal infection of mice with *H. pylori* VacA mutant fail to induce asthma protection [145].

Taken together allergic asthma is a heterogenic disease, which needs further investigation to develop curative treatments. Therefore, gaining more insight into the un-

derlying molecular mechanism of *H. pylori*-induced tolerance may provide one route for addressing unmet clinical needs for treatments of allergic diseases.

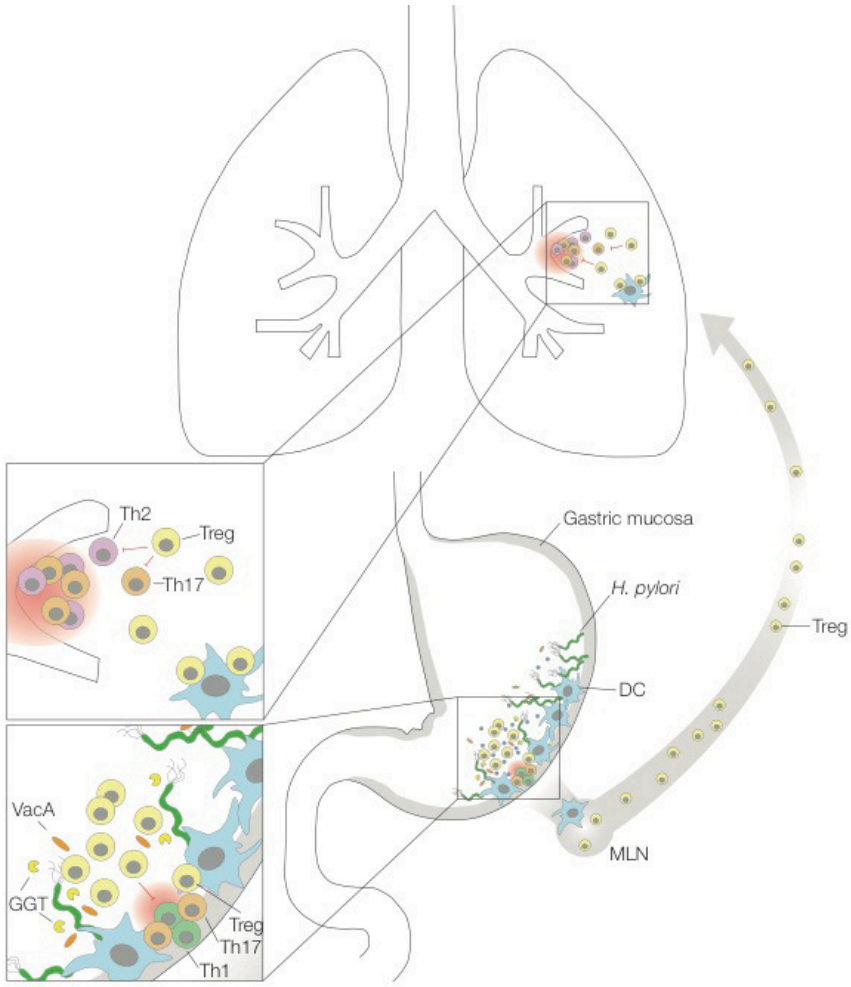

Figure 13: *H. pylori*-induced protection of allergic asthma by T_{reg} cells, VacA and GGT

H. pylori is typically acquired during early childhood and is known to cause gastric disorders, as well as prevent allergic and chronic inflammatory diseases. The *H. pylori* persistence factors GGT and VacA promote chronic infection by tolerizing DCs and thereby favoring T_{reg} differentiation. *H. pylori*-induced T_{regs} are required for the suppression of allergen-specific immune responses in the lung (modified from [165]).

AIMS OF THE THESIS

For a long time, the stomach was an immunologically neglected organ. Only recently more knowledge was gained concerning its microbial composition, but still little is known regarding the myeloid compartment in steady state or during infection, e.g. with *H. pylori* [166]. *H. pylori* infection is not only a risk factor for the development of gastric adenocarcinoma but evidence from epidemiological studies and our recent work identified *H. pylori* as beneficial in the context of allergic diseases[115,163,167]. In this regard we have identified DCs as mediators of *H. pylori*-induced immune tolerance and asthma protection[163]. However, nothing has been known regarding the role of specific DC subsets and macrophages during *H. pylori* infection in the gastric lamina propria and lung.

My first aim was to characterize the myeloid compartment in the gastric lamina propria in steady state and during *H. pylori* infection. In the next step, we aimed to identify the role of macrophages and DCs sampling *H. pylori* and studying changes of gene expression associated with *H. pylori* exposure. Beside this, we were interested in their function in regulating *H. pylori*-specific immune responses. To this end, different knockout mouse strains were used to identify the role of DC subsets in tolerance and immunity during *H. pylori* infection in the gastric lamina propria.

In the next step I investigated the role of DCs and the signaling pathways underlying *H. pylori*-mediated asthma control. Knowing that T_{reg} cells mediate the protection against asthma, I aimed to study the role of two T_{reg} mediators, IL-10 and β-catenin, in $CD11c^+$ cells by using a murine asthma model.

Further, we aimed to gain a deeper understanding of IL-18 activation upon *H. pylori* infection. We already knew from previous studies, that IL-18 is induced and essential for allergic asthma protection. IL-18 and IL-1β are regulated via caspase-1 [141,164]. We therefore aimed to identify the NLRs leading to caspase-1 and IL-18 activation upon *H. pylori* infection in DCs. Furthermore, we were interested in TLR signaling, as it transfers the signal which leads to pro-IL-1β transcription. In addition we planned to identify the bacterial PAMPs inducing IL-18 and IL-1β.

RESULTS

1. PUBLISHED RESEARCH ARTICLES

1.1 Effective treatment of allergic airway inflammation with *Helicobacter pylori* immunomodulators requires BATF3-dependent dendritic cells and IL-10

author: Daniela B. Engler, Sebastian Reuter, Yolanda van Wijck, Sabine Urban, Andreas Kyburz, Joachim Maxeiner, Helen Martin, Nir Yogev, Ari Waisman, Markus Gerhard, Timothy L. Cover, Christian Taube, and Anne Müller

Journal: PNAS. February 19, 2013; 110 (8): 3047-3052

contribution: I helped with mouse studies and performed and analyzed experiments for figure 2F, S2K and S3K.

Effective treatment of allergic airway inflammation with *Helicobacter pylori* immunomodulators requires BATF3-dependent dendritic cells and IL-10

Daniela B. Engler[a,1], Sebastian Reuter[b,1], Yolanda van Wijck[c], Sabine Urban[a], Andreas Kyburz[a], Joachim Maxeiner[b], Helen Martin[b], Nir Yogev[d], Ari Waisman[d], Markus Gerhard[e], Timothy L. Cover[f], Christian Taube[c], and Anne Müller[a,2]

[a]Institute of Molecular Cancer Research, University of Zürich, 8057 Zürich, Switzerland; [b]Medical Clinic III and [d]Institute for Molecular Medicine, Johannes Gutenberg University, 55131 Mainz, Germany; [c]Department of Pulmonology, Leiden University Medical Center, 2333 ZA, Leiden, The Netherlands; [e]Institute of Microbiology, Immunology and Hygiene, Technical University of Munich and German Center for Infection Research, 81675 Munich, Germany; and [f]Division of Infectious Diseases, Department of Medicine, Vanderbilt University School of Medicine and Veterans Affairs Tennessee Valley Healthcare System, Nashville, TN 37232-2358

Edited by Robert L. Coffman, Dynavax Technologies, Berkeley, CA, and approved July 2, 2014 (received for review June 6, 2014)

The prevalence of allergic asthma and other atopic diseases has reached epidemic proportions in large parts of the developed world. The gradual loss of the human indigenous microbiota has been held responsible for this trend. The bacterial pathogen *Helicobacter pylori* is a constituent of the normal gastric microbiota whose presence has been inversely linked to allergy and asthma in humans and experimental models. Here we show that oral or i.p. tolerization with *H. pylori* extract prevents the airway hyperresponsiveness, bronchoalveolar eosinophilia, pulmonary inflammation, and Th2 cytokine production that are hallmarks of allergen-induced asthma in mice. Asthma protection is not conferred by extracts from other enteropathogens and requires a heat-sensitive *H. pylori* component and the DC-intrinsic production of IL-10. The basic leucine zipper ATF-like 3 (BATF3)-dependent CD103$^+$CD11b$^-$ dendritic cell lineage is enriched in the lungs of protected mice and strictly required for protection. Two *H. pylori* persistence determinants, the γ-glutamyl-transpeptidase GGT and the vacuolating cytotoxin VacA, are required and sufficient for asthma protection and can be administered in purified form to prevent asthma. In conclusion, we provide preclinical evidence for the concept that the immunomodulatory properties of *H. pylori* can be exploited for tolerization strategies aiming to prevent allergen-induced asthma.

bacterial immunomodulation | allergy and asthma prevention | tolerogenic dendritic cells | bacterial persistence determinants

The prevalence of asthma and other allergic diseases has increased steadily in the course of the second half of the 20th century in both adult and pediatric, developed and developing populations (1). The lack of early childhood infections or microbial exposure due to improved sanitation, and the gradual loss of the indigenous microbiota have alternately been proposed to account for this major public health trend (2, 3). Epidemiological and experimental studies have consistently shown a strong inverse association of chronic infection with the human gastric bacterial pathogen *Helicobacter pylori* with the risk of developing allergic asthma (4–9). Chronic infection with *H. pylori* is less common in allergic individuals presenting with asthma, hay fever, or eczema than in the general population; this is especially true in children and in patients with early-onset disease (4–8). We have reported earlier that experimental infection of C57/BL6 mice with a mouse-colonizing human isolate of *H. pylori* confers robust protection against allergen-induced asthma, with particularly strong protective effects observed upon early-life exposure (9). Asthma protection could be attributed to *H. pylori*-specific tolerogenic reprogramming of dendritic cells in vitro and in vivo and to the induction of highly suppressive regulatory T cells (9, 10). Despite its striking immunomodulatory properties (11) and remarkable inverse link to various allergic diseases, the use of live *H. pylori* as a therapeutic intervention or preventive measure is unattractive due to the well-documented carcinogenic potential of chronic infection with this organism. *H. pylori* induces gastric and duodenal ulcers (12), and is also widely accepted to be the leading cause of gastric adenocarcinoma (13). Here, we have devised a strategy of *H. pylori*-specific tolerization that harnesses the bacteria's immunomodulatory properties for the prevention of asthma while avoiding the risks associated with live infection and have elucidated several key determinants of asthma protection in both the bacteria and the host.

Results

***H. pylori* Whole Cell Extract Protects Against Allergen-Induced Asthma.** To assess whether regular administration of *H. pylori* extract protects against allergen-induced asthma and thus recapitulates the effects of live infection, we treated mice with weekly doses of intragastrically administered whole cell extract from age day 7 onwards before subjecting them to ovalbumin sensitization and challenge. Control mice that had received ovalbumin but no *H. pylori* extract developed airway hyperresponsiveness to methacholine (Fig. 1 *A* and *B* and Fig. S1 *A–D*) and bronchoalveolar immune cell infiltration and eosinophilia (Fig. 1 *C* and *D*), as well as histologically evident lung inflammation and

Significance

Allergic asthma represents an increasingly common public health problem. Here, we provide preclinical evidence for the efficacy of active tolerization using *Helicobacter pylori* components as a viable strategy for asthma prevention. We use a mouse model of allergic asthma to show that regular treatment with *H. pylori* extract effectively alleviates all hallmarks of the disease. Successful treatment depends on the regulatory cytokine IL-10 and on basic leucine zipper ATF-like 3 (BATF3)-dependent dendritic cell lineages. *H. pylori* extracts lacking the γ-glutamyl-transpeptidase GGT or the vacuolating cytotoxin VacA fail to protect against asthma; conversely, both factors can be administered in purified form to achieve protection. In conclusion, the immunomodulatory properties of the common infectious agent *H. pylori* can be exploited for therapeutic purposes in an allergy model.

Author contributions: D.B.E. and A.M. designed research; D.B.E., S.R., Y.v.W., S.U., A.K., J.M., and H.M. performed research; N.Y., A.W., M.G., and T.L.C. contributed new reagents/analytic tools; D.B.E., S.R., C.T., and A.M. analyzed data; and A.M. wrote the paper.

The authors declare no conflict of interest.

This article is a PNAS Direct Submission.

[1]D.B.E. and S.R. contributed equally to this work.

[2]To whom correspondence should be addressed. Email: mueller@imcr.uzh.ch.

This article contains supporting information online at www.pnas.org/lookup/suppl/doi:10.1073/pnas.1410579111/-/DCSupplemental.

goblet cell metaplasia (Fig. 1 *E–G*). The restimulation of single cell lung preparations with ovalbumin induced the production of high levels of the Th2 cytokines IL-5 and IL-13 (Fig. 1 *H* and *I*). In contrast, mice that had received *H. pylori* extract were protected against airway hyperresponsiveness (Fig. 1 *A* and *B* and Fig. S1 *A–D*), and exhibited significantly lower levels of bronchoalveolar and pulmonary inflammation, eosinophilia and goblet cell metaplasia (Fig. 1 *C–G*). Th2 cytokine production upon allergen restimulation of lung preparations was also reduced (Fig. 1 *H* and *I*). The failure of extract-treated mice to develop allergen-induced symptoms of asthma was not due to an impaired primary response to the allergen, as the levels of ovalbumin-specific serum IgE were similar in all sensitized mice (Fig. S1*E*).

To address the specificity of the observed effects and elucidate key prerequisites of protection, we examined various administration routes and regimens, ages at treatment onset, and extracts from other gastrointestinal pathogens. Interestingly, the systemic (intraperitoneal) administration of *H. pylori* extract was as efficient as the intragastric route at conferring protection against allergen-induced asthma (Fig. S1 *F–I*). Intragastric treatment was less effective when initiated in adult mice as opposed to neonates, and four consecutive doses of extract administered to young mice before weaning were insufficient to induce full protection (Fig. S1 *F–I*). Heat-inactivated *H. pylori* extract, as well as identical amounts of extracts generated from cultures of *Escherichia coli* or *Salmonella typhimurium*, failed to confer protection against the examined hallmarks of allergic airway disease (Fig. S1 *F–I*). In conclusion, the beneficial effects of extract treatment are specific to *H. pylori* and require a heat-sensitive component of the bacteria, and are most pronounced if the treatment is initiated in young mice.

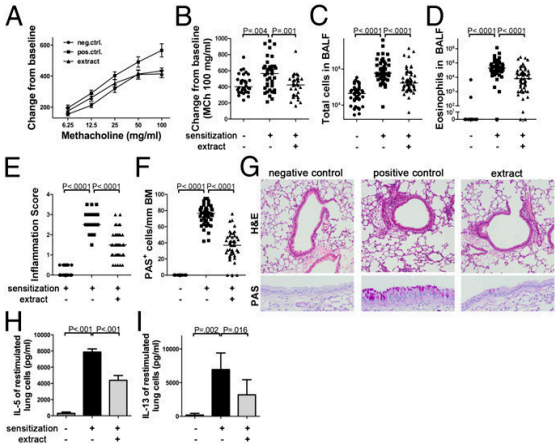

Fig. 1. Experimentally induced asthma is alleviated by treatment with *H. pylori* extract. (*A–I*) Mice were sensitized i.p. with alum-adjuvanted ovalbumin at 8 and 10 wk of age and challenged with aerosolized ovalbumin 2 wk after the second sensitization to induce asthma-like symptoms. Mock-sensitized mice served as negative controls. One group received once-weekly doses of 200 μg *H. pylori* extract intragastrically from day 7 of age until the second sensitization. (*A* and *B*) Airway hyperresponsiveness in response to increasing doses of methacholine and the highest dose of 100 mg/mL, respectively. (*C* and *D*) Total cells and eosinophils contained in 1 mL of BALF. (*E–G*) Tissue inflammation and goblet cell metaplasia as assessed on H&E and PAS-stained tissue sections; representative micrographs taken at 100× (H&E) and 400× (PAS) original magnification are shown in *G*. Pooled data from five independent studies are shown in *A–F*. (*H* and *I*) IL-5 and IL-13 secretion by single cell lung preparations restimulated with ovalbumin, as assessed by ELISA. Pooled data from two studies are shown in *H* and *I*. In scatter plots, each symbol represents one mouse; horizontal lines indicate the medians.

Successful Tolerization Against Allergen-Induced Asthma Requires IL-10 and IL-18, but Not Regulatory T Cells. *H. pylori* is known to induce the production of IL-10 in various immune cell compartments (14, 15) and high gastric levels of IL-10 ensure *H. pylori* persistence and promote *H. pylori*-specific immune tolerance (16, 17). We have shown previously that dendritic cells (DCs) play a critical role in immune tolerance to live *H. pylori*; the depletion of CD11c-positive DCs breaks tolerance and promotes clearance of the bacteria (10). To assess whether DCs produce IL-10 not only in response to live infection as shown (10), but also in response to *H. pylori* extract, cultured murine bone marrow-derived (BM) DCs were treated with increasing concentrations of extract. Indeed, BM-DCs produced and secreted large amounts of IL-10, and this was dependent on TLR2 and MyD88 signaling, but independent of TLR4 (Fig. 2*A*). A clear dose-dependent secretion of IL-10 could also be observed in human blood-derived DCs from six independent donors cultured with *H. pylori* extract (Fig. 2*B*). To address whether IL-10 is required for asthma protection conferred by extract tolerization or live infection, we administered two doses of IL-10 receptor (IL-10R)-neutralizing antibody during the challenge phase of the protocol to mice that had either received extract from the neonatal period onwards or had been infected as neonates. IL-10 signaling was required for protection against asthma in both scenarios (Fig. 2 *C–F*). We further examined the effects of extract tolerization and live infection in mice that are deficient for IL-10 production specifically in the $CD11c^+$ immune cell compartment. Although not entirely resistant to extract treatment or the beneficial effects of live infection, CD11c-Cre.$IL\text{-}10^{fl/fl}$ mice were less well protected than their Cre-negative littermates, i.e., exhibited significantly higher eosinophil counts, lung inflammation and goblet cell metaplasia (Fig. 2 *G–J*). The overall secretion of IL-10 by allergen-restimulated lung cells was reduced in CD11c-Cre.$IL\text{-}10^{fl/fl}$ mice (Fig. S2*A*), implying that $CD11c^+$ cells represent a major source of pulmonary IL-10 in this setting. In summary, we conclude that *H. pylori* extract induces IL-10 production in both murine and human DCs and that IL-10 produced by $CD11c^+$ DCs/mononuclear phagocytes, in the lungs and/or at other sites, contributes critically to protection.

Having shown previously that DC-derived IL-18 is a critical mediator of *H. pylori*-induced immune tolerance (10), we next examined the effects of *H. pylori* extract and live infection on $IL\text{-}18R^{-/-}$ mice. IL-18 signaling was absolutely required for the protective effects of live bacteria as well as extract treatment (Fig. S2 *B–E*), underscoring the tolerance-promoting role of this cytokine in the context of the *H. pylori*/host interaction. To further address whether Tregs were required for extract-mediated protection (as they are for live infection; ref. 9), we depleted $CD25^+$ Tregs (>90% depletion efficiency in the lungs, Fig. S2*F*) by applying two doses of a CD25-specific antibody before ovalbumin challenge. Treg depletion had no effect on the protection from allergic asthma conferred by *H. pylori* extract (Fig. S1 *G–J*); this result was consistent with a lack of protective activity of $CD25^+$ Tregs that were adoptively transferred from extract-treated mice to naive recipients (Fig. S1 *G–J*). *H. pylori* extract treatment of BM-DCs, in contrast to live infection, further failed to promote the expression of the Treg lineage-defining transcription factor FoxP3 in cocultured naive T cells (Fig. S2*K*), suggesting that *H. pylori* extract exerts its protective activity through the DC-intrinsic production of IL-10 (and IL-18), but independently of Tregs.

BATF3-Dependent DC Lineages Are Required for *H. pylori*-Induced Protection Against Allergic Airway Inflammation. Having identified DCs as critical mediators of *H. pylori*-specific tolerance (10) and

MICROBIOLOGY

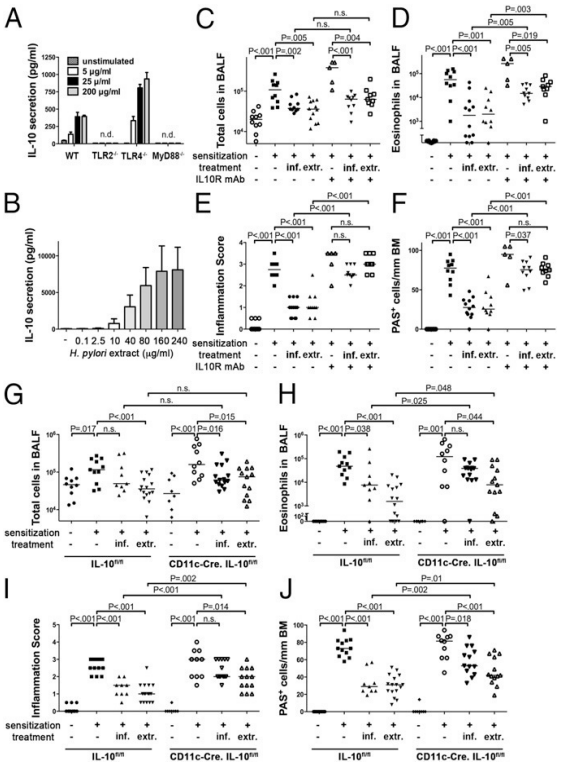

Fig. 2. IL-10 is required for *H. pylori*-induced protection against allergic asthma. (*A* and *B*) IL-10 secretion by murine bone-marrow-derived DCs of the indicated genotypes and human monocyte-derived DCs from six healthy volunteers after exposure to *H. pylori* extract. One representative experiment of three is shown in *A*, and pooled data for all six donors is shown in *B*. (*C*–*F*) Mice were treated as described in Fig. 1 or were neonatally infected with *H. pylori*; the indicated groups received 2 doses of anti-IL-10R antibody during ovalbumin challenge. (*G*–*J*) CD11c-Cre.IL-10$^{fl/fl}$ mice and their IL-10$^{fl/fl}$ littermates were either neonatally infected or received *H. pylori* extract before being subjected to ovalbumin sensitization and challenge as described in Fig. 1. Total cells (*C* and *G*) and eosinophils (*D* and *H*) contained in 1 mL of BALF. Tissue inflammation (*E* and *I*) and goblet cell metaplasia (*F* and *J*).

as key producers of protective IL-10 (Fig. 2), we next sought to dissect the role of specific DC subsets in the context of *H. pylori* infection and tolerization. To this end, we generated single cell lung preparations from extract-treated, infected, and positive as well as negative control mice and subjected them to quantitative flow cytometric analysis of various lung-infiltrating DC populations. Interestingly, despite the fact that the mice examined in this fashion exhibited very typical levels of protection (Fig. S3 *A*–*D*), their lungs were infiltrated with the same overall numbers of CD11c$^+$ MHCII$^+$ DCs as the lungs of asthmatic mice (Fig. 3*A*). However, when we distinguished between conventional and plasmacytoid DCs (cDCs, pDCs) based on their expression of B220 (also known as CD45R, a marker of the B-cell lineage that is also shared by pDCs, Fig. S3*E*), we found that CD11c$^+$ MHCII^{hi} B220$^-$ cDCs were relatively more abundant in asthmatic mice, whereas CD11c^{lo} MHCII^{lo} B220$^+$ pDCs were more abundant in the lungs of protected mice (Fig. 3 *B*–*D*). Furthermore, the total numbers of lung-infiltrating pDCs were higher than in nonsensitized negative controls (Fig. S3*F*), indicating that pDCs are actively recruited to the lungs of allergen-challenged mice that are either infected with *H. pylori* or treated with *H. pylori* extract. Another interesting difference was found among asthmatic and protected mice when we discriminated between CD11b$^+$ and CD103$^+$ cDC subsets (Fig. S3*G*). Strikingly, whereas the asthmatic lungs of positive control mice were predominantly infiltrated by CD11b$^+$ cDCs, the lungs of protected mice were relatively more infiltrated by CD103$^+$ cDCs (Fig. 3 *E*–*G*). Again, CD103$^+$ cDCs appeared to be specifically recruited to the lungs of allergen-challenged mice either infected with *H. pylori* or treated with *H. pylori* extract (Fig. S3*H*).

To assess the functional relevance of CD103$^+$ lung-infiltrating DCs in asthma protection in our model, we examined mice lacking the transcription factor basic leucine zipper ATF-like 3 (BATF3), which has previously been shown to direct the development of CD8α$^+$ lymphoid tissue DCs as well as CD103$^+$ CD11b$^-$ DCs in the lungs, intestine and skin (18). We were able to confirm that the lungs of BATF3$^{-/-}$ mice are entirely devoid of CD103$^+$ DCs, and exhibit normal and higher frequencies of pDCs and CD11b$^+$ DCs, respectively (Fig. S3 *I* and *J*). Interestingly, pure populations of mesenteric lymph node-derived DCs from BATF3$^{-/-}$ mice failed to express IL-10 upon treatment with increasing doses of *H. pylori* extract ex vivo (Fig. 3*H*). BATF3$^{-/-}$ mice were significantly less protected than wild-type mice against allergen-induced asthma upon infection with *H. pylori*, and upon treatment with *H. pylori* extract (Fig. 3 *I*–*L*), despite being colonized at comparable levels (Fig. S3*K*). In summary, BATF3-dependent CD103$^+$ DC lineages infiltrate the lungs of protected mice, and are required for the *H. pylori*-driven, IL-10-mediated protection from allergic asthma.

The *H. pylori* Persistence Determinants γ-Glutamyl Transpeptidase and Vacuolating Cytotoxin Are Required and Sufficient for Protection Against Allergic Airway Inflammation. We have shown recently that two *H. pylori* virulence determinants encoded by all clinical isolates investigated to date, the γ-glutamyl transpeptidase GGT and the vacuolating cytotoxin VacA, promote persistence through tolerogenic reprogramming of DCs (19). To examine whether GGT and/or VacA contribute to asthma protection conferred by extract tolerization, we compared the protective properties of extracts from wild-type bacteria and from GGT- or VacA-deficient isogenic mutants. Interestingly, both mutant extracts were consistently less efficient than wild-type extract at protecting allergen-sensitized and -challenged mice against bronchoalveolar and pulmonary inflammation, eosinophilia, and goblet cell metaplasia (Fig. 4 *A*–*D*). To examine whether either factor alone is sufficient to provide protection, we intraperitoneally administered either recombinant GGT or oligomeric VacA purified from culture supernatants of *H. pylori* once weekly from day 7 of age onwards. No adverse effects were observed in any of the mice, despite their young age at the time of the first doses. Strikingly, both VacA and GGT provided a level of protection against asthma that was comparable to the protection conferred by parallel whole cell extract treatment (Fig. 4 *E*–*H*). VacA was somewhat more protective than GGT at identical concentrations. VacA lacking an amino-terminal hydrophobic region of three tandem GXXXG motifs that is essential for VacA's cytotoxic activity (20) failed to protect against asthma (Fig. 4 *E*–*H*). Wild-type, but not mutant, VacA had similar effects on pulmonary Th2 cytokine production and DC infiltration (Fig. S4 *A*–*E*) as live *H. pylori* or whole cell extract (Figs. 1 and 3). IL-10R neutralization during ovalbumin challenge abrogated the protective activity of VacA, which was observed not only upon intraperitoneal administration, but also upon oral administration, and in adult as well as neonatally treated mice (Fig. S4 *F*–*I*). We conclude that GGT and VacA are key determinants of *H. pylori*-induced asthma protection and may be administered in purified form to prevent allergic asthma.

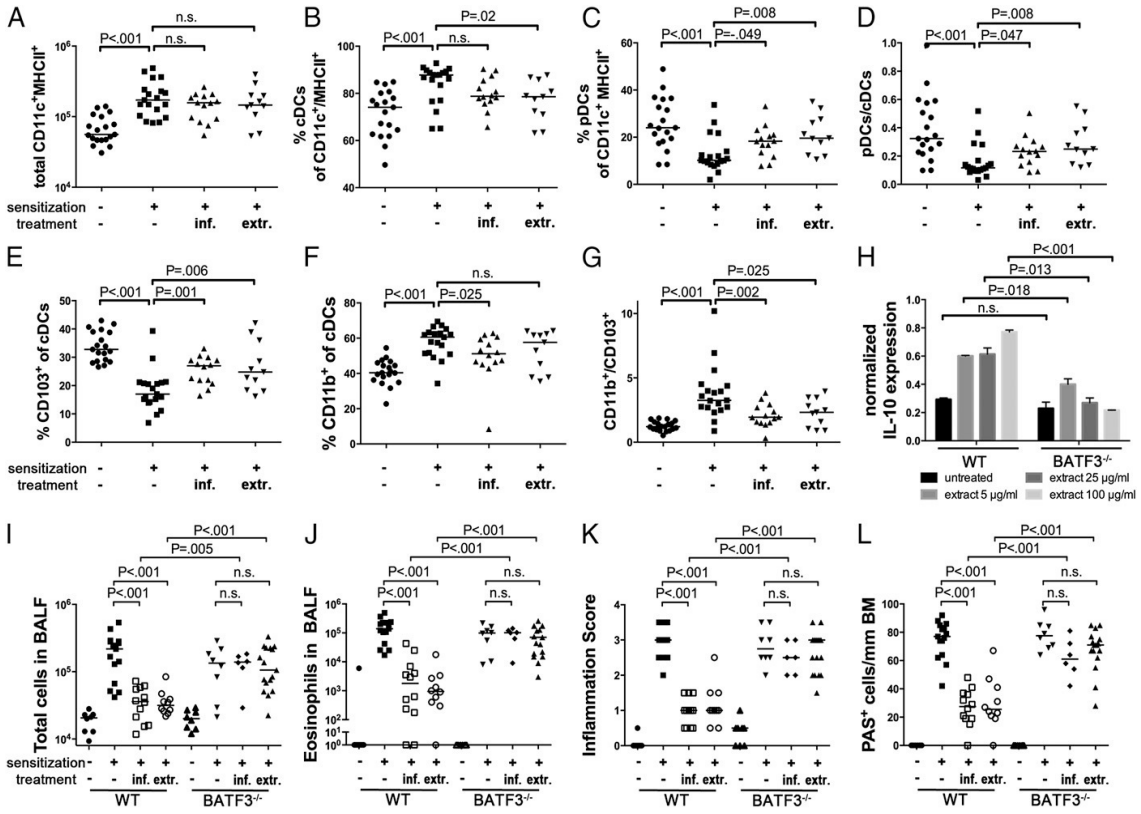

Fig. 3. CD103$^+$ conventional DCs accumulate in the lungs of *H. pylori*-infected and extract-treated mice and are required for protection. (*A*–*G*) Groups of mice treated as described in Figs. 1 and 2 were analyzed with respect to lung infiltration by pDCs and two lineages of cDCs. Data are pooled from three independent studies. (*A*) Total infiltration of CD11c$^+$MHC$^+$ cells. (*B* and *C*) Frequencies of B220$^-$ cDCs and B220$^+$ pDCs among all CD11c$^+$MHC$^+$ cells. (*D*) Ratios of pDCs to cDCs as calculated per mouse. (*E* and *F*) Frequencies of CD103$^+$ and CD11b$^+$ cells among all cDCs. (*G*) Ratios of CD11b$^+$ and CD103$^+$ cDCs as calculated per mouse. (*H*) IL-10 transcript levels normalized to GAPDH, of immunomagnetically isolated CD11c$^+$ DCs from mesenteric lymph nodes of WT and BATF3$^{-/-}$ mice, treated with the indicated increasing doses of *H. pylori* extract. (*I*–*L*) Wild-type and BATF3$^{-/-}$ mice were treated or infected as described in Figs. 1 and 2 and subjected to ovalbumin sensitization and challenge. (*I* and *J*) Total cells and eosinophils contained in 1 mL of BALF. (*K* and *L*) Tissue inflammation and goblet cell metaplasia.

Discussion

We have devised here a strategy of active tolerization for the prevention of allergic asthma that exploits the immunomodulatory properties of *H. pylori* without exposing to the risks associated with live infection. By orally or intraperitoneally administering *H. pylori* whole cell extract to allergen-sensitized mice, we were able to achieve a level of protection against asthma that was equivalent to the protection conferred by live infection (9). Extract-mediated protection was highly specific to *H. pylori*, i.e., was not conferred by extract from other Gram-negative enteropathogens such as *E. coli* or *Salmonella typhimurium*. The treatment was particularly successful when initiated in young mice, an observation that is in line with the superior protection afforded by experimental (live) infection of neonatal relative to adult mice (9). The differential susceptibility to successful tolerization of neonates and adults may be attributable to the general tolerogenic bias of the immature neonatal immune system, with its higher Treg/Teffector cell ratios and Treg-predominant responses to foreign antigens (21). Our results are in line with the epidemiological finding that children benefit more from harboring *H. pylori* than adults in terms of their asthma risk (6); similarly, early onset asthma in adolescents and young adults is more strongly inversely correlated with *H. pylori* seropositivity than adult-onset asthma (5). The data presented here thus imply that children at high risk of developing asthma are more likely than adults to benefit from *H. pylori*-specific tolerization strategies.

Having shown earlier that *H. pylori*-specific immune tolerance is a consequence of tolerogenic reprogramming of DCs by the bacteria (10), we set out to examine the contribution of specific DC lineages and their immunomodulators to immune tolerance and asthma protection in the settings of neonatal infection and neonatal-onset tolerization with *H. pylori* extract. A careful immunophenotypic analysis of the DC subsets infiltrating the lungs of protected mice revealed a preferential recruitment of CD103$^+$CD11b$^-$ conventional DCs, and to a lesser extent of B220$^+$ plasmacytoid DCs. The contribution of CD103$^+$ DCs to asthma protection was further functionally assessed in mice lacking the BATF3 transcription factor, which drives the development of CD8α$^+$ lymphoid tissue-resident DC lineages and of the closely related CD103$^+$CD11b$^-$ DC lineages in various tissues including the lung, intestine and skin (18). We were able to confirm that CD103$^+$CD11b$^-$ DCs are completely absent from the lungs of BATF3$^{-/-}$ mice, whereas all other examined subsets are present in normal numbers. BATF3$^{-/-}$ animals were equally susceptible to allergen-induced asthma as wild-type mice;

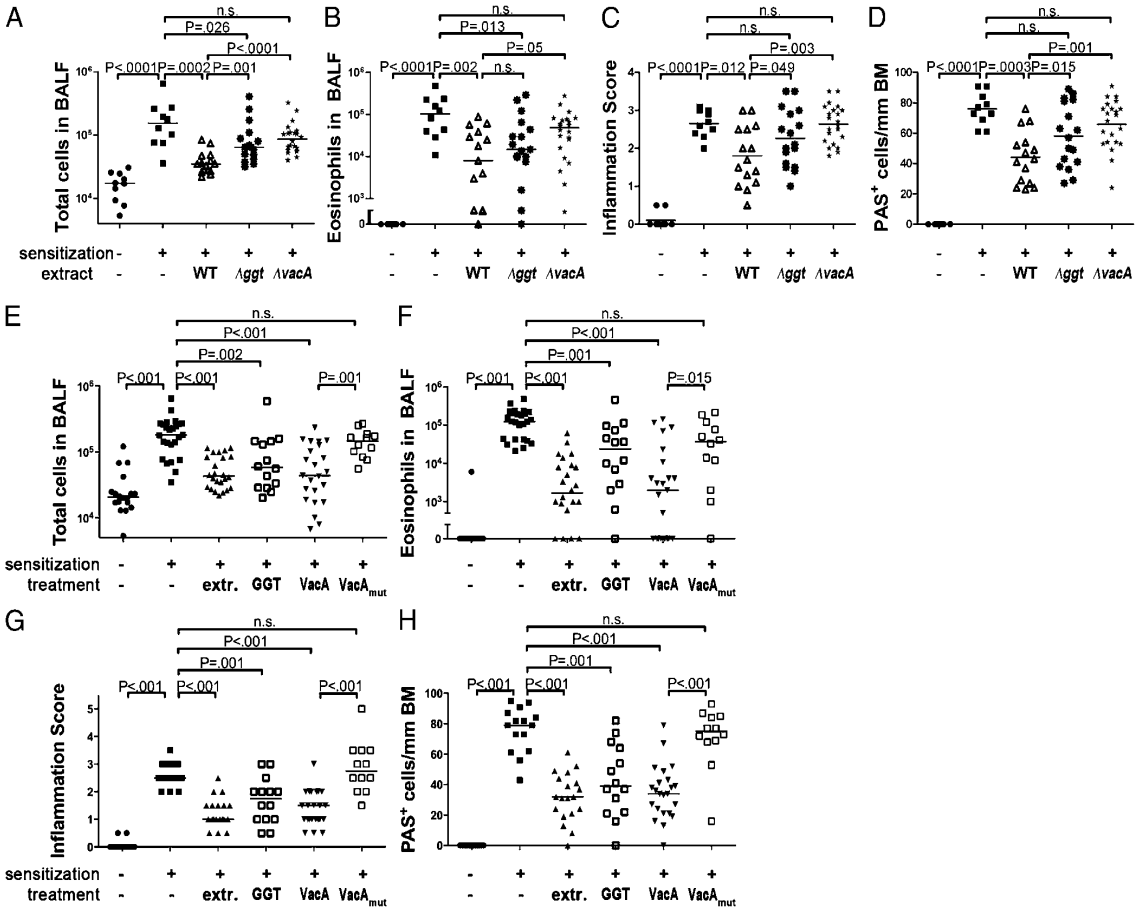

Fig. 4. *H. pylori* GGT and VacA are required and sufficient for protection against asthma. (*A–D*) Groups of mice were treated as described in Fig. 1 with *H. pylori* extract generated from either wild-type (WT) or Δ*ggt* or Δ*vacA* mutant bacteria, and were subjected to ovalbumin sensitization and challenge. (*E–H*) Mice were i.p. injected weekly with 25 μg per dose of either recombinant GGT or purified wild-type or mutant (Δ6–27) VacA starting on day 7 of age until the second sensitization. Total cells (*A* and *E*) and eosinophils (*B* and *F*) contained in 1 mL of BALF. Tissue inflammation (*C* and *G*) and goblet cell metaplasia (*D* and *H*).

however, neither regular extract treatment nor *H. pylori* colonization had any detectable beneficial effect on the examined hallmarks of asthma in this strain, indicating that BATF3-dependent DCs are strictly required for protection in both scenarios. We further found that lymph node-derived DCs from BATF3$^{-/-}$ mice fail to produce IL-10 upon treatment with *H. pylori* extract ex vivo. This observation is well in line with the requirement for IL-10 signaling proficiency and, more specifically, for the DC-intrinsic production of IL-10 for optimal *H. pylori*-mediated protection against allergic asthma. We conclude from the combined results that BATF3-dependent DC lineages suppress pulmonary allergen-specific immune responses by production of IL-10; in contrast, Tregs are not critically required for *H. pylori* extract-mediated protection, as their depletion fails to abrogate protection.

Another cytokine known to be induced by *H. pylori*, IL-18 (22), also turned out to be absolutely essential for asthma prevention in the course of our studies. IL-18 is produced upon inflammasome activation by *H. pylori* in a variety of cell types, including DCs, and promotes Treg differentiation and *H. pylori*-specific tolerance in vitro and in vivo (10, 22). Whether the DC-intrinsic production of IL-18 is required for *H. pylori* (extract)-mediated protection against asthma remains to be addressed with suitable mouse strains.

Our data further show that two *H. pylori* determinants, GGT and VacA, are required for extract-mediated protection and can be administered in purified form to prevent allergic asthma. These findings are in line with earlier reports showing that both factors have a critical role in *H. pylori* persistence and immune modulation. Mutants lacking the *ggt* gene are incapable of colonizing mice persistently (19, 23), and this phenotype has been attributed to DC tolerization by GGT in vitro and in vivo (19). Similarly, a *vacA* gene deletion mutant fails to tolerize DCs and to induce Tregs in vivo, and is therefore effectively controlled or even cleared upon onset of an adaptive immune response (19). The fact that a mutant form of VacA lacking an amino-terminal hydrophobic region of three tandem GXXXG motifs fails to protect against asthma when administered to mice in purified form suggests that membrane insertion by VacA is required for its immunomodulatory effects. The exact mechanism and relevant target cell types of VacA in vivo remain to be elucidated in detail. Taken together, our data demonstrate, to our knowledge for the first time, that the immunomodulatory properties of a very common infectious agent in humans, *H. pylori*, can be exploited for therapeutic purposes in an allergy model and lend

support to *H. pylori*-specific tolerization as a viable strategy for asthma prevention in high-risk individuals.

Materials and Methods

Animal Experimentation. C57BL/6, BATF3$^{-/-}$, IL-18R$^{-/-}$, and CD11c-Cre.IL-10fl/fl mice were orally infected with *H. pylori* PMSS1 as described (16) or received either once-weekly oral or i.p. doses of 200 μg of extract of *H. pylori* wild-type PMSS1, PMSS1Δ*ggt* or PMSS1Δ*vacA* (19), *Salmonella typhimurium*, or *E. coli* or once-weekly i.p. doses of 25 μg of recombinant GGT, or of s1m1 type VacA (wild type or Δ6–27, ref. 20) purified from *H. pylori* strain 60190. Mice were sensitized by i.p. injection of 20 μg of ovalbumin (Sigma-Aldrich) emulsified in 2.25 mg of aluminum hydroxide (Alum Imject; Pierce) at 8 and 10 wk of age and challenged with 1% aerosolized ovalbumin using an ultrasonic nebulizer (NE-U17; Omron) for 20 min daily on days 31, 32, and 33 after initial sensitization. Airway resistance measurements were performed on anesthetized, intubated and mechanically ventilated mice (FinePointe Resistance and Compliance System, Buxco Electronics) in response to increasing doses of inhaled metacholine. In vivo blocking of IL-10 signaling and depletion of Tregs was achieved by two i.p. injections of 250 μg of anti-IL-10R antibody (clone 1B1.3A) and anti-CD25 antibody (clone PC-61.5, both BioXCell), respectively, during the challenge phase. CD4^{+}CD25^{+} Tregs were adoptively transferred as described (9). Lungs were lavaged via the trachea with 1 mL of PBS. Broncho-alveolar lavage fluid (BALF) cells were counted using trypan blue dye exclusion. Differential cell counts of macrophages, lymphocytes, neutrophils, and eosinophils were performed on cytocentrifuged preparations stained with the Microscopy Hemacolor-Set (Merck). For lung histopathology, lungs were fixed by inflation and immersion in 10% (vol/vol) formalin and embedded in paraffin. Tissue sections were stained with H&E and periodic acid-Schiff and examined in blinded fashion on a BX40 Olympus microscope. Peribronchial inflammation was scored on a scale from 0 to 4. PAS-positive goblet cells were quantified per 1 mm of basement membrane. All animal experimentation was performed in accordance with federal, cantonal and institutional guidelines, and approved by the Zurich Cantonal Veterinary Authorities (no. 170/2009 to A.M.).

Preparation of *H. pylori* Extract and Purification of GGT and VacA. *H. pylori* was cultured in *Brucella* broth supplemented with 10% FCS, pelleted by centrifugation, and washed once with PBS. Bacteria were subjected to three freeze/thaw cycles and disrupted by three passes through a French pressure cell press (Stansted Fluid Power, Cell Pressure Homogenizer) at 30,000 bar. Cell debris was removed by centrifugation and the supernatant filtered through a 2-μm filter. Protein concentrations were determined by BCA Protein Kit (R&D Systems). *H. pylori* VacA was purified using published procedures (24, 25), with the following slight modifications. *H. pylori* strain 60190 was cultured in sulfite-free *Brucella* broth containing either cholesterol or 0.5% charcoal. After centrifugation of the culture, supernatant proteins were precipitated with a 50% saturated solution of ammonium sulfate. The oligomeric form of VacA was isolated by gel filtration chromatography with a Superose 6 HR 16/50 column in PBS containing 0.02% sodium azide and 1 mM EDTA. *H. pylori* GGT was purified as described (19). Protocols for lung single cell preparation, flow cytometry, cytokine ELISAs, and preparation of murine and human DCs and DC/T-cell cocultures can be found in *SI Materials and Methods*.

Statistics. All statistical analysis was performed using Graph Pad prism 5.0 software. The Mann–Whitney test was used throughout. *P* values <0.05 were considered significant.

ACKNOWLEDGMENTS. We thank Hermelijn Smits and Maria Yazdanbakhsh (Leiden University Medical Center) for their help with culturing human DCs. This study was funded by Swiss National Science Foundation Project Grant 310030_143608/1 (to A.M.), the National Institutes of Health Grants AI039657 and CA116087 (to T.L.C.), and Department of Veterans Affairs (T.L.C.).

1. Eder W, Ege MJ, von Mutius E (2006) The asthma epidemic. *N Engl J Med* 355(21): 2226–2235.
2. Blaser MJ, Falkow S (2009) What are the consequences of the disappearing human microbiota? *Nat Rev Microbiol* 7(12):887–894.
3. Strachan DP (1989) Hay fever, hygiene, and household size. *BMJ* 299(6710): 1259–1260.
4. Amberbir A, et al. (2011) Effects of Helicobacter pylori, geohelminth infection and selected commensal bacteria on the risk of allergic disease and sensitization in 3-year-old Ethiopian children. *Clin Exp Allergy* 41(10):1422–1430.
5. Chen Y, Blaser MJ (2007) Inverse associations of Helicobacter pylori with asthma and allergy. *Arch Intern Med* 167(8):821–827.
6. Chen Y, Blaser MJ (2008) Helicobacter pylori colonization is inversely associated with childhood asthma. *J Infect Dis* 198(4):553–560.
7. Reibman J, et al. (2008) Asthma is inversely associated with Helicobacter pylori status in an urban population. *PLoS ONE* 3(12):e4060.
8. Herbarth O, et al. (2007) Helicobacter pylori colonisation and eczema. *J Epidemiol Community Health* 61(7):638–640.
9. Arnold IC, et al. (2011) Helicobacter pylori infection prevents allergic asthma in mouse models through the induction of regulatory T cells. *J Clin Invest* 121(8):3088–3093.
10. Oertli M, et al. (2012) DC-derived IL-18 drives Treg differentiation, murine Helicobacter pylori-specific immune tolerance, and asthma protection. *J Clin Invest* 122(3): 1082–1096.
11. Salama NR, Hartung ML, Müller A (2013) Life in the human stomach: Persistence strategies of the bacterial pathogen Helicobacter pylori. *Nat Rev Microbiol* 11(6): 385–399.
12. Marshall BJ, Warren JR (1984) Unidentified curved bacilli in the stomach of patients with gastritis and peptic ulceration. *Lancet* 1(8390):1311–1315.
13. Parsonnet J, et al. (1991) Helicobacter pylori infection and the risk of gastric carcinoma. *N Engl J Med* 325(16):1127–1131.
14. Rad R, et al. (2009) Extracellular and intracellular pattern recognition receptors cooperate in the recognition of Helicobacter pylori. *Gastroenterology* 136(7): 2247–2257.
15. Sayi A, et al. (2011) TLR-2-activated B cells suppress Helicobacter-induced preneoplastic gastric immunopathology by inducing T regulatory-1 cells. *J Immunol* 186(2): 878–890.
16. Arnold IC, et al. (2011) Tolerance rather than immunity protects from Helicobacter pylori-induced gastric preneoplasia. *Gastroenterology* 140(1):199–209.
17. Ismail HF, Fick P, Zhang J, Lynch RG, Berg DJ (2003) Depletion of neutrophils in IL-10(-/-) mice delays clearance of gastric Helicobacter infection and decreases the Th1 immune response to Helicobacter. *J Immunol* 170(7):3782–3789.
18. Edelson BT, et al. (2010) Peripheral CD103+ dendritic cells form a unified subset developmentally related to CD8alpha+ conventional dendritic cells. *J Exp Med* 207(4): 823–836.
19. Oertli M, et al. (2013) Helicobacter pylori γ-glutamyl transpeptidase and vacuolating cytotoxin promote gastric persistence and immune tolerance. *Proc Natl Acad Sci USA* 110(8):3047–3052.
20. Vinion-Dubiel AD, et al. (1999) A dominant negative mutant of Helicobacter pylori vacuolating toxin (VacA) inhibits VacA-induced cell vacuolation. *J Biol Chem* 274(53): 37736–37742.
21. Arnold B, Schüler T, Hämmerling GJ (2005) Control of peripheral T-lymphocyte tolerance in neonates and adults. *Trends Immunol* 26(8):406–411.
22. Hitzler I, et al. (2012) Caspase-1 has both proinflammatory and regulatory properties in Helicobacter infections, which are differentially mediated by its substrates IL-1β and IL-18. *J Immunol* 188(8):3594–3602.
23. Chevalier C, Thiberge JM, Ferrero RL, Labigne A (1999) Essential role of Helicobacter pylori gamma-glutamyltranspeptidase for the colonization of the gastric mucosa of mice. *Mol Microbiol* 31(5):1359–1372.
24. Cover TL, Blaser MJ (1992) Purification and characterization of the vacuolating toxin from Helicobacter pylori. *J Biol Chem* 267(15):10570–10575.
25. Cover TL, Hanson PI, Heuser JE (1997) Acid-induced dissociation of VacA, the Helicobacter pylori vacuolating cytotoxin, reveals its pattern of assembly. *J Cell Biol* 138(4):759–769.

Supporting Information

Engler et al. 10.1073/pnas.1410579111

SI Materials and Methods

Lung Single Cell Preparation, Flow Cytometry, and Th2 Cytokine ELISAs. Lungs were dissected, enzymatically digested with 0.5 mg/mL collagenase type IA (Sigma-Aldrich) and pushed through a 70-μm nylon cell strainer. The antibodies used for staining were anti-MHCII (clone M5/114.15.2), anti-B220 (RA3-6B2), anti-CD11c (clone HL3), anti-CD103 (clone M290), and anti-CD11b (clone M1/70; all BD Pharmingen). FACS analyses were performed on a FACSCanto2 cytometer (BD Biosciences); post-acquisition analysis was done using FlowJo software (Tree Star). Cytokines in lung single-cell cultures restimulated for 72 h with 250 μg/mL ovalbumin were quantified by ELISA (IL-5, BD Pharmingen; IL-13, R&D Systems).

Preparation of Murine and Human DCs and IL-10 ELISA. For generation of murine bone-marrow-derived dendritic cells (BM-DCs), bone marrow isolated from the hind legs of donor mice (BL/6.TLR2$^{-/-}$, BL/6.TLR4$^{-/-}$, BL/6.MyD88$^{-/-}$ mice, all from Jackson Labs) was seeded at 50,000 cells per well in 96-well plates in RPMI/10% (vol/vol) FCS and 4 ng/mL GM-CSF and cultured for 5 d. For the isolation of MLN-DCs, mesenteric lymph nodes were digested in 1 mg/mL collagenase (Sigma-Aldrich) for 30 min at 37 °C with shaking before filtering through a cell strainer (40 μm; BD Biosciences) and immunomagnetic isolation of DCs using mouse-specific CD11c microbeads (Miltenyi Biotec). BM-DCs and MLN-DCs were stimulated with the indicated amounts of *Helicobacter pylori* PMSS1 extract for 16 h, and supernatants were subjected to mIL-10 ELISA (BD Pharmingen). Human monocyte-derived dendritic cells were generated from peripheral blood mononuclear cells. Venous blood was drawn from six healthy volunteers according to protocols approved by the Institutional Review Board of Leiden University Medical Center. Cells were collected after density gradient centrifugation on Ficoll, and CD14^{+} monocytes were positively isolated by magnetic-activated cell sorting (MACS) using CD14 microbeads (Miltenyi Biotec). Cells were cultured in RPMI-1640 (Invitrogen) supplemented with penicillin (100 U/mL, Astellas Pharma), streptomycin (100 μg/mL, Sigma), pyruvate (1 mM, Sigma), glutamate (2 mM, Sigma), 10% FCS, 20 ng/mL human recombinant granulocyte-macrophage colony-stimulating factor (rGM-CSF, Invitrogen/Life Technologies), and 0.86 ng/mL human rIL-4 (R&D Systems) for 6 d. On day 3, the medium and the supplements were refreshed. Monocyte-derived DCs were stimulated with *H. pylori* extract for 48 h. Secretion of IL-10 by the DCs in the supernatant was measured by ELISA (Sanquin).

DC/T-Cell Cocultures. For Treg differentiation ex vivo, BM-DC cultures were infected overnight with wild-type *H. pylori* PMSS1 or treated with 25 μg/mL *H. pylori* extract. Bacteria were killed with 200 U penicillin/0.2 mg streptomycin/mL for 6 h before the addition of T cells. CD4^{+}CD25^{-} T cells were prepared from single-cell suspensions of naive C57BL/6 spleens by immunomagnetic sorting (R&D Systems). DCs were cocultured with CD4^{+}CD25^{-} T cells at a ratio of 1:2 (0.5×10^5 DC to 1×10^5 T cells) in RPMI containing 10% FCS, 10 ng/mL rTGF-β (PeproTech), 10 ng/mL rIL-2 (R&D Systems) and 1 μg/mL anti-CD3ε (BD Bioscience). After 72 h of coculture, the cells were stained first for CD4 and CD25 and then, after fixation and permeabilization, for FoxP3 (FoxP3-APC, eBioscience). The percentage of FoxP3^{+} CD4^{+} T cells was assessed by FACS on a Cyan ADP 9 instrument (Beckman Coulter) and analyzed using FlowJo software (TreeStar).

Processing of Gastric Tissue for Plating and Colony Counting. Stomachs were retrieved and dissected longitudinally. For the quantitative assessment of *H. pylori* colonization, a stomach section containing representative amounts of antral and corpus tissue was homogenized in *Brucella* broth and serial dilutions were plated on horse blood plates for colony counting as described (1).

1. Arnold IC, et al. (2011) Tolerance rather than immunity protects from *Helicobacter pylori*-induced gastric preneoplasia. *Gastroenterology* 140(1):199–209.

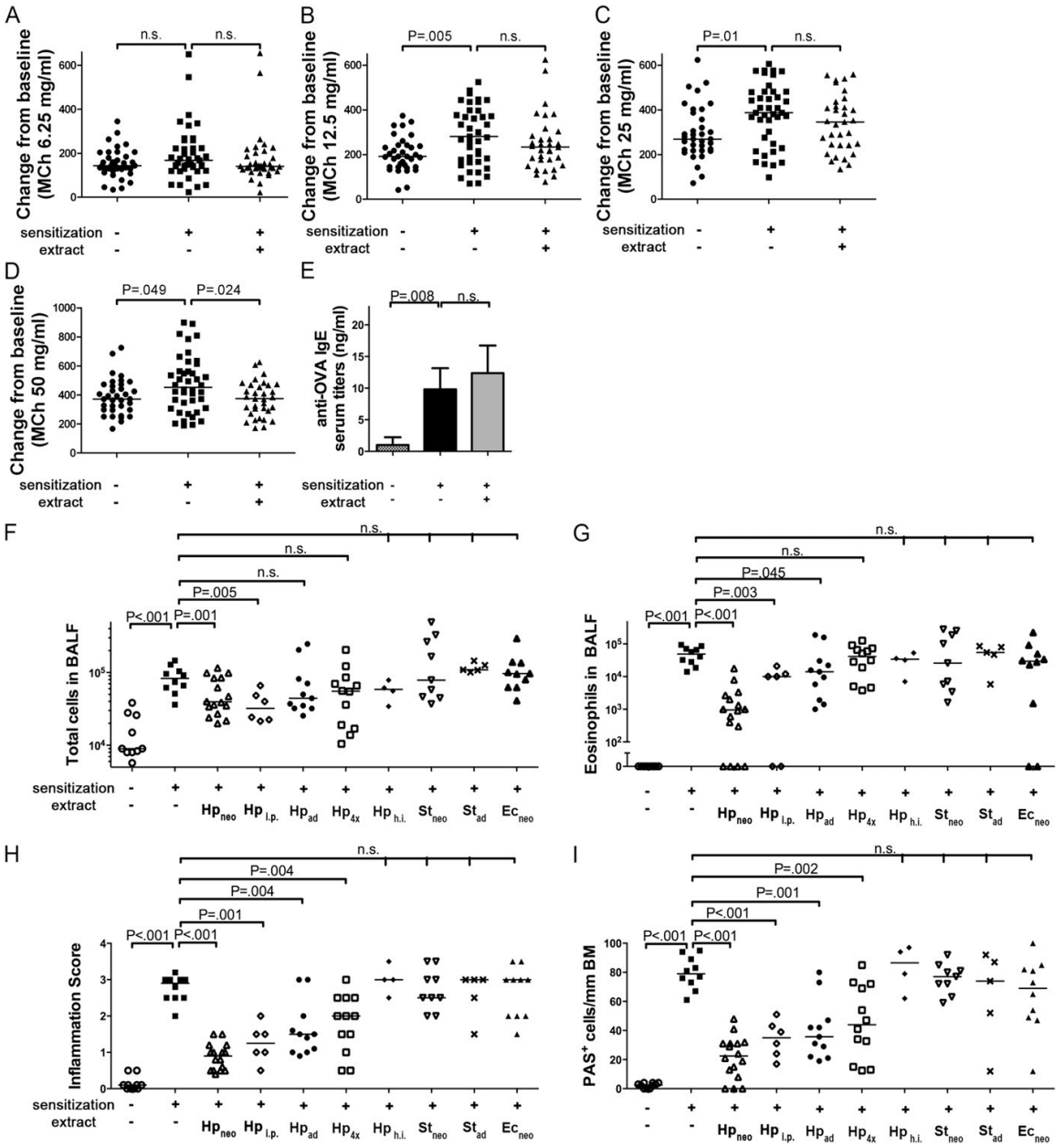

Fig. S1. The protection against asthma conferred by treatment with whole cell extract is specific to *H. pylori*, depends on a heat-sensitive component of the bacteria, and is most efficient when initiated in newborn mice. (*A*–*E*) Mice were sensitized i.p. with alum-adjuvanted ovalbumin at 8 and 10 wk of age and challenged with aerosolized ovalbumin 2 wk after the second sensitization to induce asthma-like symptoms. Mock-sensitized mice served as negative controls. One group received once-weekly doses of 200 μg of *H. pylori* extract from day 7 of age until the second sensitization. (*A*–*D*) Airway hyperresponsiveness in response to the indicated increasing doses of methacholine. (*E*) Ovalbumin-specific serum IgE titers of the groups shown in *A*–*D*. (*F*–*I*) Mice were treated as described in *A*–*E*, with the following modifications: Hp_{neo}, extract administered orally from day 7 to the second sensitization, exactly as described above; $Hp_{i.p.}$, extract administered i.p. from day 7 to the second sensitization; Hp_{ad}, extract administered orally to adult mice for 4 wk before the second sensitization; Hp_{4x}, extract administered four times orally in the first 3 wk of life only; $Hp_{h.i.}$, heat-inactivated extract administered orally from day 7 to the second sensitization; $St_{neo/ad}$, Ec_{neo}, *Salmonella typhimurium* and *Escherichia coli* extract administered orally either beginning in the neonatal period or to adults, respectively. (*F* and *G*) Total cells and eosinophils contained in 1 mL of BALF. (*H* and *I*) Tissue inflammation and goblet cell metaplasia. Data points are pooled from two independent studies.

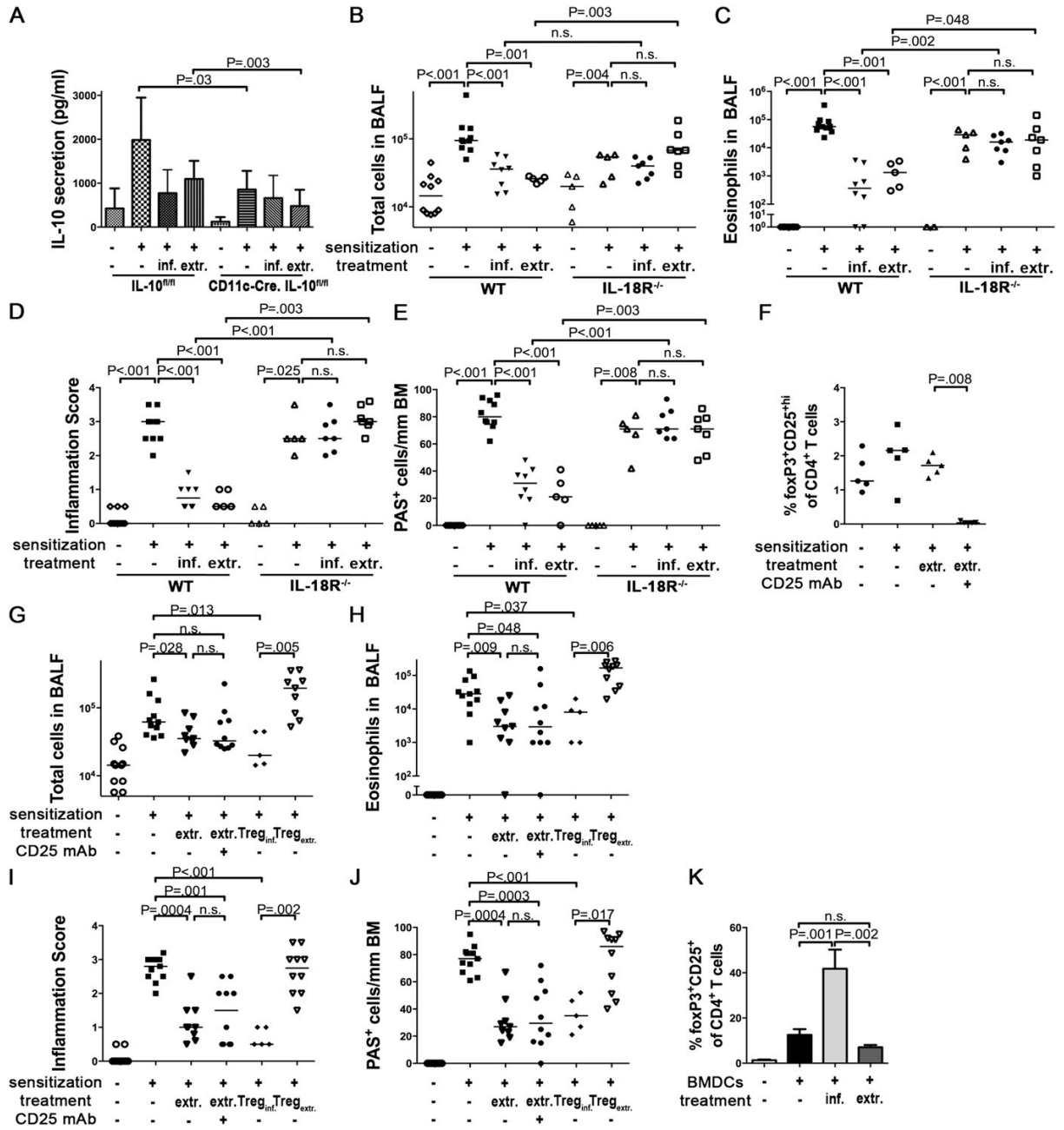

Fig. S2. The protection against asthma conferred by *H. pylori* depends on IL-10 and IL-18, but not on regulatory T cells. (*A*) CD11c-Cre.IL-10$^{fl/fl}$ mice and their IL-10$^{fl/fl}$ littermates were treated with *H. pylori* extract before being subjected to ovalbumin sensitization and challenge as described in Fig. 2 *G–J*. IL-10 secretion by single cell lung preparations restimulated with ovalbumin, as assessed by ELISA. (*B–E*) WT C57BL/6 and IL-18R$^{-/-}$ mice were neonatally infected with *H. pylori* or treated with *H. pylori* extract before being subjected to ovalbumin sensitization and challenge as described in Fig. 1. (*B* and *C*) Total cells and eosinophils contained in 1 mL of BALF. (*D* and *E*) Tissue inflammation and goblet cell metaplasia. (*F–J*) Wild-type C57BL/6 mice were treated with *H. pylori* extract before being subjected to ovalbumin sensitization and challenge. One group received two doses of anti-CD25 antibody during ovalbumin challenge. Additional sensitized and challenged groups received 100,000 immunomagnetically isolated CD4$^+$CD25$^+$ T cells from either neonatally infected donors or extract-treated donors i.v. 2 d before the first ovalbumin challenge. (*F*) Lung infiltration of CD4$^+$CD25$^+$FoxP3$^+$ T cells as assessed in lung single cell preparations of individual mice. (*G* and *H*) Total cells and eosinophils contained in 1 mL of BALF. (*I* and *J*) Tissue inflammation and goblet cell metaplasia. (*K*) BM-DCs were either infected overnight with live *H. pylori* or treated with 25 μg/mL *H. pylori* extract. Bacteria were killed with antibiotics before the addition of splenic CD4$^+$CD25$^-$ T cells at a DC:T-cell ratio of 1:2. DC/T-cell cocultures were supplemented with rTGF-β, rIL-2and anti-CD3ε. After 72 h of coculture, the cells were stained for CD4, CD25, and FoxP3 and the fraction of FoxP3$^+$ CD4$^+$ T cells was assessed by FACS.

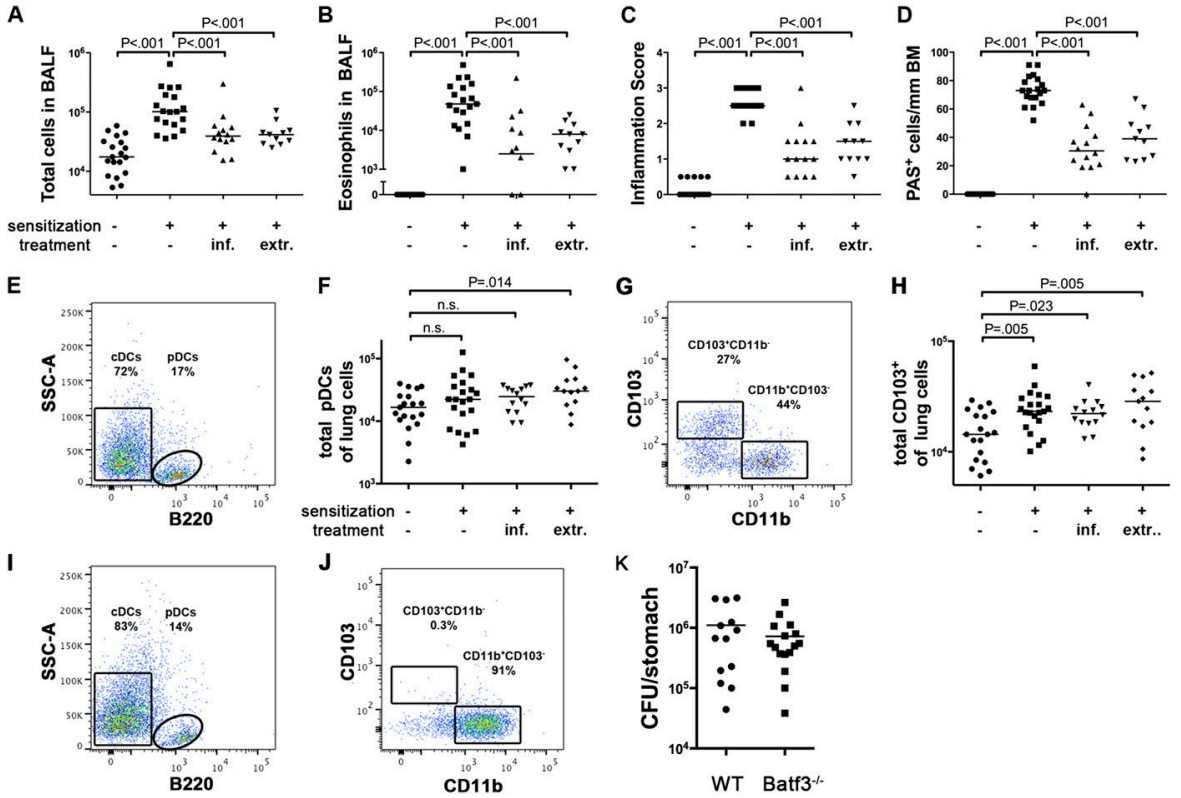

Fig. S3. CD103^{+} conventional DCs accumulate in the lungs of *H. pylori*-infected and extract-treated wild-type mice, but not basic leucine zipper ATF-like 3 (BATF3)$^{-/-}$ mice. (*A*–*D*) Total cells and eosinophils contained in 1 mL of BALF, as well as tissue inflammation and goblet cell metaplasia as assessed on H&E and PAS-stained tissue sections, of all mice for which lung DC populations are shown in Fig. 3 *A*–*G*. (*E*) Plasmacytoid DCs (pDCs) and conventional DCs (cDCs) differentially express B220; a representative scatter plot is shown for all CD11c^{+} MHCII^{+} DCs of an extract-treated mouse. (*F*) Total numbers of B220^{+} pDCs infiltrating the lungs of the mice shown in Fig. 3 *A*–*G*. (*G*) Two distinct cDC lineages can be discriminated in the lung based on CD103 and CD11b expression; a representative scatter plot is shown for an extract-treated mouse (gated on CD11c^{+} MHCII^{+} B220^{-} DCs). (*H*) Total CD103^{+} cDC infiltration into the lungs of the mice shown in Fig. 3 *A*–*G*. (*I* and *J*) BATF3$^{-/-}$ mice lack CD103^{+} cDCs, but retain CD11b^{+} cDCs and normal frequencies of pDCs. (*K*) *H. pylori* colonization of neonatally infected WT C57BL/6 and BATF3$^{-/-}$ mice as determined by plating of gastric mucosal homogenates on horse blood plates and colony counting.

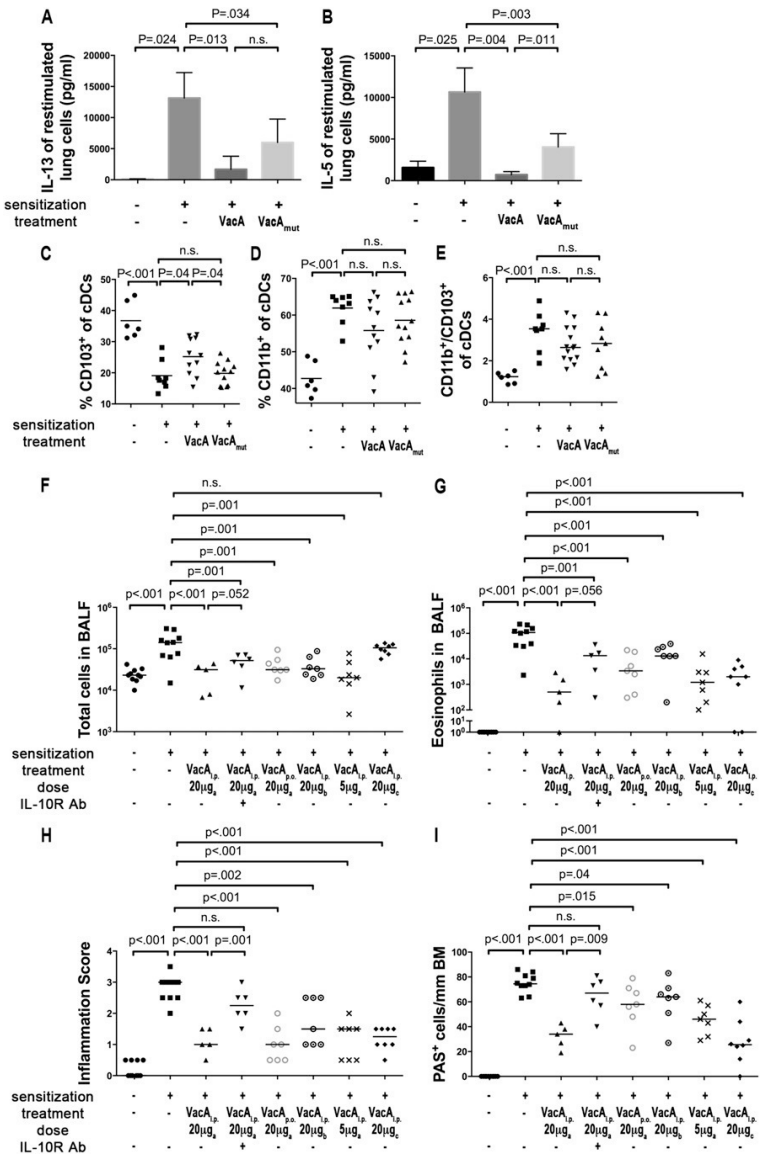

Fig. S4. VacA protects against allergic asthma when administered intraperitoneally or intragastrically. (*A–E*) Mice were i.p. injected weekly with 25 μg per dose of either recombinant GGT or purified wild-type or mutant (Δ6–27) VacA starting on day 7 of age until the second sensitization as described in Fig. 4 *E–H* (a subset of the mice of Fig. 4 *E–H* is shown here). (*A* and *B*) IL-13 and IL-5 secretion, as assessed by ELISA, of single cell lung preparations restimulated with ovalbumin. (*C* and *D*) Frequencies of $CD103^+$ and $CD11b^+$ cells among all $CD11c^+MHC^+B220^-$ cDCs infiltrating the lungs of the indicated groups of mice. (*E*) Ratios of $CD11b^+$ and $CD103^+$ cDCs as calculated per mouse. (*F* and *G*) Purified wild-type VacA was either administered intraperitoneally (i.p.) or intragastrically (p.o.) as indicated. Mice received either 5 μg or 20 μg of VacA (as indicated), either from age day 7 onwards until 2 wk before challenge (as indicated by subscript "a") or three doses only (delivered in weeks 1, 2, and 3 of life, denoted by subscript "b") or as adults (denoted by subscript "c"). Two doses of IL-10R blocking antibody were administered during challenge where indicated. (*F* and *G*) Total cells and eosinophils contained in 1 mL of BALF. (*H* and *I*) Tissue inflammation and goblet cell metaplasia. Three doses of VacA delivered before weaning were insufficient to provide full protection ("b"). Treatment of adults was almost as protective as neonatal-onset treatment (compare "c" and "a"; note that the total cell count in the adult-treated group is inconsistent with the other three readouts for reasons that are not clear); the 5-μg and 20-μg doses provided similar levels of protection; blocking IL-10 signaling abrogated protection.

1.2 *Helicobacter* urease–induced activation of the TLR2/ NLRP3/IL-18 axis protects against asthma

authors: Katrin N. Koch, Mara L. Hartung, Sabine Urban, Andreas Kyburz, Anna S. Bahlmann, Judith Lind, Steffen Backert, Christian Taube and Anne Müller

Journal: article published in Journal of Clinical Investigation, 2015

contribution: I helped with mouse studies in figure 3 and S7 and contributed with figures S7,D and E.

The Journal of Clinical Investigation BRIEF REPORT

Helicobacter urease–induced activation of the TLR2/NLRP3/IL-18 axis protects against asthma

Katrin N. Koch,[1] Mara L. Hartung,[1] Sabine Urban,[1] Andreas Kyburz,[1] Anna S. Bahlmann,[1] Judith Lind,[2] Steffen Backert,[2] Christian Taube,[3] and Anne Müller[1]

[1]Institute of Molecular Cancer Research, University of Zürich, Zürich, Switzerland. [2]Chair of Microbiology, Friedrich-Alexander University Erlangen-Nürnberg, Erlangen, Germany. [3]Department of Pulmonology, Leiden University Medical Center, Leiden, Netherlands.

Inflammasome activation and caspase-1–dependent (CASP1-dependent) processing and secretion of IL-1β and IL-18 are critical events at the interface of the bacterial pathogen *Helicobacter pylori* with its host. Whereas IL-1β promotes Th1 and Th17 responses and gastric immunopathology, IL-18 is required for Treg differentiation, *H. pylori* persistence, and protection against allergic asthma, which is a hallmark of *H. pylori*–infected mice and humans. Here, we show that inflammasome activation in DCs requires the cytoplasmic sensor NLRP3 as well as induction of TLR2 signaling by *H. pylori*. Screening of an *H. pylori* transposon mutant library revealed that pro–IL-1β expression is induced by LPS from *H. pylori*, while the urease B subunit (UreB) is required for NLRP3 inflammasome licensing. UreB activates the TLR2-dependent expression of NLRP3, which represents a rate-limiting step in NLRP3 inflammasome assembly. *ureB*-deficient *H. pylori* mutants were defective for CASP1 activation in murine bone marrow–derived DCs, splenic DCs, and human blood-derived DCs. Despite colonizing the murine stomach, *ureB* mutants failed to induce IL-1β and IL-18 secretion and to promote Treg responses. Unlike WT *H. pylori*, *ureB* mutants were incapable of conferring protection against allergen-induced asthma in murine models. Together, these results indicate that the TLR2/NLRP3/CASP1/IL-18 axis is critical to *H. pylori*–specific immune regulation.

Introduction

Persistent infection of the gastric mucosa with *H. pylori* causes gastritis (1) and represents a major risk factor for the development of gastric cancer (2) but has also been inversely linked to the risk of allergic and chronic inflammatory diseases (3, 4). The outcome of the *H. pylori*/host interaction is determined both by host and bacterial genetic factors (5) as well as the infected individual's predominant T cell response to *H. pylori*: whereas asymptomatic carriers generate *H. pylori*–specific Tregs, patients with peptic ulcer are characterized by Th1/Th2-biased, pathogenic T effector responses (6). Treg-predominant responses are particularly pronounced in children (7) and can be recapitulated in experimental models of neonatal *H. pylori* infection (8), in which they are required for protection against allergen-induced asthma (9). *H. pylori* activates caspase-1 (CASP1) in infected macrophages and DCs and induces the processing and secretion of the CASP1-dependent cytokines IL-1β and IL-18 by triggering the assembly and activation of an ASC- and NLRP3-containing inflammasome (10–12). CASP1 activation by *H. pylori* has both proinflammatory and anti-inflammatory consequences that are differentially mediated by its cytokine substrates (10). IL-1β exerts proinflammatory effects that promote Th1- and Th17-driven *H. pylori* control and gastric immunopathology (10, 11); in contrast, IL-18 signaling restricts severe gastric immunopathology and contributes to asthma protection by promoting Treg differentiation (10, 13). Here, we show using in vitro and in vivo infection models that NLRP3 inflammasome activation by *H. pylori* requires licensing through TLR2. A saturating transposon (tn) library screen revealed a critical and previously unrecognized role for *H. pylori*'s urease enzyme in promoting the TLR2-dependent transcriptional activation of NLRP3 expression, CASP1 activation, and cytokine processing as well as Treg differentiation and asthma protection.

Results and Discussion

H. pylori activates CASP1 and induces IL-1β secretion by DCs in an ASC-, NLRP3-, and TLR2-dependent manner. Having shown previously that *H. pylori* exposure activates CASP1 and induces the secretion of mature IL-1β and IL-18 in bone marrow–derived DCs (BMDCs) (10), we sought to identify host determinants of inflammasome activation by *H. pylori*. BMDCs from WT, *Nlrc4*$^{-/-}$, *Nlrp6*$^{-/-}$, *Nlrp3*$^{-/-}$, *Aim2*$^{-/-}$, and *Asc*$^{-/-}$ mice, and from mice lacking various TLRs and adaptor molecules, were cocultured with two different strains of *H. pylori* and examined with respect to CASP1 activation and IL-1β secretion. Whereas the inflammasome sensors NLRC4, NLRP6, and AIM2 were dispensable for CASP1 activation and IL-1β secretion, both processes were found to be dependent on the bipartite adaptor protein ASC as well as the cytoplasmic inflammasome sensor NLRP3 (Figure 1, A–D, and Supplemental Figure 1, A–E; supplemental material available online with this article; doi:10.1172/JCI79337DS1). Surprisingly, we found that CASP1 activation and IL-1β secretion, but not the transcriptional activation of IL-1β, required surface-exposed TLR2 (Figure 1, E–G). Other surface and endosomal TLRs known to contribute to innate immune recognition of Gram-negative pathogens, i.e., TLR4, TLR5, and TLR9 or the IL-1 receptor, were not required for IL-1β secretion (Figure 1, E–G, and Supplemental Figure 2, A–I). Similarly, we could not

Conflict of interest: The authors have declared that no conflict of interest exists.
Submitted: October 2, 2014; **Accepted:** June 11, 2015.
Reference information: *J Clin Invest*. 2015;125(8):3297–3302. doi:10.1172/JCI79337.

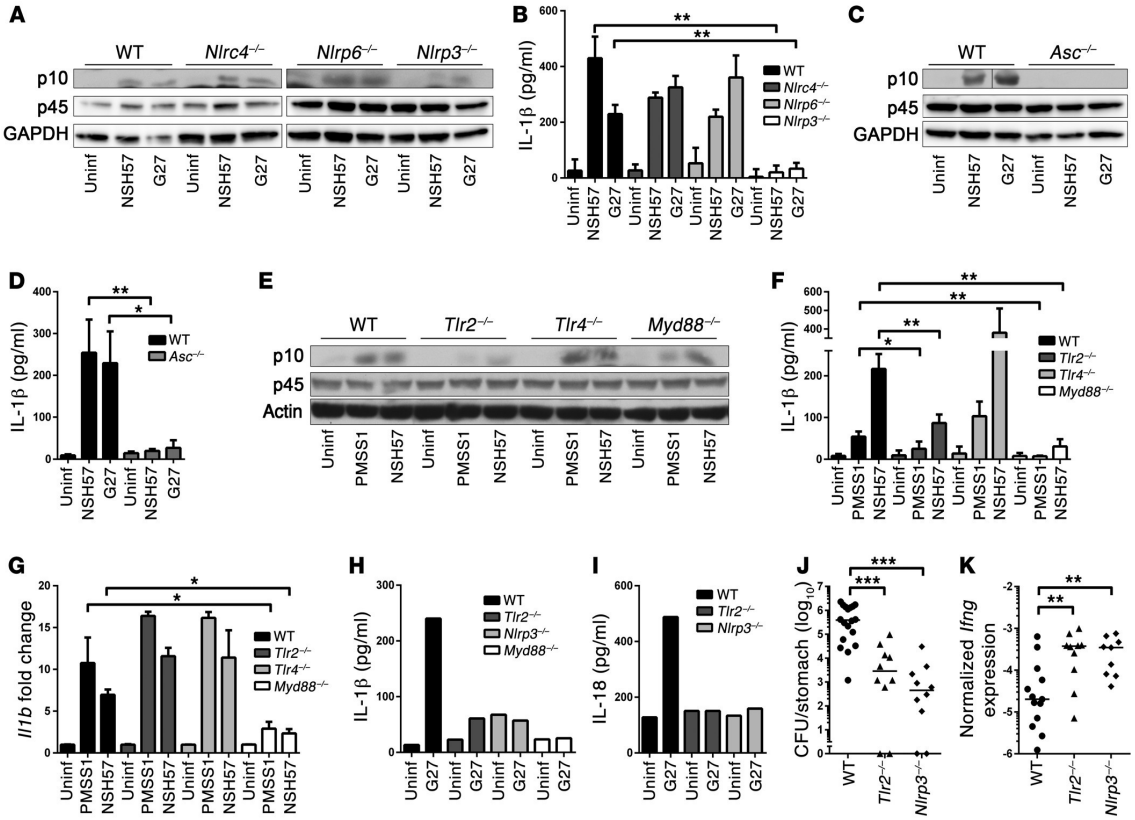

Figure 1. CASP1 activation by *H. pylori* depends on NLRP3, ASC, and TLR2. (**A**–**G**) BMDCs from mice of the indicated genotypes were infected overnight with *H. pylori* NSH57, G27, and/or PMSS1. (**A**, **C**, and **E**) Western blot analysis of CASP1 activation (p10) in the cell supernatant compared to full-length CASP1 p45 and GAPDH in the extract. Representative results of 3 independent experiments are shown (n = 3). (**B**, **D**, and **F**) IL-1β ELISA of culture supernatants; cells were prestimulated with *E. coli* LPS prior to infection. Uninf, uninfected. (**G**) *Il1b* transcription, as measured by qRT-PCR (normalized to *Gapdh* and to uninfected controls). Mean + SD of 3 independent experiments is shown (n = 3). (**H** and **I**) CD11c$^+$ splenic DCs were infected overnight with G27. (**H**) IL-1β and (**I**) IL-18 secretion was measured by ELISA. Representative data of 3 independent experiments are shown (n = 3). (**J** and **K**) Mice were infected for 1 month with PMSS1 prior to the quantification of (**J**) gastric colonization and (**K**) *Ifng* expression. Pooled data from 2 studies are shown (n = 2). Horizontal lines indicate medians. $^*P \le 0.05$, $^{**}P \le 0.01$, $^{***}P \le 0.001$, Mann-Whitney U test. Error bars represent mean + SD.

detect a contribution of the Nod-like receptor NOD2 or of the ATP sensor P2X7R to these processes (Supplemental Figure 2, J–L). Of two known adaptor molecules relaying signals downstream of the TLRs, only MyD88, but not TRIF, was involved in IL-1β expression and secretion (Figure 1, E–G, and Supplemental Figure 2, M and N). A recently identified noncanonical inflammasome activation pathway involving TRIF- and IRF3/7-mediated type I IFN production and signaling (14) was dispensable for *H. pylori*–induced inflammasome activation (Supplemental Figure 2, N–R). The critical role of TLR2, MyD88, and NLRP3 in *H. pylori*–induced IL-1β secretion was confirmed with immunomagnetically isolated CD11c$^+$ splenic DCs (Figure 1H and Supplemental Figure 2S). IL-18 secretion by splenic DCs also required TLR2 and NLRP3 (Figure 1I).

CASP1$^{-/-}$ mice, and mice lacking either IL-18 or its receptor, control *Helicobacter* infections more effectively than WT animals, because they fail to peripherally induce Tregs (10, 13). Experimental infection of *Nlrp3*$^{-/-}$ and *Tlr2*$^{-/-}$ mice with the *H. pylori* isolate PMSS1 recapitulates this phenotype: both strains were colonized at lower levels and exhibited higher gastric mucosal IFN-γ expression (Figure 1, J and K), which correlates well with higher frequencies of IFN-γ–expressing CD4$^+$ T cells in the mesenteric lymph nodes (MLNs) of *Tlr2*$^{-/-}$ mice relative to those in WT mice (Supplemental Figure 2T). The combined results suggest that *H. pylori* activates the inflammasome in a TLR2- and NLRP3-dependent manner and benefits from this process because it promotes *H. pylori* persistence.

Genome-wide screening for factors involved in IL-1β secretion reveals a role for H. pylori LPS and urease. Known activators of the NLRP3 inflammasome include both foreign and endogenous compounds, with the best-understood being urate crystals, asbestos, ATP, and bacterial pore-forming toxins (15). We were able to exclude a role for the *H. pylori* immunomodulator γ-glutamyltranspeptidase GGT and the Cag pathogenicity island in CASP1 activation and IL-1β secretion (Supplemental Figure 3, A and B). To search for *H. pylori* factors involved in inflammasome activation in a genome-wide manner, we took advantage of a previously described tn mutant library (16). As IL-1β secretion by *H. pylori*–

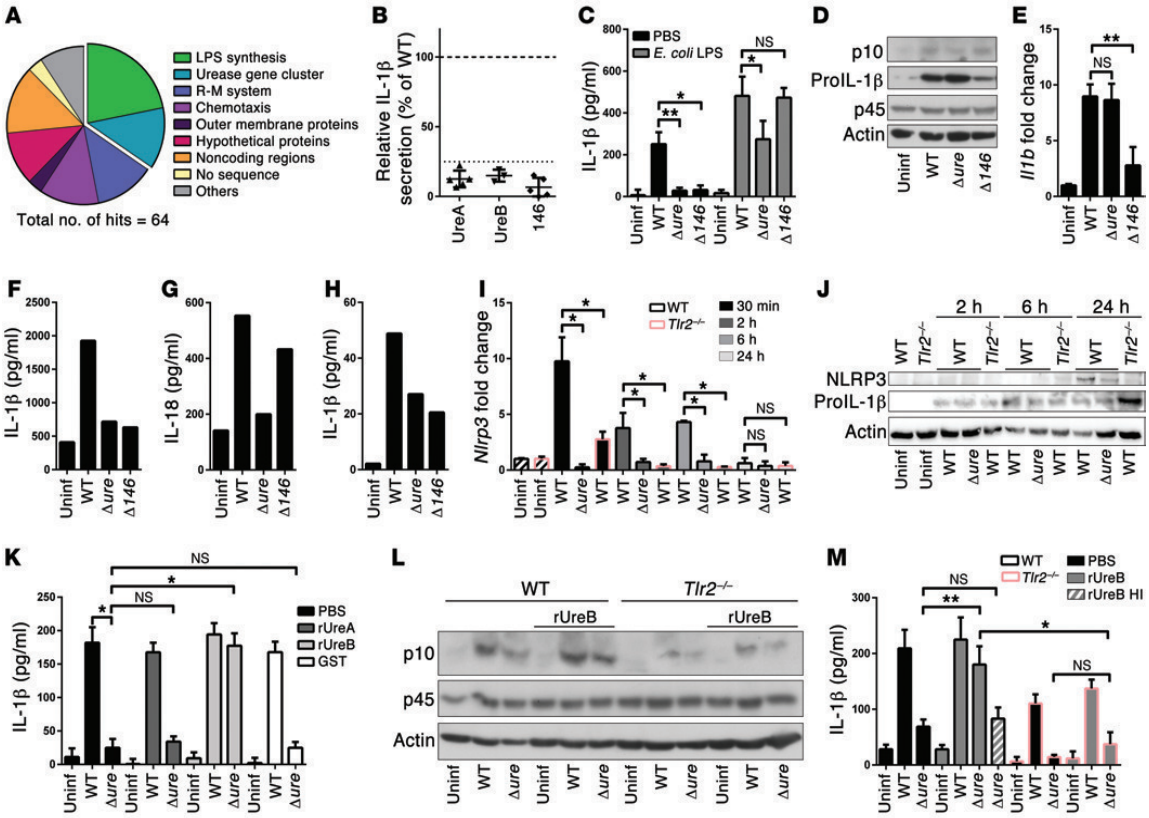

Figure 2. IL-1β secretion upon *H. pylori* infection requires LPS-induced transcriptional activation of pro–IL-1β and urease- and TLR2-dependent expression of NLRP3. (**A**) Genome-wide screening for *H. pylori* tn mutants incapable of IL-1β secretion identifies the indicated mutant categories. R-M, restriction modification. (**B**) Relative IL-1β secretion of individual tn clones with insertions in *ureA*, *ureB*, and HPG27_146. (**C**–**E** and **I**–**M**) Murine BMDCs, (**F** and **G**) splenic CD11c$^+$ DCs, and (**H**) human blood-derived DCs were infected overnight or for the indicated time points with G27 WT, Δ*ure*, or Δ*146* strains of *H. pylori* and analyzed by (**C**, **F**, **H**, **K**, and **M**) IL-1β ELISA; (**G**) IL-18 ELISA; (**D**, **J**, and **L**) CASP1 p10 and p45, pro–IL-1β, and NLRP3 Western blotting; and (**E** and **I**) qRT-PCR (normalized to *Gapdh* and to uninfected controls). BMDCs were prestimulated with *E. coli* LPS where indicated, and 1 μg/ml recombinant GST-tagged UreA, UreB (native or heat-inactivated [HI] for 10 minutes at 70°C), or GST was added to cocultures as noted. Pooled data from 3 to 4 independent experiments are show in **C**, **E**, **I**, **K**, and **M**; a representative of 2 experiments is shown in **F**–**H**. *$P \le 0.05$, **$P \le 0.01$, Mann-Whitney *U* test. Error bars represent mean + SD.

exposed DCs is dependent on CASP1 (10), we opted for IL-1β ELISA as a screening readout (Supplemental Figure 3C). The insertion sites of 64 mutants with defects in inducing IL-1β secretion (<25% of the corresponding WT infection) were sequenced and mapped to 32 different loci (Supplemental Table 1). Loci belonging to two mutant categories were identified repeatedly; these harbored tn insertions in genes involved in LPS biosynthesis and in the urease gene cluster (Figure 2, A and B). The LPS synthesis gene hit most often was LPS-1,2-glycosyltransferase (HPG27_146). LPS from *H. pylori* deficient for this gene lack the O-side chain and therefore Lewis antigens (Supplemental Figure 4A). A gene-specific deletion mutant (Δ*146*) in strain G27 recapitulated the tn mutant phenotype, as it failed to induce IL-1β secretion in BMDCs (Figure 2C). The phenotype of this mutant was attributable to its failure to induce pro–IL-1β expression at the transcriptional level, rather than to a defect in CASP1 activation, and could be rescued by *E. coli* or *H. pylori* LPS (Figure 2, C–E, and Supplemental Figure 4, B and C). IL-1β expression upon stimulation with both types of LPS was MyD88- and TLR4-dependent (Supplemental Figure 4D).

Remarkably, of the 8 tn insertions mapping to the urease gene cluster, all affected 2 genes encoding the structural urease subunits, *ureA* or *ureB* (Supplemental Table 1). A gene-specific deletion mutant lacking both UreA and UreB proteins (G27Δ*ure*, Supplemental Figure 5A) phenocopied the effect of the tn insertion mutants, which could be attributed to its failure to activate CASP1 (Figure 2, C and D). In contrast, *Il1b* transcription was normal (Figure 2E). Coculturing of murine splenic CD11c$^+$ DCs and human blood-derived DCs confirmed the defect of the *H. pylori* Δ*ure* and Δ*146* mutants with respect to IL-1β secretion; in contrast, the secretion of IL-18, which does not require transcriptional activation, was almost at WT levels in the case of the Δ*146* mutant (Figure 2, F–H). In summary, our screen identified *H. pylori* factors regulating CASP1-dependent cytokine secretion at two distinct levels, one transcriptional and one posttranslational.

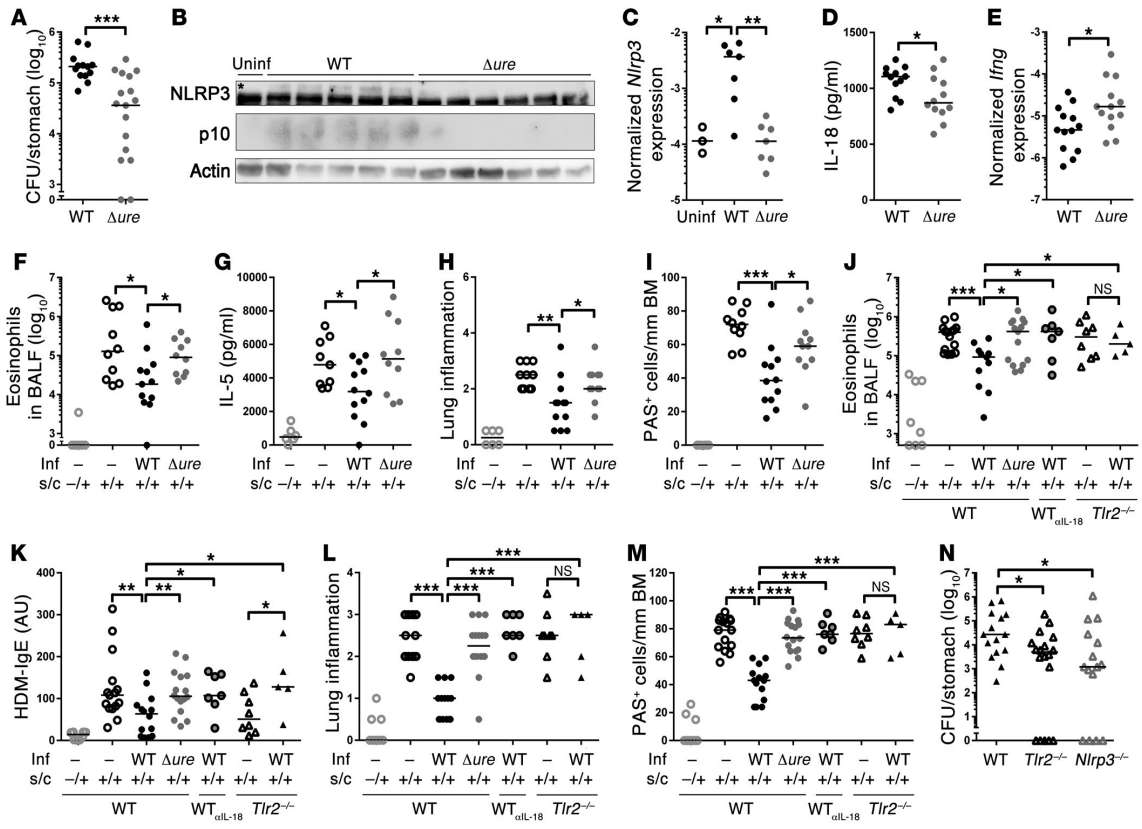

Figure 3. *H. pylori* urease is required for CASP1 activation, persistence, and asthma protection in neonatally infected mice. (**A**–**E**) Neonatal C57BL/6 mice were infected for 1 month with WT or Δ*ure H. pylori* PMSS1 and assessed with respect to (**A**) gastric colonization, (**B**) gastric mucosal NLRP3 and CASP1 (asterisk indicates the NLRP3-specific band), (**C**) *Nlrp3* expression, (**D**) IL-18, and (**E**) *Ifng* expression, as analyzed by (**B**) Western blotting, (**D**) ELISA, and/or (**C** and **E**) qRT-PCR. (**F**–**M**) Neonatally infected mice were additionally sensitized and challenged (s.c.) with (**F**–**I**) ovalbumin or (**J**–**M**) house dust mite (HDM) allergen starting at 4 weeks after infection to induce allergic asthma; αIL-18 mAb was administered weekly starting at the time of infection. Inf, infection. (**F** and **J**) Eosinophils in 1 ml of bronchoalveolar lavage fluid (BALF). (**G**) IL-5 ELISA of ovalbumin-restimulated lung single cell preparations. (**H** and **L**) Lung inflammation, as assessed on H&E-stained sections. (**I** and **M**) Goblet cell metaplasia, as quantified on PAS-stained sections. BM, basement membrane. (**K**) House dust mite–specific serum IgE, as determined by ELISA. (**N**) *H. pylori* colonization of WT, *Tlr2*$^{-/-}$, and *Nlrp3*$^{-/-}$ mice 1 month after infection. Symbols represent individual animals, and horizontal lines indicate the medians. Pooled data from 2 (**A**–**E** and **N**) and 3 (**F**–**M**) independent experiments are shown. **P* ≤ 0.05, ***P* ≤ 0.01, ****P* ≤ 0.001, Mann-Whitney *U* test.

Given the similarities in outcome of TLR2 deficiency of the host on the one hand and urease deficiency of the bacteria on the other (i.e., lack of CASP1 activation), we hypothesized that *H. pylori* urease might provide a TLR2-mediated signal to promote inflammasome/CASP1 activation. As NLRP3 expression can be primed by TLR signaling, we asked whether NLRP3 transcript and protein levels in BMDCs are affected by *H. pylori* exposure. Indeed, WT *H. pylori* infection efficiently induced NLRP3, but not AIM2 or NLRC4, expression at the transcript and protein levels in a TLR2-, MyD88-, and NF-κB–dependent manner; this was not observed in BMDCs infected with Δ*ure H. pylori* (Figure 2, I and J; Supplemental Figure 5, B–H; and data not shown). Interestingly, the defect of the Δ*ure* mutant with respect to CASP1 activation and IL-1β secretion could be rescued by recombinant UreB, but not UreA or the GST tag control; this effect was only seen in WT, but not in *Tlr2*$^{-/-}$, BMDCs (Figure 2, K–M). Heat-inactivated UreB had no effect on the two processes (Figure 2M and data not shown). Taken together, the results suggest that UreB signals via TLR2 to prime NLRP3 expression, which appears to be a rate-limiting step in *H. pylori*–induced inflammasome activation and IL-1β processing. This is particularly interesting because TLR2 has not yet been described to be activated by bacterial (non-lipo-) proteins.

H. pylori urease is required for CASP1 activation, Treg responses, and asthma protection in vivo. To investigate the consequences of LPS and urease deficiency in vivo, Δ*ure* and Δ*146* mutants were generated in the mouse-colonizing strains PMSS1 and/or SS1 and used for experimental infections of adult or neonatal C57BL/6 mice. Whereas Δ*146* failed to colonize under all circumstances (data not shown), the PMSS1Δ*ure* mutant colonized adult infected mice at WT levels for at least 3 months, without evidence of having regained urease expression (Supplemental Figure 6, A and B). In contrast, SS1Δ*ure* consistently failed to colonize (data

not shown), confirming that urease proficiency is required for mouse colonization in certain strain backgrounds (17). Interestingly, PMSS1Δ*ure* induced significantly less gastric production of IL-1β and IL-18 and less active CASP1 than the parental WT strain (Supplemental Figure 6, C–E). In line with the increased gastric IFN-γ expression of *Tlr2*$^{-/-}$ and *Nlrp3*$^{-/-}$ animals (Figure 1K), Δ*ure*-infected mice exhibited higher gastric mucosal IFN-γ expression and more IFN-γ^{+}CD4^{+} cells in the MLNs than infected WT animals (Supplemental Figure 6, F and G). A similar pattern was observed in neonatally infected animals, in which CASP1 activation, NLRP3 expression, and IL-18 secretion were also found to depend on urease proficiency of *H. pylori*; moreover, colonization levels of the Δ*ure* mutant were strongly reduced relative to the WT strain in neonatally infected mice (Figure 3, A–D). As in adult infected mice, the Δ*ure* mutant elicited higher *Ifng* expression (Figure 3E). Interestingly, *H. pylori* urease was further required for the efficient protection against allergen-induced asthma that is a hallmark of neonatally infected mice. All examined parameters of ovalbumin-induced allergic asthma, i.e., bronchoalveolar eosinophilia, lung inflammation, and goblet cell metaplasia as well as pulmonary Th2 cytokine production, were clearly reduced in infected WT animals but not in Δ*ure*-infected animals (Figure 3, F–I, and Supplemental Figure 7A). Similar results were obtained in the house dust mite model of allergic asthma (Figure 3, J–M). Moreover, protection was abrogated by a blocking antibody targeting IL-18 and in *Tlr2*$^{-/-}$ mice (Figure 3, J–M), which, similar to *Nlrp3*$^{-/-}$ mice, had a lower bacterial burden than WT mice (Figure 3N). Protection against ovalbumin-induced asthma could be adoptively transferred via immunomagnetically purified CD25^{+} Tregs from *H. pylori* infected WT donors but not Δ*ure*-infected donors; Tregs from *H. pylori* infected WT *Tlr2*$^{-/-}$ and *Nlrp3*$^{-/-}$ animals also failed to confer protection (Supplemental Figure 7, B and C). The quantification of CD25^{+}FoxP3^{+} Tregs in MLNs further revealed lower Treg frequencies in Δ*ure*-infected mice relative to infected WT mice and *Tlr2*$^{-/-}$ mice relative to WT mice (Supplemental Figure 7, D and E). In summary, the findings described here document a previously unrecognized role of *H. pylori* urease in innate immune recognition and *H. pylori* persistence that presumably is unrelated to its function in acid resistance. Here, we show that UreB promotes the TLR2-dependent expression of NLRP3, a critical component of the inflammasome that is required for CASP1 activation and IL-1β/IL-18 processing (see model in Supplemental Figure 8). Infection with urease gene deletion mutants phenocopies the effects of TLR2 and NLRP3 deficiency. The combined results confirm a critical contribution of the TLR2/NLRP3/CASP1/IL-18 axis to microbially induced immune regulation and introduce the *H. pylori* urease as a novel immunomodulator of this important human pathobiont.

Methods

Animal experimentation. C57BL/6 WT, *Casp1*$^{-/-}$, *Tlr2*$^{-/-}$, *Tlr4*$^{-/-}$, *Tlr5*$^{-/-}$, *Tlr9*$^{-/-}$, *Myd88*$^{-/-}$, *Trif*$^{-/-}$, *Nlrp3*$^{-/-}$, *Ifnar*$^{-/-}$, *Irf7*$^{-/-}$, *Nod2*$^{-/-}$, *P2rx7*$^{-/-}$, and *Aim2*$^{-/-}$ mice were originally obtained from Charles River Laboratories. *Nlrc4*$^{-/-}$ and *Asc*$^{-/-}$ mice were provided by Genentech. *Nlrp6*$^{-/-}$ mice were provided by Millenium Pharmaceuticals. *Il1r*$^{-/-}$ mice were provided by Manfred Kopf. Mice were infected orally with 10^{8} CFU *H. pylori* PMSS1 at 6 weeks or 7 days of age. Bacterial colonization was assessed by colony counting. The procedures used for asthma induction and cytokine quantification by qPCR, ELISA, and FACS are described in the Supplemental Methods.

H. pylori strains, infection of DCs, and tn library screening. *H. pylori* strains and culture conditions as well as the procedures used for the differentiation and immunomagnetic isolation of DCs and for tn library screening are described in the Supplemental Methods, along with protocols for Western blotting and purification of recombinant proteins.

Statistics. GraphPad Prism (GraphPad Software) was used for statistical analyses. All *P* values were calculated by Mann-Whitney *U* test.

Study approval. All animal experimentation was reviewed and approved by the Veterinary Office of the canton of Zurich (Zurich, Switzerland) (licenses 24/2013 and 170/2014 to A. Müller).

Acknowledgments

This study was funded by Swiss National Science Foundation grants 310030-143609 and BSCGIO_157841/1 to A. Müller. Additional funding was obtained from German Research Foundation grants CRC-796 (project B10) and CRC-1181 (project A04) to S. Backert. We thank Nina Salama for the tn library, Raffaela Semper for help with screening, and Ben Appelmelk for valuable advice on *H. pylori* LPS.

Address correspondence to: Anne Müller, Institute of Molecular Cancer Research, University of Zürich, Winterthurerstr. 190, 8057 Zürich, Switzerland. Phone: 41.44.635.3474; E-mail: mueller@imcr.uzh.ch.

1. Marshall BJ, Warren JR. Unidentified curved bacilli in the stomach of patients with gastritis and peptic ulceration. *Lancet*. 1984;1(8390):1311–1315.
2. Parsonnet J, et al. Helicobacter pylori infection and the risk of gastric carcinoma. *N Engl J Med*. 1991;325(16):1127–1131.
3. Chen Y, Blaser MJ. Helicobacter pylori colonization is inversely associated with childhood asthma. *J Infect Dis*. 2008;198(4):553–560.
4. Luther J, Dave M, Higgins PD, Kao JY. Association between Helicobacter pylori infection and inflammatory bowel disease: a meta-analysis and systematic review of the literature. *Inflamm Bowel Dis*. 2010;16(6):1077–1084.
5. Pritchard DM, Crabtree JE. Helicobacter pylori and gastric cancer. *Curr Opin Gastroenterol*. 2006;22(6):620–625.
6. Robinson K, et al. Helicobacter pylori-induced peptic ulcer disease is associated with inadequate regulatory T cell responses. *Gut*. 2008;57(10):1375–1385.
7. Harris PR, et al. Helicobacter pylori gastritis in children is associated with a regulatory T-cell response. *Gastroenterology*. 2008;134(2):491–499.
8. Arnold IC, et al. Tolerance rather than immunity protects from Helicobacter pylori-induced gastric preneoplasia. *Gastroenterology*. 2011;140(1):199–209.
9. Arnold IC, et al. Helicobacter pylori infection prevents allergic asthma in mouse models through the induction of regulatory T cells. *J Clin Invest*. 2011;121(8):3088–3093.
10. Hitzler I, et al. Caspase-1 has both proinflammatory and regulatory properties in helicobacter infections, which are differentially mediated by its substrates IL-1β and IL-18. *J Immunol*. 2012;188(8):3594–3602.
11. Kim DJ, Park JH, Franchi L, Backert S, Nunez G. The Cag pathogenicity island and interaction between TLR2/NOD2 and NLRP3 regulate IL-1beta production in Helicobacter pylori-infected dendritic cells. *Eur J Immunol*. 2013;43(10):2650–2658.
12. Semper RP, et al. Helicobacter pylori-induced IL-1β secretion in innate immune cells is regulated by the NLRP3 inflammasome and requires the cag pathogenicity island. *J Immunol*. 2014;193(7):3566–3576.

13. Oertli M, et al. DC-derived IL-18 drives Treg differentiation, murine Helicobacter pylori-specific immune tolerance, and asthma protection. *J Clin Invest*. 2012;122(3):1082–1096.
14. Rathinam VA, et al. TRIF licenses caspase-11-dependent NLRP3 inflammasome activation by gram-negative bacteria. *Cell*. 2012;150(3):606–619.
15. Broz P, Monack DM. Molecular mechanisms of inflammasome activation during microbial infections. *Immunol Rev*. 2011;243(1):174–190.
16. Salama NR, Shepherd B, Falkow S. Global transposon mutagenesis and essential gene analysis of Helicobacter pylori. *J Bacteriol*. 2004;186(23):7926–7935.
17. Eaton KA, et al. In vivo complementation of ureB restores the ability of Helicobacter pylori to colonize. *Infect Immun*. 2002;70(2):771–778.

Supplemental Figures

Supplemental Figure 1

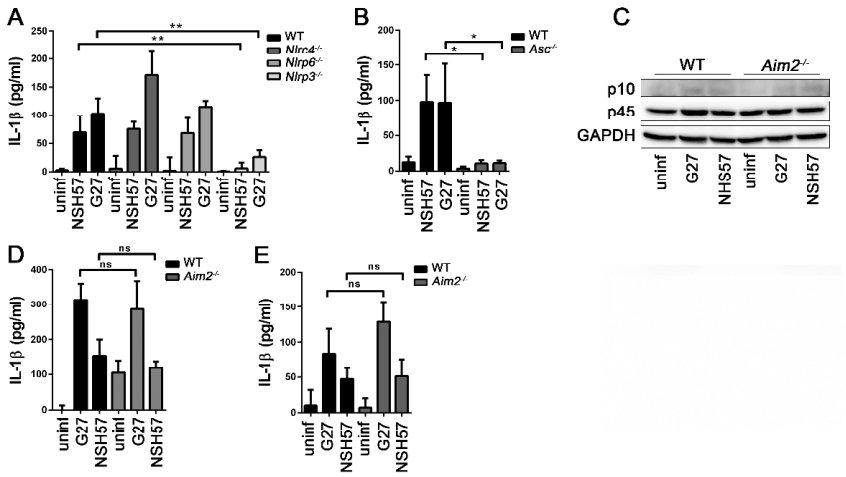

Suppl. Figure 1: IL-1β secretion by *H. pylori*-infected DCs depends on NLRP3 and ASC, but is independent of NLRC4, NLRP6 and AIM2. (**A-E)** BMDCs generated from mice of the indicated genotypes were infected overnight with *H. pylori* NSH57 and G27 at an MOI of 50, with or without prior *E. coli* LPS stimulation. **(A and B)** IL-1β ELISA of samples generated as shown in main Figure panels 1B and 1D, but without prior *E. coli* LPS stimulation. Pooled data of 3 independent experiments are shown (n=3). **(C)** WB analysis of caspase-1 activation (p10) in the cell supernatant compared to full length caspase-1 (p45) and GAPDH in the cell extract. One representative experiment of 3 is shown (n=3). **(D and E)** IL-1β ELISA of samples stimulated with 5ng/ml *E. coli* LPS for 3h prior to infection **(D)** or w/o prestimulation **(E)**. Pooled data of 3 independent experiments (n=3) are shown. Data represent mean ± SD; statistics: Mann-Whitney *U* test.

Supplemental Figure 2

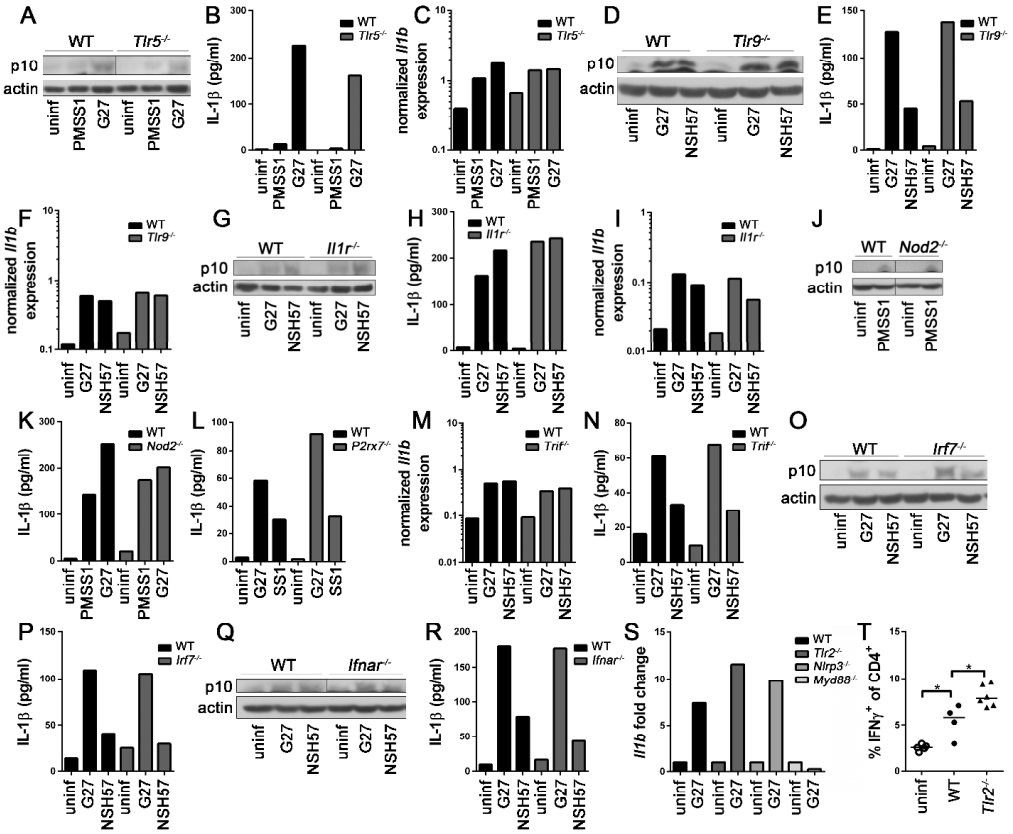

Suppl. Figure 2: Caspase-1 activation and IL-1β secretion by *H. pylori*-infected DCs is independent of TLR5 and TLR9, IL-1R, Nod2, P2X7R and the TRIF-IRF7-IFNaR axis. (**A-R)** BMDCs generated from mice of the indicated genotypes were infected overnight at an MOI of 50 with *H. pylori* NSH57, G27, SS1 and/or PMSS1. **(A, D, G, J, O and Q)** WB analysis of caspase-1 activation (p10) in the cell supernatant compared to actin expression in the cell extract. Lanes in the p10 WB in panels A, J and Q were run on the same gel, but were noncontiguous. **(B, E, H, K, L, N, P and R)** IL-1β secretion was analyzed by IL-1β ELISA of cell supernatants. **(C, F, I and M)** *Il1b* transcription was measured by qRT-PCR (normalized to *Gapdh*). **(S)** *Il1b* transcription in spleen DCs was measured by qRT-PCR and normalized to *Gapdh* and to uninfected controls. **(T)** MLN single cell suspensions derived from individual mice were re-stimulated with PMA/ionomycin and stained for IFNγ and CD4. Representative experiments are shown throughout (A-I, L, O, P and T: n=2); J and K: n=4; M, N, and Q-S: n=3). Each symbol represents one mouse. Horizontal lines indicate the median; statistics: Mann-Whitney *U* test.

Supplemental Figure 3

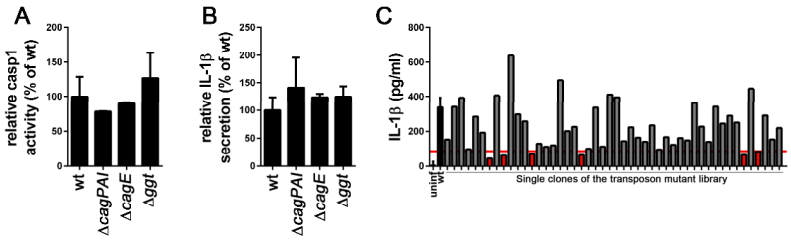

Suppl. Figure 3: IL-1β secretion by *H. pylori*-infected DCs is independent of known *H. pylori* virulence factors. (**A and B**) BMDCs generated from wild type mice were infected overnight with *H. pylori* G27 wild type and the indicated mutants and assessed with respect to caspase-1 activation (by quantification of Western blot signals for the p10 subunit, (**A**)) and IL-1β secretion (by ELISA, (**B**)). At least two and up to four experiment are pooled in A and B. Data represent mean ± SD. (**C**) Representative 96 well plate IL-1β ELISA result of the transposon mutant library screen, where all clones (in red) exhibiting IL-1β expression levels under the 75% reduction cut-off (indicated by the horizontal line) were selected for a second round of analysis.

Supplemental Figure 4

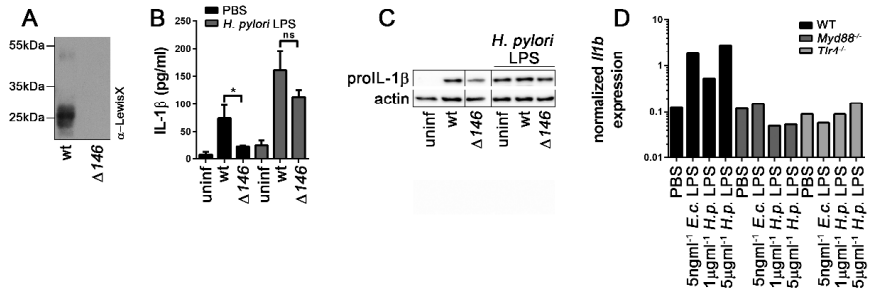

Suppl. Figure 4: *H. pylori* LPS induces the transcription of *Il1b* via TLR4 and MyD88. (A) Western blot of Lewis antigen expression of wild type G27 and the Δ*146* mutant strain. One representative blot of 3 is shown (n=3). **(B)** Wild type BMDCs were infected overnight with *H. pylori* G27 wild type and the Δ*146* mutant in the absence or presence of 1μg/ml purified *H. pylori* LPS, and assessed with respect to IL-1β secretion by ELISA. Pooled data of 3 independent experiments are shown (n=3). Data represent mean ± SD; statistics: Mann-Whitney *U* test. **(C)** BMDCs were treated as described in B and analyzed for proIL-1β expression by Western blotting of cell extract (lanes were run on the same gel, but are not contiguous). One representative experiment of 2 is shown (n=2). **(D)** Wild type, *Myd88*$^{-/-}$ and *Tlr4*$^{-/-}$ BMDCs were treated overnight with either purified *E. coli* or *H. pylori* LPS at the indicated concentrations and assessed with respect to *Il1b* expression by qRT-PCR (samples were normalized to *Gapdh*). One representative experiment of 2 is shown (n=2).

Supplemental Figure 5

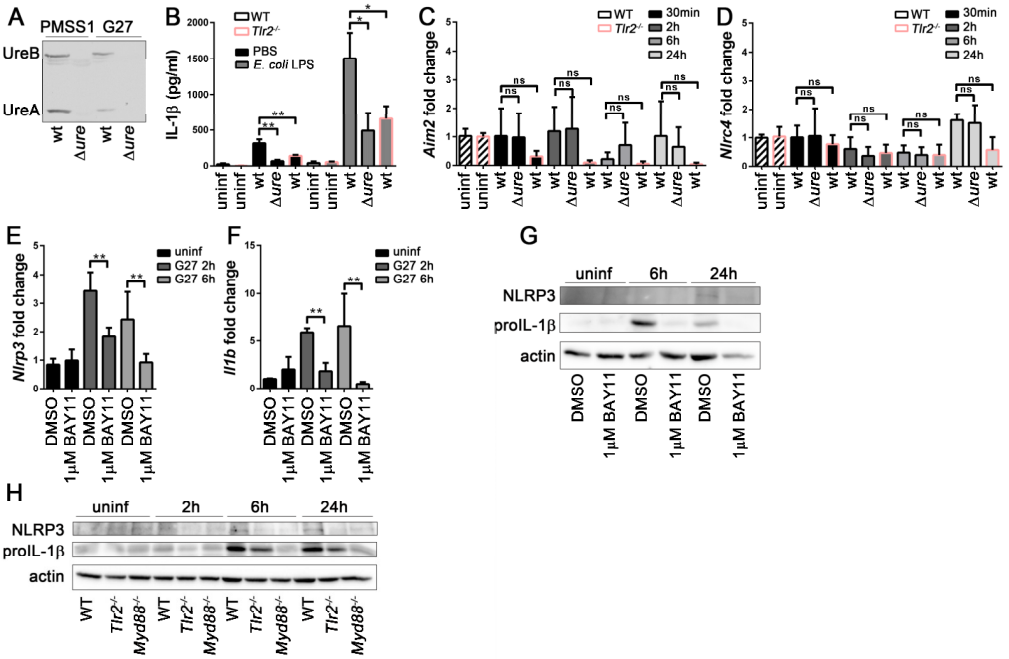

Suppl. Figure 5: Urease-proficient *H. pylori* induces the transcription of *Nlrp3*, but not of *Aim2* and *Nlrc4*, via TLR2, MyD88 and NF-κB. (A) UreA- and UreB-specific Western blot of extracts generated from PMSS1 and G27 wild type and Δ*ure* strains. One representative blot of 3 is shown (n=3). **(B-H)** BMDCs of the indicated genotypes were infected overnight with *H. pylori* G27 wild type and the Δ*ure* mutant as indicated and assessed with respect to IL-1β secretion by ELISA, and proIL-1β, AIM2, NLRC4 and NLRP3 expression by Western blotting and/or qRT-PCR. **(B)** IL-1β ELISA of the 24h-infected samples shown in Figure 2I, along with parallel samples that were additionally pre-stimulated with *E. coli* LPS for 3h. Pooled data of 3 independent experiments are shown (n=3). **(C and D)** qRT-PCR for *Aim2* **(C)** and *Nlrc4* **(D)** of the samples shown in Figure 2I. Pooled data of 4 independent experiments are shown (n=4). **(E-G)** Wild type BMDCs were treated with DMSO or the NF-κB inhibitor BAY11 for 1h prior to infection with wild type G27. Transcription of *Nlrp3* **(E)** and *Il1b* **(F)** was analyzed at the indicated time points using qRT-PCR (normalized to *Gapdh* and to completely untreated, uninfected controls). Pooled data of 3 independent experiments are shown in E and F (n=3). **(G)** NLRP3 and proIL-1β expression as analyzed by Western blotting of cell extracts relative to actin as loading control. One representative experiment of 3 is shown (n=3). **(H)** WT, *Tlr2*$^{-/-}$ and *Myd88*$^{-/-}$ BMDCs were infected for the indicated time points with wild type G27; NLRP3 and proIL-1β expression was analyzed by Western blotting of cell extracts relative to actin as loading control. One representative experiment of 3 is shown (n=3). Data in B-F represent mean ± SD; statistics: Mann-Whitney *U* test.

Supplemental Figure 6

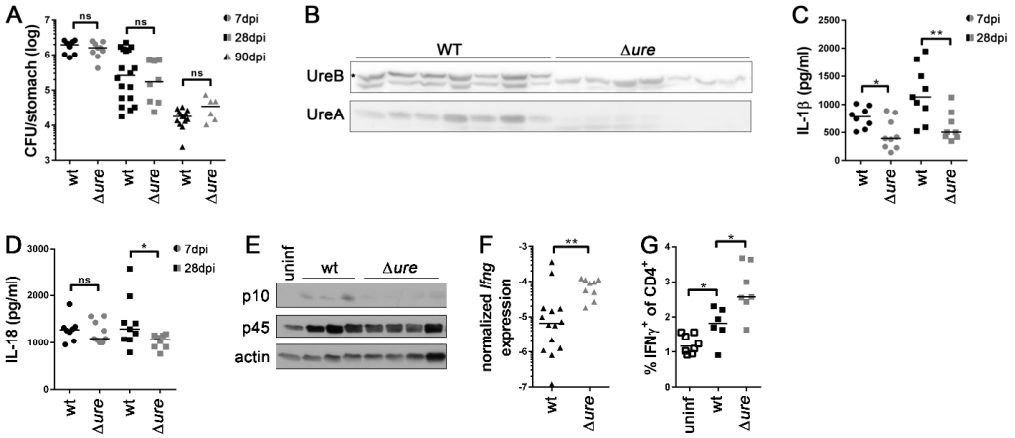

Suppl. Figure 6: *H. pylori* urease is required for inflammasome activation in adult-infected mice. **(A-G)** Mice were infected at 6 weeks of age with *H. pylori* PMSS1 wild type or the Δ*ure* mutant. **(A)** Gastric *H. pylori* colonization at the indicated time points post infection, as determined by plating and colony counting. **(B)** UreA- and UreB-specific Western blot of *H. pylori* re-isolates recovered after 28 days of infection. Each lane represents pooled re-isolates from one animal. **(C and D)** IL-1β **(C)** and IL-18 **(D)** ELISA of gastric mucosal homogenates obtained at the indicated time points post infection. Each symbol represents one animal. **(E)** Western blotting analysis of activated caspase-1 p10, full-length caspase-1 p45 and actin as loading control of gastric mucosal homogenates after 28 days of infection. Each lane represents one animal. **(F)** *Ifng* expression in the gastric mucosa after 90 days of infection, as measured by qRT-PCR and normalized to *Gapdh*. **(G)** MLN single cell suspensions derived from individual mice were re-stimulated with PMA/ionomycin and stained for IFNγ and CD4. Each symbol represents one mouse. Horizontal lines indicate the median; statistics: Mann-Whitney *U* test. Pooled data from 2 independent experiments are shown throughout (n=2); note that for technical reasons not every parameter could be analyzed for each mouse.

Supplemental Figure 7

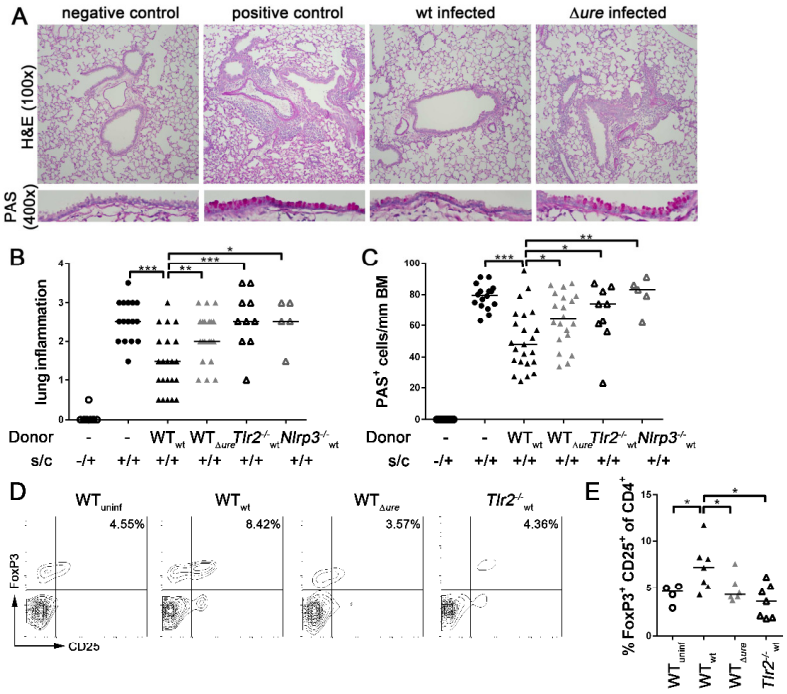

Suppl. Figure 7: TLR2, NLRP3 and *H. pylori* urease are required for the generation of asthma-suppressing Tregs. (A) Representative images of H&E- (upper panel, magnification 100x) and PAS- (lower panel, magnification 400x) stained sections of the lungs described and scored in main Figure 3H and 3I. **(B and C)** Neonatal wild type, *Tlr2*$^{-/-}$ and *Nlrp3*$^{-/-}$ mice were infected with either wild type PMSS1 or its Δ*ure* mutant for 28 days. CD4^{+}CD25^{+} Tregs were immunomagnetically isolated from Peyer's patches and MLNs of these donor mice and adoptively transferred i.v. to ovalbumin-sensitized wild type recipients one day before ovalbumin challenge (s/c, sensitized/challenged). Lung inflammation **(B)** and goblet cell metaplasia **(C)** was quantified on H&E- and PAS-stained tissue sections, respectively (BM, basement membrane). Pooled data of 3 experiments are shown (n=3). **(D and E)** Neonatal wild type and *Tlr2*$^{-/-}$ mice were infected with either wild type PMSS1 or the Δ*ure* mutant for 28 days. MLNs were isolated and stained for CD4, CD25 and FoxP3. Representative FACS plots of the CD4^{+} gate **(D)** are shown along with quantitative data for all animals **(E)**. Horizontal lines indicate the median; statistics: Mann-Whitney *U* test. Data in D and E are representative of 2 independent experiments (n=2).

Supplemental Figure 8

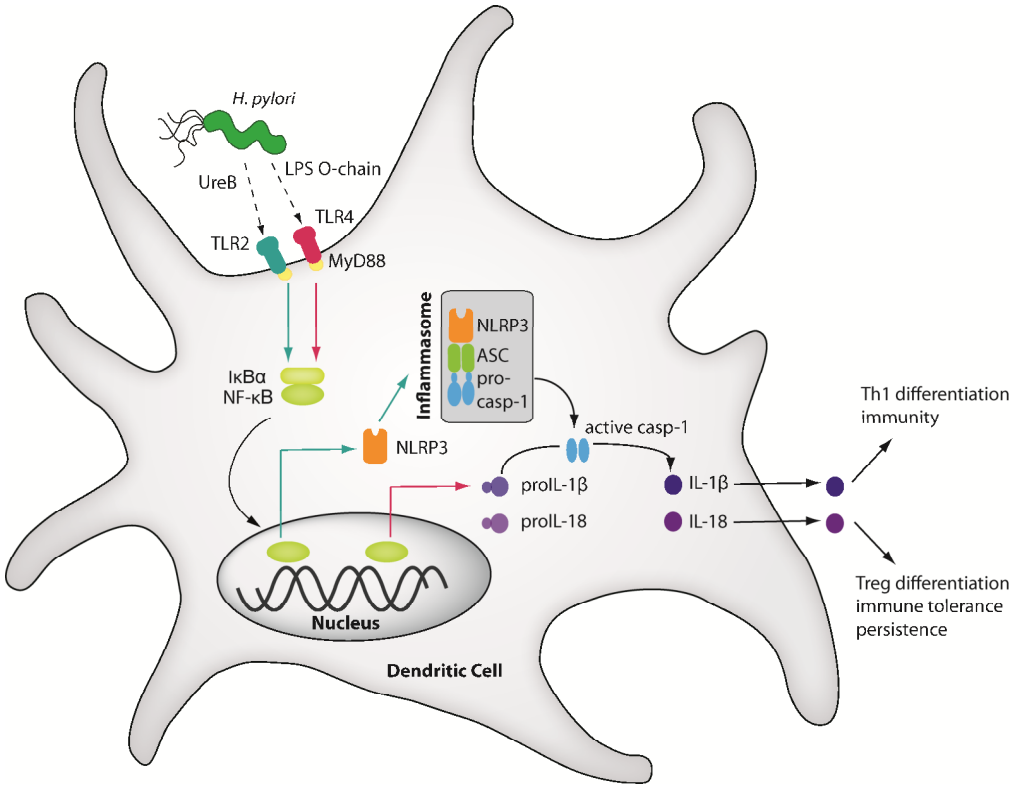

Suppl. Figure 8: Model of *H. pylori*-induced inflammasome activation. *H. pylori* LPS and the urease B subunit (UreB) collaborate to promote NLRP3 inflammasome and caspase-1 activation as well as IL-1β and IL-18 processing and secretion. *H. pylori* LPS signals via TLR4, MyD88 and NF-κB to activate *Il1b* transcription (indicated by red arrows), whereas UreB signals via TLR2, MyD88 and NF-κB to activate *Nlrp3* transcription (green arrows). The assembly of NLRP3, ASC and pro-caspase-1 is triggered through an as yet unknown mechanism leading to caspase-1 activation, and to the processing of proIL-1β and proIL-18. The mature cytokines are released and promote Th1 differentiation and *H. pylori* clearance in the case of IL-1β, and Treg differentiation, immune tolerance and persistence in the case of IL-18. Note that the pro-form of IL-18 is constitutively expressed in DCs. While shown representatively for a dendritic cell, other immune cells and gastric epithelial cells may activate the NLRP3 inflammasome in a similar manner upon exposure to *H. pylori* and may contribute as much or more mature IL-1β and IL-18 to the overall cytokine levels in the infected gastric mucosa.

Supplemental Table 1

gene #	gene name	# of hits
LPS synthesis		
HPG27_38	mannose-6-phosphate isomerase	3
HPG27_39	GDP-D-mannosedehydratase	4
HPG27_104	L-fuculose 1-phosphate aldolase	1
HPG27_146	lipopolysaccharide1,2-glycosyltransferase	5
HPG27_437	DD-heptosyl transferase	1
Urease gene cluster		
HPG27_67	ureaseB	3
HPG27_68	ureaseA	5
Restriction-modification system		
HPG27_436	type II methyltransferase	1
HPG27_746	putative type I R-M enzyme	1
HPG27_806	type I restriction enzyme M protein	1
HPG27_945	phage/colicin/tellurite resistance cluster Y protein	1
HPG27_1316	type III restriction enzyme R protein	1
HPG27_1328	putative type III restriction enzyme R	2
HPG27_1444	type III R-M system modification enzyme	1
Chemotaxis		
HPG27_95	methyl-accepting chemotaxis protein	8
Outer membrane proteins		
HPG27_739	outer membrane protein	1
HPG27_1501	putative outer membrane lipoprotein	1
Hypothetical proteins		
HPG27_773	hypothetical protein	1
HPG27_936	hypothetical protein	1
HPG27_1131	hypothetical protein	1
HPG27_1133	hypothetical protein	1
HPG27_1275	hypothetical protein	1
HPG27_1282	hypothetical protein	1
HPG27_1358	hypothetical protein	1
Others		
HPG27_487	cag pathogenicity island protein X	1
HPG27_603	putative 3-hydroxy acid dehydrogenase	1
HPG27_772	flagellar rotor protein	1
HPG27_1129	alpha carbonic anhydrase	1
HPG27_1138	aldo-keto reductase	1
	plasmid	1
	Different non coding regions	9
	No sequences due to growth deficit	2

Supplemental methods

H. pylori *strains, infection of DCs and transposon library screening*

The following *H. pylori* strains were used for *in vitro* infection of BMDCs. Strains G27, SS1 and PMSS1 have been described previously (1-3). NSH57 is a mouse-adapted derivative of strain G27 that was generated by three 3-week passages in FVB mice (4). To create the transposon library used here (generously donated by Nina R. Salama, Division of Human Biology, Fred Hutchinson Cancer Research Center, Seattle, USA), genomic DNA prepared from the original 10,000-clone G27 library (5) was transformed into NSH57 by natural transformation (4). For the analysis of individual clones with respect to their induction of IL-1β secretion by BMDCs, bacteria were cultured from frozen stocks on horse blood agar supplemented with 25 μg/ml of chloramphenicol at 37°C for 2 days under microaerophilic conditions. Colonies were picked and expanded individually o/n on fresh horse blood plates prior to inoculation of 100μl liquid cultures (Brucella broth (Difco) containing 10% FBS (Life Technologies)) in 96 well format. Liquid cultures were grown for 6h with shaking at 37°C and used for BMDC infection in 96 well flat bottom plates and for cryopreservation of individual clones. The supernatants of infected BMDCs were subjected to IL-1β ELISA after 16h of co-culture. For sequencing of the transposon flanking regions, the following primer was used: 5'-CAG TTC CCA ACT ATT TTG TCC-3'. The screen was saturated after examination of ~2500 mutants. All *H. pylori* liquid cultures were routinely assessed by light microscopy for contamination, morphology, and motility prior to use in infections.

Generation and infection of BMDC, spleen DCs and human blood-derived DCs

For the generation of BMDCs, single cell suspensions were prepared from hind leg bone marrow and seeded at 10^5 cells per well in 96 well plates for ELISA or at $2x10^6$ cells per well in 6 well plates for Western blotting in RPMI/10% FCS and 4ng/ml GM-CSF and cultured for 6 days. BMDCs were infected for 16h with *H. pylori* at a multiplicity of infection of ~50. BMDCs were pretreated for 3h with 5ng/ml LPS (Sigma Aldrich) to stimulate *Il1b* expression where indicated. BAY11-7082 (Sigma Aldrich) was added at 1μM final concentration 1h prior to infection of BMDCs to inhibit NF-κB signaling. For the isolation of splenic DCs, spleen cell suspensions were prepared by digestion using 1mg/ml CollagenaseD and 0.1% DNaseI (both from Roche) in serum-free RPMI for 1h at 37°C. DCs were immunomagnetically isolated using CD11c MicroBeads (Miltenyi Biotec) according to the manufacturer's instructions and seeded at $2x10^5$ cells per well in 96 well round bottom plates. For the generation of human DCs, peripheral blood mononuclear cells (PBMC) were isolated from buffy coats of healthy volunteer blood donors obtained from the blood donation center Zürich (ZHBSD) using Ficoll-Paque™ (GE Healthcare). $CD14^+$ monocytes were isolated from PBMCs using CD14 MicroBeads (Miltenyi Biotec) according to the manufacturer's instructions and cultured in CellGro DC medium (Cellgenix) supplemented with 1000U/ml GM-CSF and 500IU/ml IL-4 (both R&D Systems) for 6 days.

Induction and quantification of allergic asthma

Ovalbumin model: Mice were sensitized by i.p. injection of 20μg ovalbumin (Sigma-Aldrich) emulsified in 2.25mg aluminum hydroxide (Alum Imject; Pierce) at 6 and 8 weeks of age. Sensitized mice were challenged with 1% aerosolized ovalbumin using an ultrasonic nebulizer (NE-U17; Omron) for 20 min daily on days 31, 32 and 33 post initial sensitization. For Treg transfer experiments, neonatally infected donor mice were sacrificed at the age of 5 weeks and Tregs were immunomagnetically isolated from MLN and Peyer's Patches single cell suspensions ($CD4^+CD25^+$ mouse regulatory T cell isolation kit; R&D). $1x10^6$ Tregs were injected per animal into sensitized wild type recipient mice one day before the first allergen challenge. House dust mite (HDM) model: Mice were sensitized by intranasal administration of 1µg HDM (Greer) at 6 weeks of age. Mice were challenged with 10µg HDM per animal on five consecutive days, starting on day 8 after sensitization. Anti-IL-18 antibody (YIGIF74-1G7, BioXCell) was applied weekly (50µg per dose) starting at 7 days of age. After sacrifice, lungs were lavaged via the trachea with 1ml PBS. Bronchoalveolar lavage fluid (BALF) cells were counted using trypan blue dye exclusion. Differential eosinophil counts were performed on cytocentrifuged preparations stained with the Microscopy Hemacolor Set (Merck). Lungs were fixed by inflation and immersion in 10% formalin and embedded in paraffin. Tissue sections were stained with H&E and periodic acid-Schiff and examined in blinded fashion on a BX40 Olympus microscope. Peribronchial inflammation was scored on a scale from 0 to 4. PAS-positive goblet cells were quantified per 1mm of basement membrane. For lung re-stimulation, single cell suspensions were prepared by collagenase 1A (Sigma Aldrich) digestion for 45min at 37°C. Cells were seeded at $5x10^5$ cells per well and stimulated with 250µg/ml ovalbumin for 3 days. Supernatants were analyzed for secretion of IL-5 by ELISA (eBioscience) according to the manufacturer's instructions. For detection of HDM-specific IgE, plates were coated with 25µg/ml HDM antigen; HDM-bound IgE was detected using α-mouse IgE-HRP (GTX77227, GeneTex).

Western Blotting and ELISA of cell culture supernatants and extracts, and of gastric mucosal homogenates

To detect proteins in cell culture supernatants, 500µl of supernatants were TCA-precipitated and subjected to Western blotting. Cell extracts and extracts of scraped and shock frozen murine gastric mucosa were prepared using RIPA-Buffer supplemented with protease inhibitors (complete Mini, Roche). For lysis of bacteria, 200µg/ml lysozyme (Sigma Aldrich) was added to the lysis buffer. For Lewis antigen detection, bacterial lysates were treated with 125ng/ml Proteinase K (Macherey-Nagel) o/n. The following antibodies were used: α-Casp1 p10/p45 (sc514, Santa Cruz), α-NLRP3 (ab91525, abcam), α-IL-1β (AF-401-NA, R&D Systems), α-actin (sc1616, Santa Cruz), α-GAPDH (G9545, Sigma Aldrich), α-*H. pylori* Urease (ab51954, abcam), α-LewisX (ab3358, abcam). Cytokines in gastric mucosal extracts and the supernatants of infected BMDCs or splenic DCs were analyzed by ELISA (human IL-

1β and mouse IL-1β, both BD Biosciences; IL-18, eBioscience) according to the manufacturers' instructions.

Real time qRT-PCR of cytokines in cell extracts and gastric mucosal homogenates
For real-time RT-PCR of shock frozen stomach mucosa or BMDC cell pellets, total RNA was isolated using NucleoSpin RNA II kits (Macherey-Nagel). For isolation of RNA from splenic DCs, the RNeasy microkit (Qiagen) was used. RNA was reversely transcribed into cDNA using superscript III (Invitrogen). The corresponding cDNA served as a template for real-time PCR performed using the LightCycler 480 SYBR Green I master kit (Roche). Samples were normalized to GAPDH expression (conditions: Tm 60°C, 50 cycles; primers: GAPDH fw: 5'-GAC ATT GTT GCC ATC AAC GAC C-3' / GAPDH rv: 5'-CCC GTT GAT GAC CAG CTT CC-3', pro-IL-1β fw: 5'-TTG ACG GAC CCC AAA AGA TG-3' / pro-IL-1β rv: 5'-TGG ACA GCC CAG GTC AAA-3', NLRP3 fw: 5'-CCC TTG GAG ACA CAG GAC TC-3' / NLRP3 rv: 5'-GGT GAG GCT GCA GTT GTC TA-3', IFNγ fw: 5'-ATC TGG AGG AAC TGG CAA AA-3' / IFNγ rv: 5'-TTC AAG ACT TCA AAG AGT CTG AGG TA-3', AIM2 fw: 5'-CAG GCA ATT GCA TCT GAG AG-3' / AIM2 rv: 5'-CGC CTC ACA AAG ATT TTC ACT-3', NLRC4 fw: 5'-GAA GAA TCC TGT GAT CTC CAA GAG-3' / NLRC4 rv: 5'-GAT CAA ATT GTG AAG ATT CTG TGC-3').

Single cell preparations of MLN and Peyer's patches and FACS staining
Single cell suspensions of MLNs and Peyer's patches were prepared by collagenaseIV (Sigma Aldrich) digestion for 25min at 37°C. For detection of intracellular cytokines, cells were seeded at $2x10^5$ cells per well and treated with 100nM PMA (Sigma Aldrich), 1μg/ml Ionomycin (Sigma Aldrich) and 2μg/ml Monensin (Enzo LifeScience) for 4h. Fixation and permeabilization was performed with the Cytofix/Cytoperm™ Kit (BD Bioscience). The following antibodies were used for staining: CD4-FITC (RM4-5, Biolegend), CD25-Biotin (MAGM208, PartNo 860126, R&D), Streptavidin-eFluor450 (48-4317-82, eBioscience), IFNγ-PECy7 (XMG1.2, BD Biosciences), IL-17-APC (TC11-18H10.1, Biolegend) and FoxP3-APC (FJK-16s, eBioscience).

Cloning, expression and purification of recombinant proteins
UreaseA and UreaseB gene were amplified from bacterial genomic DNA using pfu-DNA polymerase (ThermoScientific) with the following primers: UreA fw: 5'-ATA TGA ATT CTT AAT TCT CCT TAA TTG TTT TT-3', UreA rv: 5'- ATA TGG ATC CAA ACT CAC CCC AAA AGA-3', UreB fw: 5'- ATA TGT CGA CCG AAC ACA TGG TAA GTT T-3', UreB rv: 5'- ATA TGA ATT CAA AAA GAT TAG CAG AAA AGA-3'. Amplified fragments were inserted into the pGEX-4T-1 plasmid (GE Healthcare) using BamHI and EcoRI restriction sites for UreaseA and SalI and EcoRI restriction sites for UreaseB (all restriction enzymes obtained from New England Biolabs). After amplification and sequencing

of the resulting plasmids, positive clones were transformed into *E. coli* BL21. Induction of overexpression of the GST-tagged proteins was done by the addition of 1mM IPTG. Bacterial cells were homogenized by sonication and precleared lysates were applied to GST GraviTrap columns (GE Healthcare). Tagged proteins were isolated according to manufacturer's instructions.

Supplemental references

1. Arnold, I.C., Lee, J.Y., Amieva, M.R., Roers, A., Flavell, R.A., Sparwasser, T., and Müller, A. 2011. Tolerance rather than immunity protects from Helicobacter pylori-induced gastric preneoplasia. *Gastroenterology* 140:199-209.
2. Covacci, A., Censini, S., Bugnoli, M., Petracca, R., Burroni, D., Macchia, G., Massone, A., Papini, E., Xiang, Z., Figura, N., et al. 1993. Molecular characterization of the 128-kDa immunodominant antigen of Helicobacter pylori associated with cytotoxicity and duodenal ulcer. *Proc Natl Acad Sci U S A* 90:5791-5795.
3. Lee, A., O'Rourke, J., De Ungria, M.C., Robertson, B., Daskalopoulos, G., and Dixon, M.F. 1997. A standardized mouse model of Helicobacter pylori infection: introducing the Sydney strain. *Gastroenterology* 112:1386-1397.
4. Baldwin, D.N., Shepherd, B., Kraemer, P., Hall, M.K., Sycuro, L.K., Pinto-Santini, D.M., and Salama, N.R. 2007. Identification of Helicobacter pylori genes that contribute to stomach colonization. *Infect Immun* 75:1005-1016.
5. Salama, N.R., Shepherd, B., and Falkow, S. 2004. Global transposon mutagenesis and essential gene analysis of Helicobacter pylori. *J Bacteriol* 186:7926-7935.

2. MANUSCRIPT

2.1 NLRP3 controls CD11b$^+$ dendritic cell differentiation at steady state and during bacterial infection

authors: Isabelle C.Arnold, Sabine Urban, Xiaozhou Zhang, Mariela Artola, Markus G. Manz, Karen Ottemann and Anne Müller

contribution: I helped with mouse studies and contributed figure 2C-F, 5B-D and F-H and contributed to figure 7

NLRP3 controls CD11b$^+$ dendritic cell differentiation at steady state and during bacterial infection

Isabelle C. Arnold,[1,*] Sabine Urban,[1] Xiaozhou Zhang,[1] Mariela Artola,[1] Markus G. Manz,[2] Karen Ottemann[3] and Anne Müller[1,*]

[1]Institute of Molecular Cancer Research and [2]Department of Hematology, University of Zürich, 8057 Zürich, Switzerland; [3]Department of Microbiology and Environmental Toxicology, Univ. of Calif. at Santa Cruz, Santa Cruz, California, USA

*For correspondence: Anne Müller, Institute of Molecular Cancer Research, University of Zürich, Winterthurerstr. 190, 8057 Zürich, Switzerland; email: mueller@imcr.uzh.ch; phone: +41 44 635 3474; fax: +41 44 635 3484

Financial disclosures: The authors have declared that no conflict of interest exists.

Words: Abstract, 185; Text, ~9300.

Abstract

The immune compartment of the gastric lamina propria is largely uncharted territory. Here, we describe the evolution and composition of the gastric, small intestinal and colonic lamina propria mononuclear phagocyte compartment during steady state and infection with the gastric pathogen *Helicobacter pylori*. We show that monocytes, CX_3CR1^{hi} macrophages and $CD11b^+$ dendritic cells are recruited to the infected stomach in a CCR2-dependent manner. All three populations, but not BATF3-dependent DCs, sample RFP^+ *H. pylori* and upregulate TLR2 upon encountering live bacteria. The differentiation of $CD11b^+$ dendritic cells in all gastrointestinal tissues requires cell-intrinsic NLRP3 expression during infection and steady state. $CD11b^+$ dendritic cells have regulatory activity in the context of *H. pylori* infection and produce IL-10 upon contact with bacteria. BATF3-dependent $CD103^+$ DC lineages on the other hand -despite their lack of direct bacterial contact- are strictly required for local Th1 cell expansion and *H. pylori* control. Humanized mice reconstituted with human hematopoietic stem cells recapitulate several features of the myeloid cell/*H. pylori* interaction. Our results reveal a clear division of labor among gastric phagocyte subsets and highlight the contribution of NLRP3 to $CD11b^+$ DC differentiation.

Key words: dendritic cells, sampling and antigen processing, inflammasome activation, innate immune receptors, immune regulation, humanized mice

Introduction

Mononuclear phagocytes (MPs) residing in the lamina propria (LP) of the gastrointestinal (GI) tract contribute critically to the control of invading pathogens and the development of immunity, as well as the induction and maintenance of immune tolerance. Specialized subsets of MPs perform distinct and complementary functions in immunity and gastrointestinal homeostasis; the MP composition differs in the lower and upper GI compartments, and in the steady state and during inflammation (1-3). Whereas the MP subsets of the small intestine and colon have been studied in detail in terms of their ontogeny, expression of surface markers and lineage-defining transcription factors, and their functional specialization, little is known about MPs residing in the gastric lamina propria. In the intestines, MPs are broadly identified as either resident (non-migratory) macrophages that are replenished from blood-derived Ly6C^{hi} monocytes and detect, engulf and neutralize pathogens and thus exert important innate effector functions, or as dendritic cells (DCs) that originate from a pre-DC-progenitor, require FLT3L for their development, migrate from mucosal tissues to draining lymph nodes via the lymph, and possess the unique ability to prime the differentiation and polarization of effector from naïve T-cells (1, 2). Intestinal LP macrophages exhibit high surface expression of the chemokine CX_3C receptor (CX_3CR) 1, as well as of F4/80 and CD64, but lack CD103. Intestinal DCs can be divided into at least two distinct lineages depending on their surface marker expression and dependence on transcription and growth factors. CD103$^+$ DCs that additionally express CD11b depend on granulocyte macrophage colony-stimulating factor (GM-CSF) (4), as well as the transcription factors Notch-2 (5) and IRF4 (6) for development. CD103$^+$CD11b$^-$ DCs in contrast require the basic leucine zipper transcription factor ATF-like (BATF)3 and IRF8 (7). Both LP dendritic cell subsets have lymph node counterparts in the form of CD11b$^+$ and CD8α^+ DCs that share the reliance on IRF4/Notch-2 and IRF8/BATF3, respectively. Functionally, IRF8/BATF3-dependent populations are endowed with superior ability to cross-present viral, tumor, and self-antigens and have a human functional equivalent in the CD141^{hi} DC subset (8), whereas IRF4/Notch-2-dependent DCs (likely human

equivalent: $CD1c^+$ DCs) have been implicated in Th17 priming (5, 6). An additional DC subset of the GI LP that is less well understood in terms of its ontogeny expresses CD11b, but neither CD103 nor macrophage markers, and intermediate levels of CX_3CR1; this population is responsive to Flt3L *in vivo* but its progenitor is controversial (9-11).

We have reported previously that *Helicobacter pylori*, a pathobiont that colonizes the human gastric mucosa of half of the world's population and is tightly associated with gastric disorders such as ulcers, chronic gastritis and gastric cancer (12), has a major impact on the functionality of dendritic cells (13-15). *H. pylori* causes a persistent, mucosa-associated but non-invasive infection that is characterized by either Treg- or Th1/Th17-predominant responses: in children and neonatally infected mice, the *H. pylori*/host interaction is generally asymptomatic and characterized by the lack of effector T-cell responses, predominance of Tregs and high level colonization (16, 17). In contrast, infected adults (especially those presenting with *H. pylori*-associated peptic ulcers), and mice infected as adults, exhibit a striking T-cell infiltrate that is dominated by effector T-cells and limits the bacterial burden without clearing *H. pylori* completely (16, 17). Rather, the large quantities of IFN-γ produced by *H. pylori*-specific Th1 cells are believed to be the direct cause of the pre-malignant lesions -i.e. epithelial hyperplasia and intestinal metaplasia- that precede the development of gastric cancer (16). The benign interaction of *H. pylori* with its host that is characteristic of pediatric populations has been linked to protective effects against allergic asthma, other forms of allergy, and against inflammatory bowel diseases in large epidemiological studies conducted in multiple areas of the world (18-20). We confirmed a protective effect of *H. pylori* in experimental models of allergic asthma induced by ovalbumin (21) and house dust mite extract (15), and in models of DSS-induced colitis (22). The protection against allergy was functionally linked to *H. pylori*-induced Tregs and further required the TLR2/NLRP3/caspase-1/IL-18 axis, as mice lacking any one of these factors fail to develop *H. pylori*-induced immune tolerance (13, 15, 22).

Here, we have conducted a detailed comparative analysis of the gastric (and small intestinal and colonic) MP populations in the steady state and during *H. pylori* infection in the stomach to dissect which subsets encounter and sample *H. pylori*, and are required for immunity on the one hand or homeostasis in the face of infection on the other. We find that gastric MP populations evolve continuously in the first weeks of life and bear more similarities to the colon than to the small intestine. Various MP subsets are recruited to the infected mucosa in a CCL2/CCR2-dependent manner, but only monocytes, $CX_3CR1^{dim}CD11b^+$ DCs and CX_3CR1^{hi} macrophages encounter RFP^+ *H. pylori*. The same cells upregulate TLR2 and NLRP3 upon contact with *H. pylori*. NLRP3 and TLR2 are required for the terminal differentiation and functionality, respectively, of $CD11b^+$ DCs during *H. pylori* infection and in the steady state. Strikingly, BATF3-dependent $CD103^+$ DCs, although never in direct contact with live bacteria, drive local Th1 responses and are required for *H. pylori* control. Our results provide evidence for a division of labor among DC subsets in an as yet poorly understood compartment of the GI tract, and highlight for the first time a critical contribution of NLRP3 to DC differentiation in GI tissues.

Results

The gastric lamina propria is dominated by myeloid populations that evolve and stabilize in the first weeks of life

Whereas the MP compartment of the colon and small intestine is well characterized in the steady state and in various pathological conditions, little is known about MP populations of the murine gastric LP, their evolution from early life to adulthood, and their functional specialization during homeostasis and bacterial infection. To address these questions, we performed a detailed parallel analysis of the gastric, small intestinal and colonic LP compartment by multicolor flow cytometry (suppl. Figure 1A). Although the overall leukocyte population was much smaller in the stomach than in the small and large intestine (suppl. Figure 1B), the frequency of myeloid cells, as defined by their expression of CD11b with or without co-expression of MHCII, was substantially higher: whereas >50% of gastric LP leukocytes are of myeloid origin, this figure is as low as 10-20% in the intestines (Figure 1A,B). Interestingly, the MP compartment of neonatal mice (analyzed at day 7 of age) differs strongly from that of adults (age 8 weeks) in all three organs and appears to be more homogeneous across organs in newborns (Figure 1B). A more detailed inspection revealed highly divergent patterns of myeloid evolution in the three organs during the first two months of life (Figure 1C-F, suppl. Figure 1C). Several interesting parallels were observed between the colon and stomach that were not shared by the SI: in particular, macrophage and $CD103^+$ $CD11b^+$ DC populations increase steadily in the first weeks of life, and contract again at or just after weaning (Figure 1C). In contrast to the adult SI, where $CD103^+$ $CD11b^+$ DCs represent the numerically dominant MP population by far, the population is relatively minor in both the adult stomach and colon in the steady state (Figure 1C,D). The stomach and colon further are populated in neonates by large numbers of MHCII-negative macrophages, $CD11b^+$ DCs and $CD103^+$ DCs that disappear within the first two weeks of life and thereafter are replaced by MHCII-positive monocytes and macrophages (Figure 1C-F, suppl. Figure 1C). In summary, the gastric LP is a predominantly myeloid organ and devoid of lymphocytes in the steady state;

the observed patterns of myeloid evolution indicate that adult-predominant myeloid lineages replace neonatal DC and macrophage lineages at approximately the time of weaning.

Experimental infection with *Helicobacter pylori* triggers the CCL2/CCR2-dependent gastric recruitment of various DC and macrophage subsets that is required for T-cell-mediated infection control

To examine how a challenge infection with the common gastric pathobiont, *Helicobacter pylori*, would affect the gastric LP compartment, we infected 6 week old mice with a mouse-colonizing human isolate of *H. pylori* and quantified the myeloid and lymphoid populations at one and three months post infection. Exposure to *H. pylori* triggered a robust influx into the gastric LP of neutrophils and $CD4^+$ T-cells; these populations were numerically dominant and increased progressively over time (Figure 2A). $CD103^+$ DCs, $CD103^+CD11b^+$ DCs, $CD11b^+$ DCs, macrophages and monocytes were recruited as well, but reached a plateau already after 1 month post infection (Figure 2B). The recruitment of $MHCII^+$ and $MHCII^-$ monocytes, and of macrophages and DC lineages to the chronically infected stomach depended strongly on the CCL2/CCR2 chemokine/receptor axis, as CCR2-deficient animals exhibited a clear defect in the recruitment of all MP lineages (Figure 2C) that was also reflected in the overall leukocyte counts at three months p.i. (Figure 2D); in contrast, the recruitment of neutrophils and $CD4^+$ T-cells was unaffected by CCR2 deficiency (Figure 2E). In wild type mice, LP T-cells exhibited a clear polarization towards both Th1 and Th17 lineages, with >70% of all T-cells producing the lineage-specific signature cytokines IFN-γ or IL-17 (or both, Figure 2F). In contrast to wild type mice, CCR2-deficient animals lacked Th1 cells, but not Th17 cells, and failed to control the infection at the three month time point (Figure 2F,G). We next generated mixed bone marrow chimeras to examine which MP populations require cell-intrinsic CCR2 signaling for gastric LP recruitment during infection. Interestingly, monocytes, macrophages and $CD11b^+$ DCs (which we consider to be *bona fide* DCs because they are absent in the gastric LP of infected $FLT3L^{-/-}$ mice, suppl.

Figure 2), but not CD103$^+$ DC lineages, failed to migrate to the infected stomach in this setting (Figure 2H,I). The combined results suggest that gastric MP populations can be divided into cell-intrinsically CCR2-dependent monocyte/macrophage/CD11b$^+$ DC lineages and CD103$^+$ DCs that are only indirectly dependent on CCR2. MP recruitment to the gastric mucosa in turn is required for proper Th1 activation and *H. pylori* control.

CX$_3$CR1^{hi} macrophages and CD11b$^+$ dendritic cells sample *H. pylori* in the murine gastric mucosa

To address which of the myeloid cells that may potentially encounter *H. pylori* in the gastric mucosa phagocytose and sample the bacteria, we generated mouse-colonizing *H. pylori* strains expressing either GFP or RFP. Both fluorescent proteins were expressed, could be detected by FACS inside cultured bone marrow-derived phagocytes, and were stable intracellularly for extended periods of time post phagocytosis (data not shown). The RFP signal proved more stable over time and therefore RFP$^+$ *H. pylori* were used in all subsequent *in vivo* experimentation. Not surprisingly, the detection of RFP signal in LP cells was most straightforward in mice with high levels of colonization. To achieve this, we infected mice neonatally (i.e. on day 7 of age), at a time when the animals develop immune tolerance rather than immunity to the infection (16). In adult mice that were infected neonatally, around 4% of the myeloid CD11b$^+$ population exhibited an RFP signal (Figure 3A). The RFP signal could further be tracked to MHCII$^+$ monocytes, macrophages and CD11b$^+$ DCs, but was largely absent in the two other DC subsets (Figure 3B,C). Infection of *CX$_3$CR1*-GFP reporter mice, in which GFP is expressed in all CX$_3$CR1-positive cells, confirmed that the RFP signal was restricted to *CX$_3$CR1*-GFP^{hi} F4/80^{hi} macrophages, CD11b$^+$ CX$_3$CR1^{dim} F4/80$^-$ DCs and CX$_3$CR1^{dim} monocytes (Figure 3D and data not shown). A similar distribution of RFP signal, albeit at a generally lower frequency, was observed in adult infected animals with significantly lower

bacterial burden (Figure 3E,F). The combined results indicate that CX_3CR1-positive macrophage, monocytes and DC populations, but not $CD103^+$ DCs, phagocytose *H. pylori* in the gastric mucosa.

RFP^+ *H. pylori* are phagocytosed by human monocytes and macrophages in mice with reconstituted human immune systems

We next established a humanized mouse model of *H. pylori* infection to assess which human myeloid cells sample RFP^+ bacteria. NOD/LtSz-scid IL2Rγ deficient (NSG) mice reconstituted at birth with human $CD34^+$ cord blood cells proved to be insufficiently permissive to myeloid cell development and rather favored lymphoid engraftment both in the spleen and the GI tract lamina propria (data not shown). Having recently developed Rag2-deficient, Il2Rγ-deficient humanized mice expressing human cytokines central to myeloid development and hematopoietic stem cell maintenance (M-CSF, IL-3, GM-CSF, thrombopoietin) under their endogenous promoters, as well as human SIRPα as a transgene, we instead opted for these "MISTRG" mice. MISTRG mice are vastly superior to NSG mice in terms of their myeloid cell engraftment in bone marrow and spleen, and the full recapitulation of human myeloid development and function (23). In the gastric LP of MISTRG mice, the frequency of $hCD45^+$ cells was low at <1% of all live cells, but roughly doubled upon infection with *H. pylori* (Figure 4A). The increase due to infection could be attributed to an influx of $CD14^+CD16^+$ monocytes (Figure 4B). A second population of myeloid cells, $CD163^+$ macrophages, were present in the gastric LP already in the steady state and did not change upon infection (Figure 4C). Both populations exhibited a clearly discernible RFP signal in on average 4 and 11% of the population upon infection (Figure 4D), suggesting that human mononuclear phagocytes indeed develop normally and acquire comparable effector functions in murine hosts. Although two major human DC populations –$CD1c^+$ DCs and $CD141^+$ DCs- were detectable in the gastric LP, their numbers and frequencies were so low (under 2%) that detecting RFP signals in these populations was impossible.

Furthermore, we found no evidence of increased LP T-cell frequencies in infected mice, and also could not detect differences in colonization levels in reconstituted relative to non-reconstituted MISTRG mice (Figure 4E and data not shown). In summary, MISTRG mice are highly permissive to human myeloid cell engraftment in the gastric LP; the recruitment of phagocytes to the infected mucosa, and their sampling of *H. pylori*, indicates that innate responses to mucosal microbes can be studied meaningfully in humanized mice.

TLR2 and NLRP3 are upregulated by mononuclear phagocytes upon exposure to *H. pylori*

As we and others have shown that both the surface-exposed toll like receptor TLR2 and the inflammasome sensor NLRP3 are critically involved in detecting *H. pylori* infection in mice and in shaping the adaptive immune response to this infection (15, 24, 25), we sought to examine the expression and regulation of these factors in gastric LP MP lineages. We first surveyed TLR2 and NLRP3 expression in various MP populations sorted from the gastric LP. Interestingly, the expression patterns of TLR2 and NLRP3 overlapped to a large extent (Figure 5A). Both were expressed strongly in macrophages but not in $CD103^+$ DCs, and at an intermediate level in $CD11b^+$ DCs (Figure 5A). TLR2 surface expression on macrophages and $CD11b^+$ DCs could be verified by FACS of LP cells, which further revealed intermediate TLR2 expression also on the surface of $MHCII^-$ monocytes and $CD103^+CD11b^+$ DCs and high expression on $MHCII^+$ monocytes (Figure 5B). *H. pylori* infection increased the fraction of $TLR2^+$ cells among monocytes, macrophages and $CD11b^+$ DCs, but not among $CD103^+$ DCs (Figure 5C). As these populations encounter RFP^+ *H. pylori* in the infected mucosa (Figure 3B,C), we quantified the mean TLR2 expression on RFP^+ and RFP^- fractions of these populations. Interestingly, RFP^+ monocytes, macrophages and $CD11b^+$ DCs showed stronger TLR2 expression than their RFP^- counterparts in the same mice (Figure 5D). Targeted qRT-PCR performed on sorted cell populations confirmed that TLR2 is indeed upregulated transcriptionally in RFP^+

macrophages and RFP$^+$ CD11b$^+$ DCs, and is part of a signature that also comprises NLRP3 (and in DCs also IL-10; Figure 5E); the same signature can be detected in sorted macrophages and CD11b$^+$ DCs from infected relative to uninfected mice, even if RFP is not used as a marker for sorting (suppl. Figure 3). No differences in TLR2 expression were observed upon infection in MP populations of mesenteric lymph nodes (Figure 5F), where TLR2 positivity was also generally much lower, indicating that the expression and upregulation of TLR2 is a feature of tissue-resident populations. We next asked whether TLR2 upregulation could be recapitulated by *H. pylori* exposure of bone-marrow-derived DCs (BM-DCs). This was indeed the case (Figure 5G); furthermore, the approximately 10 fold induction of IL-10 expression in BM-DCs upon *H. pylori* exposure was clearly dependent on TLR2 (Figure 5H). The combined results indicate that the monocytes and monocyte-derived macrophages and CD11b$^+$ DCs that encounter *H. pylori* in the infected stomach express TLR2 and NLRP3 already in the steady state, in contrast to their lymph node counterparts which are generally TLR2-negative, and further upregulate both factors upon exposure to *H. pylori*.

NLRP3 is required for CD11b$^+$ DC differentiation in the gastric lamina propria and other GI tissues

We next sought to examine the role of NLRP3 and TLR2 in MP recruitment to, and functionality in the gastric LP. We first examined the MP composition in the LP of NLRP3$^{-/-}$ mice, in the steady state and during infection, relative to wild type controls. Strikingly, the recruitment of CD11b$^+$ DCs, but not of monocytes, macrophages or CD103$^+$ DCs to the infected stomach was highly dependent on NLRP3 proficiency of the animals (Figure 6A). Consistent with the reported regulatory/anti-inflammatory function of NLRP3 in *H. pylori* infection (15), we observed an increase in gastric Th1 polarization and gastric mucosal IFN-γ expression in NLRP3$^{-/-}$ relative to wild type mice, while Th17 cells and IL-17 levels were comparable (Figure 6B,C). Interestingly, Th1 and Th17 frequencies in the MLNs were comparable in wild type and NLRP3$^{-/-}$

mice (suppl. Figure 4A). The enhanced Th1 differentiation due to lack of NLRP3 was accompanied by lower *H. pylori* colonization levels in the knock-out strain (Figure 6D). To address whether the NLRP3 dependence of $CD11b^+$ DC differentiation was evident not only during infection, but also in the steady state and in other gastrointestinal tissues, we compared the frequencies of $CD11b^+$ DCs (Figure 6E) and of other DC subsets and macrophages (suppl. Figure 4B) in the LP of stomach, small intestine and colon. Interestingly, although all other examined cell types were present at normal frequencies, $CD11b^+$ DCs were absent in all GI tissues in the steady state. We next treated both wild type and $NLRP3^{-/-}$ mice with the antibiotics ampicillin, neomycin, metronidazole and vancomycin to eliminate the bulk of microbial sources of NLRP3 activation. This treatment failed to reduce $CD11b^+$ DC frequencies in the colons of wild type mice to $NLRP3^{-/-}$ levels (suppl. Figure 4C), indicating that non-microbial NLRP3 activation may be more important than microbial NLRP3 ligands in promoting the differentiation of $CD11b^+$ DCs. To address whether the NLRP3 dependence of $CD11b^+$ DC differentiation was cell-intrinsic, we generated bone marrow chimeras in which NLRP3-proficient and –deficient cells were analyzed in the same environment. Interestingly, NLRP3 was clearly required in a cell-intrinsic manner in $CD11b^+$ DCs for their differentiation in the gastric mucosa (Figure 6F,G). Having shown earlier that $TLR2^{-/-}$ and $NLRP3^{-/-}$ mice share very similar phenotypes in terms of allergy protection driven by *H. pylori* (15), we speculated that the requirement of $CD11b^+$ DC differentiation for NLRP3 might extend to TLR2. Although $TLR2^{-/-}$ mice exhibited similarly elevated gastric LP Th1 responses (Figure 6H,I) and the concomitant reduced colonization levels (Figure 6J), phenocopying $NLRP3^{-/-}$ mice in this regard, the dysregulation of T-cell responses could not be attributed to reduced $CD11b^+$ DC frequencies in the $TLR2^{-/-}$ animals (suppl. Figure 4D). As observed in the MLNs of $NLRP3^{-/-}$ mice, MLN T-cell responses were normal in $TLR2^{-/-}$ mice (suppl. Figure 4E). The combined results suggest that $CD11b^+$ DCs have a critical role in maintaining gastric homeostasis, especially during chronic infection, require NLRP3-mediated cues from the environment for their differentiation in GI tissues, and are dependent on TLR2 signals for their functionality.

The selective loss of CD103$^+$ DCs reveals a division of labor among gastric lamina propria DC subsets

We next sought to examine the functional contribution of CD103$^+$ DCs to *H. pylori*-specific immunity in mice that lack the transcription factor BATF3. BATF3$^{-/-}$ animals exhibit strongly reduced numbers of CD103$^+$ DCs, and moderately reduced CD103$^+$CD11b$^+$ DCs, but have normal complements of all other cell types in their gastric LP, both in the steady state and during infection (Figure 7A). Interestingly, BATF3$^{-/-}$ mice have a clear defect in generating local Th1 responses (Figure 7B,C) and in controlling the infection (Figure 7D), although their MLN T-cell responses were normal (Figure 7E). The findings suggest that CD103$^+$ DCs, despite never encountering RFP$^+$ *H. pylori* directly (Figure 3C) nevertheless have a prominent and non-redundant role in providing the local signals driving Th1 expansion.

Discussion

Our comparative analysis of MP evolution in early life revealed the stomach to be a predominantly myeloid organ, with little or no lymphocyte contribution to the overall leukocyte population; this was in sharp contrast to both the small and large intestine, where lymphocytes are the dominant immune cell compartments. The neonatal stomach is special in that it is populated by MP subsets that disappear later in life, at least in the steady state: MHCII-negative monocytes/macrophages, $CD103^+$ DCs and $CD11b^+$ DCs are all initially present at day 7, and gradually decline within the first 2-4 weeks of life. The dramatic loss of entire populations is not observed in the small intestine, which shows more or less gradual increases in all MP populations as well as in overall cellularity. Upon infection with *H. pylori*, the composition of the gastric LP changes profoundly, with a robust but numerically modest increase observed in all three DC subsets as well as monocytes and macrophages, and a numerically much more striking increase observed in neutrophils and $CD4^+$ T-cells. Virtually all infiltrating T-cells are activated and polarized to produce Th1 and/or Th17 cytokines; this is in contrast to the naïve stomach, where T-cells are extremely scarce. As reported previously (16) only the exposure of adult mice results in strong T-cell infiltration and a concomitant control of the infection; in contrast, neonatal exposure fails to attract T-cells (even as infected mice age), explaining why neonatally infected mice sustain high levels of *H. pylori* colonization for life (16). In the neonatal stomach, *H. pylori* initially encounters $CD103^+$ DCs and $CD11b^+$ DC and $MHCII^-$ macrophage/monocyte populations that are not found at such high numbers in the adult stomach; the differences in the dominant APC populations at the time of first encounter may account for the differences in T-cell recruitment and polarization.

The increase in MP numbers in the infected gastric mucosa is highly dependent on CCR2; bone marrow chimera experiments revealed, however, that only certain lineages (monocytes, macrophages and $CD11b^+$ DCs) show a cell-intrinsic requirement of CCR2 signaling for their tissue recruitment. *Bona fide* DC populations ($CD103^+$ $CD11b^+$ and $CD103^+$ $CD11b^-$) are present in normal numbers in the infected mucosa

even if they lack CCR2. This finding is in agreement with previous reports showing that Ly6C^{hi}CCR2^{+} monocytes give rise to macrophages and Cx$_3$CR1^{dim} CD11b^{+} MPs in both healthy and inflamed colon in a process that involves downregulation of Ly6C, and upregulation of MHCII, CD11c, CX$_3$CR1 and (in macrophages) F4/80 and CD64 (9), whereas the two CD103^{+} DC subsets arise from Flt3L-dependent pre-DC progenitors that neither express nor require CCR2 (26, 27). Bain et al further raise the intriguing possibility that Cx$_3$CR1^{dim} CD11b^{+} MPs represent an intermediate cell type in arrested development under conditions of inflammation (9). This view is challenged by genetic tracing experiments linking CD11b^{+} DCs to a pre-DC progenitor (28); more recent evidence confirmed that intestinal CD11b^{+} MPs are indeed classical DCs derived from Flt3 ligand-dependent, DC-committed precursors despite the fact that a large fraction of these cells expresses CCR2 (11). Our data indicate that CX$_3$CR1^{dim} CD11b^{+} MPs, which are very abundant in the *H. pylori*-infected mucosa, exhibit properties of both DCs and macrophages, as they are largely absent in Flt3L-deficient mice, but share many surface receptors (CX$_3$CR1, TLR2) and the cell-intrinsic developmental CCR2 requirement with macrophages.

The generation of RFP-expressing bacteria allowed us to address which MP populations encounter *H. pylori* in the infected mucosa. To our surprise, we found that MHCII^{+} monocytes, macrophages and CD11b^{+} DCs, but not Flt3-dependent CD103^{+} DC lineages, showed evidence of recent *H. pylori* encounters. This was particularly striking as CD103^{+} DCs were absolutely required for the generation of the Th1 response that ultimately controls *H. pylori* in the stomach. The result implies that antigen transfer occurs among MP populations, either locally in the infected mucosa, or in the draining lymph nodes; our data are reminiscent of a recent report demonstrating transfer of (fed) antigens from intestinal CX$_3$CR1-positive macrophages to CD103^{+} DCs in models of oral tolerance (29). The bacterially derived RFP signal further allowed us to study the consequences of *H. pylori* contact for MP gene expression by comparison of transcripts between RFP-positive and –negative fractions of the same MP populations. Not surprisingly, we found the anti-inflammatory cytokine IL-10 to be induced in CD11b^{+} DCs upon *H. pylori* contact; this

finding is in agreement with our previous observation that the DC-intrinsic production of IL-10 (which we examined in *CD11c*-Cre x IL-10$^{fl/fl}$ mice) is required for *H. pylori*-induced immune tolerance and the protection against allergic asthma that is a hallmark of neonatally infected mice (30). We further found that TLR2 and NLRP3 transcripts are co-induced upon *H. pylori* contact in CD11b$^+$ DCs, a finding that is in line with our and others' earlier observations that both TLR2 and NLRP3 are required for inflammasome activation and IL-1β and IL-18 processing by caspase-1 upon *H. pylori* infection of BM-DCs (15, 24, 25). In contrast to CD11b$^+$ DCs, CD103$^+$ DCs express very low TLR2 at steady state, do not encounter *H. pylori* and thus are unlikely to serve as important sources of inflammasome-dependent cytokines. As the TLR2/NLRP3/caspase-1/IL-18 axis is required for tolerogenic responses to *H. pylori*, but not for immunity (13, 15), we propose that CD11b$^+$ DCs are the main drivers of tolerance- and homeostasis-promoting processes in the infected stomach.

Quite unexpectedly, we found NLRP3 to be cell-intrinsically required for the local differentiation of CD11b$^+$ DCs, not only in the stomach during infection, but throughout the GI tract in both the steady state and during infection. Whether this property of NLRP3 is linked to its role as a cytoplasmic sensor and trigger of inflammasome activation currently remains unclear. It will be of interest to investigate whether microbial or host-derived PAMPs or DAMPs serve as signals for CD11b$^+$ DC differentiation in tissues; our preliminary data obtained in antibiotic-treated mice indicate that microbial stimuli are not the predominant source of NLRP3 activation. Also, it will be interesting to see whether CD11b$^+$ DCs at other mucosal tissues of the body populated by a resident microbiota, such as the airways, share the developmental requirement for NLRP3.

Interestingly, gastric CD103$^+$ DC populations neither express NLRP3 in the steady state, nor do they induce it upon *H. pylori* infection, nor is their frequency in the LP altered due to NLRP3 deficiency. Strikingly, we found BATF3-dependent CD103$^+$ DCs, which appear to never be in direct contact with live *H. pylori*, to be strictly required for immunity as their loss abrogated immune control driven by Th1-polarized T-cells.

These data are in line with previous evidence of a critical role of BATF3-dependent CD103$^+$ DCs in Th1 activation and/or expansion in models of *Leishmania major* infection (31) and immune protection against a newly identified protist, *Tritrichomonas musculis*, which colonizes the murine intestine and triggers strongly Th1-polarized T-cell responses (32). Our data support a model where BATF3-dependent DCs are dispensable for T-cell priming -as we find Th1 frequencies in the MLNs to be relatively normal- but rather are required for local Th1 expansion in the tissue. BATF3-dependent CD103$^+$ DCs of the GI tract are better known for their potency at driving CD8$^+$ T cell immunity (7, 26, 27) and for their role in priming Treg differentiation through the production of retinoic acid (33), although their exclusive, non-redundant role in promoting Treg-driven tolerance was recently challenged in an oral tolerization model (34). Our data, as well as the results from the *Leishmania* and *Tritrichomonas musculis* models, attribute an additional Th1-promoting function to this versatile DC subset, at least in the GI tract. In summary, we show here that the gastric lamina propria is populated by a complex network of mononuclear phagocytes in the steady state and especially during infection, which orchestrates a fine balance of maintaining tissue homeostasis while effectively controlling invading pathogens.

Methods

Animal experimentation. C57BL/6 WT, B6.SJL-Cd45.1, *Tlr2*$^{-/-}$, *Nlrp3*$^{-/-}$, Ccr2$^{-/-}$, *Batf3* $^{-/-}$*and CX*$_3$*CR1*$^{GFP/+}$ mice were originally obtained from the Jackson laboratory. All strains, as well as MISTRG, were bred and maintained under specific pathogen–free conditions in accredited animal facilities at the University of Zürich. All animal experimentation was reviewed and approved by the Zürich Cantonal Veterinary Office (licences ZH170/2014, ZH24/2013 and ZH235/2015 to A.M.). For the generation of bone-marrow chimeras, B6 WT mice were irradiated with 10.5 Gy and reconstituted i.v. with an equal number of BM cells from WT CD45.1 and Ccr2$^{-/-}$ CD45.2 or *Nlrp3*$^{-/-}$ CD45.2 mice (1.5x10^7 cells/ mouse). Mice were rested for 6 weeks before being used in experiments. For the generation of humanized mice, newborn MISTRG mice were injected intra-hepatically with 2.5×10^5 CD34$^+$ cells 3 days after birth. CD34$^+$ cells were isolated from human cord blood with immunomagnetic beads (Miltenyi Biotec) with a yield of 0.5–4×10^6 CD34$^+$ cells per donor (purity >90%) and were stored in liquid nitrogen until use. Mice were infected with *H. pylori* 4 weeks after reconstitution and analysed 4 weeks later. For the depletion of gut commensal microbiota, animals were given ampicillin (1 g l^{-1}; Sigma), vancomycin (500 mg l^{-1}; Applichem), neomycin sulphate (N; 1 g l^{-1}; Applichem), and metronidazole (1 g l^{-1}; Sigma) in drinking water for 7 weeks as described (35) prior to analysis.

***H. pylori* strains, culture conditions and colony counting**

Mice were infected orally on two consecutive days with 10^8 CFU *H. pylori* PMSS1 at 6 weeks or 7 days of age and analyzed at 1 and 3 months p.i. unless specified otherwise. The *H. pylori* strain used in this study, PMSS1, is a clinical isolate of a patient with duodenal ulcer and the parental strain of the mouse-derivative Sydney strain 1 (SS1*)* (16). The PMSS1 RFP isogenic mutant was described previously (36). *H. pylori* was grown on horse blood agar plates and in liquid culture as described previously (16). Cultures were routinely assessed by light microscopy for contamination, morphology, and motility.

Infection of mouse BMDCs. Murine bone marrow stem cells from donor mice were used to generate BMDCs by flushing the femur and tibia. Cells were resuspended in RPMI-1640 medium supplemented with 10% fetal bovine serum, 100 U ml^{-1} penicillin/streptomycin and 20ng/ml GM-CSF (PeproTech), and seeded at a density of $0.7x10^6$ cells/ml. Cells were cultured at 37°C for 6 days and additional medium was added every 3 days. At day 7, cells were washed and resuspended in RPMI-1640 medium supplemented with 10% fetal bovine serum and 10% Brucella Broth (Becton Disckinson) prior to infection with *H. pylori*.

Leukocyte Isolation. For lamina propria leukocyte isolation, gastrointestinal tissues were opened longitudinally, washed and cut into pieces. Peyer's patches were removed from the small intestine. Pieces were incubated in Hanks' balanced salt solution with 10% FCS and 5 mM EDTA at 37°C to remove epithelial cells. Tissue was digested at 37 °C for 50 min in a shaking incubator with 15 mM HEPES, 500 U/ml of type IV collagenase (Sigma-Aldrich) and 0.05 mg ml^{-1} DNase I in RPMI-1640 medium supplemented with 10% fetal bovine serum and 100 U ml^{-1} penicillin/streptomycin. Cells were then layered onto a 40/80% Percoll gradient, centrifuged, and the interface was washed in PBS with 0.5% BSA. MLN cell suspensions were prepared by digesting the tissue with 500 U/ml of type IV collagenase in RPMI-1640 medium for 15 min followed by pushing through a cell strainer using a syringe plunger.

Flow cytometry, cell sorting and counting. For surface staining, cells were stained in PBS with 0.5% bovine serum albumin with a fixable viability dye and a combination of the following antibodies: anti-mouse CD45 (30-F11), CD45.1 (A20), CD45.2 (104), CD11c (N418), MHCII (M5/114.15.2), F4/80 (BM8), CD103 (M2E7), CD11b (M1/70), Ly6G (1A8), Ly6C (HK1.4), CD4 (RM4-5) and TCRβ (H57-597) (all from BioLegend); anti-mouse Siglec-F (E50-2440) (from BD Biosciences); anti-mouse CD282/TLR2 (6C2, Affymetrix); anti-human CD45 (HI30), CD14 (M5E2), CD16 (3G8), CD33 (P67.6) and CD163 (GHI/61) (all from BioLegend). Fc block (anti-CD16/CD32, Affymetrix) was included to minimize nonspecific antibody binding. For intracellular cytokine staining of T cells, cells were incubated for 3.5 h in complete IMDM medium containing 0.1 µM

phorbol 12-myristate 13-acetate and 1 µM ionomycin with 1:1,000 Brefeldin A (eBioscience) and GolgiStop solutions (BD Biosciences) at 37 °C in a humidified in a humidified incubator with 5% CO2. Following surface staining, cells were fixed and permeabilized with the Cytofix/Cytoperm Fixation/Permeabilization Solution Kit (BD Biosciences) according to the manufacturer's instructions. Cells were stained for 50 min with antibodies to IL-17A (TC11-18H10.1) and IFNγ (XMG1.2, Biolegend). Total leukocyte counts were determined by adding countBright™ Absolute Counting Beads (Life technologies) to each sample prior to analysis. Samples were analyzed on a LSRII Fortessa (BD Biosciences) or sorted on a FACSAriaIII (BD Biosciences) to a purity of >95%. Analysis was performed using FlowJo software (Tree Star, Ashland, OR).

Quantitative PCR. RNA was isolated from scraped gastric mucosa, BMDCs or from FACS-sorted cells using the RNeasy Mini kit (QIAGEN) according to the manufacturer's instructions. Complementary DNA synthesis was performed using Superscript III reverse transcriptase (QIAGEN). Quantitative PCR reactions for the candidate genes were performed using TaqMan gene expression assays (Ifng Mm01168134_m1, Il17a Mm00439618_m1, Il10 Mm01288386_m1, Tlr2 Mm00442346_m1, Nalp3 Mm00840904_m1, Hprt Mm03024075_m1; Applied Biosystems) or SYBR Green (GAPDH fw: 5'-
GAC ATT GTT GCC ATC AAC GAC C-3' / GAPDH rv: 5'-CCC GTT GAT GAC CAGCTT CC-3', IL-10 fw: 5'-CAG AGC CAC ATG CTC CTA GA-3' / IL-10 rv: 5'-TGT CCA GCT GGT CCT TTG TT -3'; Tm 60°C, 50 cycles) Complementary DNA samples were analyzed in duplicate using a Light Cycler 480 detection system (Roche) and gene expression levels for each sample were normalized to HPRT or GAPDH expression. Mean relative gene expression was determined, and the differences were calculated using the 2ΔC(t) method.

Statistical Analysis. Statistical analysis was performed with Prism 6.0 (GraphPad Software). The nonparametric Mann-Whitney test was used for all statistical comparisons. Differences were considered statistically significant when $p < 0.05$.

Author contributions

I.C.A. designed, performed and analyzed most of the experiments and co-wrote the manuscript; S.U., and X.Z. contributed several *in vivo* experiments and performed BM-DC infections. M.A. performed qPCRs. M.G.M. and K.O. provided critical tools and intellectual input and A.M. supervised the studies and co-wrote the manuscript.

Acknowledgements

This work was supported by the Swiss National Science Foundation Temporary Backup Schemes Consolidator Grant BSCGIO_157841/1 to A.M. and the clinical research priority program on Human Hemato-Lymphatic Diseases, University of Zurich. We thank all members of the Müller lab as well as Melanie Greter and Maries van den Broek for helpful discussions. We are grateful to Lubor Borsig for sharing $CCR2^{-/-}$ mice, and to the technical staff of the Department of Hematology for preparing human cord blood HSCs.

References

1. Cerovic V, Bain CC, Mowat AM, and Milling SW. Intestinal macrophages and dendritic cells: what's the difference? *Trends Immunol.* 2014;35(6):270-7.
2. Lavin Y, Mortha A, Rahman A, and Merad M. Regulation of macrophage development and function in peripheral tissues. *Nat Rev Immunol.* 2015;15(12):731-44.
3. Mowat AM, and Agace WW. Regional specialization within the intestinal immune system. *Nat Rev Immunol.* 2014;14(10):667-85.
4. Greter M, Helft J, Chow A, Hashimoto D, Mortha A, Agudo-Cantero J, Bogunovic M, Gautier EL, Miller J, Leboeuf M, et al. GM-CSF controls nonlymphoid tissue dendritic cell homeostasis but is dispensable for the differentiation of inflammatory dendritic cells. *Immunity.* 2012;36(6):1031-46.
5. Lewis KL, Caton ML, Bogunovic M, Greter M, Grajkowska LT, Ng D, Klinakis A, Charo IF, Jung S, Gommerman JL, et al. Notch2 receptor signaling controls functional differentiation of dendritic cells in the spleen and intestine. *Immunity.* 2011;35(5):780-91.
6. Persson EK, Uronen-Hansson H, Semmrich M, Rivollier A, Hagerbrand K, Marsal J, Gudjonsson S, Hakansson U, Reizis B, Kotarsky K, et al. IRF4 transcription-factor-dependent CD103(+)CD11b(+) dendritic cells drive mucosal T helper 17 cell differentiation. *Immunity.* 2013;38(5):958-69.
7. Edelson BT, Kc W, Juang R, Kohyama M, Benoit LA, Klekotka PA, Moon C, Albring JC, Ise W, Michael DG, et al. Peripheral CD103+ dendritic cells form a unified subset developmentally related to CD8alpha+ conventional dendritic cells. *J Exp Med.* 2010;207(4):823-36.
8. Haniffa M, Shin A, Bigley V, McGovern N, Teo P, See P, Wasan PS, Wang XN, Malinarich F, Malleret B, et al. Human tissues contain CD141hi cross-presenting dendritic cells with functional homology to mouse CD103+ nonlymphoid dendritic cells. *Immunity.* 2012;37(1):60-73.
9. Bain CC, Scott CL, Uronen-Hansson H, Gudjonsson S, Jansson O, Grip O, Guilliams M, Malissen B, Agace WW, and Mowat AM. Resident and pro-inflammatory macrophages in the colon represent alternative context-dependent fates of the same Ly6Chi monocyte precursors. *Mucosal Immunol.* 2013;6(3):498-510.
10. Cerovic V, Houston SA, Scott CL, Aumeunier A, Yrlid U, Mowat AM, and Milling SW. Intestinal CD103(-) dendritic cells migrate in lymph and prime effector T cells. *Mucosal Immunol.* 2013;6(1):104-13.
11. Scott CL, Bain CC, Wright PB, Sichien D, Kotarsky K, Persson EK, Luda K, Guilliams M, Lambrecht BN, Agace WW, et al. CCR2(+)CD103(-) intestinal dendritic cells develop from DC-committed precursors and induce interleukin-17 production by T cells. *Mucosal Immunol.* 2015;8(2):327-39.
12. Salama NR, Hartung ML, and Muller A. Life in the human stomach: persistence strategies of the bacterial pathogen Helicobacter pylori. *Nat Rev Microbiol.* 2013;11(6):385-99.
13. Oertli M, Sundquist M, Hitzler I, Engler DB, Arnold IC, Reuter S, Maxeiner J, Hansson M, Taube C, Quiding-Jarbrink M, et al. DC-derived IL-18 drives Treg differentiation, murine Helicobacter pylori-specific immune tolerance, and asthma protection. *J Clin Invest.* 2012;122(3):1082-96.
14. Oertli M, Noben M, Engler DB, Semper RP, Reuter S, Maxeiner J, Gerhard M, Taube C, and Muller A. Helicobacter pylori gamma-glutamyl transpeptidase and vacuolating cytotoxin promote gastric persistence and immune tolerance. *Proc Natl Acad Sci U S A.* 2013;110(8):3047-52
15. Koch KN, Hartung ML, Urban S, Kyburz A, Bahlmann AS, Lind J, Backert S, Taube C, and Muller A. Helicobacter urease-induced activation of the TLR2/NLRP3/IL-18 axis protects against asthma. *J Clin Invest.* 2015;125(8):3297-302.

16. Arnold IC, Lee JY, Amieva MR, Roers A, Flavell RA, Sparwasser T, and Müller A. Tolerance rather than immunity protects from Helicobacter pylori-induced gastric preneoplasia. *Gastroenterology.* 2011;140(1):199-209.
17. Harris PR, Wright SW, Serrano C, Riera F, Duarte I, Torres J, Pena A, Rollan A, Viviani P, Guiraldes E, et al. Helicobacter pylori gastritis in children is associated with a regulatory T-cell response. *Gastroenterology.* 2008;134(2):491-9.
18. Blaser MJ, Chen Y, and Reibman J. Does Helicobacter pylori protect against asthma and allergy? *Gut.* 2008;57(5):561-7.
19. Castano-Rodriguez N, Kaakoush NO, Lee WS, and Mitchell HM. Dual role of Helicobacter and Campylobacter species in IBD: a systematic review and meta-analysis. *Gut.* 2015.
20. Zhou X, Wu J, and Zhang G. Association between Helicobacter pylori and asthma: a meta-analysis. *Eur J Gastroenterol Hepatol.* 2013;25(4):460-8.
21. Arnold IC, Dehzad N, Reuter S, Martin H, Becher B, Taube C, and Müller A. Helicobacter pylori infection prevents allergic asthma in mouse models through the induction of regulatory T cells. *J Clin Invest.* 2011;121(3088-93.
22. Engler DB, Leonardi I, Hartung ML, Kyburz A, Spath S, Becher B, Rogler G, and Muller A. Helicobacter pylori-specific protection against inflammatory bowel disease requires the NLRP3 inflammasome and IL-18. *Inflamm Bowel Dis.* 2015;21(4):854-61.
23. Rongvaux A, Willinger T, Martinek J, Strowig T, Gearty SV, Teichmann LL, Saito Y, Marches F, Halene S, Palucka AK, et al. Development and function of human innate immune cells in a humanized mouse model. *Nat Biotechnol.* 2014;32(4):364-72.
24. Semper RP, Mejias-Luque R, Gross C, Anderl F, Muller A, Vieth M, Busch DH, Prazeres da Costa C, Ruland J, Gross O, et al. Helicobacter pylori-Induced IL-1beta Secretion in Innate Immune Cells Is Regulated by the NLRP3 Inflammasome and Requires the Cag Pathogenicity Island. *J Immunol.* 2014;193(3566-76.
25. Kim DJ, Park JH, Franchi L, Backert S, and Nunez G. The Cag pathogenicity island and interaction between TLR2/NOD2 and NLRP3 regulate IL-1beta production in Helicobacter pylori-infected dendritic cells. *Eur J Immunol.* 2013;43(2650-8
26. Bogunovic M, Ginhoux F, Helft J, Shang L, Hashimoto D, Greter M, Liu K, Jakubzick C, Ingersoll MA, Leboeuf M, et al. Origin of the lamina propria dendritic cell network. *Immunity.* 2009;31(3):513-25.
27. Varol C, Vallon-Eberhard A, Elinav E, Aychek T, Shapira Y, Luche H, Fehling HJ, Hardt WD, Shakhar G, and Jung S. Intestinal lamina propria dendritic cell subsets have different origin and functions. *Immunity.* 2009;31(3):502-12.
28. Schraml BU, van Blijswijk J, Zelenay S, Whitney PG, Filby A, Acton SE, Rogers NC, Moncaut N, Carvajal JJ, and Reis e Sousa C. Genetic tracing via DNGR-1 expression history defines dendritic cells as a hematopoietic lineage. *Cell.* 2013;154(4):843-58.
29. Mazzini E, Massimiliano L, Penna G, and Rescigno M. Oral tolerance can be established via gap junction transfer of fed antigens from CX3CR1(+) macrophages to CD103(+) dendritic cells. *Immunity.* 2014;40(2):248-61.
30. Engler DB, Reuter S, van Wijck Y, Urban S, Kyburz A, Maxeiner J, Martin H, Yogev N, Waisman A, Gerhard M, et al. Effective treatment of allergic airway inflammation with Helicobacter pylori immunomodulators requires BATF3-dependent dendritic cells and IL-10. *Proc Natl Acad Sci U S A.* 2014;111(32):11810-5.
31. Martinez-Lopez M, Iborra S, Conde-Garrosa R, and Sancho D. Batf3-dependent CD103+ dendritic cells are major producers of IL-12 that drive local Th1 immunity against Leishmania major infection in mice. *Eur J Immunol.* 2015;45(1):119-29.

32. Chudnovskiy A, Mortha A, Kana V, Kennard A, Ramirez JD, Rahman A, Remark R, Mogno I, Ng R, Gnjatic S, et al. Host-Protozoan Interactions Protect from Mucosal Infections through Activation of the Inflammasome. *Cell.* 2016;167(2):444-56 e14.
33. Coombes JL, Siddiqui KR, Arancibia-Carcamo CV, Hall J, Sun CM, Belkaid Y, and Powrie F. A functionally specialized population of mucosal CD103+ DCs induces Foxp3+ regulatory T cells via a TGF-beta and retinoic acid-dependent mechanism. *J Exp Med.* 2007;204(8):1757-64.
34. Veenbergen S, van Berkel LA, du Pre MF, He J, Karrich JJ, Costes LM, Luk F, Simons-Oosterhuis Y, Raatgeep HC, Cerovic V, et al. Colonic tolerance develops in the iliac lymph nodes and can be established independent of CD103(+) dendritic cells. *Mucosal Immunol.* 2016;9(4):894-906.
35. Diehl GE, Longman RS, Zhang JX, Breart B, Galan C, Cuesta A, Schwab SR, and Littman DR. Microbiota restricts trafficking of bacteria to mesenteric lymph nodes by CX(3)CR1(hi) cells. *Nature.* 2013;494(7435):116-20.
36. Keilberg D, Zavros Y, Shepherd B, Salama NR, and Ottemann KM. Spatial and Temporal Shifts in Bacterial Biogeography and Gland Occupation during the Development of a Chronic Infection. *MBio.* 2016;7(5).

Figure 1

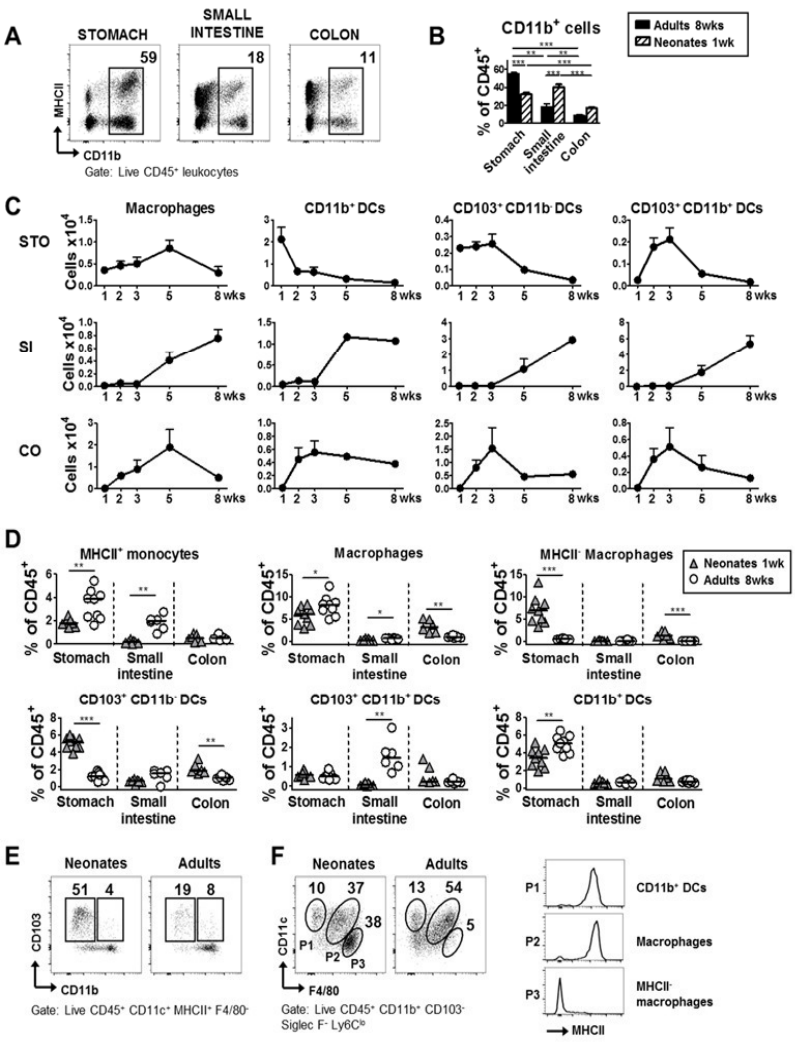

Figure 1. Comparative analysis of the evolution and composition of the gastric, small intestinal and colonic lamina propria (LP) mononuclear phagocyte (MP) populations in the steady state. The indicated MP subsets were isolated from the LP of stomach, small intestine and colon at the indicated age and analyzed by flow cytometry. **(A)** Representative FACS plots of CD11b$^+$ myeloid cells in the stomach, small intestine and colon, in % of live CD45$^+$ leukocytes. **(B)** Frequencies of CD11b$^+$ myeloid cells in the three compartments in adult (8 week old) and neonatal (1 week old) mice. Pooled data from 5-9 mice per group are shown. **(C)** Absolute counts per organ of macrophages and of CD11b$^+$, CD103$^+$, CD103$^+$CD11b$^+$ DCs at the indicated ages. Between 3 and 5 mice were pooled for each time point. STO, stomach, SI, small intestine, CO, colon. In B and C, data are represented as mean +SEM. **(D)** Frequencies of the indicated MP populations, as assessed at 1 and 8 weeks of age. Horizontal lines indicate medians. In B and D, * indicates $p<0.05$, ** $p<0.01$, ***$p<0.001$, as calculated by Mann-Whitney test. Data are pooled from 2 independent studies (9 mice total per group). **(E, F)** Representative FACS plots of DC subsets (E),macrophages and CD11b$^+$ DCs (F) in 1 week old (neonate) and 8 week old (adult) mice. Histograms in the right panels show the MHCII expression of macrophages and CD11b$^+$ DCs.

Figure 2

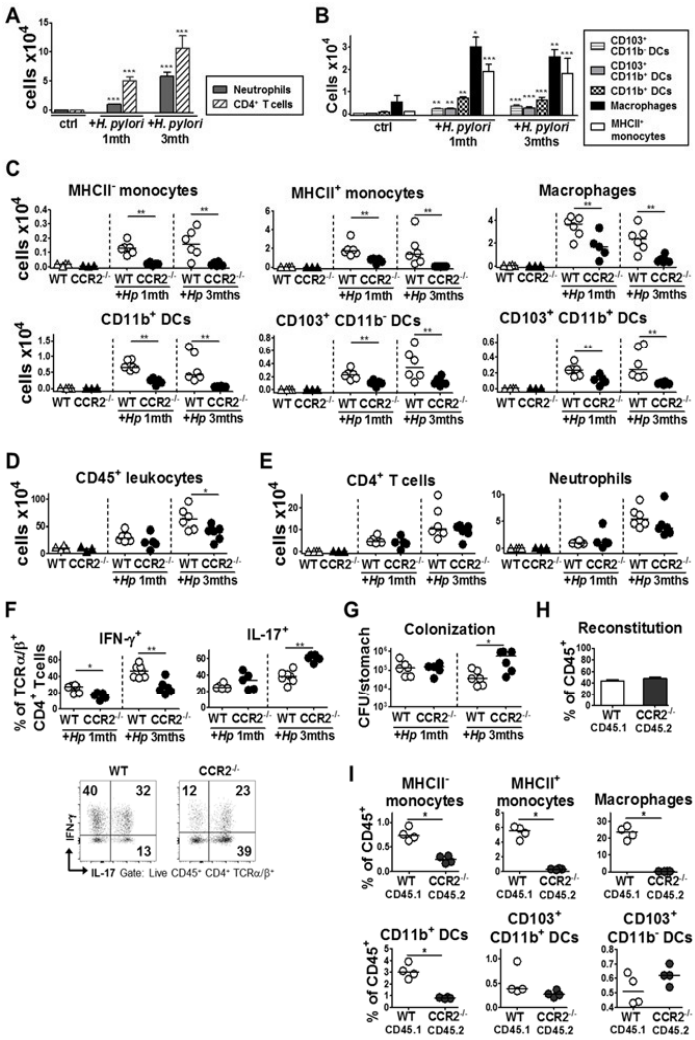

Figure 2. Cell-intrinsic dependence of monocytes, macrophages and CD11b$^+$ DCs on CCR2 for recruitment to the gastric lamina propria. (A, B) Absolute counts of neutrophils and CD4$^+$ T-cells (A) and of various MP populations (B) in the LP of mice in the steady state and at 1 and 3 months post infection (p.i.) with *H. pylori*. Data are represented as mean +SEM. P-values were calculated relative to uninfected controls. **(C)** Absolute counts of the indicated gastric LP MP populations in WT and CCR2$^{-/-}$ mice in the steady state and at 1 and 3 months p.i. with *H. pylori*. **(D-F)** Absolute counts of all leukocytes (D), CD4$^+$ T-cells and neutrophils (E), and IFN-γ$^+$ and IL-17$^+$ CD4$^+$ T-cells (F) in the gastric LP of WT and CCR2$^{-/-}$ mice in the steady state and at 1 and 3 months p.i. with *H. pylori*. In F, representative FACS plots are shown. **(G)** *H. pylori* colonization of the mice shown in A-F, represented as CFU per stomach. Data in C-G are representative of 2 independently conducted time courses. **(H, I)** Adult WT mice were reconstituted with 1:1 mixed bone marrow from CD45.1$^+$ WT and CD45.2$^+$ CCR2$^{-/-}$ donors. Mice were allowed to reconstitute for six weeks prior to a six week infection with *H. pylori*. The reconstitution efficiency in % of all CD45$^+$ cells is shown in H. The frequencies of the indicated MP populations is shown in I. In C,D,E,F,G and I, horizontal lines indicate medians. * indicates p<0.05, ** p<0.01, ***p<0.001, as calculated by Mann-Whitney test.

Figure 3

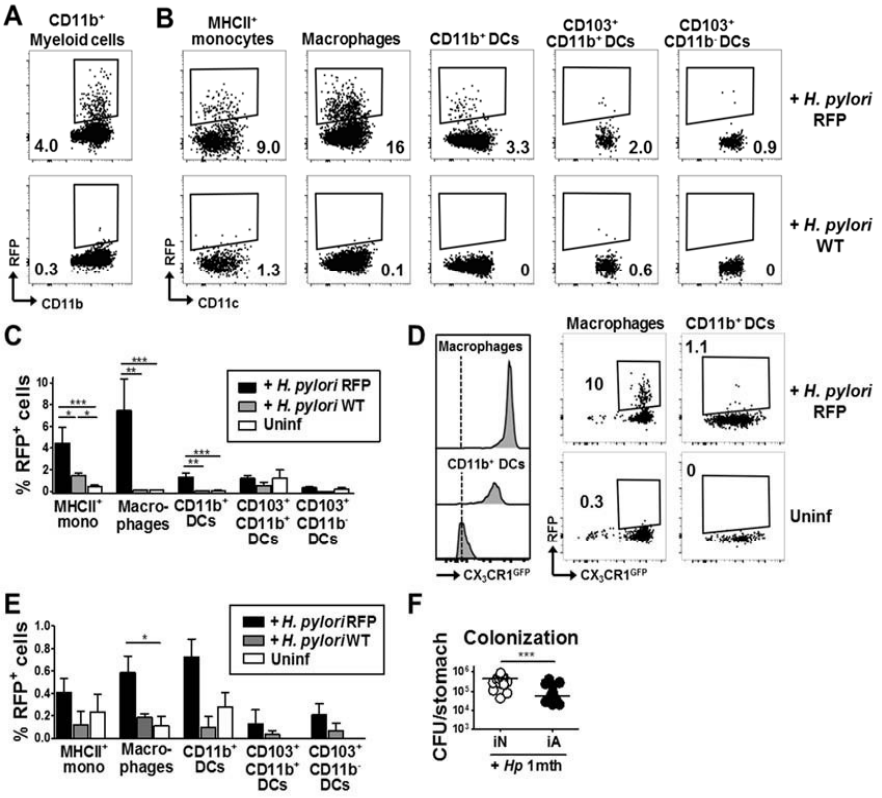

Figure 3. Monocytes, macrophages and CD11b$^+$ DCs, but not other DC subsets, encounter RFP$^+$ *H. pylori* in the gastric LP. Mice were infected at 1 week of age (A-D) or 6 weeks of age (E) with RFP$^+$ or WT (RFP$^-$) *H. pylori* prior to the analysis of gastric LP MP populations. **(A)** Frequency of RFP$^+$ cells among all CD11b$^+$ gastric LP myeloid cells isolated from mice infected with RFP$^+$ or WT *H. pylori.* **(B)** Frequencies of RFP$^+$ cells among the indicated gastric LP MP populations isolated from mice infected with RFP$^+$ or WT *H. pylori* for 3 months. Representative FACS plots are shown in A and B. **(C)** Frequencies of RFP$^+$ cells among the indicated gastric LP MP populations isolated from mice infected neonatally with RFP$^+$ or WT *H. pylori* relative to uninfected mice. Between 6 and 8 mice were analyzed per group. Data are represented as mean +SEM. **(D)** *CX$_3$CR1*-GFP reporter mice were infected with RFP$^+$ *H. pylori* or WT *H. pylori.* Frequencies of RFP$^+$ cells among *CX$_3$CR1*-GFP^{hi} gastric LP macrophages and *CX$_3$CR1*-GFP^{dim} CD11b$^+$ DCs are shown in representative FACS plots. The histograms in the left panel show the *CX$_3$CR1*-GFP expression of the two populations relative to WT (non-transgenic, bottom panel) cells. **(E)** Frequencies of RFP$^+$ cells among the indicated gastric LP MP populations isolated from mice infected as adults with RFP$^+$ or WT *H. pylori* relative to uninfected mice. Between 3 and 12 mice were analyzed per group. Data are represented as mean +SEM. **(F)** *H. pylori* colonization of the mice shown in C and E, represented as CFU per stomach: horizontal lines indicate medians.

Figure 4

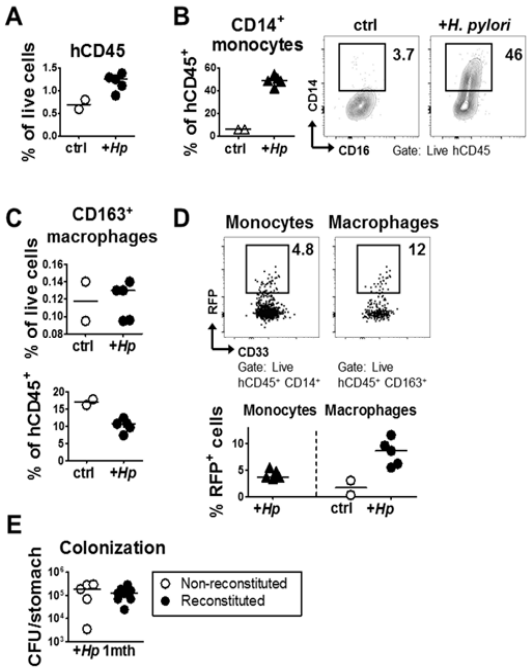

Figure 4. Human CD163$^+$ macrophages and CD14$^+$ monocytes encounter RFP$^+$ *H. pylori* in the gastric LP of humanized MISTRG mice. MISTRG mice were intrahepatically injected on day 2 of age with 2.5 x10^5 CD34$^+$ cord blood hematopoietic stem cells and allowed to reconstitute for 6 weeks prior to infection with RFP$^+$ *H. pylori* for 1 month. LP phagocytes were analyzed by flow cytometry. **(A)** Reconstitution efficiency as assessed in the gastric LP. **(B)** Frequency of CD14$^+$ monocytes in % of all human leukocytes in the gastric LP of *H. pylori*-infected relative to uninfected mice. Representative FACS plots are shown in the panels on the right. **(C)** Frequency of CD163$^+$ macrophages in % of live cells (top panel) and of human leukocytes (bottom panel) in the gastric LP of *H. pylori*-infected relative to uninfected mice. **(D)** Frequency of RFP$^+$ cells among CD14$^+$ monocytes and CD163$^+$ macrophages in the gastric LP of *H. pylori*-infected relative to uninfected mice. Representative FACS plots and pooled data are shown. Note that monocytes were too scarce in the uninfected LP to allow for a meaningful analysis of their baseline RFP fluorescence. **(E)** *H. pylori* colonization of the mice shown in A-D, as well as of 3 additional reconstituted and 5 un-reconstituted MISTRG mice. Horizontal lines indicate medians.

Figure 5

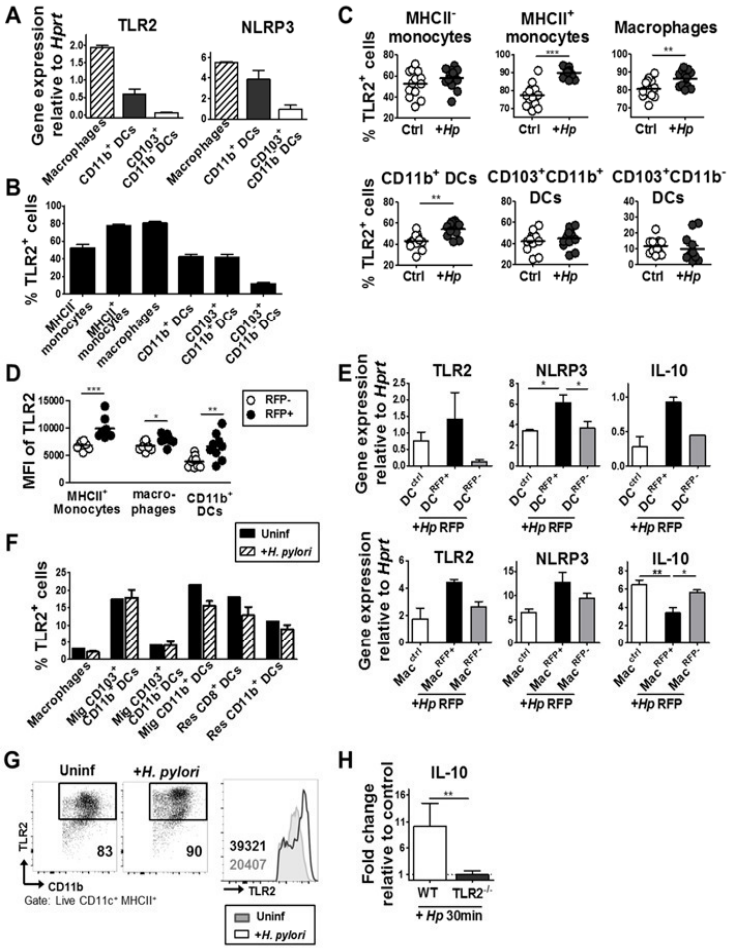

Figure 5. Phagocytes that have encountered *H. pylori* in the gastric mucosa express and upregulate TLR2 and NLRP3. (A) Expression of TLR2 and NLRP3 by gastric macrophages, CD11b$^+$ and CD103$^+$ DCs, as determined by qRT-PCR of gastric LP populations FACS-sorted and analyzed in 2 pools of 4 mice. Data are represented as mean +SEM of 2 independent experiments. **(B)** Frequencies of TLR2$^+$ cells among the indicated gastric LP MP populations. Data are represented as mean +SEM of 13 mice. **(C)** Frequencies of TLR2$^+$ cells among the indicated gastric LP MP populations of *H. pylori*-infected relative to uninfected mice (analyzed one month p.i.). Horizontal lines indicate medians. Data are pooled from 3 independent studies. **(D)** MFI of TLR2 expression on RFP$^+$ and RFP$^-$ monocytes, macrophages and CD11b$^+$ DCs. Data are from 1 month-infected mice and pooled from 3 independent studies. **(E)** Expression of TLR2, NLRP3 and IL-10 by gastric CD11b$^+$ DCs (top panel) and macrophages (bottom panel), as determined by qRT-PCR of FACS-sorted RFP$^+$ and RFP$^-$ populations from 2 pools of 4 mice each. Data are represented as mean +SEM of 2 independent experiments. CD11b$^+$ DCs and macrophages from uninfected donors were sorted and analyzed as well. **(F)** Frequencies of TLR2$^+$ cells among the indicated MLN macrophage and DC populations of *H. pylori*-infected relative to uninfected mice shown in C. Data are represented as mean +SEM. mig, migratory; res, resident. **(G)** Bone marrow (BM)-derived DCs were infected with *H. pylori* at a multiplicity of infection of 50 for 24h prior to staining for TLR2 expression. **(H)** WT and TLR2$^{-/-}$ BM-DCs were infected with *H. pylori* for 30 min prior to qRT-PCR analysis of IL-10 expression. Data are represented as mean +SEM of three independent experiments.

Figure 6

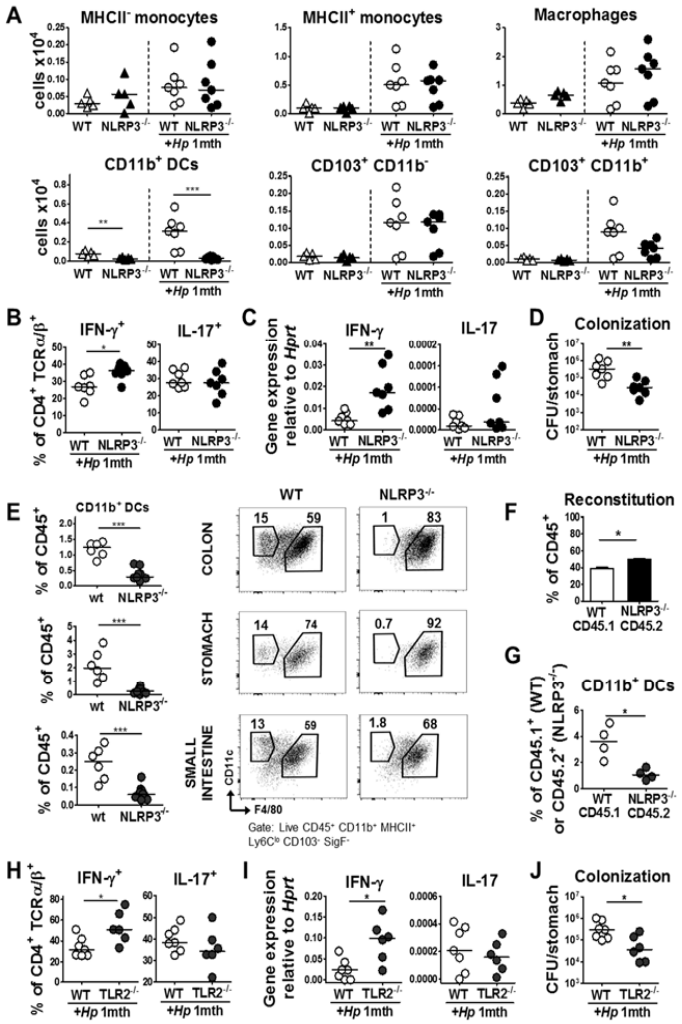

Figure 6. NLRP3 is required for the terminal differentiation of CD11b⁺ DCs. NLRP3$^{-/-}$ and WT mice were infected with *H. pylori* for one month and their gastric LP leukocytes were analyzed by FACS. **(A)** Absolute counts of the indicated gastric LP MP populations in WT and NLRP3$^{-/-}$ mice in the steady state and at 1 month p.i. with *H. pylori*. **(B)** Frequencies of IFN-γ⁺ and IL-17⁺ cells among all CD4⁺ T-cells of *H. pylori*-infected WT and NLRP3$^{-/-}$ mice. **(C)** IFN-γ and IL-17 expression in the gastric mucosa of *H. pylori*-infected WT and NLRP3$^{-/-}$ mice, as determined by qRT-PCR. **(D)** *H. pylori* colonization of the mice shown in A-C. Data in A-D are from 1 study that is representative of 4 independent ones. **(E)** Frequencies of CD11b⁺ DCs among CD45⁺ cells in the LP of colon, stomach and small intestine of WT and NLRP3$^{-/-}$ mice. Representative FACS plots are shown on the right. **(F,G)** Adult WT mice were reconstituted with 1:1 mixed bone marrow from CD45.1⁺ WT and CD45.2⁺ NLRP3$^{-/-}$ donors. Mice were allowed to reconstitute for 6 weeks prior to a 6 week infection with *H. pylori*. The reconstitution efficiency is shown in F. The frequencies of CD11b⁺ DCs are shown in G. **(H-J)** TLR2$^{-/-}$ and WT mice were infected with *H. pylori* for one month and their gastric LP leukocytes were analyzed by FACS. Frequencies of IFN-γ⁺ and IL-17⁺ cells among all CD4⁺ T-cells are shown in H. IFN-γ and IL-17 expression in the gastric mucosa, as determined by qRT-PCR, is shown in I. *H. pylori* colonization is shown in J. Data in H-J are representative of 4 independent experiments.

Figure 7

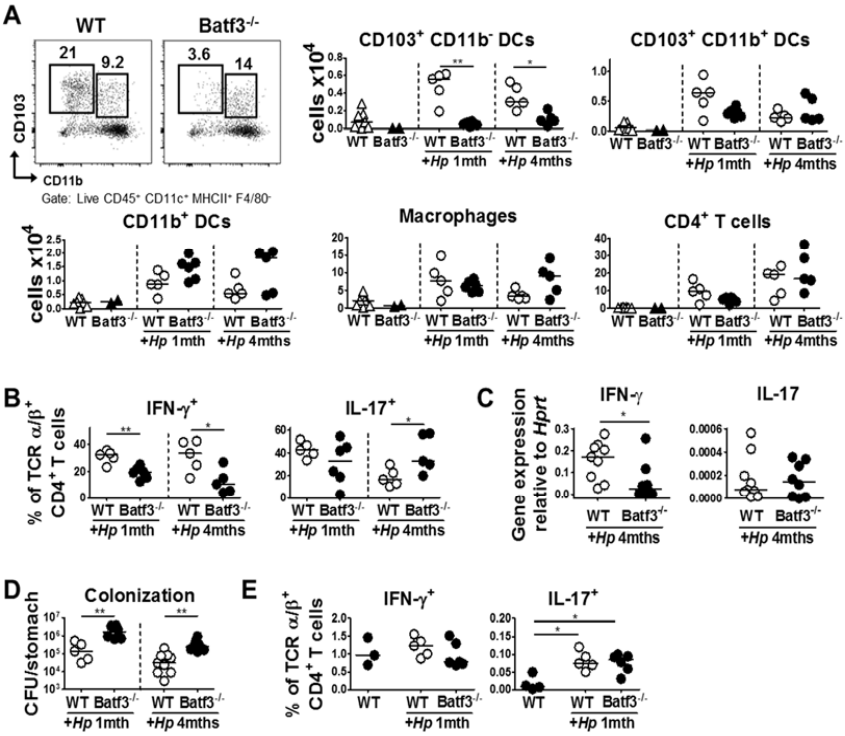

Figure 7. BATF3-dependent DCs are required for Th1 responses and *H. pylori* control. BATF3$^{-/-}$ and WT mice were infected with *H. pylori* for one or four months and their gastric LP leukocytes were analyzed by FACS. **(A)** Absolute counts of the indicated gastric MP and T-cell populations in WT and BATF3$^{-/-}$ mice in the steady state and at one and four months p.i. with *H. pylori*. Representative FACS plots show the specific loss of gastric CD103^{+} CD11b^{-} DCs due to BATF3 deficiency. **(B)** Frequencies of IFN-γ^{+} and IL-17^{+} cells among CD4^{+} T-cells of the mice shown in A. **(C)** IFN-γ and IL-17 expression in the gastric mucosa of the mice shown in A. **(D)** *H. pylori* colonization of the mice shown in A-C. **(E)** Frequencies of IFN-γ^{+} and IL-17^{+} cells among all CD4^{+} T-cells in the MLNs of *H. pylori*-infected WT and BATF3$^{-/-}$ mice; Uninfected WT mice are shown for comparison. In all panels horizontal lines indicate medians. * indicates p<0.05, ** p<0.01, ***p<0.001, as calculated by Mann-Whitney test.

Supplemental Figure 1

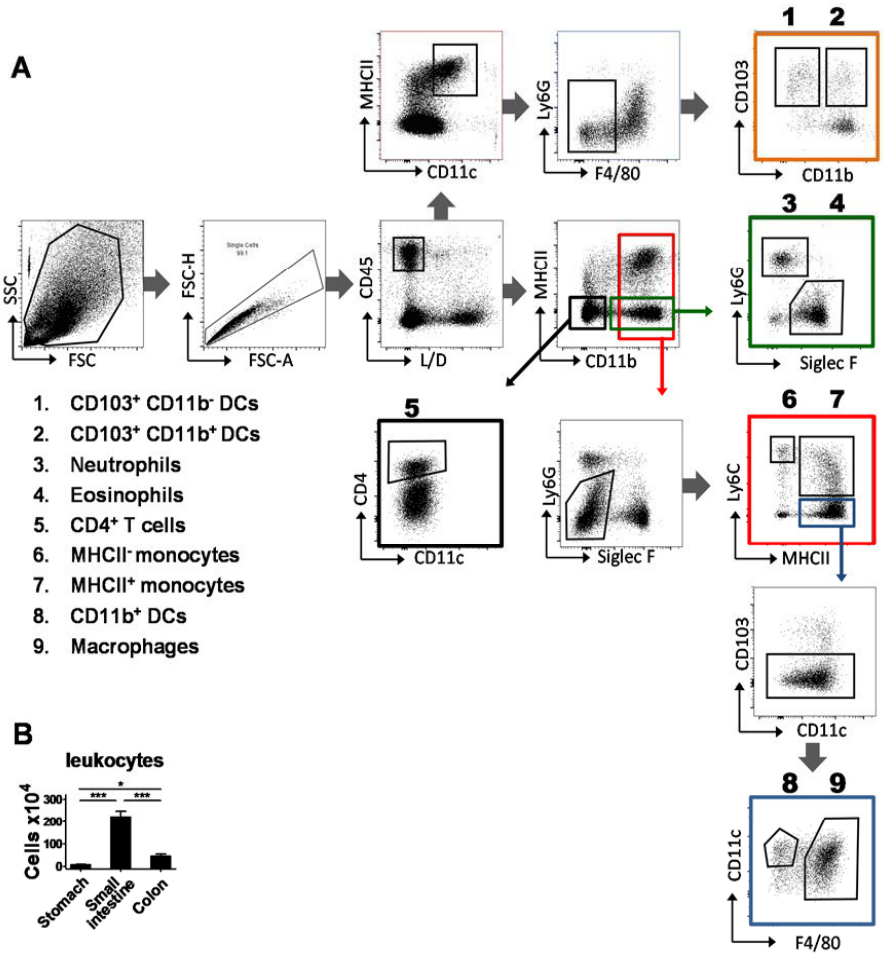

Suppl. Figure 1. Leukocyte populations evolve in the first 8 weeks of life in the gastrointestinal tract. (A) Gating strategy used for the identification and quantification of nine leukocyte populations (1-9) that were isolated by enzymatic digestion and percoll gradient centrifugation and analyzed by flow cytometry. (B) Absolute counts per organ of $CD45^+$ leukocytes of the three indicated gastrointestinal compartments of the mice shown in Figure 1. (C) Absolute counts per organ of total leukocytes, monocytes and macrophages as assessed at the indicated ages. Between 3 and 5 mice were pooled for each time point. STO, stomach, SI, small intestine, CO, colon. In B and C, data are represented as mean +SEM.

Supplemental Figure 2

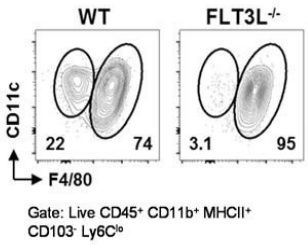

Suppl. Figure 2. CD11b$^+$ DCs require FLT3L for their differentiation. Representative FACS plots of CD11b$^+$ DCs (population circled on the left) and macrophages (population on the right) in WT and FLT3L$^{-/-}$ mice.

Supplemental Figure 3

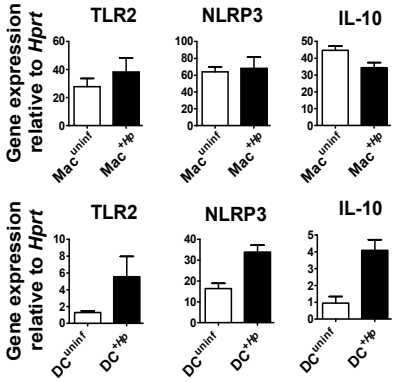

Suppl. Figure 3. CD11b$^+$ DCs and macrophages respond to *H. pylori* in the gastric lamina propria. Expression of TLR2, NLRP3 and IL-10 of FACS-sorted gastric macrophages (Mac) and CD11b$^+$ DCs, as determined by qRT-PCR in 2 pools each of 4 infected and uninfected mice. Data are represented as mean +SEM.

Supplemental Figure 4

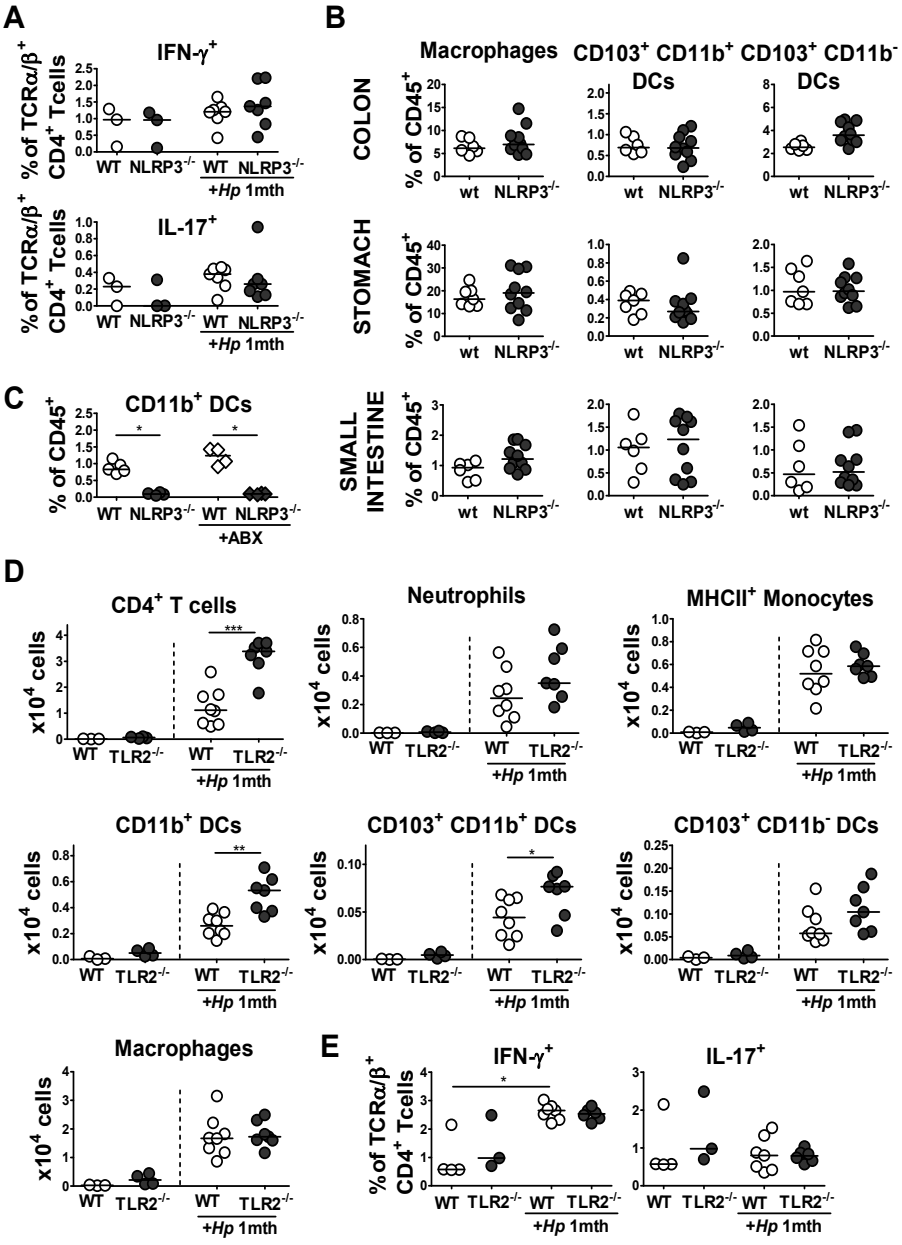

Suppl. Figure 4. CD11b$^+$ DCs require NLRP3 for their differentiation in GI tissues and TLR2 signaling for their functionality. (A) Frequencies of IFN-γ$^+$ and IL-17$^+$ cells among all CD4$^+$ T-cells in the MLNs of *H.*

pylori-infected WT and NLRP3$^{-/-}$ mice as well as three uninfected controls each. Data are from the mice shown in Figure 6A-D, and representative of 4 independent experiments. (B) Frequencies of the indicated DC and macrophage populations in the colons, small intestine and stomach of the WT and NLRP3$^{-/-}$ mice shown in Figure 6E. (C) Frequencies of CD11b^{+} DCs in the colons of WT and NLRP3$^{-/-}$ mice that were either treated or not with antibiotics for 7 weeks. In all panels horizontal lines indicate medians. (D) Absolute counts of the indicated T-cell, neutrophil and MP populations in the gastric LP of the uninfected and *H. pylori*-infected WT and TLR2$^{-/-}$ mice shown in Figure 6H-J. (E) Frequencies of IFN-γ^{+} and IL-17^{+} cells among all CD4^{+} T-cells in the MLNs of the *H. pylori*-infected WT and TLR2$^{-/-}$ mice shown in Figure 6H-J and in panel D.

3. UNPUBLISHED DATA

3.1 The role of β-catenin signaling in DCs during *H. pylori* infection

contribution I planned, conducted and analyzed all experiments, except for lung histology readouts, which were analyzed by Christian Taube.

3.1.1 The regulation of β-catenin signaling *in vitro* during *H. pylori* infection

β-catenin is an important regulator of homeostasis and attenuation of allergic asthma [104,168]. In DCs, β-catenin can be activated by several pathways. One of them is TRL2 signaling, which favors a tolerogenic immune response [99]. As we have shown previously that *H. pylori* induces TLR2 signaling, we aimed to investigate whether *H. pylori* induces β-catenin signaling in DCs of the stomach mucosa and the lung. In addition, we investigated if this is TLR2 dependent.

To this end, the expression of the β-catenin target genes *AXIN2*, a member of the β-catenin destruction complex and *CYCLIND1* (CCND1), which is required for the progression through the G1 phase of the cell cycle, were measured *ex vivo* in bone marrow-derived DCs and $CD11c^+$ enriched spleen DCs. Their expression was compared in DCs from wild type (wt) and TLR2-deficient mice. The transcriptional expression was studied by the means of RT-qPCR analysis. As expected, *H. pylori* infection leads to an increase of CCND1 and AXIN2 transcripts in $CD11c^+$ spleen DCs of wild type mice. This increase is absent in spleen $CD11c^+$ DCs of TLR2 deficient mice (Figure 14A, B).

We next explored which signal induces TLR2-dependent β-catenin activation upon *H. pylori* infection. Having shown previously that the virulence factor urease promotes TLR2 signaling in DCs, we aimed to identify its role for β-catenin signaling [169]. As the activation of β-catenin leads to its stabilization, the protein level of β-catenin was studied after *H. pylori* infection by means of Western Blotting. To this end, BMDCs were cocultured with wt- or ureaseB-deficient *H. pylori*. The results showed that β-catenin stabilizes after *H. pylori* infection, and this stabilization is at least partly urease-dependent (Figure 14C, D). In line with this a slightly reduced expression of AXIN2 in the BMDCs was observed (Figure 14E).

Besides this, it is known that *H. pylori* infection induces IL-10 signaling in tolerogenic DCs favoring T_{reg} induction [164]. We hypothesized that IL-10 secretion after *H. pylori* infection is TLR2-mediated and β-catenin-dependent in DCs. Therefore $CD11c^+$ spleen DCs either from wt or $TLR2^{-/-}$ mice were cocultured with *H. pylori* and the IL-10 expression was evaluated by RT-qPCR. In line with their reduced β-catenin signaling, also the IL-10 expression was diminished in spleen DCs of $TRL2^{-/-}$ mice (Figure 14F) suggesting that β-catenin signaling might be part of the pathway activating IL-10 during *H. pylori* infection of DCs. β-catenin signaling is known to induce IL-10 expression in DCs after exposure to various stimuli such as TGF-β receptor, WNT or TLR2 activation [97]. To assess the role of β-catenin in DCs during *H. pylori* infection, we crossed mice harboring floxed β-catenin alleles [170] with transgenic mice expressing the cre recombinase under the regulation of the CD11c promoter [171]. These mice

are deficient for β-catenin expression in all DC subsets and also in some intestinal macrophages, as they express high levels of CD11c. BMDCs of wt and β-catenin$^{DC-/-}$ mice were cocultured with *H. pylori*. BMDCs from the β-catenin$^{DC-/-}$ mice failed to induce IL-10 transcription, and the IL-10 secretion was reduced, but not totally inhibited by the depletion of β-catenin signaling (Figure 14G, H). Taking together, the results suggest that *H. pylori* induces β-catenin signaling via the TLR2 receptor, which is to a certain degree dependent on *H. pylori* ureaseB. Moreover, *H. pylori*-induced IL-10 transcription is dependent on TLR2 receptor signaling and is at least partially regulated by β-catenin.

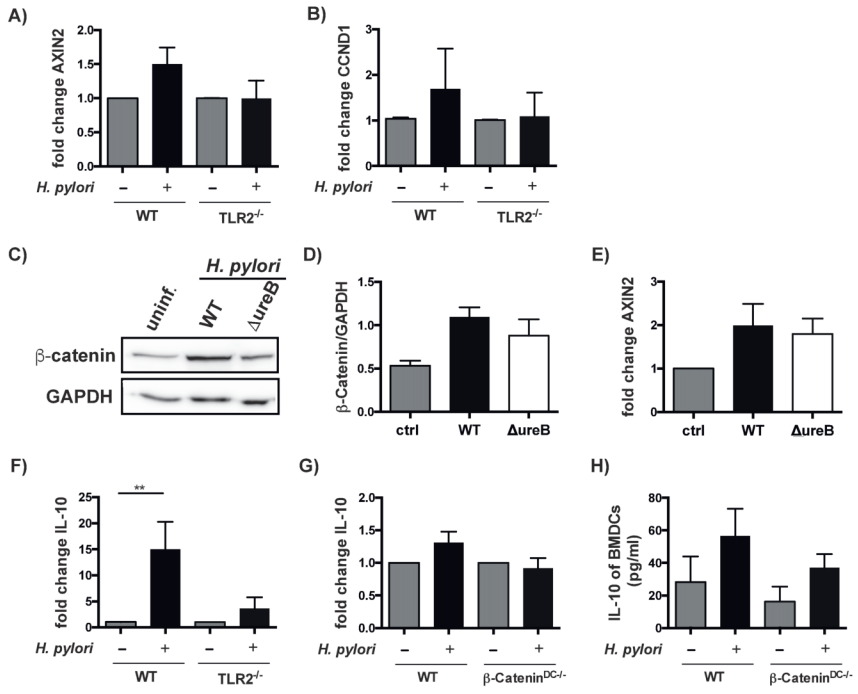

Figure 14: *H. pylori* induces β-catenin activity and IL-10 expression by TLR2 stimulation

Spleen DCs from C57BL/6 wild type mice and TLR2$^{-/-}$ mice were isolated and immunomagnetically enriched for CD11c^{+} cells and infected with *H. pylori* (G27 strain) for 2hrs. The fold change of AXIN2 (A) and CCND1 (B) was assessed by RT-qPCR. BMDCs of C57BL/6 were isolated and cultured with GM-CSF. At day 6, cells were infected with wt *H. pylori* or Δurease *H. pylori*. After 24hrs infection the protein level of β-catenin was visualized by Western Blotting analysis (C) and quantified (D). 2hrs after infection the expression of AXIN2 was assessed by RT-qPCR (E). BMDCs of TLR2$^{-/-}$ and β-catenin$^{DC-/-}$ and control β-catenin$^{DCfl/fl}$ mice were isolated and cultured with GM-CSF. At day 6, cells were infected with *H. pylori* for 2hrs and the IL-10 expression was analyzed by RT-qPCR (F and G). After 24hrs of infection IL-10 was analyzed in the supernatant of the cells by ELISA (H). Data of A, B are pooled from four-, C-E representative from three-, F-H pooled from two independent experiments. Statistical significance was tested by a nonparametric Mann-Whitney U, ** = p<0,01.

3.1.2 *H. pylori* infection increases β-catenin signaling in human monocyte-derived DCs in an urease-dependent manner

After we had determined that β-catenin signaling during *H. pylori* infection in murine BMDCs is at least partially dependent on *H. pylori* urease activity, we set out to confirm this also in human monocyte-derived (MO)-DCs. To this end, mononuclear cells were isolated from human blood samples and enriched for $CD14^+$ $CD11c^+$ cells and cultured with hGM-CSF and hIL-4. In human MO-DCs, *H. pylori* leads to a significant increase of the expression of the β-catenin target genes *AXIN2* and *IL-10* as well as to a slight *CCND1* upregulation. This effect was entirely dependent on ureaseB production by *H. pylori* (Figure 15).

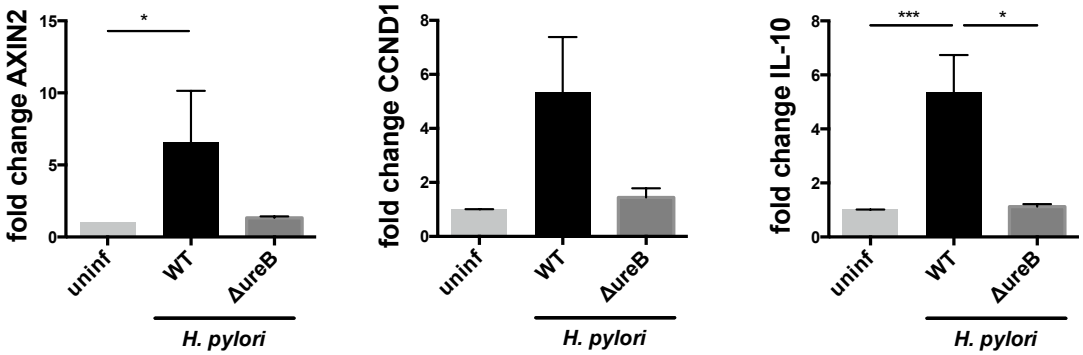

Figure 15: *H. pylori* urease is required for β-catenin target gene activation in human MO-DCs

MO-DCs were isolated from human blood samples and enriched for $CD14^+$ and $CD11c^+$ and cultured with hIL-4 and hGM-CSF. At day six, cells were infected with *H. pylori* or with ΔureB *H. pylori* for 2hrs. Fold change of AXIN2, CylinD1 and IL-10 expression were analyzed by RT-qPCR.

3.1.3. Loss of β-catenin signaling in $CD11c^+$ cells has little if any effect on *H. pylori* induced immune tolerance

β-Catenin signaling in $CD11c^+$ cells plays not an essential role in H. pylori colonization

β-catenin is known to promote intestinal DC tolerogenic activities in steady state. Less is known about the role of β-catenin in gastric DCs. We assessed the role of β-catenin in $CD11c^+$ cells in the stomach, first focusing on its role in controlling *H. pylori* colonization. We observed an *H. pylori*-mediated induction of β-catenin stabilization - and IL-10 transcription *in vitro*, which points in the direction that β-catenin signaling has an anti inflammatory function during *H. pylori* infection and might therefore favor the colonization and persistence of the bacterium in the stom-

ach. To assess this, we made again use of the β-catenin$^{DC-/-}$ mice. As we know that *H. pylori*-induced tolerance can be best studied in the neonatal infection model, β-catenin$^{DCfl/-}$ mice and β-catenin$^{CD11c-/-}$ mice were infected six days after birth, during the neonatal window, for one month. In addition, mice were also infected at the age of four weeks for one month, to mimic the inflamed stomach of symptomatic carriers.

The colonization of neonatal and adult mice was reduced in the β-catenin$^{DCfl/-}$ strain and slightly more in the β-Catenin$^{DC-/-}$ mice compared to the cre^{-} littermate controls (Figure 16A). As expected a generally lower colonization level was observed in the adult infected mice after one month of infection compared to the neonatally infected mice. From previous studies we know that reduced colonization correlates inversely with the inflammation of the stomach, characterized by an increased T_H1 response. Therefore, we expected in the knockout mice, which show a reduced colonization, an accompanying increase in IFN-γ expression, with the most conspicuous differences in adult infected mice. As the neonatal tolerogenic phenotype leads to a much lower T cell infiltration in the gastric LP compared to the adult LP, we analyzed the IFN-γ expression with two different readouts. In neonatally infected mice we studied the IFN-γ expression in the scraped mucosa of the stomach by means of RT-qPCR (Figure 16B). In contrast, in adult infected mice the expression of IFN-γ was detected directly by flow cytometry in LP CD4^{+} T cells (Figure 16C). Neonatally infected mice did not show a great increase of IFN-γ expression in the stomach mucosa (Figure 16B). Surprisingly, we also did not observe an increase of T_H1 producing T cells in the stomach mucosa of adult infected mice. In both cases the IFN-γ level was independent of the presence of β-catenin alleles. In contrast to the neonatal phenotype, we observed in the adult infected β-catenin$^{DC-/-}$ mice a slight increase of T_H1-cells producing IFN-γ in the MLNs (Figure 16D). This goes in line with the reduced colonization in the stomach. As the neonatal phenotype is characterized by a tolerogenic response, we investigated the effect on IL-10 expression. Compared to this, we could observe an increased IL-10 expression in the stomach mucosa of mice deficient for β-catenin in CD11c^{+} DCs (Figure 16E).

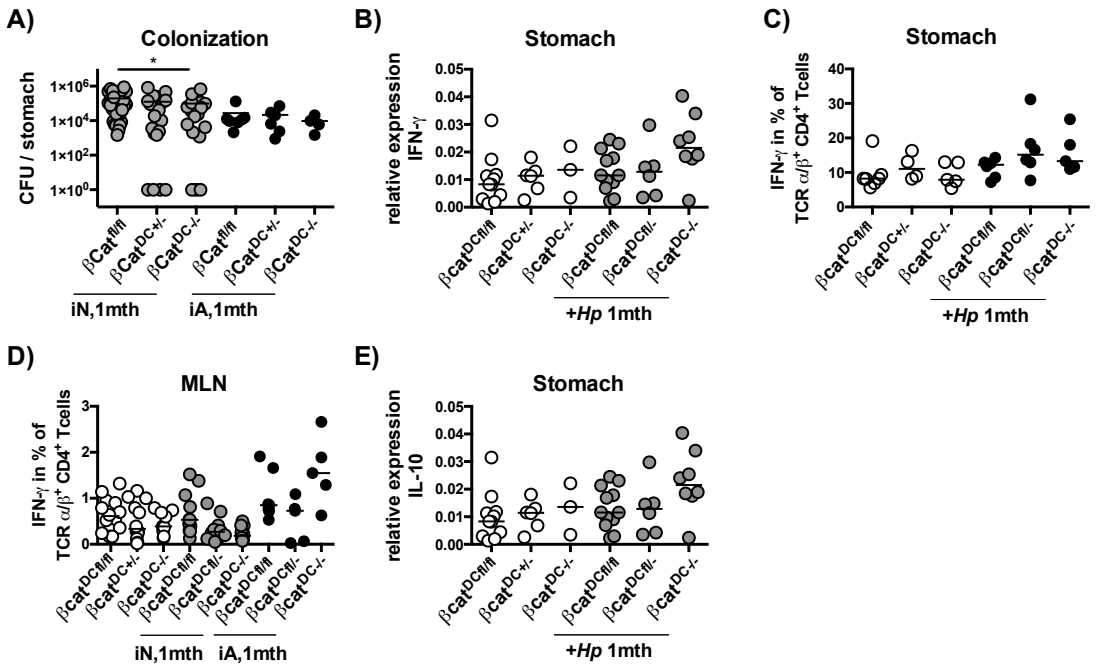

Figure 16: β-catenin signaling in CD11c$^+$ cells plays no essential role in controlling T_H1 responses and *H. pylori* colonization in the gastric mucosa of infected mice

β-catenin$^{DCfl/fl}$, β-catenin$^{DCfl/-}$ and β-catenin$^{DC-/-}$ mice were infected with RFP-expressing *H. pylori* (PMSS1) strain at six to seven days of age (grey dots; iN) or at the age of four weeks (black dots, iA) for one month. We studied the gastric colonization (A), IFN-γ expression in the stomach mucosa by RT-pPCR (iN) (B) and the % of IFN-γ-expressing T cells in the stomach by flow cytometry (iA) (c). In MLN the % of IFN-γ expressing T cells of iN infected and iA infected mice were assessed by flow cytometry (D). IL-10 expression in stomach mucosa was analyzed by RT-qPCR (iN) (E). A & D are pooled data of four-, B, E of two- and C of one representative independently performed experiments. The horizontal bars in each graph indicates the medians.

β-Catenin signaling in CD11c$^+$ cells plays no role in H. pylori uptake and H. pylori induced TLR2 upregulation on myeloid cells

From our manuscript by Arnold *et al.* we know that *H. pylori* encounters CD11b$^+$ DCs, macrophages and inflammatory monocytes in the gastric lamina propria. Therefore, we wanted to address if β-catenin signaling is important in these cells to phagocytose *H. pylori*. Mice were infected as neonates with an RFP-expressing *H. pylori* strain. The RFP signal is detectable in different myeloid cell subsets by flow cytometry analysis (ref. manuscript Arnold *et al.,* 2017). No RFP signal was detectable in the CD103$^+$CD11b$^+$ DCs and CD103$^+$CD11b$^-$ DCs (Figure 17A). An RFP signal was detected in the three expected myeloid cell subsets. However, the loss of β-catenin resulted in less RFP signal in the macrophage compartment (CD11b$^+$CD11c$^{hi/dim}$F4/80$^+$CX3CR1^{hi}). Knowing that β-catenin is activated via TRL2 signaling and TLR2 expression is upregulated on *H. pylori*-infected cells (ref. manuscript Arnold *et al.,* 2017), we set out to study a potential feedback loop of β-catenin signaling on TLR2 expression. Therefore, we compared the TLR2 expression on *H. pylori*-positive myeloid cells of β-catenin$^{DC-/-}$ mice and β-catenin$^{DCfl/fl}$ mice with their wt littermates. Using flow cytometry analysis, we observed an increase of TLR2 expression (MFI) in myeloid cells that had phagocytosed *H. pylori*. TLR2 expression did not increase after infection on *bona fide* DCs in the stomach. However, this increase on CD11b$^+$ DCs, monocytes and macrophages is independent of the presence of the β-catenin alleles (Figure 17B). The differences in *H. pylori* uptake in macrophages do not negatively affect the TLR2 expression in macrophages.

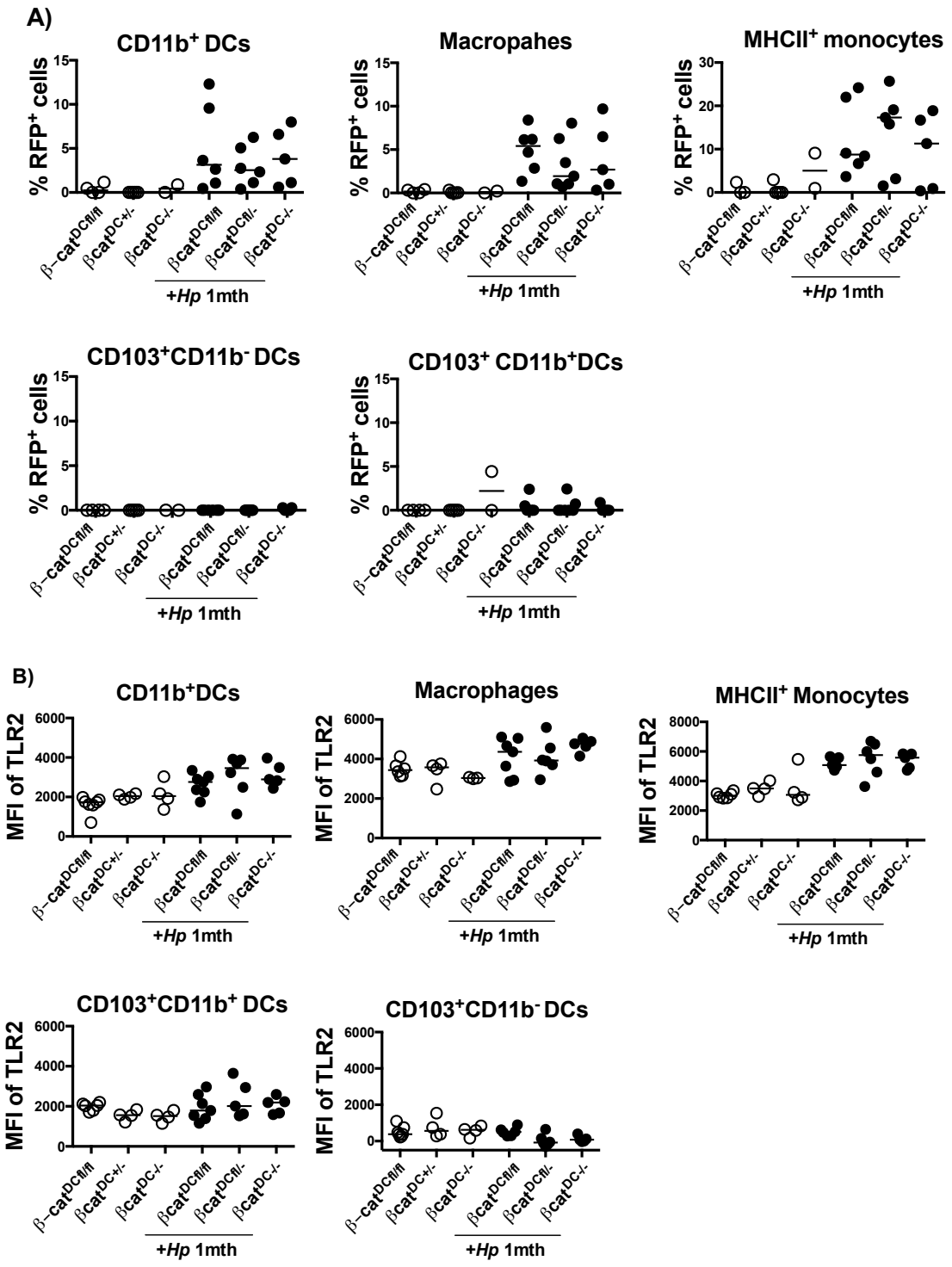

Figure 17: β-catenin signaling in CD11c$^+$ cells is not required for *H. pylori* uptake by gastric macrophages or DCs

β-catenin$^{DC-/-}$, β-catenin$^{DC-/fl}$ and cre$^-$ littermates were neonatally infected with *H. pylori* expressing RFP for one month. RFP-positive signal was assessed by flow cytometry analysis in lamina propria CD11b$^+$ DCs, macrophages, monocytes and CD103$^+$CD11b$^+$ and CD103$^+$CD11b$^-$ DCs (A) and TLR2 expression in the same myeloid cells was quantified by flow cytometry (B). The figure shows data from one experiment.

3.1.4 β-catenin signaling in CD11c$^+$ cells contributes to *H. pylori*-induced allergic asthma protection

A recent study showed WNT1/β-catenin signaling in the lung to be essential to attenuate allergic airway diseases, by inhibiting the ability of DCs to migrate to mesenteric lymph nodes [168]. As we know that DCs play an essential role in *H. pylori*-induced allergic asthma protection, we investigated a potential role of β–catenin activation in CD11c$^+$ cells during *H. pylori*-mediated asthma protection. β-catenin$^{DC-/-}$ mice β-catenin$^{DC-/fl}$ and their cre-negative littermates were infected as neonates and sensitized intranasally with house dust mite (HDM) extract at the age of four weeks and challenged two weeks later five times in a row with HDM intranasally. Control mice were left either untreated or sensitized/challenged with HDM as a positive control. Two days after the last challenge the lungs were analyzed, focusing on lung inflammation and goblet cell metaplasia, two characteristics of allergic airway pathology. β-catenin$^{DC-/-}$ mice are less well protected compared to their cre-negative littermates and their β-catenin$^{DCfl/-}$ littermates. This is indicated in a slightly increased lung inflammation score (Figure 18A) and goblet cell metaplasia as determined by PAS staining of lung sections (Figure 18B). Figure 18 C and D done in separate experiments show that β-catenin$^{DC-/-}$ mice induce symptoms of allergic asthma after sensitization and challenge comparable to wt mice. To sum up, β-catenin signaling in CD11c$^+$ cells seems to have an effect on *H. pylori*-induced protection against allergic asthma.

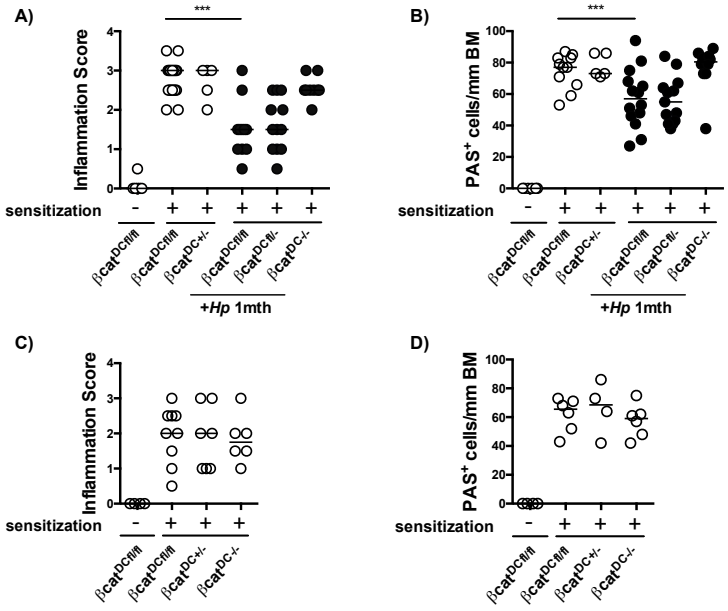

Figure 18: β-catenin signaling in CD11c^{+} cells contributes to *H. pylori*-induced allergic asthma protection

β-catenin$^{DC-/-}$, β-catenin$^{DCfl/-}$ and wt littermate mice were neonatally infected with *H. pylori* and sensitized four weeks after infection intranasally with house dust mite (HDM) allergen. Two weeks later, mice were challenged with HDM on five consecutive days. Two days after the last challenge, lung inflammation was assessed on H&E-stained sections (A&C) and goblet cell metaplasia was quantified on PAS-stained sections (B&D). Data are pooled from two independent experiments each.

3.2 Methods and Material

Animal experiments

C57BL/6 mice were purchased from Janvier and TLR2$^{-/-}$, CD11cCre and β-Catenin$^{fl/fl}$ mice were originally obtained from the Jackson laboratory. All strains were bred and maintained under specific-pathogen-free condition in individually ventilated cages in an accredited animal facility of the University Zurich. All experiments were approved by the Zurich Cantonal Veterinary Office, under the licenses ZH170/2014 and ZH24/2013.

H. pylori strains, culture conditions and colony counting

For the *in vitro* infection *H. pylori* strain G27 were used and for the *in vivo* studies mice were infected with *H. pylori* strain PMSS1. They have been described previously in Covacci *et al*. 1993 and Arnold *et al.,* 2011 [172,173]. The RFP PMSS1 isogenic mutant strain was designed by our collaborator Karen Ottemann and was described before in [174]. For the infection *in vitro* and *in vivo,* bacteria were cultured from frozen stocks on horse blood agar plates containing 12µg/ml Vancomycin, 100µg/ml Bacitracin and 15µg/ml Nalidic Acid at 37°C for 2 days under microaerophilic conditions. They were inoculated for 6 hours in 20ml liquid culture (Brucella broth (Difco) containing 10% FBS (Life Technologies)). Liquid cultures were grown with shaking at 37°C in microaerophilic conditions. For *in vitro* infection *H. Pylori* was cultured for 6hrs or overnight for *in vivo* infection. The Δurease *H. pylori* mutant was cultured on plates and in liquid culture supplemented additionally with 25µg/ml of Chloramphenicol. Mice were infected intragastrically either on day 7 after birth or at the age of 6 weeks with 10^7-10^8 CFU *H. pylori* PMSS1 always for four weeks. All *H. pylori* liquid cultures were routinely assessed by light microscopy for contamination, morphology, and motility prior to use.

HDM-induced allergic asthma

For the induction of HDM-induced allergic asthma six weeks after infection, mice were sensitized i.p. with 1ug of house dust mite extract (HDM) (Greer) dissolved in PBS. Beginning on day 8 post-sensitization, mice were challenged i.p with 10ug HDM on five consecutive days. Two days after the last challenge, mice were sacrificed with CO_2 and were analyzed for asthmatic readouts. For the lung histopathology, lungs were fixed by perfusion and immersion in 10% (vol/vol) formalin and analyzed by our collaborators in Leiden. In short, tissue was embedded in paraffin and the tissue sec-

tions were stained with H&E and periodic acid-Schiff and analyzed blindly with a BX40 Olympus microscope. Goblet cell metaplasia was quantified as the number of PAS-positive goblet cells per 1mm of the basement membrane. The peribronchial inflammation was scored from 0-4, with four being the most inflamed condition.

Generation and infection of BMDC, spleen DCs and human blood-derived DCs

For the generation of murine bone marrow derived DCs (BMDCs), the femur and tibia of donor mice (C57BL/6, TLR2$^{-/-}$ and β-Catenin$^{DC-/-}$) were flushed with full RPMI medium (10% (vol/vol) FCS, 100 U/ml penicillin/streptomycin). Cells were treated with red cell blood lysis buffer (Roche) for 1min, the reaction was stopped with RPMI medium. 2x10^6 cells were seeded in 6well plates for WB or 50.000 cells in 96-well plates for ELISA in full RPMI medium and 20ng/ml GM-CSF. The same volume of medium was added every 3 days during the whole period of 7 days. BMDCs were infected for 16h with *H. pylori* at a multiplicity of infection of ~50.

For the isolation of splenic DCs, cell suspensions were prepared by digestion using 1mg/ml CollagenaseD and 0.1% DNaseI (both from Roche) in serum-free RPMI for 1h at 37°C. Erythrocytes were lysed with 1ml ACK lysis buffer for 2 min. DCs were immunomagnetically isolated using CD11c MicroBeads (Miltenyi Biotec) according to the manufacturer's instruction and seeded at 2x10^5 cells per well in 96 well round bottom plates. Cells were infected with *H. pylori* at a multiplicity of infection of ~50 directly after seeding for two or four hours.

For the generation of human DCs, peripheral blood mononuclear cells (PBMC) were isolated from buffy coats using Ficoll-Paque^{TM} (GE Healthcare) of healthy volunteers obtained from the blood donation centre Zürich (ZHBSD). CellGro DC medium (Cellgenix) supplemented with 1000U/ml GM-CSF and 500IU/ml IL-4 (both R&D Systems) for 6 days. Cells were infected with *H. pylori* at a multiplicity of infection of ~50 for two hours.

Leukocyte isolation

To isolate the leukocyte population of the lamina propria the stomach was isolated and opened longitudinally and cut into three pieces and stored in RPMI medium. To remove epithelial cells the stomach was washed with Hanks' balanced salt solution with 10% FCS and 5 mM EDTA at 37°C. To digest the stomach, it was incubated in RPMI (10% FCS and 100 U/ml penicillin/streptomycin) supplemented with 0.05 mg/ml DNase I and 500 U/ml of type CollagenaseIV (Sigma-Aldrich) for 50min, at 37°C in a shaking incubator. To enrich the leucocyte population cells were layered on

a 40/80% Percoll gradient and centrifuged for 18min. The interface was collected and washed in PBS with 0.5% BSA.

Flow cytometry, cell counting

To perform a surface staining cells were stained in PBS and 0.5% bovine serum albumin with a fixable viability dye and FC- block to reduce unspecific antibody binding, with the following antibodies: anti-mouse CD45 (30-F11), CD45.1 (A20), CD45.2 (104), CD11c (N418), MHCII (M5/114.15.2), F4/80 (BM8), CD103 (M2E7), CD11b (M1/70), Ly6G (1A8), Ly6C (HK1.4), CD4 (RM4-5) and TCRβ (H57-597) (all from BioLegend); anti-mouse CD282/TLR2 (6C2, Affymetrix). For the intracellular T cell staining, cells were incubated in complete IMDM medium, which was supplemented with 0.1uM phorbol 12-myriste 13-acetate and 1ul ionomycin with 1:1000 Brefeldin A (eBioscience) and GolgiStop solution for 3.5 hrs at 37°C with 5% CO_2. After the staining, cells were fixed and permeabilized with Cytofix/Cytperm Fixation/Permeabilization Solution Kit following the manufacturer`s instruction. Cells were stained with the antibodies IFN-γ (XMG1.2, Biolegend) and IL-17 (TC11-18H10.1) for 50 min. Before the analysis countBright^{TM} absolute counting beads (Life technologies) were added to each sample. All samples were analyzed on a LSRII Fortessa (BD Biosciences). The analysis was performed with the FlowJo software (Tree-Star).

Western Blot

BMDCs were sonicated with a BIORUPTOR® (Diagenode) for 5 minutes. The protein extracts of BMDCs were made in RIPA-Buffer (50mM Tris-HCl, pH 8.0, 150mM sodium chloride, 1% NP-40, 0.5% sodium deoxycholate, 0.1% SDS) supplemented with 2mM sodium orthovanadate, 15mM sodium pyrophosphate, 10mM sodium fluoride and 1X complete protease inhibitor cocktail (Roche). Samples were diluted 1:5 with loading dye and heated up to 90°C for 5min. The same volume of the sample was separated in an 8% Tris-glycine SDS-Polyacrylamide gel followed by transfer onto nitrocellulose membranes. Membranes were probed with antibodies against β-catenin (1/2000, AbCam) and GAPDH (1/5000, Sigma Aldrich). The membrane was analyzed using a FUSION Solo (Vilber Lourmat) with Fusion software. Pictures were analyzed and quantified using ImageJ software.

ELISA

The supernatants of infected BMDCs were subjected to IL10-ELISA after 24hrs of co-culture. To quantify IL-10 abundance the mouse BD OptEIA IL-10 ELISA (Bioscience) was used according to the manufacturer's instructions. Samples were diluted 1:2 using assay diluent. Plates were analyzed after 10-15 minutes developing time, using a microplate reader SpectraMax i3 (Molecular Devices) with SoftMax Pro 6.4 software.

Quantitative RT-PCR

RNA was isolated from scraped stomach mucosa and BMDCs using the NucleoSpin® RNA II Kit (Macherey-Nagel) or from spleen DCs and MO-DCs using the RNeasy Mini kit (QIAGEN) according to manufacture's instructions. The RNA concentration was determined by the NanoDrop® ND-1000 Spectrophotometer (WITEC AG) and adjusted to 1υg RNA per sample. Complementary DNA synthesis was performed using SuperScriptIII reverse transcriptase (Invitrogen) in a T3000 Thermocycler (Biometra). Quantitative PCR reactions for the candidate genes were performed using either SYBER-Green or TaqMan gene expression assay. The following TaqMan probes were used: (Ifnγ Mm01168134_m1, Il17a Mm00439618_m1, Il10 Mm01288386_m1, AXIN2 Mm00443610_m1, HPRT Mm03024075_m1). SYBER Green primers are listed below and were designed with an annealing temperature of 60°C and 50 cycles. Complementary cDNA was analyzed on a Lightcycler 480 instrument. Samples were measured in duplicates and the relative gene expression was normalized to GAPDH or HPRT. The mean relative gene expression was determined, normalized to the internal control and calculated using the 2ΔC(t) or respectively the 2ΔΔC(t) method.

Species	**Target sequence**		**Sequence**
murine	AXIN2	fw	AAC CTA TGC CCG TTT CCT CT
		rw	CCA CAC ATT TCT CCC TCT CC
	IL-10	fw	CAG AGC CAC ATG CTC CTA GA
		rw	TGT CCA GCT GGT CCT TTG TT
	GAPDH	fw	GAC ATT GTT GCC ATC AAC GAC C
		rw	CCC GTT GAT GAC CAG CTT CC
human	AXIN2	fw	GCT GAC GGA TGA TTC CAT GT
		rw	ACT GCC CAC ACG ATA AGG AG
	IL-10	fw	AAG GGC AAT TTA ATC CAAA GGT T
		rw	TTT GGT TTC CTC ACC CTA CTG T
	RPLPO	fw	CAG CAG CTG GCA CCT TAT TGG
		rw	CCA GCT CTG GAG AAA CTG CTG

Statistical analysis

Statistical analysis was performed with Prism 6.0 (GraphPad Software). The nonparametric Mann-Whitney U test was used for all statistical comparisons. Median values are indicated. Stars are used to show the statistically significance according to the p-value: * $p<0.05$, ** $p<0.01$.

DISCUSSION

1. THE ROLE OF MACROPHAGES AND CD11b$^+$ DCs IN *H. PYLORI* INFECTION

1.1 The MP compartment differs between gastric, small intestinal and colonic mucosa

Much is known about the murine myeloid compartment of the colon and the intestine. Most studies of the intestinal tract focus on understanding the regional specification of different cell populations and their function in homeostasis in an adult setting [175,176]. Others have studied the microbial composition during early development or how nutrition can shape cell maturation and composition [177,178]. Besides this a lot of research focuses on inflammatory dysfunction of the gut such as IBD or the interplay between immune system, microbiota and dietary habits [179]. However, there is only little literature about the composition and the function of the myeloid compartment in the gastric lamina propria. In general not much literature focuses on the developmental differences in these myeloid compartments - stomach, intestine and colon - from the neonatal period towards adult age [180]. Therefore, we compared the three organs during development and made several unexpected findings. First, myeloid cells are the main population in the gastric mucosa in steady state, which is in clear contrast to the colon and intestine, where lymphocytes are the dominant cell type. The gastric lamina propria is colonized with myeloid cells such as CD103$^+$, CD11b$^+$ DCs and macrophages, which decrease from neonatal age until adult age in steady state. One week after birth the overall amount of CD11b$^+$ DCs is the highest compared to all other cell types and decreases gradually afterwards. The same is true for the *bona fide* DCs three weeks after birth. At the time of weaning the amount of CD103$^+$ DCs decreases. This trend stands in clear contrast to the myeloid compartment of the small intestine, which shows a gradual increase of all major cell subsets. Overall, the colon and the gastric lamina propria show many similarities except the development of CD11b$^+$ DCs, leading to the hypothesis, that both organs might have similar functions with regard to their immunologic compartment.

Several studies were performed mainly to identify the tolerogenic or inflammatory role of DCs during *H. pylori* infection, but did not focus on the cell composition in the gastric mucosa. A previous publication of Kao *et al*. has investigated the effect on DCs directly after a *H. pylori* infection in cryo- and paraffin-embedded sections of the stomach. They made use of GFP-expressing *H. pylori* and observed an influx of DCs

into the gastric lamina propria of mice as early as 6 and 48hrs after infection. However, five days after infection these authors hardly saw any DCs in the stomach and speculated that in an acute infection DCs are recruited very rapidly and then immediately migrate to the draining lymph nodes [181]. Another study has focused on human samples and detected an increased amount of DCs in the stomach of infected patients [182]. We were now able to investigate the behavior of all myeloid cells over the time of one and three months, and saw an increase of the absolute cell amount of all myeloid cells during infection. The main incoming cells are lymphocytes followed by neutrophils, macrophages, inflammatory monocytes and the various DC subsets. In the adult infection model, these lymphocytes have a clear T_H1 polarization. This goes in line with previous studies in our lab, showing that adult-infected mice induce a T_H1 response. In contrast, neonatally infected mice fail to induce a T_H1 response and rather are skewed towards T_{reg} differentiation. This difference in T cell differentiation might be explained by the fact that during the neonatal phase the overall amount of regulatory $CD11b^+$ DCs and macrophages is higher compared to an adult stomach

1.2 CCR2 dependent recruitment of macrophages and DCs

As described above, *H. pylori* infection triggers an influx of T cells, neutrophils and also of specific myeloid cells in the gastric mucosa. We could show that this influx of myeloid cells is dependent on CCR2 signaling. However, only $CX3CR1^{dim}CD11b^+$ MPs, monocytes and macrophages are dependent on cell-intrinsic CCR2 signaling for their recruitment during *H. pylori* infection, as we could show in bone marrow chimera experiments. In contrast *bona fide* $CD103^+$ DCs do not rely on CCR2 and are present in normal cell numbers in infected mixed chimera mice. This leads to the assumption, that during inflammation, $Ly6C^{hi}CX3CR1^{dim}$ monocytes, resident $CX3CR1^{hi}$ macrophages and $CX3CR1^{dim}CD11b^+$ MPs are replenished by CCR2-dependent blood borne $Ly6C^{hi}$ monocytes, which enter the gastric lamina propria. These results go in line with previous studies in the intestine and colon [66,183]. Bain *et al.* showed that also in the colon $Ly6C^{hi}CX3CR1^{dim}$ monocytes and $CX3CR1^{hi}$ macrophages are replenished by $Ly6c^{hi}$ monocytes in a CCR2-dependent manner using a dextran-induced colitis model. They showed, that this holds true even for the steady state. Besides this, they observed that during inflammation, $Ly6C^{hi}$ monocytes do not fully develop into macrophages in their model, but rather arrest as $Ly6C^{hi}CX3CR1^{dim}$ inflammatory monocytes. In contrary, we observed also an increase of macrophages beside $Ly6C^{hi}$ monocytes after infection with *H. pylori* in wt mice. This suggests that an *H. pylori*

infection don not lead to a total disruption of monocyte differentiation into CX3CR1^{hi} macrophages. These differences in the studies may be explained by the use of totally different models, as *H. pylori* has also a regulatory function, which might allow the development towards tolerogenic macrophages. However, this needs to be further investigated by means of cytokine profiling. Moreover, we observed a strong dependency of CX3CR1^{dim}CD11b^{+} MPs on CCR2. Further characterization of this population revealed that these cells are on the one hand FLT3-dependent but additionally express TLR2 and CX3CR1 and are CCR2-dependent. This leads to the suggestion that these cells in the gastric mucosa exhibit properties of *bona fide* DCs as well as of macrophages. Beside this, it is now clear that some *bona fide* CD11b^{+} DCs are able to express CCR2 and also pre-DCs might express CCR2 [30,33,184]. Bain *et al.* found in steady state and in a colitis model, that CD11b^{+}CCR2^{+} DCs are FLT3-dependent and derive from DC progenitors, and cannot be replenished by Ly6C^{hi} monocytes [66]. This supports the hypothesis of CD11b^{+} DCs being *bona fide* DCs.

1.3 CD11b^{+} DCs, Ly6C^{+} monocytes and macrophages phagocytose *H. pylori* in the gastric mucosa

The gastrointestinal tract promotes the absorption of nutrients and allows the growth of commensals but at the same time has to distinguish them from harmful microorganisms. It is still a matter of discussion how antigen sampling pathways handle luminal antigens in the stomach and the intestine. It is now well-accepted that antigens are taken up by specialized microfold cells in the Peyer`s Patches [185]. Several papers reported that CX3CR1-expressing mononuclear cells are able to form transepithelial dendrites to take up soluble antigens in the intestine [71,73]. Consequently, we were interested in understanding the uptake of *H. pylori* in the stomach and the potential role of CX3CR1^{hi} macrophages and CX3CR1^{dim}CD11b^{+} DCs. To better follow this process *in vivo*, our collaborator Karen Ottemann generated a PMSS1 *H. pylori* strain expressing RFP under the urease promoter. This strain can be detected *in vitro* 48hrs after infection of BMDC culture and *in vivo* even after one month of infection. To specifically detect *H. pylori* in CX3CR1^{+} mononuclear cells, we infected the CX3CR1$^{GFP/+}$ reporter mice with RFP-expressing *H. pylori*. We could detect an RFP signal in inflammatory monocytes, CX3CR1^{hi} macrophages and CX3CR1^{dim}CD11b^{+} DCs. To our surprise, we could not detect a RFP signal in any CD103^{+} DC subset. This was unexpected, as CD103^{+} DCs are essential for a T_H1 response and for controlling *H. pylori* colonization. These findings go in line with the literature, as several publications argue that CX3CR1^{+} macrophages are essential for soluble antigen and patho-

gen uptake in the intestine [73,185,186]. Niess *et al.* revealed that CX3CR1$^{GFP/GFP}$ mice, which harbor a GFP-knock-in instead of the CX3CR1 gene, cannot extend dendrites into the gut lumen [71]. These mice were deficient of developing oral tolerance against ovalbumin. Mazzini *et al*. further raised the hypothesis that in the intestine, soluble fed antigens can be taken up via transepithelial dendrites only by CX3CR1^{hi} macrophages [73]. They report that CX3CR1^{hi} macrophages can transfer the antigen via gap junction to CD103^{+} DCs. Thereby the gap junction protein Cx43 functions as a docking molecule. It allows DCs to acquire membrane domains containing a MHCII complex of the macrophages, potentially via trogocytosis. Only CD103^{+} DCs not CX3CR1^{hi} macrophages are able to migrate to the lymph nodes, where they induce T cell response [7,72]. Surprisingly, we do not see a significant increase of CD103^{+} DCs in the MLN after infection with *H. pylori*. Probably this is due to the analysis of the whole MLN, which also drains the small intestine and colon. The stable cell number of circulating CD103^{+} DCs from the gut might outnumber and mask the invading CD103^{+} DCs cells from the stomach. Beside this, we could not detect an increase in the CX3CR1^{dim} population in the MLN after *H. pylori* infection supporting the hypothesis by Schulz *et al*., that these cells do not migrate to the lymph nodes and that the antigen transfer to CD103^{+} DCs might occur locally in the stomach [72]. Until now, no reports investigated the role of CX3CR1^{dim}CD11b^{+} DCs in antigen uptake. Cerovic *et al*. only showed that these cells are able to migrate to the lymph nodes and prime T cells [187]. The role of this DC subset in origin and function needs to be further investigated in the gastrointestinal tract. This leads to the suggestion that beside DCs also other cells are necessary to build up the immune response in the MLNs. Up to now we cannot rule out that *H. pylori* antigen travels to the MLN via the lymph in a non-cell-associated fashion. However, we do not see any RFP signal in any MLN cell and cannot detect any live bacteria in the MLN by plating even under conditions when we detect a robust RFP signal in the myeloid compartment of the stomach. Additionally, a technical limitation of RFP-detection in MLN cells after the death of bacteria could also be an explanation.

Until now, the importance of the CX3CR1-dependent mechanism is still under debate, as it was only observed in the duodenum so far [73]. However, our own data suggest, that at least in the gastric LP CX3CR1 macrophages are able to take up *H. pylori.* In a next step the potential interaction between CD103^{+} DCs and CX3CR1 macrophages via gap junctions and the effect for an *H. pylori* infection might be studied. To this end Gja1$^{fl/fl}$ x Itagx-Cre mice, whose Cx43 is conditionally deleted in CD11c^{+} cells, could be used. To further study the role of CX3CR1^{+} mononuclear cells during *H. py-*

lori infection in more detail, we are currently investigating the phenotype of mice depleted for $CD11c^{+}CX3CR1^{+}$ cells by using CD11cCre x CX3CR1Stop-DTR mice. In the future we will also study the more specific depletion of macrophages by using LysMCre or CD64Cre x CX3CR1Stop-DTR mice.

To sum up, we could show that *H. pylori* is taken up by $CX3CR1^{hi}$ macrophages, monocytes as well as $CX3CR1^{dim}$ $CD11b^{+}$ DCs *in vivo*, which nicely supports the existing literature. However, the role of these cells in *H. pylori* infection has not further been studied so far.

1.4 Upregulation of tolerogenic mediators after *H. pylori* encounter

1.4.1 H. pylori encounter leads to an upregulation of TLR2 and NLRP3 transcription in mononuclear phagocytes

Having figured out which cells are taking up *H. pylori,* we were interested in investigating the transcriptional consequences for these cells. We focused on IL-10, TLR2 and NLRP3 expression. We and others could show that TLR2 and NLRP3 are important for *H. pylori* detection and for the induction of a tolerogenic immune response [85,169,188]. Specifically, we could show that the TLR2/NLRP3/IL-18 axis is induced after *H. pylori* infection of BMDCs, leading to a tolerogenic phenotype [169]. This will be discussed in more detail in the next chapter. Additionally, we know from several studies with different knockout mice that $TLR2^{-/-}$, $NLRP3^{-/-}$, $Caspase\text{-}1^{-/-}$ and $IL\text{-}18^{-/-}$ mice copy the phenotype of T_{reg} or DC depletion in mice during *H. pylori* infection. This phenotype is characterized by increased inflammation and severe pathology [164,169]. To now study the effect at the transcriptional level on cells phagocytosing *H. pylori,* we infected mice with RFP-expressing *H. pylori* and compared sorted RFP^{+} cells with RFP^{-} cells from the same mice. *H. pylori*-encountered $CD11b^{+}$ DCs and macrophages expressed more TLR2 and NLPR3. In contrast to $CD11b^{+}$ DCs, the expression of TLR2 and NLRP3 in $CD103^{+}$ DCs, which do not take up *H. pylori,* was much lower in general and did not increase after infection. We hypothesized based on these findings that the contact of *H. pylori* leads to an upregulation of TLR2/NLRP3 transcription. NLRP3 and TLR2 signaling are tightly linked to a tolerogenic immune response during *H. pylori* infection. The combined results suggest that $CD11b^{+}$ DCs favor a tolerogenic immune response in *H. pylori* infected stomachs. In addition, we found this cell type is dominant and most abundant in the murine gastric LP during the time of the tolerogenic window, between the first two weeks after birth. This

might explain the tolerogenic response against a neonatal *H. pylori* infection, which is not so pronounced in an adult infection.

1.4.2 H. pylori encounter induces IL-10 expression in CD11b$^+$ DCs

To further confirm the assumption that *H. pylori*-exposed CD11b$^+$ DCs favor immune tolerance, we studied their IL-10 expression upon *H. pylori* encounters in the same setup. We focused on IL-10 as a classical and mainly tolerogenic immune regulator [189]. The same CD11b$^+$ DCs which upregulate TLR2 and NLRP3 also have an increased IL-10 expression, supporting the hypothesis that these cells gain a tolerogenic phenotype upon *H. pylori* contact in the stomach. This goes in line with the results from Engler *et al.* where we could show that DC-specific IL-10 expression is essential for *H. pylori*-mediated protection against OVA-induced asthma, by making use of the CD11c-Cre x IL-10$^{fl/fl}$ mice. Mice deficient for IL-10 in CD11c$^+$ cells were not protected from allergic asthma by *H. pylori* anymore, compared to their IL-10 proficient littermates. Furthermore, these mice revealed increased inflammation and concomitantly less bacterial colonization in the gastric mucosa, supporting the tolerogenic role of DC-specific IL-10 signaling [190]. In contrast to the sorted DCs, we could observe a reduction of IL-10 transcripts in sorted RFP$^+$ CX3CR1^{hi} macrophages, suggesting a diminished tolerogenic function after *H. pylori* contact. This is surprising, as we know from literature that CX3CR1$^+$ macrophages regulate anergy during immune homeostasis and also inflammation mainly by expressing IL-10. Further, Bain *et al.* observed no significant changes in their transcription profiles during infection [66]. Taken together, all these data support the assumption that CD11b$^+$ DCs favor a tolerogenic, rather than inflammatory environment upon *H. pylori* encounter.

2. THE ANTI-INFLAMMATORY ROLE OF TLR2/NLRP3 IN *H.PYLORI* INFECTION

2.1 *H. pylori* induces TLR2-dependent NLRP3 transcription

It is known that IL-18 signaling is activated upon *H. pylori* infection. However, for a long time the underlying signaling pathway was not known. To this end, we initially asked which pattern recognition receptor was able to induce caspase-1. Neither NLRC4, NLRC6 nor AIM2 were required. Only NLRP3 and ASC were essential. In the next step, by studying the relevant TLRs activating NLPR3, we only identified TLR2 activation as being essential in inducing IL-1β and IL-18 expression. In line with this,

Kim *et al.* observed a dependency of IL-18 and IL-1β on TLR2/NLRP3 signaling. In contrast, we observed the transcription of pro IL-1β to be dependent on *H. pylori* LPS, which signals via TLR4/MyD88.

As we know that urease induces TLR2, we wanted to understand the molecular mediators inducing NLRP3. Therefore, we studied the role of NF-κB, as it is known to induce NLRP3 upon *E-coli* LPS treatment [84]. A further publication revealed that several bacterial products or isolated PAMPS are able to induce this signaling pathway not only in DCs [191,192]. Rapsinski *et al.* could show that insoluble amyloids in biofilms of *Salmonella Typhimurium* and *Escherichia coli* induced IL-1β by the activation of TLR2 and NLRP3. In this publication, the authors studied TLR2-induced NLRP3 activation in HEK and BMDM cells. It suggests that this pathway is not only restricted to DCs *in vitro* [193]. This supports our findings of TLR2 and NLRP3 upregulation in DCs and in macrophages upon *H. pylori* encounter. In a next step we now plan to investigate in $TLR2^{-/-}$ mice whether NLRP3 expression is also dependent on TLR2 in these cells.

2.2 Urease B induces IL-1β and NLRP3 expression

As mentioned in the previous section we investigated the role of ureaseB during *H. pylori* infection. We were curious to know which bacterial factors induce IL-1β and NLRP3 activation. Therefore, we performed a screen with a transposon library to find mutants that lack the ability to trigger IL-1β secretion. UreaseA and B, two urease subunits from the urease enzyme, were repeatedly detected in this screen. Urease is active in the bacterial cytosol and periplasm and catalyzes the hydrolysis of urea to carbon dioxide and ammonia. This leads to an increase of the pH to a neutral level and the ability for *H. pylori* to survive and colonize the human stomach. The finding that also other *Helicobacter* strains express urease despite living in non-acidic conditions leads to the hypothesis of additional essential functions of urease for the bacterium [194]. UreaseB can be secreted by *H. pylori*. We consequently suggested that ureaseB might act as a PAMP. We observed that only ureaseB but not A was able to rescue the IL1-β and caspase-1 activity after an infection with a urease mutant strain. This supports that not the catalytic activity but rather a structural part is essential for the rescue. In contrast, we could not rescue this phenotype in $TLR2^{-/-}$ DCs stressing the interaction between ureaseB and TLR2. Moreover, our results conclude that urease activates NF-κB, which concomitantly induces NLRP3 transcription via MyD88, a classical adaptor for NF-κB signaling.

However it needs to be mentioned, that neither ureaseB nor TLR2 signaling is able to lead to the assembly of the inflammasome by itself. Both were only able to induce transcription of NLRP3 which elucidates that further factors are necessary for the assembly. Summarizing the literature, it seems that *H. pylori* infection induces the NLRP3 inflammasome assembly by a variety of signals, rather than one specific ligand alone. Semper *et al.* observed a dependency of CagA and VacA on the inflammasome assembly in BMDCs [188]. We observed with both factors minor effects on the IL-1β expression suggesting that they might play a role in the assembly. Semper *et al.* further suggest, that the generation of ROS and potassium efflux is responsible for NLRP3 activation. A blockage of potassium by additional KCL into the cell culture and a treatment with a ROS inhibitor reduced the IL-1β production. A potential link could be the ability of the *H. pylori* virulence factor VacA to induce ROS and a potassium influx. Another report underlines the speculated NLRP3 activation by bacterial products; here K^+-dependent activation was observed for the bacterial toxin nigericin derived from *Streptomyces hygroscopicus* [195]. Further reports point out that NLRP3 can be activated by increased intracellular $Ca2^+$ concentrations [196,197]. CagA can regulate the $Ca2^+$ concentration in a PLC-dependent manner. This leads to the hypothesis that CagA might be important for NLRP3 regulation, knowing that CagA interacts with many host proteins within the cell to regulate growth, morphology and motility [198]. If we consider, that more than one factor induces the assembly of the inflammasome it might be of interest to make use of recombinant proteins to analyze the effect more in detail.

To sum up, we could show that ureaseB is important to activate NLRP3 in a TLR2-dependent manner, to induce inflammasome activation and to secrete IL-1β and IL-18.

2.3 NLRP3- an anti-inflammatory regulator

In the last year, the view on the NLRP3 signaling which favors the secretion of the cytokines IL-1β and IL-18 as a sole pro-inflammatory mediator has changed. This goes in line with our data and a previous publication from our lab, showing that NLRP3 activation in *H. pylori* infection favors a tolerogenic milieu. Engler *et al.* could show, that NLRP3 via IL-18 protects mice from spontaneous colitis [199]. Several other publications underline the anti-inflammatory function, especially of IL-18, in the gastrointestinal tract [200,201]. Dupaul-Chicoine *et al*. observed, that the application of IL-18 rescued the mucosal tissue damage in caspase-$1^{-/-}$ mice [200]. In our lab, Hitzler *et al*. identified IL-18 as a mediator regulating tolerogenic responses to *H. pylori* [141].

Here we linked this IL-18 activation with the increase in T_{reg} expression [169]. This induction was not only seen in MLN but also in the lung, explaining one reason for the *H. pylori*-mediated protection against allergic asthma [164].

2.4 NLRP3 is required for CD11b$^+$ DC differentiation in gastrointestinal tissues

Even though NLRP3 is the best-studied NLR and represents a pivotal host mechanism to sense diverse danger signals, its functionality and role in MP recruitment in the gastric LP is poorly investigated. From previous studies we know that NLRP3 is mostly expressed in macrophages and CD11b$^+$ DCs and to a lower extent in CD103$^+$ DCs. To further investigate NLRP3 function, we first compared the MP composition in wt and NLRP3$^{-/-}$ mice. To our surprise, the NLRP3 knockout mice showed a defect in recruiting CD11b$^+$ DCs in steady state and during *H. pylori* infection. By studying mixed chimera to investigate the cell-intrinsic requirement of NLRP3 during *H. pylori* infection, we observed a dependency of the CD11b$^+$ DC differentiation on NLRP3 expression in the gastric LP. These mice are characterized by a reduced colonization and concomitant increased T_H1 response in the gastric LP. Consequently, we also studied the intestine and colon, where we observed the same effects for CD11b$^+$ DCs in NLPR3$^{-/-}$ mice. As the digestive tract is highly exposed to commensals and pathogens, which might affect the cell composition, we depleted the microbiota by antibiotic treatment [202,203]. But the results revealed that a non-microbiota regulated activation of NRP3 is essential for CD11b$^+$ DC migration. As several studies point out the dependency of NLRP3 signaling on TLR2 activation, we expected the same phenotype also in the recruitment of CD11b$^+$ DCs in TLR2$^{-/-}$ mice [169,193]. However, our data show that TLR2 signaling is not essential for CD11b$^+$ DC recruitment to, or differentiation in the LP. This suggests that the dysregulated T_H1 response in the TLR2$^{-/-}$ mice is not caused by the absence of CD11b$^+$ DCs. As we know from BDMC studies that TLR2-deficient cells are unable to produce IL-10 we could in the next step investigate if sorted CD11b$^+$ DCs of TLR2$^{-/-}$ mice show a functional dysregulation evidenced by reduced IL-10 expression. The absence of CD11b$^+$ DCs in NLRP3$^{-/-}$ mice and the potential dysregulation of CD11b$^+$ DCs in TLR2$^{-/-}$ mice might be one reason for the increased T_H1 response observed in both strains in the stomach LP.

Guarda *et al.* showed that NLRP3 is not homogenously expressed in myeloid cells by using NLRP3/GFP reporter mice, suggesting that NLRP3 might have differential importance depending on the cell type. To better study the expression of NLRP3 in the LP and organs, one should consider making use of this mouse strain [204]. In this

regard, several studies reviled the expression of NLRP3 not only in myeloid cells but also in lymphoid- and epithelial cells [205,206]. Bruchard *et al.* showed that NLRP3 is not only a member of the inflammasome but functions also as a transcription factor in T_H2 cells. They identified that NLRP3 directly binds IFR4 and concomitantly induces IRF4 dependent IL4 expression. It would be interesting to study if NLRP3 also binds IRF4 in $CD11b^+$ DCs. As IRF4 is an essential transcription factor of $CD11b^+$ DCs, a NLRP3 deficiency might influence the differentiation or migration of $CD11b^+$ DCs as we observed in Arnold *et al.*. This binding can be investigated by chromatin- immunoprecipitation (ChIP). Beside this Bruchard *et al.* found that a NLRP3 deficiency in T_H2 cells leads to a reduction of IL-4, IL-5 and IL-13, but did not affect their activation or proliferation. In contrast to T_H2, NLRP3 is irrelevant for the cytokine production of T_H1 cells. These data led to the assumption that altered T_H2 cytokine secretion might deregulate the T cell balance and explain the overshooting T_H1 response we observe in $NLRP3^{-/-}$ mice after *H. pylori* infection.

For the intestine, it is known that TLR2 and NLRP3 have an additional function in epithelial cells by regulating the barrier function. TLR2 and NLRP3 are important for epithelial integrity in intestinal epithelial cells during colitis, which is disrupted in TLR2- and NLRP3-deficient mice. Moreover, NLRP3 in epithelial cells is essential for the protection against *Citrobacter rodentium* and subsequently the prevention of pathology in this case [207,208]. As we made use of whole body TLR2 and NLRP3 knockout mice, we might have caused an imbalance in the barrier function, which might lead to a dysregulation of the T_H1 response in the gastric mucosa of these mice. This T_H1 difference between infected and control mice was only local in the LP and not observed in the MLN. This argues for an effect caused by resident cells, which might be the $CD11b^+$ DCs as well as epithelial cells or after infection also local T cells infiltrating the stomach.

Taken together, we observed an NLRP3-dependent $CD11b^+$ DC recruitment in the gastrointestinal LP in steady state and after infection. These observations raise the question if the recruitment problem of $CD11b^+$ DCs is specific for the gastrointestinal tract or if we could observe this phenotype also in other mucosal tissue. Studying in this regard the pulmonary LP would be of high interest, knowing that NLPR3 is essential for *H. pylori*-conferred allergic asthma protection [169,206]. But also an investigation of the bone marrow might be of interest to study if this effect is a developmental or a migratory defect.

3. THE PLEITROPIC ROLE OF BATF3-DEPENDENT DCs DURING *H. PYLORI* INFECTION

3.1 BATF3-dependent DCs regulate the T_H1 response against *H. pylori* in the GI tract

From literature it is already known that BATF3-dependent DCs have pleiotropic functions. It is well established that BATF3-dependent $CD103^+$ and $CD8^+$ DCs have superior antigen cross-presentation capacities relative to the other DC subsets. They consequently play an essential role in antiviral and anti tumor immunity through the generation of $CD8^+$ cytotoxic T cells [45,209,210].

As we know that $CD103^+$ DCs are not in direct contact with *H. pylori,* we were interested to study their role during infection using $BATF3^{-/-}$ mice lacking $CD103^+$ DCs. To this end, we could show that compared to $CD11b^+$ DCs, these cells are important to build up immunity, as BATF3-deficient mice are not able to mount a proper T_H1 response. These findings go in line with recent publications underlining the role of BATF3-dependent DC in regulating T_H1 responses. In the model of *Leishmania major* infection, $CD103^+$ DCs play an essential role in activating a T_H1 response, here via the production of IL-12 [47]. However we could not evaluate the IL-12 involvement during *H. pylori* infection in $CD103^+$ DCs, due to technical difficulties of detection by FACS and qRT-PCR. Chudnovskiy *et al*. recently identified *Tritrichomonas musculis*, which colonizes the intestine and favors a T_H1 response by BATF3-dependent $CD103^+$ and IRF4-dependent DCs [211]. As we did not observe any changes in the T cell polarization in the MLNs we concluded that the BATF3-dependent DCs are not essential for T cell priming in the MLNs. This argues for a local induction of a T_H1 response in the lamina propria by these cells.

These newer results stand in contrast to several publications describing $CD103^+$ DCs as cells driving tolerogenic immune response in various organs. Several studies report $CD103^+$ DCs in the gut as regulatory mediators by providing retinoic acid to T_{reg} cells leading to their induction [35,212]. $CD103^+$ DCs have been reported to induce *de novo* production of T_{reg} cells also in the spleen and lung [38,213]. These controversial results together suggest a high plasticity of $CD103^+$ DCs at least in the gastrointestinal tract. However, the observation that BATF3-dependent $CD103^+$ DCs also regulate immunity is not limited to the GI tract, as Furuhashi *et al.* showed that pulmonary $CD103^+$ DCs are prone to prime naïve CD4 cells towards T_H1/T_H17 differentiation [214]. These data are supported by an additional study, pointing out a high plasticity of pulmonary $CD103^+$ DCs, which allows switching from a tolerogenic towards a

T_H1/T_H17 response *in vitro* and *in vivo* [215]. Taken together, we could show that *H. pylori* infection skews the CD103$^+$ DC response towards a regional inflammatory one in the intestine and once more underlines the plasticity of this DC subset depending on the signals the cells receive.

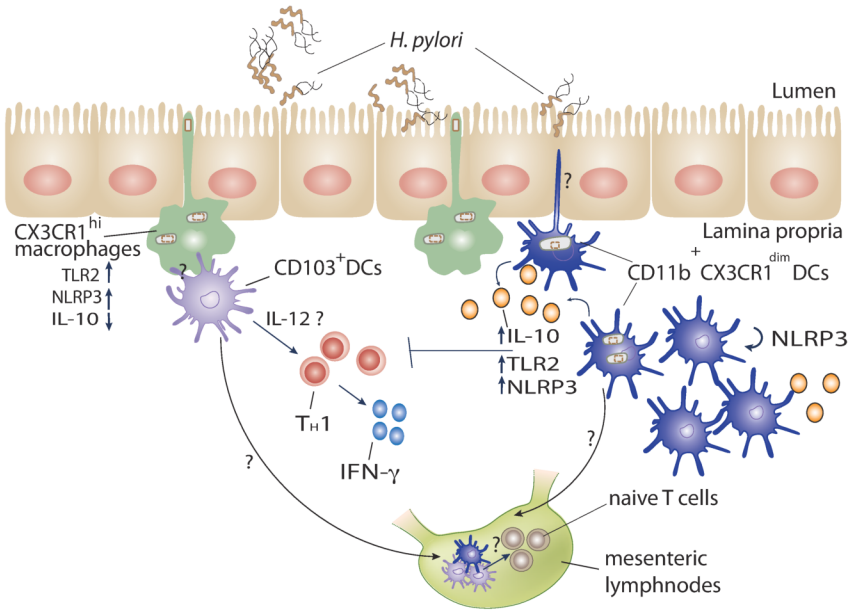

Figure 19: The role of gastric myeloid cells during *H. pylori* infection

H. pylori is sampled by CX3CR1^{hi}macrophages, CD11b$^+$ DCs and CX3CR1^{dim} monocytes. As we currently have little information regarding the role of monocytes yet, they are not depicted here. DCs and macrophages, which sample *H. pylori,* upregulate TLR2 and NLRP3. DCs also upregulate IL-10 transcription. Compared to this, macrophages, which are known to have a tolerogenic function in steady state, downregulate IL-10 transcription after *H. pylori* uptake. In contrast to these cells, CD103$^+$ DCs are not able to sample *H. pylori*, even though the promote a T_H1 immune response during *H. pylori*. This priming happens locally in the LP. Further open questions are if CD103$^+$ DCs interact with CX3CR1^{hi} macrophages potentially via gap junction and how CD103$^+$ DCs regulate T_H1 response - via an increased IL-12 expression. In contrast to CD103$^+$ DCs, CD11b$^+$ DCs dampen T_H1 responses and thereby reduce inflammation and favor *H. pylori* persistence. This speaks for the tolerogenic function of this cell type during *H. pylori* infection in the gastric LP. In addition the differentiation of this cell type at least in the gastrointestinal tract is dependent on NLRP3 expression.

3.2 The role of CD103$^+$ DCs in the lung of *H. pylori*-infected mice

In contrast to the well-established role of CD103$^+$ DCs in T_H1 and CD8$^+$ T cell responses their contribution in regulating T_H2 responses is still controversially discussed. Reports range from CD103$^+$ DCs being essential for a proper T_H2 response to their ability to do the contrary [38,50,54]. It has to be mentioned that each result was obtained in different infection models. Consequently we studied the role of this DC subset also *in H. pylori*-induced asthma protection. BATF3-dependent DCs were es-

sential for *H. pylori*-induced asthma protection, as BATF3$^{-/-}$ mice revealed an increased asthmatic phenotype characterized by increased goblet cell metaplasia, IL-5 and IL-13 production. In addition, we found an increased influx of CD103^{+} DCs in *H. pylori*-protected lungs compared to allergic lungs. In an *ex vivo* study comparing MLN DCs of BATF3$^{-/-}$ mice with DCs of wt mice, we observed an increased IL-10 expression after treatment with *H. pylori* extract only in the wt mice indicating that CD103^{+} DCs are an important source of IL-10. In line with this finding, Khare *et al.* also observed a pulmonary tolerance dependent on CD103^{+} DCs. Here CD103^{+} DCs were able to favor T_{reg} induction in an *ex vivo* co-culture and induce Aldh1a2, which together with TGF-β primes T_{reg} cells [38]. We did not specifically investigate the cytokine profile of CD103^{+} DCs in *H. pylori*-induced asthma protection so far. This would be of interest, to clarify the phenotype of CD103^{+} DCs and the underlying mechanism during *H. pylori* infection in comparison for instance to the inflammatory phenotype of the same DC subset in the stomach of *H. pylori*-infected mice.

Beside CD103^{+} DCs regulating the T_H2 response, we now know that also subsets of CD11b^{+} DCs are able to regulate T_H2 responses. By making use of IRF4$^{-/-}$ mice or mice specifically depleted for Notch2 in DCs, we can address the question in the context of an *H. pylori*-induced asthma protection. To sum up, we saw that in the lung of *H. pylori* infected mice, CD103^{+} DC are essential to protect mice from allergic asthma potentially by their IL-10 expression.

4. THE ROLE OF β-CATENIN SIGNALING IN *H.PYLORI* INFECTION

4.1 The effect of *H. pylori* infection on β-catenin signaling in DCs

As mentioned before, it now becomes clear that DC subsets are able to induce divergent immune responses depending on the antigens they detect. β-catenin activation in DCs, either dependent or independent of WNT is known to shape immune responses towards tolerance. Manoharan *et al.* reviled a TLR2 induced β-catenin signaling via the PI3K/AKT pathway promoting vitamin A metabolism and IL-10 secretion. This protected the mice against T_H17/T_H1-mediated autoimmune neuroinflammation [99,216]. As TLR2 is activated by *H. pylori* secreted ureaseB, we consequently wanted to study the potential activation of β-catenin upon *H. pylori* infection. We observed in spleen DCs that the activation of β-catenin target genes is dependent on TLR2 receptor signaling. This goes in line with the literature, suggesting that β-catenin is activated by TLR2 [216]. In addition, Nakayama *et al*. showed that VacA is

able to induce β-catenin signaling via TLR2/AKT activation [107]. However, we could not confirm a dependency of β-catenin activation on AKT signaling (data not shown).

Our data suggest, that *H. pylori* ureaseB induces several tolerogenic-signaling pathways via TLR2 activation. On the one hand, ureaseB induces NLRP3-dependent activation of IL-18 and IL-1β. It further induces β-catenin signaling. From gastric cancer and breast cancer cells it is known that IL-1β is able to activate β-catenin signaling. This leads to the hypothesis, that β-catenin is not only activated by TLR2 directly but might be activated via NLRP3/IL1-β [217]. As an infection with *H. pylori in vitro* mainly leads to a tolerogenic IL-18-driven phenotype, the activation of β-catenin via IL-1β is probably not so strong. However, this pathway needs to be confirmed in DCs first. Beside this, we should think of studying the β-catenin expression not only in TLR2- but also in NLRP3-deficient mice.

As the reduction of β-catenin target genes in TLR2-deficient cells was not statistically significant, we consequently suggest that β-catenin is not exclusively activated via TLR2 signaling in spleen DCs upon *H. pylori* infection, but might be activated by different pathways as discussed in the following. Beside ureaseB and VacA, also CagA is known to induce β-catenin signaling independent of TLR2. In the context of gastric cancer it is known that CagA interacts with E-cadherin and thereby inhibits the β-catenin/E-cadherin interaction in gastric cells [106]. This leads to the deregulation of β-catenin activation and subsequently to the accumulation of nuclear β-catenin. However this is not consistent, as some studies observed a disruption of E-cadherin independent of CagA [218]. Another study observed an activation of the β-catenin target gene CyclinD1 independent of CagA [129,219]. Making use of human monocyte DCs we could not observe that CagA is important for activating CyclinD1 (data not shown), arguing that this might be an epithelial cell-specific phenotype.

One possible signaling pathway that can be studied in DCs, and is independent of TLR2 is the effect of *H. pylori* on E-cadherin and the concomitant uncoupling of β-catenin from E-cadherin. Jiang *et al.* observed β-catenin induction and a maturation of BMDCs after E-cadherin disruption [98]. In addition to E-cadherin and TLR2 stimulation, further signaling pathways such as FAS, TGF-β and PLC-γ2 are able to activate β-catenin in DCs [97,100,101,220]. However, further studies are warranted to elucidate how this pathway might work.

As β-catenin activation favors tolerogenic pathways, it is not surprising that it induces IL-10 secretion. Manoharan *et al.* found that TLR2 signaling induces IL-10 via several pathways. It can be activated via ERK directly, which favors SOCS3 activation and concomitantly an inhibition of IL-12, IL-23 and IL-6, leading to a suppression of

T_H1/T_H17 responses [99]. Beside this, they found that IL-10 transcription is induced via the PI3K-dependent phosphorylation of AKT, which inhibits GSK3β by phosphorylation. This leads to an activation of TCF4 and β-catenin in the nucleus and induces IL-10 as well as RALDH transcription. From previous studies we know the importance of IL-10 signaling for *H. pylori-induced* tolerogenic immune responses. Consequently, we analyzed the IL-10 expression in BMDCs of TLR2-deficient mice and mice deficient for β-catenin in $CD11c^+$ cells after *H. pylori* infection. IL-10 signaling is strongly reduced in DCs from TLR2-deficient mice and to a lesser extent in β-catenin deficient DCs. These results suggest that *H. pylori* infection induces IL-10 signaling in DCs mainly via TLR2. It also points out that TLR2 is able to induce IL-10 synergistically with other β-catenin-independent pathways. This supports the findings of Manoharan *et.al*., who found that TLR2 induces ERK signaling and β-catenin activation to induce IL-10 signaling in DCs [99].

To sum up we could demonstrate that *H. pylori* is able to induce β-catenin signaling via a urease-dependent TLR2 activation beside other, until now unknown pathways. Moreover these results point out that *H. pylori*-induced TLR2 signaling favors IL-10 secretion at least partly via β-catenin.

4.2 The role of β-catenin signaling in $CD11c^+$ cells in *H. pylori*-induced immune tolerance

We found that *H. pylori* exposure of DCs drives the TLR2-dependent and also -independent activation of β-catenin target genes including IL-10. We consequently hypothesized that β-catenin has a tolerogenic function in DCs *in vivo*. To this end, we generated mice that are deficient for β-catenin in DCs in all organs. As a drawback of this model, macrophages in the gastrointestinal tract and alveolar macrophages in the lung also express high levels of CD11c. Therefore we could not rule out an ectopic depletion of β-catenin in these cells as well [221,222]. To circumvent this, a DC specific Cre- strain such as FLT3 or Zbtb46 should be used, to nail the phenotype down to DCs. We first studied the effect of β-catenin on the colonization level of *H. pylori* in the stomach mucosa. As expected, we observed a reduced colonization in neonatally infected and slight reduction in adult infected mice. This observation is underlined by a slightly increased IFN-γ expression in the stomach mucosa of neonatally infected β-catenin-deficient mice. In the adult infection we did not observe a great difference in IFN-γ-expressing T cells, which goes in line with only a slight decrease in the colonization level. These data support the publications stating that β-catenin activa-

tion in CD11c$^+$ cells induces a tolerogenic phenotype [216]. In contrast, the picture in the MLN is different compared to the stomach. Here we observed an increase of IFN-γ only in the adult infection and no obvious changes of IFN-γ expressing T cells in the neonatal infection. This leads to the suggestion that the T_H1 response in the lamina propria is locally shaping the inflammatory condition, at least in the neonatally infected model. As mentioned before, it needs to be further studied if this local immune response is also shaped by NK-cells or local T cells. As a neonatal infection induces a tolerogenic condition, we wanted to study the effect of β-catenin depletion on the IL-10 production in the stomach mucosa. In contrast and against our hypothesis, we observed an increase in IL-10 expression inversely correlated to the amount of β-catenin alleles in uninfected and *H. pylori* infected mice. This stands in contrast to the literature, showing that β-catenin depletion leads to a reduction in IL-10 secretion [104]. However it also underlines the complexity of IL-10 regulation and favors the controversial discussion still ongoing in literature. This suggests that β-catenin might have a negative feedback on other IL-10 producing cells, as for instance T_H1, T_H2, or T_H17 cells [189]. Another observation of Cohen *et al.* was an increased IL-12 expression in CD103$^+$ and CD8$^+$ DCs by overexpressing β-catenin in DCs [223]. However we did not further investigate the IL-12 expression in CD103$^+$ DCs yet, to confirm this connection. From our *in vitro* study we know that β-catenin is upregulated in a TRL2-dependent manner. Beside this, we observed an upregulation of TLR2 and NLRP3 in cells being in contact with *H. pylori*. This upregulation is however not dependent on an intrinsic feedback loop regulated by β-catenin signaling. The only difference we observed was that macrophages of mice deficient for β-catenin in CD11c$^+$ cells, take up slightly less *H. pylori*. If this is a direct effect of the depletion of β-catenin in these cells or a bystander effect from DC needs to be further investigated by comparing the expression of β-catenin in these cell populations.

To sum up, the role of β-catenin in DCs and potentially macrophages during *H. pylori* immune regulation appears to be minor one by studying the colonization and the T_H1 response.

5. MECHANISMS OF ASTHMA PROTECTION

5.1 Host factors regulating *H. pylori*-induced asthma protection

5.1.1 IL-10 is a critical regulator for asthma protection

Recently, we and others have shown that DCs are essential for immune tolerance and to build up a T_H2 cell-driven airway inflammation [164,224]. Previous publications revealed in genome-wide association studies, that IL-10 is an important risk factor for asthma predisposition [225,226]. Moreover, lower levels of IL-10 serum were found in asthmatic patients [225,227]. From our *in vitro* studies we already knew that DCs are able to induce IL-10 secretion upon *H. pylori* infection. Consequently, we investigated the role of DCs and IL-10 in *H. pylori*-mediated asthma protection in more detail. We showed that IL-10 is produced to a great extent by pulmonary $CD11c^+$ DCs, as the IL-10 expression was reduced by half in CD11c-Cre x $IL\text{-}10^{fl/fl}$ mice. In addition, we could show that IL-10 in DCs is important for *H. pylori*-induced allergic asthma protection, as this was lost in CD11c-Cre x $IL\text{-}10^{fl/fl}$ mice. The protection is comparable to mice treated with anti-IL-10R antibodies [190]. These findings are supported by a publication in which constitutive IL-10-secreting DCs were transferred and prevented lung inflammation [228]. As mentioned before, we not only studied the effect of live infection but also the effect of the bacterial extract and found that also here IL-10 is important for extract-mediated asthma protection.

From the literature it is known that IL-10 is regulated via a TNFα-mediated negative feedback loop during airway inflammation [229]. IL-10 induces the apoptosis in eosinophils and thereby reduces the secretion of IL-5 and consequently asthma symptoms directly. We could show that *H. pylori* extract induces IL-10 secretion in DCs and that this depends on TLR2 and MyD88 signalling. This goes in line with our results, revealing a diminished IL-10 expression in $TLR2^{-/-}$ mice after infection. Thus also *H. pylori*-infected $TLR2^{-/-}$ mice are not able to protect from asthmatic symptoms. In myeloid DCs and macrophages MyD88, the adapter molecule downstream of TLR2, induces IL-10 expression [230]. Beside this IL-10 can be regulated by several further mechanisms like DC-SIGN, dectin1 or as discussed above via β-catenin [231].

We also started to elucidate the DC subsets regulating the IL-10 secretion in the lung after *H. pylori* infection. We identified $CD103^+CD11b^-$ DCs to be essential for an asthma protection. We observed that DCs lacking this population have a reduced IL10 expression *ex vivo*, suggesting a potential role of $CD103^+$ DCs in IL-10 regulation. Due to technical problems we were not able to define the IL-10 expression directly in $CD103^+$ DCs of the lung. However, it should be mentioned that DCs are not the only

source of IL-10 in the lung. Interstitial macrophages are known to produce IL-10 and to regulate lung homeostasis [232]. A recent paper showed that interstitial macrophages constitutively express IL-10 via TLR4/MyD88. Unfortunately Kawano *et al.* did not study the role of CD103$^+$ DCs in their setup [233]. As we know from Koch *et al*. that *H. pylori* LPS is able to induce TLR4 signalling in DCs, this might also be true for interstitial macrophages [169]. In addition, the transfer of infected interstitial macrophages into HDM-sensitized mice would clarify if these cells were able to rescue asthma symptoms. To sum up, our data support the assumption that IL-10 signalling in DCs is required for allergic asthma protection conferred by infection and also by *H. pylori* extract. The source of IL-10 should be studied in more detail regarding the role of macrophages.

5.1.2 The role of T_{reg} cells in asthma protection

In a previous publication from our lab, Oertli *et al*. showed that T_{reg} cells are essential for asthma protection in the neonatal infection model [164]. We observed now an increase of Foxp3$^+$ T_{reg} cells in MLN and PP after infection. This increase was neither visible in mice infected with urease mutant *H. pylori* nor in infected TLR2$^{-/-}$ mice. Additionally, the wt T_{reg} cells were not only increased in number after an infection with *H. pylori*, they also revealed tolerogenic properties. T_{reg} cells, isolated from infected mice and transferred into uninfected, sensitized wt recipients, were able to alleviate asthma symptoms. This protection was not observed with T_{reg} cells from mice infected with urease mutant *H. pylori.* This again indicates the importance of the TLR2/NLRP3/IL-18 pathway for an *H. pylori*-induced tolerance, by priming T_{reg} cells. In the last years, T_{regs} got into the focus as being essential during the sensitization phase of allergic asthma [234]. However, until now, we could not explain the tolerogenic effect of T_{reg} cells in *H. pylori*-induced allergic asthma and immune tolerance. To elucidate the effect *H. pylori* has on T_{reg} cells we analysed potential DNA modifications in the epigenome of T_{reg} cells in the MLN. The T_{reg}-specific demethylated region (TSDR) within the FOXP3 locus can be demethylated in the thymus. This results in the stabilization of Foxp3 expression and thereby guarantees full functionality and long-term stability of T_{reg} cells [235,236]. Therefore, we compared sorted Foxp3$^+$ cells from *H. pylori*-infected versus Foxp3$^+$ cells from MLNs of uninfected mice. With the use of DNA methylation analysis we investigated the methylation status at 12 TSDR regions. We observed a higher demethylation in Foxp3$^+$ cells from infected mice. This suggests that the demethylation might confer the long-lasting protection against various allergic diseases such as asthma or food allergy (Kyburz *et al.* 2017, in preparation).

Surprisingly, extract-induced asthma protection was not dependent on T_{reg} cells. Depletion of T_{regs} with an anti-CD25 antibody has no effect on extract protection, even though extract protection is dependent on $CD103^+$ DCs and IL-10 [190]. This indicates, that the extract induces other, T_{reg}-independent, signaling pathways in the lung. This goes in line with the literature, as the role of T_{reg} cells in asthma protection is still controversially discussed, and some publications support the idea that asthma protection is not based on T_{reg} cells. In this regard, it might be of interest to study the role of pDCs in more detail. Besides the increase of $CD103^+$ DCs, we additionally saw an increase of pDCs. They are not known as classical IL-10 inducers but can mediate tolerance by suppressing mature DCs via induction of T_{reg} cells, IDO- or PDL1 production (rev. [230,237]). Taken together, T_{reg} induction is not essential for extract-induced asthma protection but essential for alleviating asthma symptoms in neonatal *H. pylori* infection. Thereby *H. pylori* induces a stable T_{reg} differentiation which conveys one way of asthma protection.

5.1.3 β-catenin signaling in $CD11c^+$ cells is a critical mediator of protection

Another signaling pathway which is known to play an important role in asthma protection and the induction of IL-10 is the β-catenin pathway. We and others suggest an important immune modulatory effect of β-catenin signaling on inflammatory processes in allergic asthma. β-catenin signaling has immunosuppressive functions mainly in DCs, preventing the induction and secretion of pro-inflammatory cytokines and the subsequent airway inflammation [238-240]. We observed the *H. pylori*-dependent activation of β-catenin *in vitro.* Consequently, we wanted to study the role of β-catenin in DCs during *H. pylori*-induced allergic asthma protection. Mice deficient for β–catenin in $CD11c^+$ cells were not protected from goblet cell metaplasia and lung inflammation, two hallmarks of allergic asthma. These results support previous findings by Reuter *et al.* showing that β-catenin signaling in DCs plays an essential role during allergic asthma protection. Recently, Yan *et al*. could show that curcumin induces β-catenin signaling in DCs, which protects from various hallmarks of OVA-induced asthma such as lung inflammation and goblet cell metaplasia [241]. In humans, Bae *et al.* observed that β-catenin loss of function mutations correlate with an increased asthma risk [242].

Taken together, our findings underline the importance of β-catenin signaling in DCs and potentially also macrophages during *H. pylori*-induced allergic asthma protection. However, only a minor importance of β-catenin in regulating the tolerogenic

immune response in the stomach was observed, as discussed above. This underlines once again the divergent functionality of cells in different organs.

5.2. Bacterial determinants of asthma protection

5.2.1 The role of VacA and GGT in allergic asthma protection

We identified two immunomodulators of *H. pylori,* GGT and VacA, which are both able to induce tolerogenic DCs and required for the induction of suppressive T_{reg} cells. Moreover, VacA mutants failed to confer asthma protection [145]. Therefore we investigate the ability of purified VacA and GGT to protect from asthma symptoms [190]. Purified VacA and GGT protect nearly as good as a live infection of mice.

The effect of GGT might be traced back to the general function of GGT to convert glutathione and glutamine to glutamate on dendritic cells and directly on T cells. Schmees *et al.* showed that *H. pylori* GGT induces a cell cycle arrest and thereby inhibits T cell proliferation [243]. This goes in line with another publication revealing that reduced extracellular glutamine levels affect T cell proliferation, activation and effector cytokine expression [244]. Bussilon *et al.* have suggested that the tolerogenic properties might be caused by Cox2, which is induced upon GGT exposure of gastric epithelial cells and is known to inhibit T_H1 responses [146,147]. These data go in line with our experiments hinting towards an inhibition of T_{reg} differentiation when co-cultures of infected dendritic cells and T cells were supplemented with glutamine and glutathione. Käbisch *et al.* recently shed light into the molecular mechanism of GGT on human dendritic cells. They reported that glutamate, the product of GGT, induces DCs by inhibiting cAMP signaling and reducing IL-6 secretion in response to *H. pylori* infection [245]. All these data support that GGT is an immunomodulator, which induces tolerogenic by programming DCs and T cells to favour persistence and to prevent from allergic diseases.

Compared to GGT, purified VacA protected even better from asthma symptoms, especially when the protein was given during the neonatal phase. From the literature it is known that VacA is able to induce NLRP3 inflammasome activation [188]. Moreover, VacA is necessary for T_{reg} differentiation [145]. As also NLRP3/IL-18 signaling induces T_{reg} differentiation this suggests that VacA might signal via the NLRP3/IL-18 pathway. Moreover, VacA induces the PI3K/Akt pathway favouring GSK3β inhibition and concomitant β-catenin activation [107]. We could show that β-catenin is important for IL-10 secretion after *H. pylori* infection. In addition IL-10 expression is essential for VacA-induced asthma protection, as IL-10 depletion abrogates this protection.

Furthermore, it is known that PI3K is involved in IL-10 signaling [246]. Thus, it would be interesting to address whether VacA signals via PI3K to induce IL-10. Another question, which needs to be answered, is whether VacA signals via IL-18. Thus, we should observe that VacA protection is abolished in NLRP3$^{-/-}$ and IL-18$^{-/-}$ mice.

The tolerogenic properties of VacA are further confirmed by the previously mentioned DNA methylation of the TSD region in the Foxp3 locus. We observed that VacA treatment increased the demethylation of the regions in Foxp3^{+} cells from MLNs (manuscript Kyburz *et al.,* 2017). This might explain one immunomodulatory pathway how VacA favours tolerogenicity and alleviates asthma symptoms.

To sum up, these results point out that we are still on the road of understanding the complexity of this cellular interplay of myeloid- but also other immune cells. This complexity makes us aware that we need to investigate the molecular mechanisms more carefully to further improve treatment strategies against diseases such as allergic asthma.

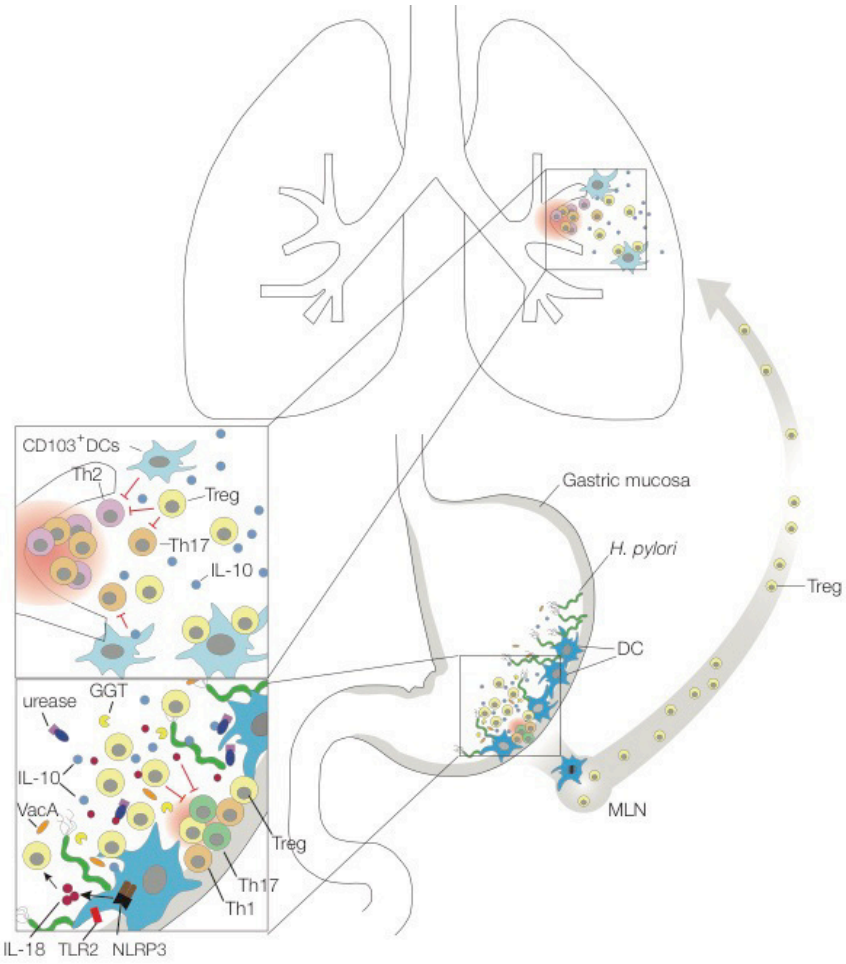

Figure 20: Host- and bacterial factors contribute to the protection of allergic asthma during an *H. pylori* infection

The *H. pylori* immunomodulators GGT and VacA promote chronic infection by tolerizing DCs and thereby inducing T_{reg} differentiation. *H. pylori*-induced T_{regs} are required for the suppression of allergen-specific immune responses. VacA protection depends on $CD103^{+}$ DCs and IL-18 secretion. IL-18 can be induced by urease-dependent TLR2/NLRP3 activation in DCs. Treg- and DC-derived IL-10 contributes to *H. pylori*-specific allergy prevention in the lung (modified from [163]).

CONCLUDING REMARKS

It is now well established that DC subsets have a pleiotropic function depending on the stimuli they receive and the tissue they populate. It is known that *H. pylori* induces tolerogenic DCs, which favors bacterial persistence in the stomach. We could show, that this property is tightly linked to the protection against allergic asthma [247]. However, not much more was known about the role of DCs in the gastric lamina propria. Here we studied the function of DCs in more detail during steady state and *H. pylori* infection in the gastric LP, and in the lung during allergic asthma.

We showed that the development of $CD11b^+$ DCs is dependent on intrinsic NLRP3 expression in the gut LP and identified these cells as tolerogenic regulators during *H. pylori* infection in the gastric LP. In addition we observed that these cells sample *H. pylori* as efficiently as $CX3CR1^{hi}$ macrophages and $Ly6C^{hi}$ monocytes and subsequently upregulate NLRP3 and TLR2 expression. In contrast to tolerogenic $CD11b^+$ DCs, $CD103^+$ DCs favor a T_H1 response in the gastric LP (manuscript Arnold *et al*.). This stands in contrast to our findings in the allergic lung, where $CD103^+$ DCs are infiltrating and driving asthma protection [190]. This underlines once again the pleiotropic function of DC cells in various organs. Beside $CD103^+$ DCs being essential, we identified DC specific IL-10 secretion and β-catenin activation to be important for asthma protection, highlighting the tolerogenic function of DCs. Beside DCs, T_{reg} cells develop during *H. pylori* persistence in an IL-18 dependent manner. Until now, not much was known regarding the cellular activation of IL-18 in DCs during *H. pylori* infection. Here we identified the urease *H. pylori* subunit ureaseB as an immunosuppressive factor that serves as PAMP for TLR2. Signaling via TLR2 induces NLRP3 inflammasome activation, thereby activating the secretion of IL-18, which in turn promotes a T_{reg} response.

However there are still a lot of open questions regarding the role of DCs during *H. pylori* infection and the mechanism of allergy protection. As NLRP3 was shown to regulate IRF4 expression in T cells, it would be of high interest to follow up the role of NLRP3 in IRF4-dependent $CD11b^+$ DCs [206]. Besides it would be of interest to elucidate the role of macrophages as we observed that macrophages take up *H. pylori* and therefore might also represent regulators of the persistence. In addition, it was shown that interstitial macrophages in the lung and macrophages in the gastric LP are potent tolerogenic mediators, as they secrete IL-10 [65,232]. The depletion of $CX3CR1^+$ macrophages, with a LysM-Cre system would be of interest to study these

effects. In the lung, this system will only deplete interstitial macrophages, as alveolar macrophages do not express CX3CR1 [248]. By answering these questions, we can further shed light on the development of persistent bacterial colonization and elucidate key players of allergic asthma protection.

Taken together, with this work we gained more insight into the division of labor among different DC subsets and the molecular pathways regulating immune suppression and inflammation.

ABBREVIATION

APC	antigen presenting cell
ASC	apoptosis-associated speck-like protein containing c-Terminal CARD
b-catenin	beta catenin
β-Trcp	β-transducin repeat-containing protein
BATF	Basic Leucine Zipper ATF-Like *Transcription Factor*
BCL9	B-cell CLL/lymphoma 9 protein
BMDCs	bowne marrow derived DCs
CBP	CREB-binding protein
CCND1	cyclinD1
CCR	C-C Motif Chemokine Receptor
CDP	conventional dendritic cell precursor
cDC	classical dendritic cells
cMoP	common monocyte progenitors
CK1α	casein kinase 1α
CX3C	chemokine receptor
DC	dendritic cell
DVL	disheveled
EAE	experimental autoimmune encephalomyelitis
E-cadherin	epithelial cadherin
ERK	extracellular signal-related kinase
FACS	fluorescence activated cell sorting
FLT3	FMS-like tyrosine kinase 3
FoxP3	forkhead box P3
Fzd	Frizzled
GGT	gamma glutamyl transpeptidase
GMP	granulocyte monocyte progenitors
GSK3β	glycogen synthase kinase 3β
H. pylori	*helicobacter pylori*
IDO	Indolamin-2,3-Dioxygenase
Ig	Immunoglobulin
IFN	type I interferon
IL	interleukin
ILC2	group 2 innate lymphoid cell
IRAKs	IL-1R-associated kinases
IRF	the interferon-regulatory factor
JNK	JUN N-terminal kinase
KLF4	Kruppel-like factor 4 is a zinc-finger transcription factor,
LEF	lymphoid enhancer factor
LN	lymph nodes
LP	lamina propria
LPS	lipopolysaccharide
LRP5/6,	low-density lipoprotein receptor-related protein 5/6
MAL	MyD88-adaptor-like proteins

MAPK	mitogen-activated protein kinases
MFI	mean fluoresence intensity
MLN	mesenteric lymph nodes
MDP	monocyte and dendritic *cell* progenitors
MPS	mononuclear phagocyte system
MyD88	myeloid differentiation primary-response protein 88
NF-κB	nuclear factor-κB
NLR	Nod-like receptors
PAMPs	pathogen-associated molecular pattern
pDC	plasmacytoid
PP	Peyer`s Patch
PRR	pattern recognition receptors
PYGO	Pygopus
RALDH 1/2	retinaldehyde dehydrogenase 1/2
RIG-I	retinoic acid inducible gene I
RORγT	retinoid-related orphan receptor γT
TCF	T-cell factor
Teff	effector T cells
TFH	T follicular helper
TGFβ	transforming growth factor β
TH	T helper
T_H2	T helper 2
TLR	toll like receptors
TNKS	tankyrase-1
Treg	regulatory T cells
Tr1	Type 1 regulatory T cell
TRIF	TIR domain-containing adaptor protein inducing TFNβ
TRAM	TRIF- related adaptor molecule
TRAF	TNF receptor-associated factors
TSDR	Treg-specific demethylated region
TSLP	thymic stromal lymphopoeitin
wt	wild type
VacA	Vacuolating cytotoxin A

REFERENCES

1. Gordon, S. Elie Metchnikoff: father of natural immunity. *European journal of immunology* **38**, 3257-3264 (2008).
2. van Furth, R.*, et al.* [Mononuclear phagocytic system: new classification of macrophages, monocytes and of their cell line]. *Bull World Health Organ* **47**, 651-658 (1972).
3. Steinman, R.M. & Cohn, Z.A. Identification of a novel cell type in peripheral lymphoid organs of mice. I. Morphology, quantitation, tissue distribution. *The Journal of experimental medicine* **137**, 1142-1162 (1973).
4. Schlenner, S.M.*, et al.* Fate mapping reveals separate origins of T cells and myeloid lineages in the thymus. *Immunity* **32**, 426-436 (2010).
5. Sathe, P.*, et al.* Lymphoid tissue and plasmacytoid dendritic cells and macrophages do not share a common macrophage-dendritic cell-restricted progenitor. *Immunity* **41**, 104-115 (2014).
6. Hettinger, J.*, et al.* Origin of monocytes and macrophages in a committed progenitor. *Nature immunology* **14**, 821-830 (2013).
7. Bogunovic, M.*, et al.* Origin of the lamina propria dendritic cell network. *Immunity* **31**, 513-525 (2009).
8. Cisse, B.*, et al.* Transcription factor E2-2 is an essential and specific regulator of plasmacytoid dendritic cell development. *Cell* **135**, 37-48 (2008).
9. Satpathy, A.T.*, et al.* Zbtb46 expression distinguishes classical dendritic cells and their committed progenitors from other immune lineages. *The Journal of experimental medicine* **209**, 1135-1152 (2012).
10. Murphy, T.L.*, et al.* Transcriptional Control of Dendritic Cell Development. *Annual review of immunology* **34**, 93-119 (2016).
11. Ginhoux, F.*, et al.* The origin and development of nonlymphoid tissue CD103+ DCs. *The Journal of experimental medicine* **206**, 3115-3130 (2009).
12. Dalod, M., Chelbi, R., Malissen, B. & Lawrence, T. Dendritic cell maturation: functional specialization through signaling specificity and transcriptional programming. *EMBO J* **33**, 1104-1116 (2014).
13. Mildner, A. & Jung, S. Development and function of dendritic cell subsets. *Immunity* **40**, 642-656 (2014).
14. Yanagihara, S., Komura, E., Nagafune, J., Watarai, H. & Yamaguchi, Y. EBI1/CCR7 is a new member of dendritic cell chemokine receptor that is up-regulated upon maturation. *Journal of immunology* **161**, 3096-3102 (1998).
15. Forster, R., Davalos-Misslitz, A.C. & Rot, A. CCR7 and its ligands: balancing immunity and tolerance. *Nature reviews. Immunology* **8**, 362-371 (2008).
16. Pulendran, B., Tang, H. & Manicassamy, S. Programming dendritic cells to induce T(H)2 and tolerogenic responses. *Nature immunology* **11**, 647-655 (2010).
17. Veldhoen, M., Hocking, R.J., Atkins, C.J., Locksley, R.M. & Stockinger, B. TGFbeta in the context of an inflammatory cytokine milieu supports de novo differentiation of IL-17-producing T cells. *Immunity* **24**, 179-189 (2006).

18. Chang, H.C.*, et al.* The transcription factor PU.1 is required for the development of IL-9-producing T cells and allergic inflammation. *Nature immunology* **11**, 527-534 (2010).
19. Koch, M.A.*, et al.* The transcription factor T-bet controls regulatory T cell homeostasis and function during type 1 inflammation. *Nature immunology* **10**, 595-602 (2009).
20. Schmidt, A., Oberle, N. & Krammer, P.H. Molecular mechanisms of treg-mediated T cell suppression. *Frontiers in immunology* **3**, 51 (2012).
21. Banchereau, J.*, et al.* Immunobiology of dendritic cells. *Annual review of immunology* **18**, 767-811 (2000).
22. Jung, S.*, et al.* In vivo depletion of CD11c+ dendritic cells abrogates priming of CD8+ T cells by exogenous cell-associated antigens. *Immunity* **17**, 211-220 (2002).
23. Murphy, K.M. Transcriptional control of dendritic cell development. *Advances in immunology* **120**, 239-267 (2013).
24. Russ, B.E., Prier, J.E., Rao, S. & Turner, S.J. T cell immunity as a tool for studying epigenetic regulation of cellular differentiation. *Front Genet* **4**, 218 (2013).
25. Guilliams, M.*, et al.* From skin dendritic cells to a simplified classification of human and mouse dendritic cell subsets. *European journal of immunology* **40**, 2089-2094 (2010).
26. Gurka, S., Hartung, E., Becker, M. & Kroczek, R.A. Mouse Conventional Dendritic Cells Can be Universally Classified Based on the Mutually Exclusive Expression of XCR1 and SIRPalpha. *Frontiers in immunology* **6**, 35 (2015).
27. Bachem, A.*, et al.* Expression of XCR1 Characterizes the Batf3-Dependent Lineage of Dendritic Cells Capable of Antigen Cross-Presentation. *Frontiers in immunology* **3**, 214 (2012).
28. Grajales-Reyes, G.E.*, et al.* Batf3 maintains autoactivation of Irf8 for commitment of a CD8alpha(+) conventional DC clonogenic progenitor. *Nature immunology* **16**, 708-717 (2015).
29. Schlitzer, A.*, et al.* IRF4 transcription factor-dependent CD11b+ dendritic cells in human and mouse control mucosal IL-17 cytokine responses. *Immunity* **38**, 970-983 (2013).
30. Lewis, K.L.*, et al.* Notch2 receptor signaling controls functional differentiation of dendritic cells in the spleen and intestine. *Immunity* **35**, 780-791 (2011).
31. Lee, H.*, et al.* Phenotype and function of nasal dendritic cells. *Mucosal immunology* **8**, 1083-1098 (2015).
32. Bekiaris, V., Persson, E.K. & Agace, W.W. Intestinal dendritic cells in the regulation of mucosal immunity. *Immunological reviews* **260**, 86-101 (2014).
33. Scott, C.L.*, et al.* CCR2(+)CD103(-) intestinal dendritic cells develop from DC-committed precursors and induce interleukin-17 production by T cells. *Mucosal immunology* **8**, 327-339 (2015).
34. Worbs, T.*, et al.* Oral tolerance originates in the intestinal immune system and relies on antigen carriage by dendritic cells. *The Journal of experimental medicine* **203**, 519-527 (2006).
35. Coombes, J.L.*, et al.* A functionally specialized population of mucosal CD103+ DCs induces Foxp3+ regulatory T cells via a TGF-beta and retinoic acid-

dependent mechanism. *The Journal of experimental medicine* **204**, 1757-1764 (2007).
36. Iwata, M.*, et al.* Retinoic acid imprints gut-homing specificity on T cells. *Immunity* **21**, 527-538 (2004).
37. Steimle, A. & Frick, J.S. Molecular Mechanisms of Induction of Tolerant and Tolerogenic Intestinal Dendritic Cells in Mice. *J Immunol Res* **2016**, 1958650 (2016).
38. Khare, A.*, et al.* Cutting edge: inhaled antigen upregulates retinaldehyde dehydrogenase in lung CD103+ but not plasmacytoid dendritic cells to induce Foxp3 de novo in CD4+ T cells and promote airway tolerance. *Journal of immunology* **191**, 25-29 (2013).
39. Mucida, D.*, et al.* Reciprocal TH17 and regulatory T cell differentiation mediated by retinoic acid. *Science* **317**, 256-260 (2007).
40. Stock, A., Booth, S. & Cerundolo, V. Prostaglandin E2 suppresses the differentiation of retinoic acid-producing dendritic cells in mice and humans. *The Journal of experimental medicine* **208**, 761-773 (2011).
41. Zelante, T.*, et al.* CD103(+) Dendritic Cells Control Th17 Cell Function in the Lung. *Cell Rep* **12**, 1789-1801 (2015).
42. Matteoli, G.*, et al.* Gut CD103+ dendritic cells express indoleamine 2,3-dioxygenase which influences T regulatory/T effector cell balance and oral tolerance induction. *Gut* **59**, 595-604 (2010).
43. Fallarino, F.*, et al.* The combined effects of tryptophan starvation and tryptophan catabolites down-regulate T cell receptor zeta-chain and induce a regulatory phenotype in naive T cells. *Journal of immunology* **176**, 6752-6761 (2006).
44. Johansson-Lindbom, B.*, et al.* Functional specialization of gut CD103+ dendritic cells in the regulation of tissue-selective T cell homing. *The Journal of experimental medicine* **202**, 1063-1073 (2005).
45. Hildner, K.*, et al.* Batf3 deficiency reveals a critical role for CD8alpha+ dendritic cells in cytotoxic T cell immunity. *Science* **322**, 1097-1100 (2008).
46. Hashimoto, D., Miller, J. & Merad, M. Dendritic cell and macrophage heterogeneity in vivo. *Immunity* **35**, 323-335 (2011).
47. Martinez-Lopez, M., Iborra, S., Conde-Garrosa, R. & Sancho, D. Batf3-dependent CD103+ dendritic cells are major producers of IL-12 that drive local Th1 immunity against Leishmania major infection in mice. *European journal of immunology* **45**, 119-129 (2015).
48. Mashayekhi, M.*, et al.* CD8alpha(+) dendritic cells are the critical source of interleukin-12 that controls acute infection by Toxoplasma gondii tachyzoites. *Immunity* **35**, 249-259 (2011).
49. Laffont, S., Siddiqui, K.R. & Powrie, F. Intestinal inflammation abrogates the tolerogenic properties of MLN CD103+ dendritic cells. *European journal of immunology* **40**, 1877-1883 (2010).
50. Plantinga, M.*, et al.* Conventional and monocyte-derived CD11b(+) dendritic cells initiate and maintain T helper 2 cell-mediated immunity to house dust mite allergen. *Immunity* **38**, 322-335 (2013).
51. Tussiwand, R.*, et al.* Klf4 expression in conventional dendritic cells is required for T helper 2 cell responses. *Immunity* **42**, 916-928 (2015).

52. Persson, E.K.*, et al.* IRF4 transcription-factor-dependent CD103(+)CD11b(+) dendritic cells drive mucosal T helper 17 cell differentiation. *Immunity* **38**, 958-969 (2013).
53. Denning, T.L.*, et al.* Functional specializations of intestinal dendritic cell and macrophage subsets that control Th17 and regulatory T cell responses are dependent on the T cell/APC ratio, source of mouse strain, and regional localization. *Journal of immunology* **187**, 733-747 (2011).
54. Nakano, H.*, et al.* Pulmonary CD103(+) dendritic cells prime Th2 responses to inhaled allergens. *Mucosal immunology* **5**, 53-65 (2012).
55. Sichien, D., Lambrecht, B.N., Guilliams, M. & Scott, C.L. Development of conventional dendritic cells: from common bone marrow progenitors to multiple subsets in peripheral tissues. *Mucosal immunology* (2017).
56. Hashimoto, D.*, et al.* Tissue-resident macrophages self-maintain locally throughout adult life with minimal contribution from circulating monocytes. *Immunity* **38**, 792-804 (2013).
57. Bain, C.C.*, et al.* Constant replenishment from circulating monocytes maintains the macrophage pool in the intestine of adult mice. *Nature immunology* **15**, 929-937 (2014).
58. Varol, C.*, et al.* Intestinal lamina propria dendritic cell subsets have different origin and functions. *Immunity* **31**, 502-512 (2009).
59. Scott, C.L., Henri, S. & Guilliams, M. Mononuclear phagocytes of the intestine, the skin, and the lung. *Immunological reviews* **262**, 9-24 (2014).
60. Jaensson, E.*, et al.* Small intestinal CD103+ dendritic cells display unique functional properties that are conserved between mice and humans. *The Journal of experimental medicine* **205**, 2139-2149 (2008).
61. Mildner, A., Yona, S. & Jung, S. A close encounter of the third kind: monocyte-derived cells. *Advances in immunology* **120**, 69-103 (2013).
62. Geissmann, F., Jung, S. & Littman, D.R. Blood monocytes consist of two principal subsets with distinct migratory properties. *Immunity* **19**, 71-82 (2003).
63. Jakubzick, C.*, et al.* Minimal differentiation of classical monocytes as they survey steady-state tissues and transport antigen to lymph nodes. *Immunity* **39**, 599-610 (2013).
64. Varol, C., Mildner, A. & Jung, S. Macrophages: development and tissue specialization. *Annual review of immunology* **33**, 643-675 (2015).
65. Bain, C.C. & Mowat, A.M. Macrophages in intestinal homeostasis and inflammation. *Immunological reviews* **260**, 102-117 (2014).
66. Bain, C.C.*, et al.* Resident and pro-inflammatory macrophages in the colon represent alternative context-dependent fates of the same Ly6Chi monocyte precursors. *Mucosal immunology* **6**, 498-510 (2013).
67. Zigmond, E.*, et al.* Macrophage-restricted interleukin-10 receptor deficiency, but not IL-10 deficiency, causes severe spontaneous colitis. *Immunity* **40**, 720-733 (2014).
68. Shouval, D.S.*, et al.* Interleukin-10 receptor signaling in innate immune cells regulates mucosal immune tolerance and anti-inflammatory macrophage function. *Immunity* **40**, 706-719 (2014).

69. Hadis, U.*, et al.* Intestinal tolerance requires gut homing and expansion of FoxP3+ regulatory T cells in the lamina propria. *Immunity* **34**, 237-246 (2011).
70. Flannigan, K.L., Geem, D., Harusato, A. & Denning, T.L. Intestinal Antigen-Presenting Cells: Key Regulators of Immune Homeostasis and Inflammation. *The American journal of pathology* **185**, 1809-1819 (2015).
71. Niess, J.H.*, et al.* CX3CR1-mediated dendritic cell access to the intestinal lumen and bacterial clearance. *Science* **307**, 254-258 (2005).
72. Schulz, O.*, et al.* Intestinal CD103+, but not CX3CR1+, antigen sampling cells migrate in lymph and serve classical dendritic cell functions. *The Journal of experimental medicine* **206**, 3101-3114 (2009).
73. Mazzini, E., Massimiliano, L., Penna, G. & Rescigno, M. Oral tolerance can be established via gap junction transfer of fed antigens from CX3CR1(+) macrophages to CD103(+) dendritic cells. *Immunity* **40**, 248-261 (2014).
74. Coombes, B.K. & Mahony, J.B. Dendritic cell discoveries provide new insight into the cellular immunobiology of DNA vaccines. *Immunol Lett* **78**, 103-111 (2001).
75. Varol, C., Zigmond, E. & Jung, S. Securing the immune tightrope: mononuclear phagocytes in the intestinal lamina propria. *Nature reviews. Immunology* **10**, 415-426 (2010).
76. Medzhitov, R., Preston-Hurlburt, P. & Janeway, C.A., Jr. A human homologue of the Drosophila Toll protein signals activation of adaptive immunity. *Nature* **388**, 394-397 (1997).
77. Akira, S., Uematsu, S. & Takeuchi, O. Pathogen recognition and innate immunity. *Cell* **124**, 783-801 (2006).
78. Jin, M.S.*, et al.* Crystal structure of the TLR1-TLR2 heterodimer induced by binding of a tri-acylated lipopeptide. *Cell* **130**, 1071-1082 (2007).
79. Kang, J.Y.*, et al.* Recognition of lipopeptide patterns by Toll-like receptor 2-Toll-like receptor 6 heterodimer. *Immunity* **31**, 873-884 (2009).
80. Verstak, B.*, et al.* MyD88 adapter-like (Mal)/TIRAP interaction with TRAF6 is critical for TLR2- and TLR4-mediated NF-kappaB proinflammatory responses. *The Journal of biological chemistry* **284**, 24192-24203 (2009).
81. O'Neill, L.A., Golenbock, D. & Bowie, A.G. The history of Toll-like receptors - redefining innate immunity. *Nature reviews. Immunology* **13**, 453-460 (2013).
82. Lechtenberg, B.C., Mace, P.D. & Riedl, S.J. Structural mechanisms in NLR inflammasome signaling. *Curr Opin Struct Biol* **29**, 17-25 (2014).
83. Martinon, F., Burns, K. & Tschopp, J. The inflammasome: a molecular platform triggering activation of inflammatory caspases and processing of proIL-beta. *Mol Cell* **10**, 417-426 (2002).
84. Bauernfeind, F.G.*, et al.* Cutting edge: NF-kappaB activating pattern recognition and cytokine receptors license NLRP3 inflammasome activation by regulating NLRP3 expression. *Journal of immunology* **183**, 787-791 (2009).
85. Kim, D.J., Park, J.H., Franchi, L., Backert, S. & Nunez, G. The Cag pathogenicity island and interaction between TLR2/NOD2 and NLRP3 regulate IL-1beta production in Helicobacter pylori infected dendritic cells. *European journal of immunology* **43**, 2650-2658 (2013).

86. Kiura, K., Kataoka, H., Yasuda, M., Inoue, N. & Shibata, K. The diacylated lipopeptide FSL-1 induces TLR2-mediated Th2 responses. *FEMS Immunol Med Microbiol* **48**, 44-55 (2006).
87. Dillon, S*., et al.* Yeast zymosan, a stimulus for TLR2 and dectin-1, induces regulatory antigen-presenting cells and immunological tolerance. *The Journal of clinical investigation* **116**, 916-928 (2006).
88. Yang, D*., et al.* Eosinophil-derived neurotoxin acts as an alarmin to activate the TLR2-MyD88 signal pathway in dendritic cells and enhances Th2 immune responses. *The Journal of experimental medicine* **205**, 79-90 (2008).
89. Kaji, R., Kiyoshima-Shibata, J., Nagaoka, M., Nanno, M. & Shida, K. Bacterial teichoic acids reverse predominant IL-12 production induced by certain lactobacillus strains into predominant IL-10 production via TLR2-dependent ERK activation in macrophages. *Journal of immunology* **184**, 3505-3513 (2010).
90. Suryawanshi, A*., et al.* Canonical wnt signaling in dendritic cells regulates Th1/Th17 responses and suppresses autoimmune neuroinflammation. *Journal of immunology* **194**, 3295-3304 (2015).
91. Willert, K*., et al.* Wnt proteins are lipid-modified and can act as stem cell growth factors. *Nature* **423**, 448-452 (2003).
92. van Amerongen, R. & Nusse, R. Towards an integrated view of Wnt signaling in development. *Development* **136**, 3205-3214 (2009).
93. Rubinfeld, B*., et al.* Association of the APC gene product with beta-catenin. *Science* **262**, 1731-1734 (1993).
94. Aberle, H., Bauer, A., Stappert, J., Kispert, A. & Kemler, R. beta-catenin is a target for the ubiquitin-proteasome pathway. *EMBO J* **16**, 3797-3804 (1997).
95. Bilic, J*., et al.* Wnt induces LRP6 signalosomes and promotes dishevelled-dependent LRP6 phosphorylation. *Science* **316**, 1619-1622 (2007).
96. Valenta, T., Hausmann, G. & Basler, K. The many faces and functions of beta-catenin. *EMBO J* **31**, 2714-2736 (2012).
97. Suryawanshi, A., Tadagavadi, R.K., Swafford, D. & Manicassamy, S. Modulation of Inflammatory Responses by Wnt/beta-Catenin Signaling in Dendritic Cells: A Novel Immunotherapy Target for Autoimmunity and Cancer. *Frontiers in immunology* **7**, 460 (2016).
98. Jiang, A*., et al.* Disruption of E-cadherin-mediated adhesion induces a functionally distinct pathway of dendritic cell maturation. *Immunity* **27**, 610-624 (2007).
99. Manoharan, I*., et al.* TLR2-dependent activation of beta-catenin pathway in dendritic cells induces regulatory responses and attenuates autoimmune inflammation. *Journal of immunology* **193**, 4203-4213 (2014).
100. Qian, C*., et al.* Fas signal promotes the immunosuppressive function of regulatory dendritic cells via the ERK/beta-catenin pathway. *The Journal of biological chemistry* **288**, 27825-27835 (2013).
101. Vander Lugt, B*., et al.* TGF-beta suppresses beta-catenin-dependent tolerogenic activation program in dendritic cells. *PloS one* **6**, e20099 (2011).
102. Clevers, H. & Nusse, R. Wnt/beta-catenin signaling and disease. *Cell* **149**, 1192-1205 (2012).

103. Silva-Garcia, O., Valdez-Alarcon, J.J. & Baizabal-Aguirre, V.M. The Wnt/beta-catenin signaling pathway controls the inflammatory response in infections caused by pathogenic bacteria. *Mediators of inflammation* **2014**, 310183 (2014).
104. Manicassamy, S.*, et al.* Activation of beta-catenin in dendritic cells regulates immunity versus tolerance in the intestine. *Science* **329**, 849-853 (2010).
105. Shan, M.*, et al.* Mucus enhances gut homeostasis and oral tolerance by delivering immunoregulatory signals. *Science* **342**, 447-453 (2013).
106. Murata-Kamiya, N.*, et al.* Helicobacter pylori CagA interacts with E-cadherin and deregulates the beta-catenin signal that promotes intestinal transdifferentiation in gastric epithelial cells. *Oncogene* **26**, 4617-4626 (2007).
107. Nakayama, M.*, et al.* Helicobacter pylori VacA-induced inhibition of GSK3 through the PI3K/Akt signaling pathway. *The Journal of biological chemistry* **284**, 1612-1619 (2009).
108. Polk, D.B. & Peek, R.M., Jr. Helicobacter pylori: gastric cancer and beyond. *Nat Rev Cancer* **10**, 403-414 (2010).
109. Marshall, B.J. & Warren, J.R. Unidentified curved bacilli in the stomach of patients with gastritis and peptic ulceration. *Lancet* **1**, 1311-1315 (1984).
110. Moodley, Y.*, et al.* Age of the association between Helicobacter pylori and man. *PLoS Pathog* **8**, e1002693 (2012).
111. Fox, J.G.*, et al.* Helicobacter hepaticus sp. nov., a microaerophilic bacterium isolated from livers and intestinal mucosal scrapings from mice. *J Clin Microbiol* **32**, 1238-1245 (1994).
112. Haesebrouck, F.*, et al.* Gastric helicobacters in domestic animals and nonhuman primates and their significance for human health. *Clin Microbiol Rev* **22**, 202-223, Table of Contents (2009).
113. Hunt, R.H.*, et al.* Helicobacter pylori in developing countries. World Gastroenterology Organisation Global Guideline. *J Gastrointestin Liver Dis* **20**, 299-304 (2011).
114. Brown, L.M. Helicobacter pylori: epidemiology and routes of transmission. *Epidemiol Rev* **22**, 283-297 (2000).
115. Blaser, M.J. & Falkow, S. What are the consequences of the disappearing human microbiota? *Nat Rev Microbiol* **7**, 887-894 (2009).
116. Weyermann, M., Rothenbacher, D. & Brenner, H. Acquisition of Helicobacter pylori infection in early childhood: independent contributions of infected mothers, fathers, and siblings. *Am J Gastroenterol* **104**, 182-189 (2009).
117. Banatvala, N. & Feldman, R. The epidemiology of Helicobacter pylori: missing pieces in a jigsaw. *Commun Dis Rep CDR Rev* **3**, R56-59 (1993).
118. Peek, R.M., Jr. & Crabtree, J.E. Helicobacter infection and gastric neoplasia. *J Pathol* **208**, 233-248 (2006).
119. Ferlay, J.*, et al.* Estimates of worldwide burden of cancer in 2008: GLOBOCAN 2008. *Int J Cancer* **127**, 2893-2917 (2010).
120. Kimura, M.*, et al.* Vacuolating cytotoxin purified from Helicobacter pylori causes mitochondrial damage in human gastric cells. *Microb Pathog* **26**, 45-52 (1999).

121. Cover, T.L., Krishna, U.S., Israel, D.A. & Peek, R.M., Jr. Induction of gastric epithelial cell apoptosis by Helicobacter pylori vacuolating cytotoxin. *Cancer Res* **63**, 951-957 (2003).
122. Cover, T.L. & Blaser, M.J. Purification and characterization of the vacuolating toxin from Helicobacter pylori. *The Journal of biological chemistry* **267**, 10570-10575 (1992).
123. Ilver, D., Barone, S., Mercati, D., Lupetti, P. & Telford, J.L. Helicobacter pylori toxin VacA is transferred to host cells via a novel contact-dependent mechanism. *Cell Microbiol* **6**, 167-174 (2004).
124. Nguyen, V.Q., Caprioli, R.M. & Cover, T.L. Carboxy-terminal proteolytic processing of Helicobacter pylori vacuolating toxin. *Infect Immun* **69**, 543-546 (2001).
125. Telford, J.L.*, et al.* Gene structure of the Helicobacter pylori cytotoxin and evidence of its key role in gastric disease. *The Journal of experimental medicine* **179**, 1653-1658 (1994).
126. Blaser, M.J. & Berg, D.E. Helicobacter pylori genetic diversity and risk of human disease. *The Journal of clinical investigation* **107**, 767-773 (2001).
127. Atherton, J.C., Peek, R.M., Jr., Tham, K.T., Cover, T.L. & Blaser, M.J. Clinical and pathological importance of heterogeneity in vacA, the vacuolating cytotoxin gene of Helicobacter pylori. *Gastroenterology* **112**, 92-99 (1997).
128. Atherton, J.C.*, et al.* Mosaicism in vacuolating cytotoxin alleles of Helicobacter pylori. Association of specific vacA types with cytotoxin production and peptic ulceration. *The Journal of biological chemistry* **270**, 17771-17777 (1995).
129. Jones, K.R., Whitmire, J.M. & Merrell, D.S. A Tale of Two Toxins: Helicobacter Pylori CagA and VacA Modulate Host Pathways that Impact Disease. *Front Microbiol* **1**, 115 (2010).
130. Cover, T.L. & Blanke, S.R. Helicobacter pylori VacA, a paradigm for toxin multifunctionality. *Nat Rev Microbiol* **3**, 320-332 (2005).
131. Rossi, M.*, et al.* Evidence for conserved function of gamma-glutamyltranspeptidase in Helicobacter genus. *PloS one* **7**, e30543 (2012).
132. Shibayama, K.*, et al.* Metabolism of glutamine and glutathione via gamma-glutamyltranspeptidase and glutamate transport in Helicobacter pylori: possible significance in the pathophysiology of the organism. *Mol Microbiol* **64**, 396-406 (2007).
133. Chevalier, C., Thiberge, J.M., Ferrero, R.L. & Labigne, A. Essential role of Helicobacter pylori gamma-glutamyltranspeptidase for the colonization of the gastric mucosa of mice. *Mol Microbiol* **31**, 1359-1372 (1999).
134. Moran, A.P., Lindner, B. & Walsh, E.J. Structural characterization of the lipid A component of Helicobacter pylori rough- and smooth-form lipopolysaccharides. *J Bacteriol* **179**, 6453-6463 (1997).
135. Rad, R.*, et al.* Extracellular and intracellular pattern recognition receptors cooperate in the recognition of Helicobacter pylori. *Gastroenterology* **136**, 2247-2257 (2009).
136. Sayi, A.*, et al.* TLR-2-activated B cells suppress Helicobacter-induced preneoplastic gastric immunopathology by inducing T regulatory-1 cells. *Journal of immunology* **186**, 878-890 (2011).

137. Uno, K.*, et al.* Toll-like receptor (TLR) 2 induced through TLR4 signaling initiated by Helicobacter pylori cooperatively amplifies iNOS induction in gastric epithelial cells. *Am J Physiol Gastrointest Liver Physiol* **293**, G1004-1012 (2007).
138. Gringhuis, S.I., den Dunnen, J., Litjens, M., van der Vlist, M. & Geijtenbeek, T.B. Carbohydrate-specific signaling through the DC-SIGN signalosome tailors immunity to Mycobacterium tuberculosis, HIV-1 and Helicobacter pylori. *Nature immunology* **10**, 1081-1088 (2009).
139. Smith, S.M. Role of Toll-like receptors in Helicobacter pylori infection and immunity. *World J Gastrointest Pathophysiol* **5**, 133-146 (2014).
140. Salama, N.R., Hartung, M.L. & Muller, A. Life in the human stomach: persistence strategies of the bacterial pathogen Helicobacter pylori. *Nat Rev Microbiol* **11**, 385-399 (2013).
141. Hitzler, I.*, et al.* Caspase-1 has both proinflammatory and regulatory properties in Helicobacter infections, which are differentially mediated by its substrates IL-1beta and IL-18. *Journal of immunology* **188**, 3594-3602 (2012).
142. Kim, K.M.*, et al.* Helicobacter pylori gamma-glutamyltranspeptidase induces cell cycle arrest at the G1-S phase transition. *J Microbiol* **48**, 372-377 (2010).
143. Gerhard, M.*, et al.* A secreted low-molecular-weight protein from Helicobacter pylori induces cell-cycle arrest of T cells. *Gastroenterology* **128**, 1327-1339 (2005).
144. Gebert, B., Fischer, W., Weiss, E., Hoffmann, R. & Haas, R. Helicobacter pylori vacuolating cytotoxin inhibits T lymphocyte activation. *Science* **301**, 1099-1102 (2003).
145. Oertli, M.*, et al.* Helicobacter pylori gamma-glutamyl transpeptidase and vacuolating cytotoxin promote gastric persistence and immune tolerance. *Proceedings of the National Academy of Sciences of the United States of America* **110**, 3047-3052 (2013).
146. Busiello, I.*, et al.* Helicobacter pylori gamma-glutamyltranspeptidase upregulates COX-2 and EGF-related peptide expression in human gastric cells. *Cell Microbiol* **6**, 255-267 (2004).
147. Meyer, F., Ramanujam, K.S., Gobert, A.P., James, S.P. & Wilson, K.T. Cutting edge: cyclooxygenase-2 activation suppresses Th1 polarization in response to Helicobacter pylori. *Journal of immunology* **171**, 3913-3917 (2003).
148. Lambrecht, B.N. & Hammad, H. The immunology of asthma. *Nature immunology* **16**, 45-56 (2015).
149. Eder, W., Ege, M.J. & von Mutius, E. The asthma epidemic. *N Engl J Med* **355**, 2226-2235 (2006).
150. Kay, A.B. Pathology of mild, severe, and fatal asthma. *American journal of respiratory and critical care medicine* **154**, S66-69 (1996).
151. Sigurs, N., Bjarnason, R., Sigurbergsson, F. & Kjellman, B. Respiratory syncytial virus bronchiolitis in infancy is an important risk factor for asthma and allergy at age 7. *American journal of respiratory and critical care medicine* **161**, 1501-1507 (2000).
152. Kusel, M.M.*, et al.* Early-life respiratory viral infections, atopic sensitization, and risk of subsequent development of persistent asthma. *J Allergy Clin Immunol* **119**, 1105-1110 (2007).

153. Gilliland, F.D*., et al.* Obesity and the risk of newly diagnosed asthma in school-age children. *Am J Epidemiol* **158**, 406-415 (2003).
154. Kim, H.Y., DeKruyff, R.H. & Umetsu, D.T. The many paths to asthma: phenotype shaped by innate and adaptive immunity. *Nature immunology* **11**, 577-584 (2010).
155. Lamblin, C*., et al.* Bronchial neutrophilia in patients with noninfectious status asthmaticus. *American journal of respiratory and critical care medicine* **157**, 394-402 (1998).
156. Wilson, R.H*., et al.* Allergic sensitization through the airway primes Th17-dependent neutrophilia and airway hyperresponsiveness. *American journal of respiratory and critical care medicine* **180**, 720-730 (2009).
157. Bentley, A.M., Kay, A.B. & Durham, S.R. Human late asthmatic reactions. *Clin Exp Allergy* **27 Suppl 1**, 71-86 (1997).
158. Fahy, J.V. Type 2 inflammation in asthma--present in most, absent in many. *Nature reviews. Immunology* **15**, 57-65 (2015).
159. Busse, W.W*., et al.* Randomized, double-blind, placebo-controlled study of brodalumab, a human anti-IL-17 receptor monoclonal antibody, in moderate to severe asthma. *American journal of respiratory and critical care medicine* **188**, 1294-1302 (2013).
160. Lin, H*., et al.* Omalizumab rapidly decreases nasal allergic response and FcepsilonRI on basophils. *J Allergy Clin Immunol* **113**, 297-302 (2004).
161. Wenzel, S*., et al.* Dupilumab in persistent asthma with elevated eosinophil levels. *N Engl J Med* **368**, 2455-2466 (2013).
162. Luther, J., Dave, M., Higgins, P.D. & Kao, J.Y. Association between Helicobacter pylori infection and inflammatory bowel disease: a meta-analysis and systematic review of the literature. *Inflamm Bowel Dis* **16**, 1077-1084 (2010).
163. Arnold, I.C*., et al.* Helicobacter pylori infection prevents allergic asthma in mouse models through the induction of regulatory T cells. *The Journal of clinical investigation* **121**, 3088-3093 (2011).
164. Oertli, M*., et al.* DC-derived IL-18 drives Treg differentiation, murine Helicobacter pylori-specific immune tolerance, and asthma protection. *The Journal of clinical investigation* **122**, 1082-1096 (2012).
165. Kyburz, A. & Muller, A. Helicobacter pylori and Extragastric Diseases. *Curr Top Microbiol Immunol* **400**, 325-347 (2017).
166. Kienesberger, S*., et al.* Gastric Helicobacter pylori Infection Affects Local and Distant Microbial Populations and Host Responses. *Cell Rep* **14**, 1395-1407 (2016).
167. Engstrand, L. & Lindberg, M. Helicobacter pylori and the gastric microbiota. *Best Pract Res Clin Gastroenterol* **27**, 39-45 (2013).
168. Reuter, S*., et al.* The Wnt/beta-catenin pathway attenuates experimental allergic airway disease. *Journal of immunology* **193**, 485-495 (2014).
169. Koch, K.N*., et al.* Helicobacter urease-induced activation of the TLR2/NLRP3/IL-18 axis protects against asthma. *The Journal of clinical investigation* **125**, 3297-3302 (2015).

170. Brault, V.*, et al.* Inactivation of the beta-catenin gene by Wnt1-Cre-mediated deletion results in dramatic brain malformation and failure of craniofacial development. *Development* **128**, 1253-1264 (2001).
171. Caton, M.L., Smith-Raska, M.R. & Reizis, B. Notch-RBP-J signaling controls the homeostasis of CD8- dendritic cells in the spleen. *The Journal of experimental medicine* **204**, 1653-1664 (2007).
172. Arnold, I.C.*, et al.* Tolerance rather than immunity protects from Helicobacter pylori-induced gastric preneoplasia. *Gastroenterology* **140**, 199-209 (2011).
173. Covacci, A.*, et al.* Molecular characterization of the 128-kDa immunodominant antigen of Helicobacter pylori associated with cytotoxicity and duodenal ulcer. *Proceedings of the National Academy of Sciences of the United States of America* **90**, 5791-5795 (1993).
174. Keilberg, D. & Ottemann, K.M. How Helicobacter pylori senses, targets and interacts with the gastric epithelium. *Environ Microbiol* **18**, 791-806 (2016).
175. Kayama, H. & Takeda, K. Functions of innate immune cells and commensal bacteria in gut homeostasis. *J Biochem* **159**, 141-149 (2016).
176. Mowat, A.M. & Agace, W.W. Regional specialization within the intestinal immune system. *Nature reviews. Immunology* **14**, 667-685 (2014).
177. Sun, M., He, C., Cong, Y. & Liu, Z. Regulatory immune cells in regulation of intestinal inflammatory response to microbiota. *Mucosal immunology* **8**, 969-978 (2015).
178. Marques, T.M.*, et al.* Programming infant gut microbiota: influence of dietary and environmental factors. *Curr Opin Biotechnol* **21**, 149-156 (2010).
179. Goto, Y., Kurashima, Y. & Kiyono, H. The gut microbiota and inflammatory bowel disease. *Curr Opin Rheumatol* **27**, 388-396 (2015).
180. Woodmansey, E.J. Intestinal bacteria and ageing. *J Appl Microbiol* **102**, 1178-1186 (2007).
181. Kao, J.Y.*, et al.* Helicobacter pylori-secreted factors inhibit dendritic cell IL-12 secretion: a mechanism of ineffective host defense. *Am J Physiol Gastrointest Liver Physiol* **291**, G73-81 (2006).
182. Bimczok, D.*, et al.* Human primary gastric dendritic cells induce a Th1 response to H. pylori. *Mucosal immunology* **3**, 260-269 (2010).
183. Tamoutounour, S.*, et al.* CD64 distinguishes macrophages from dendritic cells in the gut and reveals the Th1-inducing role of mesenteric lymph node macrophages during colitis. *European journal of immunology* **42**, 3150-3166 (2012).
184. Satpathy, A.T.*, et al.* Notch2-dependent classical dendritic cells orchestrate intestinal immunity to attaching-and-effacing bacterial pathogens. *Nature immunology* **14**, 937-948 (2013).
185. Cerovic, V., Bain, C.C., Mowat, A.M. & Milling, S.W. Intestinal macrophages and dendritic cells: what's the difference? *Trends in immunology* **35**, 270-277 (2014).
186. Hapfelmeier, S.*, et al.* Microbe sampling by mucosal dendritic cells is a discrete, MyD88-independent step in DeltainvG S. Typhimurium colitis. *The Journal of experimental medicine* **205**, 437-450 (2008).
187. Cerovic, V.*, et al.* Intestinal CD103(-) dendritic cells migrate in lymph and prime effector T cells. *Mucosal immunology* **6**, 104-113 (2013).

188. Semper, R.P.*, et al.* Helicobacter pylori-induced IL-1beta secretion in innate immune cells is regulated by the NLRP3 inflammasome and requires the cag pathogenicity island. *Journal of immunology* **193**, 3566-3576 (2014).
189. Saraiva, M. & O'Garra, A. The regulation of IL-10 production by immune cells. *Nature reviews. Immunology* **10**, 170-181 (2010).
190. Engler, D.B.*, et al.* Effective treatment of allergic airway inflammation with Helicobacter pylori immunomodulators requires BATF3-dependent dendritic cells and IL-10. *Proceedings of the National Academy of Sciences of the United States of America* **111**, 11810-11815 (2014).
191. Shimada, K.*, et al.* Caspase-1 dependent IL-1beta secretion is critical for host defense in a mouse model of Chlamydia pneumoniae lung infection. *PloS one* **6**, e21477 (2011).
192. Segovia, J.*, et al.* TLR2/MyD88/NF-kappaB pathway, reactive oxygen species, potassium efflux activates NLRP3/ASC inflammasome during respiratory syncytial virus infection. *PloS one* **7**, e29695 (2012).
193. Rapsinski, G.J.*, et al.* Toll-like receptor 2 and NLRP3 cooperate to recognize a functional bacterial amyloid, curli. *Infect Immun* **83**, 693-701 (2015).
194. Ge, Z.*, et al.* Helicobacter hepaticus urease is not required for intestinal colonization but promotes hepatic inflammation in male A/JCr mice. *Microb Pathog* **45**, 18-24 (2008).
195. Munoz-Planillo, R.*, et al.* K(+) efflux is the common trigger of NLRP3 inflammasome activation by bacterial toxins and particulate matter. *Immunity* **38**, 1142-1153 (2013).
196. Lee, G.S.*, et al.* The calcium-sensing receptor regulates the NLRP3 inflammasome through Ca2+ and cAMP. *Nature* **492**, 123-127 (2012).
197. Horng, T. Calcium signaling and mitochondrial destabilization in the triggering of the NLRP3 inflammasome. *Trends in immunology* **35**, 253-261 (2014).
198. Marlink, K.L.*, et al.* Effects of Helicobacter pylori on intracellular Ca2+ signaling in normal human gastric mucous epithelial cells. *Am J Physiol Gastrointest Liver Physiol* **285**, G163-176 (2003).
199. Engler, D.B.*, et al.* Helicobacter pylori-specific protection against inflammatory bowel disease requires the NLRP3 inflammasome and IL-18. *Inflamm Bowel Dis* **21**, 854-861 (2015).
200. Dupaul-Chicoine, J.*, et al.* Control of intestinal homeostasis, colitis, and colitis-associated colorectal cancer by the inflammatory caspases. *Immunity* **32**, 367-378 (2010).
201. Hirota, S.A.*, et al.* NLRP3 inflammasome plays a key role in the regulation of intestinal homeostasis. *Inflamm Bowel Dis* **17**, 1359-1372 (2011).
202. Donaldson, G.P., Lee, S.M. & Mazmanian, S.K. Gut biogeography of the bacterial microbiota. *Nat Rev Microbiol* **14**, 20-32 (2016).
203. Conlon, M.A. & Bird, A.R. The impact of diet and lifestyle on gut microbiota and human health. *Nutrients* **7**, 17-44 (2014).
204. Guarda, G.*, et al.* Differential expression of NLRP3 among hematopoietic cells. *Journal of immunology* **186**, 2529-2534 (2011).
205. Anderson, O.A., Finkelstein, A. & Shima, D.T. A2E induces IL-1ss production in retinal pigment epithelial cells via the NLRP3 inflammasome. *PloS one* **8**, e67263 (2013).

206. Bruchard, M.*, et al.* The receptor NLRP3 is a transcriptional regulator of TH2 differentiation. *Nature immunology* **16**, 859-870 (2015).
207. Song-Zhao, G.X.*, et al.* Nlrp3 activation in the intestinal epithelium protects against a mucosal pathogen. *Mucosal immunology* **7**, 763-774 (2014).
208. Zaki, M.H.*, et al.* The NLRP3 inflammasome protects against loss of epithelial integrity and mortality during experimental colitis. *Immunity* **32**, 379-391 (2010).
209. Zelenay, S.*, et al.* The dendritic cell receptor DNGR-1 controls endocytic handling of necrotic cell antigens to favor cross-priming of CTLs in virus-infected mice. *The Journal of clinical investigation* **122**, 1615-1627 (2012).
210. Fuertes, M.B.*, et al.* Host type I IFN signals are required for antitumor CD8+ T cell responses through CD8{alpha}+ dendritic cells. *The Journal of experimental medicine* **208**, 2005-2016 (2011).
211. Chudnovskiy, A.*, et al.* Host-Protozoan Interactions Protect from Mucosal Infections through Activation of the Inflammasome. *Cell* **167**, 444-456 e414 (2016).
212. Sun, C.M.*, et al.* Small intestine lamina propria dendritic cells promote de novo generation of Foxp3 T reg cells via retinoic acid. *The Journal of experimental medicine* **204**, 1775-1785 (2007).
213. Yamazaki, S.*, et al.* CD8+ CD205+ splenic dendritic cells are specialized to induce Foxp3+ regulatory T cells. *Journal of immunology* **181**, 6923-6933 (2008).
214. Furuhashi, K.*, et al.* Mouse lung CD103+ and CD11bhigh dendritic cells preferentially induce distinct CD4+ T-cell responses. *American journal of respiratory cell and molecular biology* **46**, 165-172 (2012).
215. Semmrich, M.*, et al.* Directed antigen targeting in vivo identifies a role for CD103+ dendritic cells in both tolerogenic and immunogenic T-cell responses. *Mucosal immunology* **5**, 150-160 (2012).
216. Manicassamy, S. & Pulendran, B. Retinoic acid-dependent regulation of immune responses by dendritic cells and macrophages. *Semin Immunol* **21**, 22-27 (2009).
217. Perez-Yepez, E.A., Ayala-Sumuano, J.T., Lezama, R. & Meza, I. A novel beta-catenin signaling pathway activated by IL-1beta leads to the onset of epithelial-mesenchymal transition in breast cancer cells. *Cancer Lett* **354**, 164-171 (2014).
218. Weydig, C., Starzinski-Powitz, A., Carra, G., Lower, J. & Wessler, S. CagA-independent disruption of adherence junction complexes involves E-cadherin shedding and implies multiple steps in Helicobacter pylori pathogenicity. *Exp Cell Res* **313**, 3459-3471 (2007).
219. Udhayakumar, G., Jayanthi, V., Devaraj, N. & Devaraj, H. Interaction of MUC1 with beta-catenin modulates the Wnt target gene cyclinD1 in H. pylori-induced gastric cancer. *Mol Carcinog* **46**, 807-817 (2007).
220. Capietto, A.H.*, et al.* Down-regulation of PLCgamma2-beta-catenin pathway promotes activation and expansion of myeloid-derived suppressor cells in cancer. *The Journal of experimental medicine* **210**, 2257-2271 (2013).

221. Landsman, L. & Jung, S. Lung macrophages serve as obligatory intermediate between blood monocytes and alveolar macrophages. *Journal of immunology* **179**, 3488-3494 (2007).
222. Arnold, I.C.*, et al.* CD11c(+) monocyte/macrophages promote chronic Helicobacter hepaticus-induced intestinal inflammation through the production of IL-23. *Mucosal immunology* **9**, 352-363 (2016).
223. Cohen, S.B.*, et al.* Beta-catenin signaling drives differentiation and proinflammatory function of IRF8-dependent dendritic cells. *Journal of immunology* **194**, 210-222 (2015).
224. van Rijt, L.S.*, et al.* In vivo depletion of lung CD11c+ dendritic cells during allergen challenge abrogates the characteristic features of asthma. *The Journal of experimental medicine* **201**, 981-991 (2005).
225. Nie, W., Fang, Z., Li, B. & Xiu, Q.Y. Interleukin-10 promoter polymorphisms and asthma risk: a meta-analysis. *Cytokine* **60**, 849-855 (2012).
226. Hyun, M.H., Lee, C.H., Kang, M.H., Park, B.K. & Lee, Y.H. Interleukin-10 promoter gene polymorphisms and susceptibility to asthma: a meta-analysis. *PloS one* **8**, e53758 (2013).
227. Raeiszadeh Jahromi, S.*, et al.* Serum levels of IL-10, IL-17F and IL-33 in patients with asthma: a case-control study. *J Asthma* **51**, 1004-1013 (2014).
228. Henry, E.*, et al.* Dendritic cells genetically engineered to express IL-10 induce long-lasting antigen-specific tolerance in experimental asthma. *Journal of immunology* **181**, 7230-7242 (2008).
229. Obonyo, M.*, et al.* Deficiencies of myeloid differentiation factor 88, Toll-like receptor 2 (TLR2), or TLR4 produce specific defects in macrophage cytokine secretion induced by Helicobacter pylori. *Infect Immun* **75**, 2408-2414 (2007).
230. Boonstra, A.*, et al.* Macrophages and myeloid dendritic cells, but not plasmacytoid dendritic cells, produce IL-10 in response to MyD88- and TRIF-dependent TLR signals, and TLR-independent signals. *Journal of immunology* **177**, 7551-7558 (2006).
231. Kumar, S.*, et al.* IL-10 production from dendritic cells is associated with DC SIGN in human leprosy. *Immunobiology* **218**, 1488-1496 (2013).
232. Rubtsov, Y.P.*, et al.* Regulatory T cell-derived interleukin-10 limits inflammation at environmental interfaces. *Immunity* **28**, 546-558 (2008).
233. Kawano, H.*, et al.* IL-10-producing lung interstitial macrophages prevent neutrophilic asthma. *Int Immunol* **28**, 489-501 (2016).
234. Zhang, H.*, et al.* Subsets of regulatory T cells and their roles in allergy. *Journal of translational medicine* **12**, 125 (2014).
235. Polansky, J.K.*, et al.* DNA methylation controls Foxp3 gene expression. *European journal of immunology* **38**, 1654-1663 (2008).
236. Toker, A.*, et al.* Active demethylation of the Foxp3 locus leads to the generation of stable regulatory T cells within the thymus. *Journal of immunology* **190**, 3180-3188 (2013).
237. Matta, B.M., Castellaneta, A. & Thomson, A.W. Tolerogenic plasmacytoid DC. *European journal of immunology* **40**, 2667-2676 (2010).
238. Bao, Z.*, et al.* Glycogen synthase kinase-3beta inhibition attenuates asthma in mice. *American journal of respiratory and critical care medicine* **176**, 431-438 (2007).

239. Kim, K.K.*, et al.* Epithelial cell alpha3beta1 integrin links beta-catenin and Smad signaling to promote myofibroblast formation and pulmonary fibrosis. *The Journal of clinical investigation* **119**, 213-224 (2009).
240. Reuter, S., Beckert, H. & Taube, C. Take the Wnt out of the inflammatory sails: modulatory effects of Wnt in airway diseases. *Lab Invest* **96**, 177-185 (2016).
241. Yang, X.*, et al.* Curcumin reduces lung inflammation via Wnt/beta-catenin signaling in mouse model of asthma. *J Asthma*, 1-6 (2016).
242. Bae, S.*, et al.* Beta-catenin promoter polymorphism is associated with asthma risk in Korean subjects. *Clin Biochem* **45**, 1187-1191 (2012).
243. Schmees, C.*, et al.* Inhibition of T-cell proliferation by Helicobacter pylori gamma-glutamyl transpeptidase. *Gastroenterology* **132**, 1820-1833 (2007).
244. Wustner, S.*, et al.* Helicobacter pylori gamma-glutamyltranspeptidase impairs T-lymphocyte function by compromising metabolic adaption through inhibition of cMyc and IRF4 expression. *Cell Microbiol* **17**, 51-61 (2015).
245. Kabisch, R., Semper, R.P., Wustner, S., Gerhard, M. & Mejias-Luque, R. Helicobacter pylori gamma-Glutamyltranspeptidase Induces Tolerogenic Human Dendritic Cells by Activation of Glutamate Receptors. *Journal of immunology* **196**, 4246-4252 (2016).
246. Martin, M.*, et al.* Role of the phosphatidylinositol 3 kinase-Akt pathway in the regulation of IL-10 and IL-12 by Porphyromonas gingivalis lipopolysaccharide. *Journal of immunology* **171**, 717-725 (2003).
247. Oertli, M. & Muller, A. Helicobacter pylori targets dendritic cells to induce immune tolerance, promote persistence and confer protection against allergic asthma. *Gut Microbes* **3**, 566-571 (2012).
248. Yu, Y.R.*, et al.* A Protocol for the Comprehensive Flow Cytometric Analysis of Immune Cells in Normal and Inflamed Murine Non-Lymphoid Tissues. *PloS one* **11**, e0150606 (2016).

ACKNOWLEDGMENTS

First I would like to thank my supervisor Anne Müller for giving me the opportunity to do my PhD in her lab. Even though the topics were challenging, I was glad to always have the possibility to receive your scientific support. Your motivation and enthusiasm for the projects were always inspiring over the last years.

Furthermore, I would like to acknowledge my committee members Melanie Greter, Maries van den Broek and Manfred Kopf for their input, critical discussions, helpful input and constant support.

Beside this, I would like to thank the whole IMCR for the atmosphere, which makes it a great place to work. I would like to thank all the people making the IMCR running so smoothly, especially Odete and Farah, who helped me in any occasion and always made my day even brighter.

A special thanks goes to all present and past members of the lab who created such a friendly and good working atmosphere. It was a great pleasure working with you, discussing with you, getting technical assistance and sharing so many hours in the mouse house together. Thanks for being so helpful, when I again had crutches "running" around or other health issues. It was great not only spending time together at work but also becoming close friends and sharing leisure times together. I strongly hope that this will continue.

I am grateful to my family for their emotional and also financial support during my whole education. Without you, I would not have been at this point where I am standing now - once again in another city. Thanks for always being there for me, but at the same time always letting me go my way and supporting it.

Last but not least, I would like to thank all my friends, especially Katha, Phillip, Katja, Tine and Katharina for the great moments during the last four years outside of work.

APPENDIX

1. PUBLISHED RESEARCH ARTICLES

1.1 Lymphotoxin β receptor signalling executes *Helicobacter pylori*-driven gastric inflammation in a T4SS-dependent manner.

authors: Mejías-Luque R, Zöller J, Anderl F, Loew-Gil E, Vieth M, Adler T, Engler D., Urban S, Browning JL, Müller A, Gerhard M, Heikenwalder M

journal: GUT, 2016

contribution: I contributed to figure S5 and S6

ORIGINAL ARTICLE

Lymphotoxin β receptor signalling executes *Helicobacter pylori*-driven gastric inflammation in a T4SS-dependent manner

Raquel Mejías-Luque,[1,2] Jessica Zöller,[3] Florian Anderl,[1] Elena Loew-Gil,[1] Michael Vieth,[4] Thure Adler,[5] Daniela B Engler,[6] Sabine Urban,[6] Jeffrey L Browning,[7] Anne Müller,[6] Markus Gerhard,[1,2] Mathias Heikenwalder[3,8]

▸ Additional material is published online only. To view please visit the journal online (http://dx.doi.org/10.1136/gutjnl-2015-310783).

For numbered affiliations see end of article.

Correspondence to
Professor Mathias Heikenwälder, Schneckenburgerstrasse 8, Munich 81675, Germany; heikenwaelder@helmholtz-muenchen.de, mheikenwaelder@dkfz.de
Division of Chronic Inflammation and Cancer (German Cancer Research Center) DKFZ, or Professor Markus Gerhard, Trogerstrasse 30, Munich, 81675, Germany; markus.gerhard@tum.de, Institut für Medizinische Mikrobiologie, Immunologie und Hygiene, Technische Universität München, Germany

RM-L, JZ, MG and MH contributed equally.

Received 23 September 2015
Revised 14 March 2016
Accepted 21 March 2016

ABSTRACT

Objective Lymphotoxin β receptor (LTβR) signalling has been implicated in inflammation-associated tumour development in different tissues. We have analysed the role of LTβR and alternative NF-κB signalling in *Helicobacter pylori*-mediated gastric inflammation and pathology.

Design We analysed several ligands and receptors of the alternative NF-κB pathway, RelB, p52 nuclear translocation and target genes in tissue samples of *H. pylori*-infected patients with different degrees of gastritis or early gastric tumours by in situ hybridisation, immunohistochemistry, Western blot and real-time PCR analyses. Molecular mechanisms involved in LTβR activation by *H. pylori* were assessed in vitro using human gastric cancer cell lines and distinct *H. pylori* isolates. The effects of blocking or agonistically activating LTβR on gastric pathology during challenge with a human pathogenic *H. pylori* strain were studied in a mouse model.

Results Among the tested candidates, LT was significantly increased and activated alternative NF-κB signalling was observed in the gastric mucosa of *H. pylori*-infected patients. *H. pylori* induced LTβR–ligand expression in a type IV secretion system-dependent but CagA-independent manner, resulting in activation of the alternative NF-κB pathway, which was further enhanced by blocking canonical NF-κB during infection. Blocking LTβR signalling in vivo suppressed *H. pylori*-driven gastritis, whereas LTβR activation in gastric epithelial cells of infected mice induced a broadened pro-inflammatory chemokine milieu, resulting in exacerbated pathology.

Conclusions LTβR-triggered activation of alternative NF-κB signalling in gastric epithelial cells executes *H. pylori*-induced chronic gastritis, representing a novel target to restrict gastric inflammation and pathology elicited by *H. pylori*, while exclusively targeting canonical NF-κB may aggravate pathology by enhancing the alternative pathway.

Significance of this study

What is already known on this subject?
- Activation of alternative NF-κB signalling through Lymphotoxin β receptor (LTβR) has been implicated in inflammation-driven tumour development and progression in different tissues.
- *Helicobacter pylori* infection leads to early activation of the canonical NF-κB signalling pathway.
- Polymorphisms in the *LTA* gene were associated with increased risk for gastric cancer development.
- Increased levels of chemokines regulated by alternative NF-κB signalling (eg, CXCL13) have been observed in *H. pylori*-infected subjects.

What are the new findings?
- *H. pylori* infection triggers LTβR signalling and alternative NF-κB activation in gastric epithelial cells, contributing to gastric inflammation.
- Blocking LTβR signalling during *H. pylori* infection reduces gastric inflammation, while activation of LTβR leads to a more severe pathology.
- Activated alternative NF-κB exacerbates gastric inflammation even in the absence of *H. pylori*.

How might it impact on clinical practice in the foreseeable future?
- Our results suggest that blocking *H. pylori*-induced LTβR signalling might represent an interesting therapeutic approach after antibiotic treatment to control the gastric inflammation elicited by the bacterium. This strategy might be also considered in combination with inhibition of canonical NF-κB, since blocking the canonical pathway alone might have deleterious effects by enhancing the alternative NF-κB pathway. This combinatorial or sequential approach may be able to prevent the well-described progression of gastric pathology even after eradication of *H. pylori* and should be evaluated in clinical trials in high-risk populations.

To cite: Mejías-Luque R, Zöller J, Anderl F, *et al*. *Gut* Published Online First: [*please include* Day Month Year] doi:10.1136/gutjnl-2015-310783

INTRODUCTION

Chronic gastritis induced by colonisation of the gastric mucosa by *Helicobacter pylori* can progress to atrophic gastritis, intestinal metaplasia, dysplasia and ultimately to gastric carcinoma.[1] The pro-inflammatory environment triggered by the

bacterial infection initiates rapid activation of distinct signalling cascades, particularly NF-κB, thereby setting the molecular basis for malignant transformation.[2]

The severity of the inflammatory response to the bacterium and the risk for gastric cancer (GC) development upon infection have been directly linked to the presence of certain bacterial virulence factors, mainly the *cag* pathogenicity island (*cag*PAI), which encodes different components of a type IV secretion system (T4SS) necessary for translocation of Cytotoxin-associated gene A into the host cells.[3] Another component of this T4SS, the CagL protein, interacts with and activates the integrin α5β1 on gastric epithelial cells, which initiates the delivery of CagA into the target cells.[4] Inside the epithelial cell, CagA interacts with host cell molecules such as the phosphatase SHP-2 and triggers a number of downstream signalling pathways with oncogenic activity. At the same time, inflammatory signalling is induced as a consequence of this interaction. While CagA delivery mainly results in the induction of interleukin (IL)-8, the activation of canonical NF-κB signalling is mainly T4SS dependent,[5] highlighting the important role of this pathway in *H. pylori*-induced pathology.

Activation of canonical NF-κB signalling in gastric epithelial cells and infiltrating immune cells has been well documented during *H. pylori* infection;[2 6–8] however, only few data about the functional role of alternative NF-κB pathway in the context of *H. pylori*-driven pathology are available.

The alternative NF-κB pathway is activated via a distinct set of receptors of the tumour necrosis factor superfamily (TNFSF),[9] including BAFFR, Fn14, CD40, herpes virus entry mediator and the lymphotoxin β receptor (LTβR). The latter is triggered by either binding of LTα1β2 heterotrimers expressed by activated T, B, natural killer (NK) cells and lymphoid tissue inducer cells, or LIGHT (homologous to **l**ymphotoxin exhibits **i**nducible expression and competes with HSV **g**lycoprotein D for binding to **h**erpes virus entry mediator, a receptor expressed on **T** lymphocytes), a TNFSF member expressed on T lymphocytes.[9–11] Under pathological conditions, LTs and LIGHT can also be expressed by epithelial cells.[12 13] LTβR is mainly expressed on epithelial and stromal cells, thereby enabling the communication with lymphocytes. Receptor activation leads to the formation of the RelB/p52 NF-κB complex, which mechanistically relies on inducible processing of the precursor p100 to p52 after activation of NF-κB inducing kinase (NIK). The precursor p100 functions as an IκB-like molecule that keeps RelB located in the cytoplasm.[14] Following ligand binding, proteosomal processing of p100 to p52 results in the formation of RelB/p52 heterodimers capable of translocating into the nucleus,[15 16] inducing the expression of several target genes, including alternative NF-κB-specific CXCL13 and other NF-κB target genes (CXCL10, CCL2 or CCL20) that could be linked to active alternative NF-κB signalling.[12 17] Interestingly, some of these chemokines have been reported to be upregulated in stomachs of *H. pylori*-infected subjects.[18–21] However, the upstream events leading to the secretion of these chemokines during *H. pylori* infection are still mostly uncharacterised.

The LT system (LT/LIGHT and LTβR) is crucial for formation and maintenance of tertiary lymphoid organs (TLOs), thereby contributing to cancer development in several tissues.[22–25] However, the role of LTβR signalling in *H. pylori*-driven gastritis and progression to GC remained unknown. Here, we provide evidence that LTβR signalling is essential in executing *H. pylori*-induced chronic inflammation, a precursor of gastric carcinogenesis.

MATERIAL AND METHODS

Cell culture and *H. pylori* strains

AGS, Kato III and SNU-1 (American Type Culture Collection (ATCC)), AZ521 (Japanese Collection of Research Biosources), St3051 and St2957, NUGC-4 and MKN45 were grown in Dulbecco's Modified Eagle Medium (DMEM)/10% fetal calf serum (FCS) (Gibco).[26] Cells were maintained at 37°C in a CO_2 atmosphere and routinely tested for *Mycoplasma* contamination.

H. pylori strains G27,[27] SS1, PMSS1[28] and P12[29] were grown on Wilkins–Chalgren blood agar plates and maintained under microaerophilic conditions. G27 isogenic strains G27Δ*CagA*, G27Δ*CagE*, G27Δ*CagF* and G27Δ*CagI*, G27Δ*BabA*, G27Δ*SabA*, G27Δ*VacA*, G27Δ*gGT*, G27Δ*UreA/B*, PMSS1Δ*CagE*[30] and P12*slt* (kindly provided by Ivo Boneca) were grown in plates containing either 20 μg/mL of kanamycin or 15 μg/mL of chloramphenicol under the same conditions. *H. pylori* clinical isolates were obtained from the Städtisches Klinikum München. Two of the seven clinical isolates were CagA positive (see online supplementary figure S4B).

Histology and immunohistochemistry

Human gastric tissue samples were obtained from the paraffin-embedded tissue bank of the Institut für Pathologie, Klinikum Bayreuth Germany, after approval of the local ethics committee. Patients did not receive antibiotics, nonsteroidal anti-inflammatory drugs (NSAID) or proton pump inhibitor (PPI) drugs before biopsy. Paraffin sections were stained with H&E or various primary and secondary antibodies (see online supplementary table S2). Briefly, sections were incubated in Bond Primary antibody diluent (Leica) and staining was performed on a BOND-MAX immunohistochemistry robot (Leica Biosystems) using BOND polymer refine detection solution for diaminobenzidine (DAB). Image acquisition was performed with a Leica SCN400 slide scanner. The number of cells positively stained for different markers was determined using SlidePathTissueIA image analysis software (Leica) on whole gastric mucosa sections and normalised to tissue area. Pictures for representation were taken by scanning whole tissue sections using a Leica SCN400 slide scanner.

Animal experiments

Female C57BL/6 mice (6–8 weeks) were obtained from Harlan Laboratories (Rossdorf, Germany). All animal studies were conducted in compliance with European guidelines for the care and use of laboratory animals (licenses 63/2008 and 24/2013 to AM) and were approved by the Zurich Cantonal Veterinary Office.

The systemic antagonist mLTβR-mIgG1 (LTβR–Ig) and a control murine monoclonal IgG1 antibody, MOPC-21, were prepared at Biogen Idec and stored at −80°C until used. One week prior to infection, mice were injected intraperitoneally with 100 μg of either substance on day 7 and day 2. On day 0, 2 and 5, mice were infected orogastrically with one dose of 10^9 colony-forming units (cfu) of the *H. pylori* strain PMSS1 and further injected once per week with 100 μg of either LTβR–Ig or MOPC-21 for 1 month. *H. pylori* infection was confirmed by counting cfu from stomach homogenates and efficacy of LTβR–Ig treatment was confirmed by loss of splenic follicular dendritic cell (FDC) networks visualised by anti-FDC-M1 staining. Agonistic activation of the alternative NF-κB signalling pathway was performed by treating mice twice a week with

50 µg ACH6 antibody (kindly provided by Dr Jeffrey Browning/Biogen Idec).

Statistics

Normally distributed data were analysed by one-way analysis of variance (ANOVA) with Dunnett's or Bonferroni's correction for multiple comparisons or Student's t test where indicated, while Mann–Whitney U test or ANOVA Kruskal–Wallis with Dunn's comparison test was used to compare not normally distributed data. Statistical significance was defined when $p<0.05$.

RESULTS

LTβR ligand expression and activation of alternative NF-κB signalling in *H. pylori*-induced gastritis and early gastric tumours

We first assessed mRNA expression of several ligands activating the alternative NF-κB signalling (eg, BAFF, CD40L, LTα, LTβ and TWEAK). We observed significant induction of LTβ mRNA in *H. pylori*-induced gastritis (see online supplementary figure S1A). Thus, we investigated the identity of putative LTβ-responsive cells by in situ hybridisation for LTβR in human gastric tissue samples presenting different degrees of gastric inflammation or early gastric tumours associated with *H. pylori* infection (see online supplementary table S1). We observed that gastric epithelial cells display LTβR mRNA expression that was not affected by the severity of gastric disease (figure 1A and see online supplementary figure S1B). In the same stomach samples increased levels of LTβ were corroborated on protein level, predominantly expressed by inflammatory cells (T and B cells) infiltrating the gastric mucosa (figure 1B, C and see online supplementary figure S1C). Moreover, we detected LTβ protein expression in $LT\beta R^+$ epithelial cells in *H. pylori*-induced gastritis as well as in gastric tumours (figure 1C and see online supplementary figure S1D), suggesting cell autonomous and non-autonomous LTβR signalling. Interestingly, LTβ expression was higher in intestinal-type compared with diffuse-type GCs (see online supplementary figure S1E).

Alternative NF-κB signalling activation was assessed by RelB and p52 nuclear translocation in epithelial cells, which was higher in gastritis and in gastric tumour samples, when compared with controls (figure 1B, D, E and see online supplementary figure S1F).

Furthermore, we analysed expression of LTβR downstream target genes in *H. pylori*-induced moderate gastritis samples (figure 1F). Enhanced expression of CXCL13 and several other chemokines related to LTβR signalling (CCL17, CCL20, CXCL10 and CCL2) was found in patients with *H. pylori*-associated gastritis compared with controls (figure 1F). Furthermore, increased expression of A20, an endogenous inhibitor of canonical NF-κB, corroborated concomitant canonical NF-κB signalling activation in *H. pylori* infection.

H. pylori activates LTβR signalling and alternative NF-κB in human GC cells

To investigate whether *H. pylori* activates LTβR signalling in gastric epithelial cells and to define the molecular mechanisms involved, we initially characterised a panel of human GC cell lines. Except AZ521, all cell lines analysed expressed LTβR (see online supplementary figure S2A). Interestingly, constitutive p100 processing was detected in some cell lines including AZ521 and NUGC-4 (see online supplementary figure S2B). Constitutive activation of alternative NF-κB signalling was not LTβR-ligand dependent, since under basal conditions none of the cell lines studied expressed LTα, LTβ or LIGHT (see online supplementary figure S2C). In parallel, we also analysed canonical NF-κB signalling. All GC cell lines analysed expressed TNFR1 at different levels, while canonical NF-κB activation—examined by pRelA—was observed in most of the cell lines independently of basal expression of TNFα (see online supplementary figure S2C,D). Based on these results, we selected the cell lines MKN45 and St3051, which express LTβR at different levels but lack constitutive activation of the alternative NF-κB pathway, for further experiments.

We first infected these GC cell lines with the *H. pylori* strain G27 at different multiplicity of infection (MOI) for 12 h. *H. pylori* stimulation at low MOI (2–10) resulted in dose-dependent induction of p100 expression and cleavage to p52 (figure 2A and see online supplementary figure S2E). At higher infectious doses (MOI 20–50) we found a reduction in p100 processing, which we observed to be a consequence of cell death occurring at high MOI (data not shown). Thus, we selected MOI 10 for further investigations. As expected, *H. pylori* infection also resulted in a dose-dependent phosphorylation of p65 (see online supplementary figure S2F), demonstrating activation of canonical NF-κB.

We next examined the kinetics of alternative NF-κB signalling activation in a time course study. p100 expression was upregulated 6 h post-infection, while its processing was apparent earliest after 8 h (figure 2B and see online supplementary figure S2G), reaching a plateau of p52 at 10 h, which was maintained even at 24 h post-infection. Using different clinical *H. pylori* isolates we confirmed p100 processing (figure 2C).

We further investigated whether p100 processing to p52 correlated with LTβR-ligand expression. We detected LT mRNA upregulation already 3 h post-infection (figure 2D), which was approximately 4–5 h before first signs of p100 processing (figure 2B). Notably, expression of LTβ was induced at a much higher level when compared with LTα in both cell lines, while LTβR expression did not change (see online supplementary figure S2H).

Next, we analysed the expression of different chemokines regulated by LTβR signalling at 12 h post-infection. Similar to results obtained from patients, significant induction of CXCL13, CXCL10 and CCL20 in response to *H. pylori* infection was found in GC cells (figure 2E and see online supplementary figure S2I). A20 levels were also significantly enhanced (figure 2E and see online supplementary figure S2I).

H. pylori-induced LTβR ligand upregulation activates alternative NF-κB in a secondary loop post-infection

H. pylori can interact with host receptors, for example, MUC5AC[31] or TNFR1,[32] which prompted us to investigate whether *H. pylori* directly interacted with the LTβR and triggered downstream signalling. However, no interaction between LTβR and *H. pylori* was detected via immunoprecipitation (see online supplementary figure S3A).

As *H. pylori*-induced LT expression precedes p100 processing (shown in figure 2B, D), we hypothesised that LTs might activate LTβR signalling in a secondary loop post-infection. Thus, we scavenged $LT\alpha_1\beta_2$ and LIGHT using an LTβR–Ig fusion protein. LTβR–Ig treatment during *H. pylori* infection did not affect LTα and LTβ mRNA levels (see online supplementary figure S3B and data not shown). However, LTβR–Ig treatment suppressed p100 processing, whereas the isotype control MOPC-21 did not (figure 3A). This suggests that LTβR ligands induce activation of LTβR signalling in response to *H. pylori* infection.

LT expression can be regulated by canonical NF-κB.[33] Therefore, we analysed whether this pathway also regulates LT

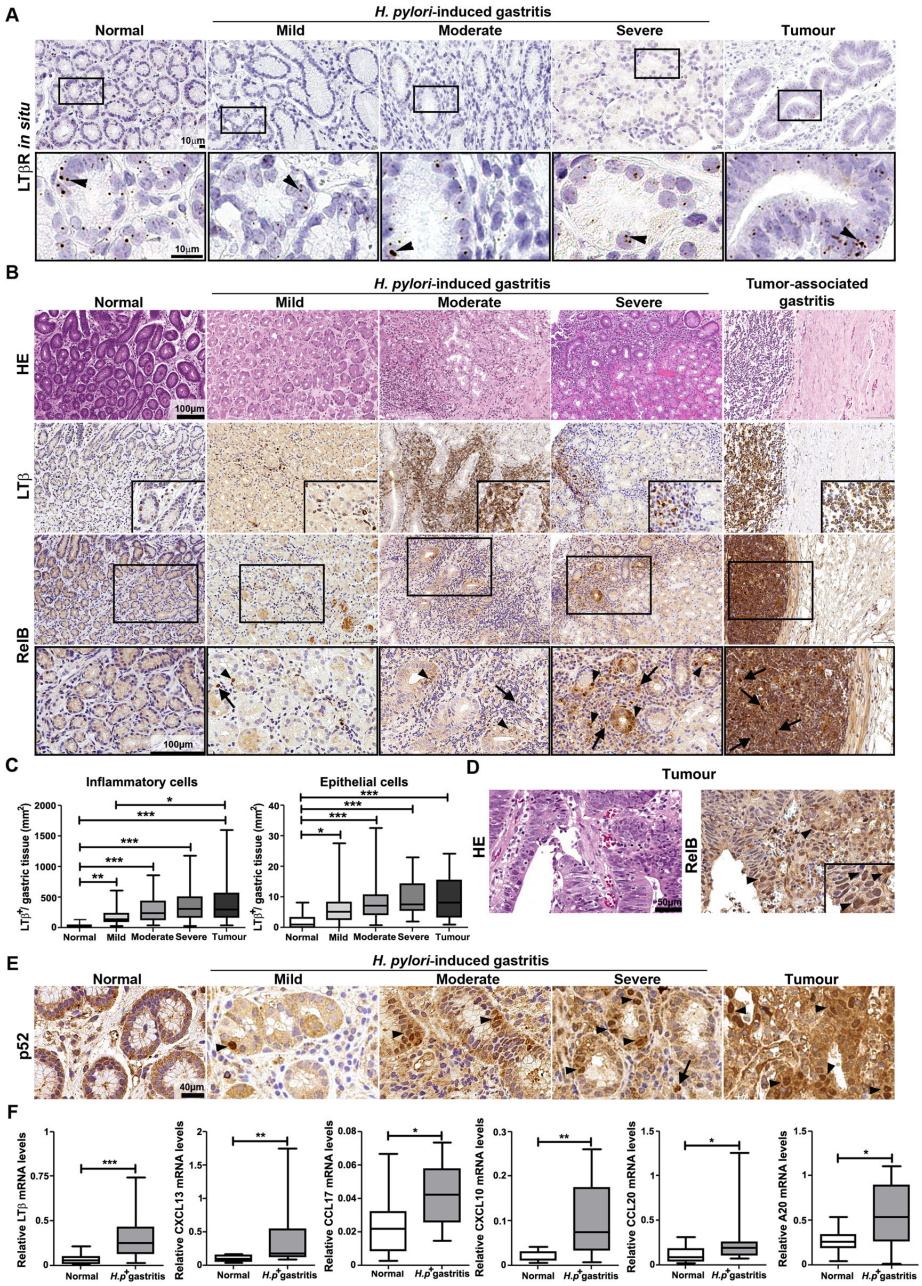

Figure 1 Lymphotoxin β receptor (LTβR) signalling is activated in *Helicobacter pylori*-induced gastritis and gastric tumours. (A) LTβR mRNA expression detected in human normal gastric mucosa, in mild, moderate and severe gastritis caused by *H. pylori* infection, as well as in early gastric adenocarcinomas detected by in situ hybridisation. (B) Representative images of LTβ and RelB expression in human gastric tissue samples detected by immunohistochemistry. Arrowheads indicate RelB nuclear expression in epithelial cells. Arrows denote expression in immune cells. (C) Quantification of $LT\beta^+$ cells (median and minimum to maximum values) in human normal gastric mucosa (n=20), mild (n=26), moderate (n=24) and severe gastritis (n=17), as well as in early gastric adenocarcinoma (n=23) tissue samples. (D) Representative image of RelB expression in gastric tumours detected by immunohistochemistry. Arrows indicate $RelB^+$ nuclei. (E) Representative images of p52 expression in human gastric samples. Arrowheads indicate p52 nuclear expression in epithelial cells. Arrows denote expression in immune cells. (F) Whiskers (median and minimum to maximum) box plots show relative mRNA levels of CXCL13, CCL17, CXCL10, CCL20, CCL2 and A20 detected in human normal gastric mucosa (n=11) and *H. pylori*-induced gastritis (n=11). *p≤0.05, **p≤0.01, ***p≤0.001. (analysis of variance Kruskal–Wallis, Dunn's multiple comparison test.)

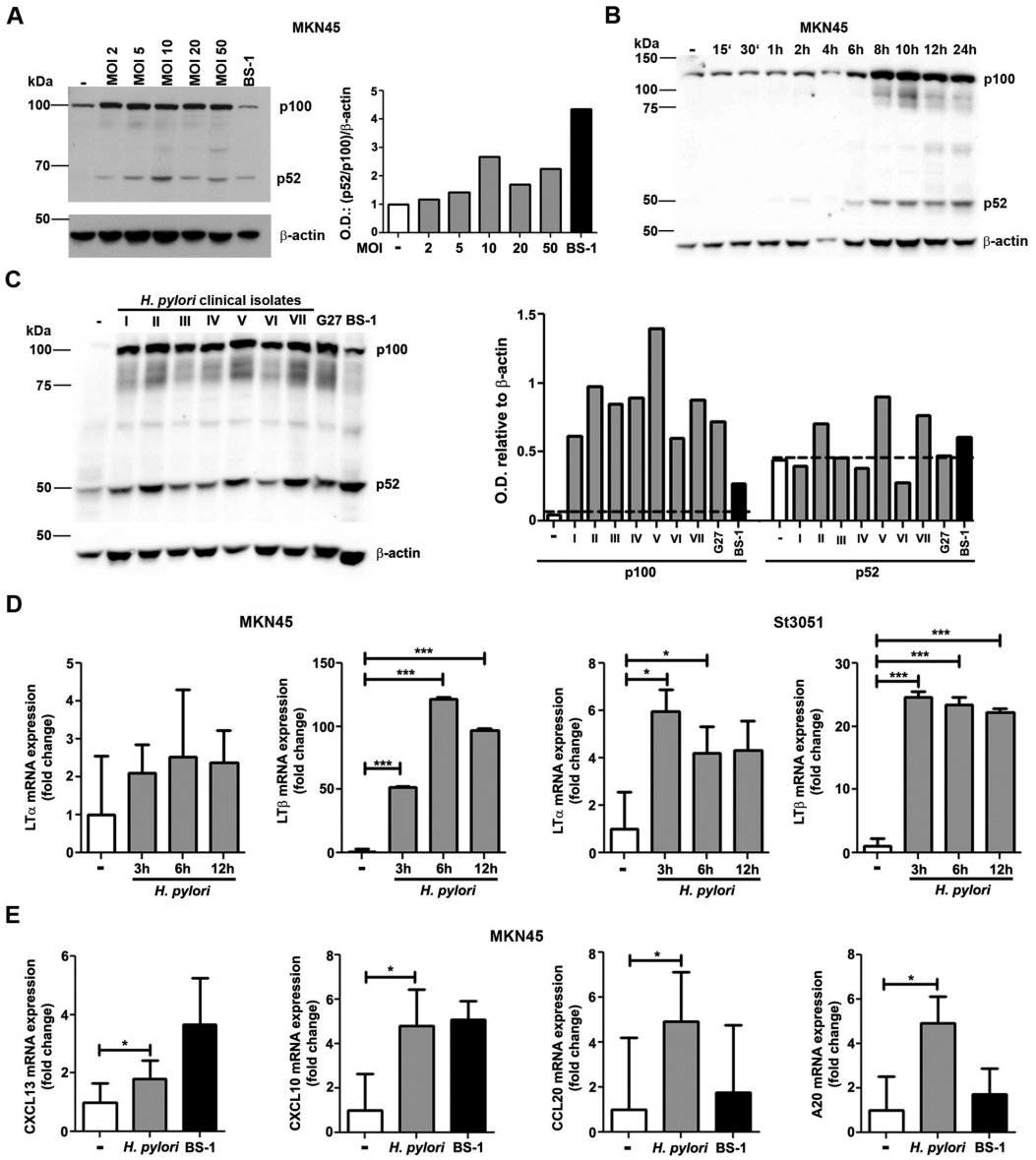

Figure 2 *Helicobacter pylori* activates alternative NF-κB signalling. (A) MKN45 and St3051 cells were infected with *H. pylori* G27 strain at the indicated MOI and p100 processing to p52 was analysed by western blot. The agonist of lymphotoxin β receptor (LTβR) signalling BS-1 (0.5 μg/mL) was used as positive and β-actin as loading control. One representative blot and band quantification showing the ratio between p100 and p52 levels from three independent experiments is shown. OD, optical density (arbitrary units). (B) MKN45 GC cells were infected with *H. pylori* G27 strain at MOI 10 for different time points and processing of p100 to p52 was analysed by western blot. The agonist BS-1 (0.5 μg/mL for 12 h) was used as positive control. β-actin was used as loading control. One representative blot is shown. (C) p100 processing to p52 detected by western blot in MKN45 cells infected with different clinical isolates (I–VII) at MOI 10 for 12 h. One representative of three independent experiments is shown. (D) mRNA expression levels (mean±SD) of LTα and LTβ upon *H. pylori* G27 strain infection at MOI 10 for 3 (n=3), 6 (n=4) and 12 h (n=4) in MKN45 and St3051 cells (ANOVA, Dunnett's multiple comparison test). (E) CXCL13, CXCL10, CCL20 and A20 mRNA expression upon *H. pylori* G27 strain infection at MOI 10 for 12 h. The agonist BS-1 (0.5 μg/mL) was used as positive control. Ct values were normalised to Glyceraldehyde-3-phosphate dehydrogenase (GADPH). Results (mean±SD) from three independent experiments are presented as fold induction. *p≤0.05, ***p≤0.001. (Control and *H. pylori*-infected cells were compared using Student's t test.)

expression in GC cells. Upon TNFα stimulation, LTβ expression was significantly induced, while only minor effects were detected on LTα mRNA levels. As a control, A20 was induced (see online supplementary figure S3C). We confirmed regulation of LTα and LTβ by canonical NF-κB upon *H. pylori* infection by using an inhibitor of human IκB kinase 2 (IKK2)

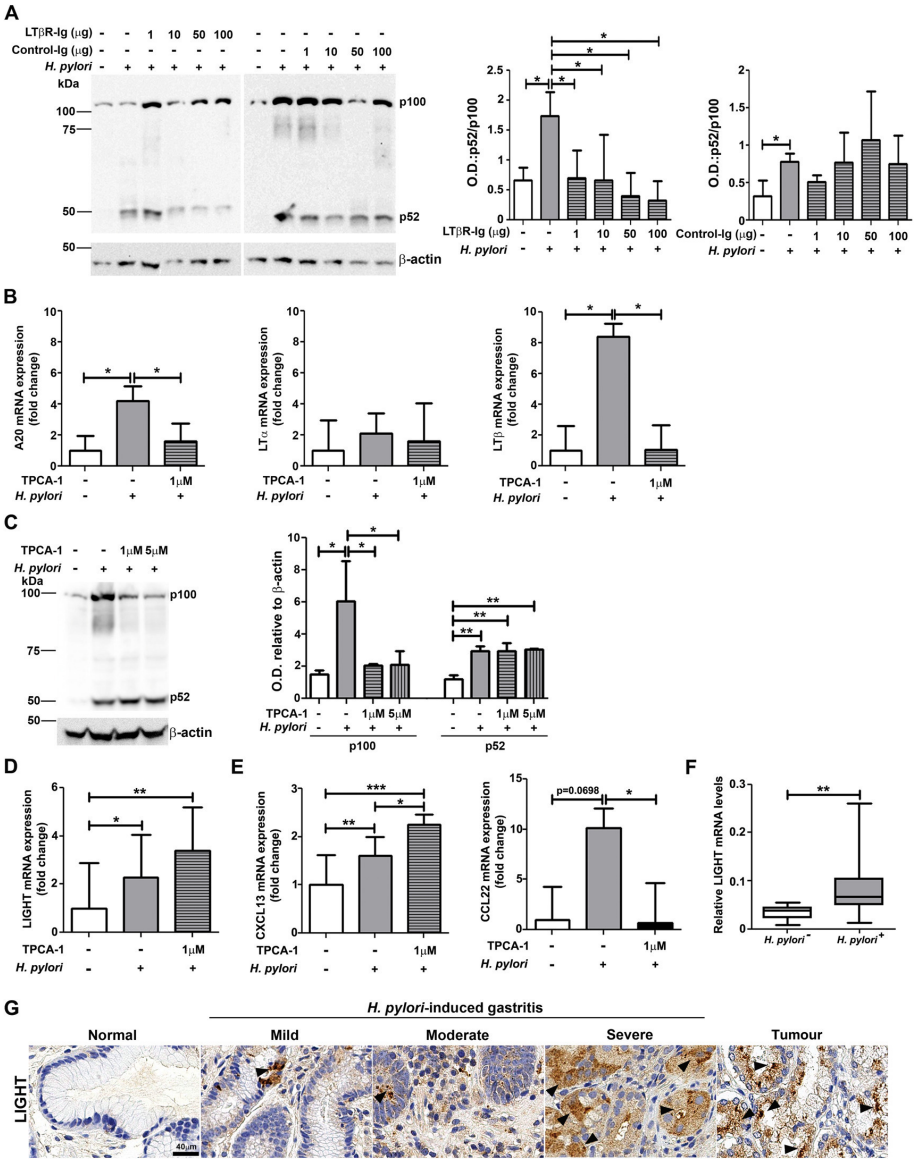

Figure 3 Activation of lymphotoxin β receptor (LTβR) signalling is induced by secreted LT and LIGHT (homologous to **l**ymphotoxin exhibits **i**nducible expression and competes with HSV **g**lycoprotein D for binding to **h**erpes virus entry mediator, a receptor expressed on **T** lymphocytes) in response to *Helicobacter pylori* infection. (A) MKN45 cells were incubated with LTβR–Ig or the isotype control MOPC21 for 1 h before *H. pylori* infection at MOI 10. p100 processing to p52 was evaluated by western blot after 12 h infection. β-actin served as loading control. One representative blot and quantification of three independent experiments (mean±SD) are shown. (B) A20, LTα and LTβ mRNA levels were analysed by real-time PCR in MKN45 cells after 12 h infection with the *H. pylori* strain G27 (MOI 10). Cells were incubated with the inhibitor of human IκB kinase 2 (IKK2) TPCA-1 1 h prior to infection. Ct values were normalised to GADPH. Results expressed as mean±SD from three independent experiments are shown. (C) MKN45 cells were incubated with TPCA-1 for 1 h before infection with the *H. pylori* strain G27 (MOI 10). Cell lysates were obtained after 12 h infection and levels of p100/p52 were assessed by western blot. β-actin was used as loading control. One representative blot and quantification (mean±SD) of three independent experiments are shown. (D) LIGHT mRNA expression levels after infection of MKN45 cells with the *H. pylori* strain G27 at MOI 10 for 12 h. Cells were incubated with TPCA-1 for 1 h before infection. Results (mean±SD) from three independent experiments are shown. (E) CXCL13 and CCL22 mRNA levels in MKN45 cells infected with *H. pylori* G27 (MOI 10, 12 h). Where indicated, cells were incubated with TPCA-1 1 h before infection. Ct values were normalised to GADPH. Results (mean±SD) from three independent experiments are shown. (F) Whiskers (median and minimum to maximum) box plot showing relative mRNA levels of LIGHT in gastric *H. pylori*-induced and *H. pylori*-negative gastritis (n=11). (G) Representative images of LIGHT expression in human gastric tissue samples detected by immunohistochemistry. Arrows indicate positive cells. *p≤0.05, **p≤0.01, ***p≤0.001. ((A–E) analysis of variance (ANOVA), Bonferroni's multiple comparison test; (F) ANOVA Kruskal–Wallis, Dunn's multiple comparison test.)

[5-(p-Fluorophenyl)-2-ureido]thiophene-3-carboxamide (see online supplementary figure S3D). Reduced levels of A20 were detected after TPCA-1 treatment (figure 3B), while the expression of LTα was slightly affected. Remarkably, LTβ levels were significantly reduced (figure 3B), confirming that LTβ expression is regulated by canonical NF-κB in gastric cells. When assessing p100 processing we observed lower levels of p100 in the presence of TPCA-1 (figure 3C and see online supplementary figure S3E). Remarkably, cleavage of p100 to p52 was still found to a similar extent when compared with untreated controls, suggesting a canonical NF-κB-independent LTβR ligand to drive p100 processing in the absence of LTs.

Besides LTs, LIGHT was reported to activate LTβR. Therefore, we studied LIGHT expression in gastric cells post-*H. pylori* challenge. While no or minor upregulation was detected after activation of canonical NF-κB using TNFα (see online supplementary figure S3C), we observed induction of LIGHT expression upon *H. pylori* infection (figure 3D), which was even further enhanced when blocking canonical NF-κB by TPCA-1. Likewise, expression of the LTβR signalling-specific target gene CXCL13 was increased when blocking canonical NF-κB (figure 3E), while expression of the canonical pathway target CCL22 was completely abrogated (figure 3E). This suggests that canonical NF-κB negatively regulates LTβR activation through repressing LIGHT in *H. pylori* infection. Notably, expression of other TNFSF ligands such as BAFF or CD40L was not detected, neither under basal conditions nor after *H. pylori* infection or TPCA-1 treatment in GC cells (data not shown). In line, the expression of TWEAK was not upregulated upon bacterial infection or inhibition of canonical NF-κB (see online supplementary figure S3F), supporting the fact that LIGHT may be responsible for inducing p100 processing after blocking canonical NF-κB pathway. In parallel, *H. pylori*-triggered upregulation of LIGHT mRNA expression was confirmed in human gastric biopsies with moderate gastritis (figure 3F). LIGHT protein expression was mainly increased in epithelial cells of human gastric tissue samples presenting different degrees of gastric inflammation and in early gastric tumours associated with *H. pylori* infection (figure 3G).

*H. pylori cag*PAI but not CagA is required for LTβR-mediated activation of alternative NF-κB

To determine whether the expression of LTs and subsequent activation of LTβR signalling was influenced by *H. pylori* virulence factors, we infected epithelial cells with different mutant strains. A functional T4SS was necessary to induce LT expression, since cells infected with the mutant strain G27Δ*CagE* expressed lower levels of LT compared with cells infected with the wild-type strain (figure 4A). Notably, LIGHT expression did not depend on a functional T4SS, confirming canonical NF-κB-independent regulation of LIGHT (see online supplementary figure S4A).

When analysing p100 processing, we observed that lack of CagA left p100 levels and p100 cleavage unaltered, while

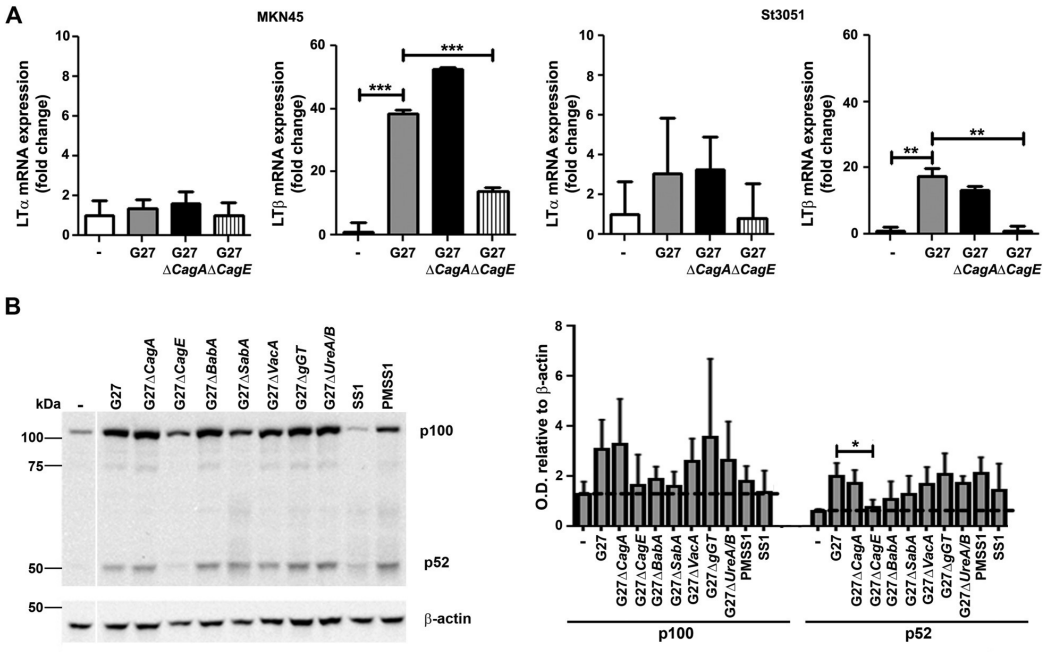

Figure 4 Activation of alternative NF-κB is independent of CagA. (A) mRNA expression levels of lymphotoxin (LT)α and LTβ in MKN45 and St3051 cells after infection with wild-type *Helicobacter pylori* G27 strain and the isogenic mutant strains G27Δ*CagA* and G27Δ*CagE*. Ct values were normalised to GADPH. Results (mean±SD) from four independent experiments are shown (analysis of variance, Bonferroni's multiple comparison test). (B) MKN45 cells were infected with the *H. pylori* wild-type strains G27, PMSS1 and SS1 and the G27 isogenic mutant strains G27Δ*CagA*, G27Δ*CagE*, G27Δ*BabA*, G27Δ*SabA*, G27Δ*VacA*, G27Δ*gGT* and G27Δ*UreA/B* at MOI 10 for 12 h. p100 processing to p52 was detected by western blot. β-actin was used as loading control. One representative blot and quantification of three independent experiments is shown. *p≤0.05, **p≤0.01, ***p≤0.001. (G27 wt and G27Δ*CagE*-infected cells were compared using Student's t test.)

bacteria devoid of functional *cag*PAI (SS1, G27Δ*CagE*, G27Δ*CagF*, G27Δ*CagI*) did not induce p100 expression and processing (figure 4B, see online supplementary figure S4B, C). In line, clinical isolates lacking CagA induced p100 processing (figure 2E and see online supplementary figure S4D). Thus, CagA is not necessary for LT-mediated activation of alternative NF-κB signalling in gastric cells.

Another described *H. pylori* effector molecule translocated into target host cells through the T4SS is peptidoglycan.[34] To determine whether peptidoglycan could be involved in LT-mediated activation of alternative NF-κB, we infected cells with a strain deficient in lytic transglycosylase activity (P12*slt*), which is involved in bacterial muropeptide release. Processing of p100 to p52 was reduced in cells infected with the *slt*-deficient strain (see online supplementary figure S4E), suggesting that peptidoglycan may be involved in activation of alternative NF-κB.

A functional T4SS is necessary to induce ligand expression and alternative NF-κB activation in vivo

In order to validate our results in vivo, C57BL/6 mice were infected with the pathogenic *H. pylori* strain PMSS1[28 30] and analysed for LTα, LTβ and LIGHT mRNA expression. One month post-infection, mice presented significantly increased gastric levels of all LTβR ligands (figure 5A), confirming a correlation between *H. pylori* infection and LT/LIGHT upregulation in vivo. Since our in vitro data suggested the involvement of a functional T4SS in alternative NF-κB activation, we also infected mice with PMSS1 strain deficient for CagE. mRNA levels of LTα, LTβ and LIGHT were lower in mice infected with *H. pylori* PMSS1Δ*CagE* when compared with mice infected with the wild-type strain (figure 5B), even though they were colonised at higher levels (figure 5C). In addition, mice infected with CagE-deficient bacteria showed less gastric inflammation (figure 5D), as previously reported.[30] Specifically, lower infiltration of T and B cells was detected in the stomach of mice infected with PMSS1Δ*CagE* when compared with mice infected with wild-type bacteria (figure 5E). Infection of mice with wild-type PMSS1 induced activation of alternative NF-κB in gastric epithelial cells, as detected by nuclear translocation of RelB (figure 5E). Notably, lack of CagE correlated with reduced nuclear RelB translocation, confirming that activation of alternative NF-κB signalling by *H. pylori* requires a functional T4SS. Moreover, the expression of canonical as well as alternative NF-κB signalling target genes such as A20, murine IL-8 homologue KC, CXCL13, CXCL10, CCL2 and CCL20 was reduced in the gastric mucosa of mice infected with bacteria deficient for CagE (figure 5F).

Blocking LTβR signalling in vivo reduces *H. pylori*-induced gastric inflammation

We next assessed whether LTβR signalling is correlatively or causally linked with gastric inflammation and pathology triggered by *H. pylori* in vivo. Thus, we treated *H. pylori*-infected mice with LTβR–Ig (see online supplementary figure S5A) to study the effects of blocking LTβR signalling on bacterial colonisation and gastric inflammation induced by *H. pylori*. Efficacy of LTβR–Ig treatment was confirmed by staining LTβR-dependent FDCs in spleen[25] (see online supplementary figure S5B). Interestingly, LTβR–Ig-treated mice presented a higher gastric bacterial load when compared with MOPC-21-injected mice (figure 6A), suggesting that LTβR signalling is important to control bacterial burden. Higher *H. pylori* colonisation was accompanied by less gastric inflammation (figure 6B), indicating that LTβR signalling is an important driver of gastric pathology induced by the bacterium. Remarkably, LTβR–Ig-injected mice displayed less $CD3^+$ and $CD4^+$ cells infiltrating the stomach (figure 6C and see online supplementary figure S5C). In addition, less $B220^+$ cells were detected upon LTβR–Ig treatment in the gastric mucosa of infected mice (figure 6C), demonstrating a reduced inflammatory response after blocking LTβR signalling. Moreover, mice treated with LTβR–Ig presented lower nuclear translocation of RelB in gastric epithelial cells (figure 6C), confirming treatment efficacy.

We further assessed whether blocking LTβR signalling upon *H. pylori* infection altered the expression levels of several chemokines. We observed decreased levels of KC, CXCL10, CCL20 and CCL2 in the stomach of mice injected with LTβR–Ig (figure 6D), correlating with the lower inflammation found in the gastric mucosa.

Activation of LTβR signalling enhances gastric pathology induced by *H. pylori*

We next determined the effect of enhanced LTβR signalling during *H. pylori* infection. We injected *H. pylori*-infected mice with ACH6, a murine agonist of LTβR[35] (figure 7 and see online supplementary figure S5A). ACH6-triggered activation of LTβR led to a decrease in gastric bacterial load (figure 7A), accompanied by higher gastric inflammation (figure 7B). We observed slightly lower levels of $CD3^+$ cells in *H. pylori*-infected animals treated with the agonist (figure 7C), while no major differences were detected in $CD4^+$ or $F480^+$ macrophages (see online supplementary figure S6A). Interestingly, animals treated with the agonist presented more B cells than infected control mice (see online supplementary figure S6B). In line, the expression of CXCL13 was enhanced in mice injected with ACH6 (figure 7D). We also observed increased expression of the LTβR target genes LIGHT, ICAM—involved in leucocyte recruitment—and CCL2 (figure 7D), while KC and CCL20 levels remained unchanged (see online supplementary figure S6C).

DISCUSSION

Activation of LTβR triggers and maintains TLOs during chronic infection.[36] Notably, lymphoid neogenesis and TLO formation were reported as a histological hallmark of chronic *H. pylori* infection,[37–39] suggesting a possible role of the LTβR signalling pathway in *H. pylori*-driven pathology.

The involvement of NIK in *H. pylori*-induced NF-κB activation was reported in gastric epithelial cells,[40 41] and p100/p52 processing upon *H. pylori* infection was reported in B lymphocytes.[42] However, in the latter study, activation of alternative NF-κB reflected by p100 processing was not found in the GC cell line AGS. In addition, p100/p52 staining of human gastric samples from *H. pylori*-infected subjects showed only cytoplasmic staining that was weaker compared with infiltrating lymphocytes, leading to the conclusion that the alternative NF-κB pathway was not activated in epithelial cells upon *H. pylori* infection. In our study, we have detected p100 processing in different human gastric cell lines. Importantly, activation of the alternative NF-κB pathway was corroborated in epithelial and immune cells in gastritis and gastric tumour samples from *H. pylori*-infected patients. Likewise, mice infected with *H. pylori* showed increased nuclear translocation of RelB in gastric epithelial cells, demonstrating that *H. pylori* activates alternative NF-κB in vitro and in vivo.

Canonical and alternative NF-κB signalling are closely related and crosstalk at different levels, for example, expression of

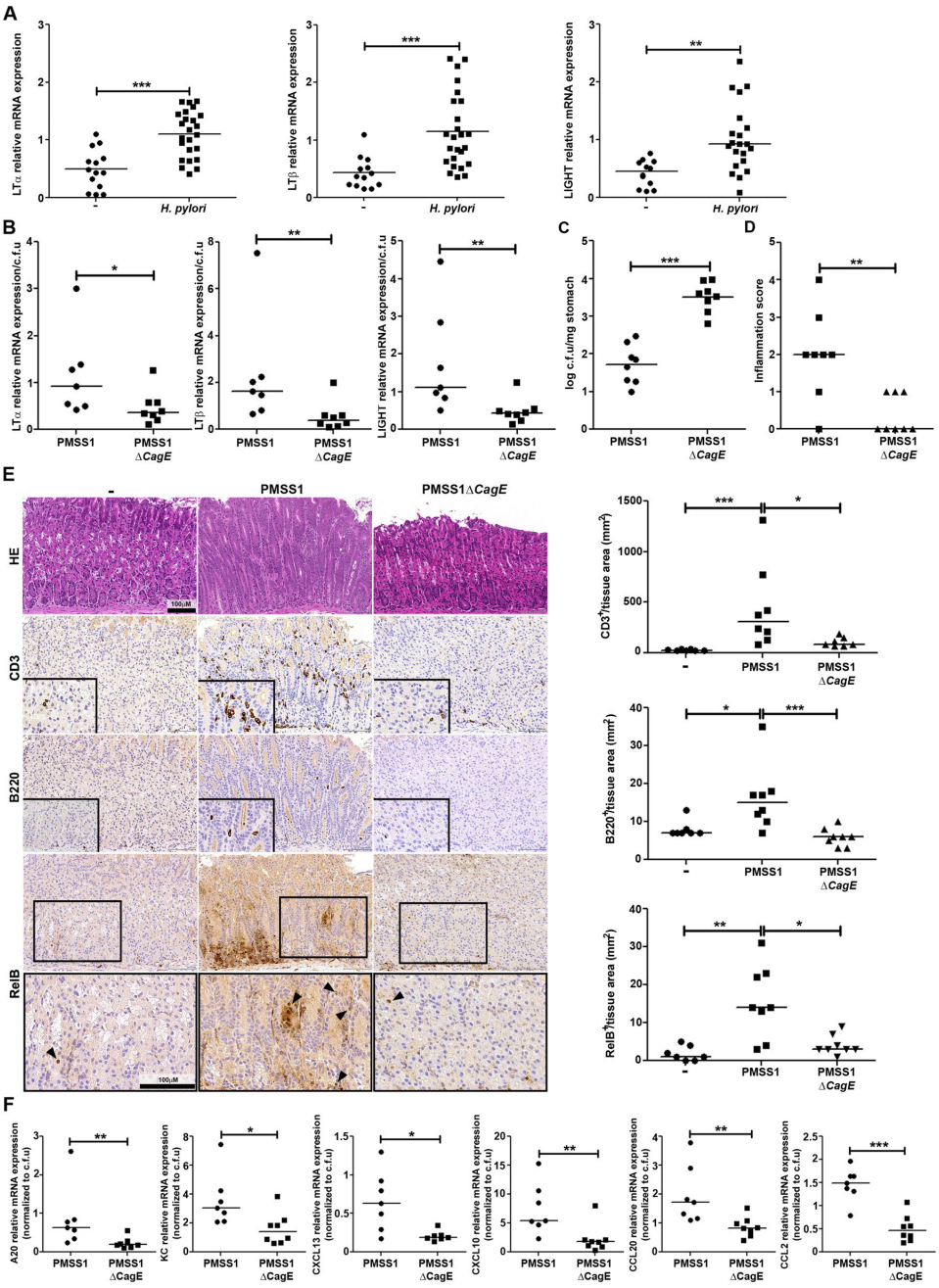

Figure 5 *Helicobacter pylori* activates alternative NF-κB in vivo in a type IV secretion system (T4SS)-dependent manner. (A) Lymphotoxin (LT)α, LTβ and LIGHT (homologous to **l**ymphotoxin exhibits **i**nducible expression and competes with HSV **g**lycoprotein D for binding to **h**erpes virus entry mediator, a receptor expressed on **T** lymphocytes) mRNA levels in mice infected for 1 month with the *H. pylori* strain PMSS1. Ct values were normalised to GADPH. (B–F) Mice were infected for 1 month with the *H. pylori* strain PMSS1 or an isogenic strain lacking CagE. (B) LTα, LTβ and LIGHT mRNA levels in infected mice. Ct values were normalised to GADPH. (C) Colony-forming units (cfu) per mg of stomach. (D) Inflammatory score. Activity and chronicity of infection was evaluated in antrum and corpus of murine stomach samples according to the updated Sydney system. (E) Murine stomach samples were stained for CD3, B220 and RelB by immunohistochemistry. Representative pictures are shown. $CD3^+$ and $B220^+$ cells and $RelB^+$ nuclei were calculated per area of tissue (mm^2). (F) Relative mRNA expression levels of A20, KC, CXCL13, CXCL10, CCL20 and CCL2 in the stomach of *H. pylori*-infected mice. Ct values were normalised to GADPH. *p≤0.05, **p≤0.01, ***p≤0.001. ((A), (B) and (F) (Mann–Whitney U test); (E) analysis of variance Kruskal–Wallis, Dunn's multiple comparison test.)

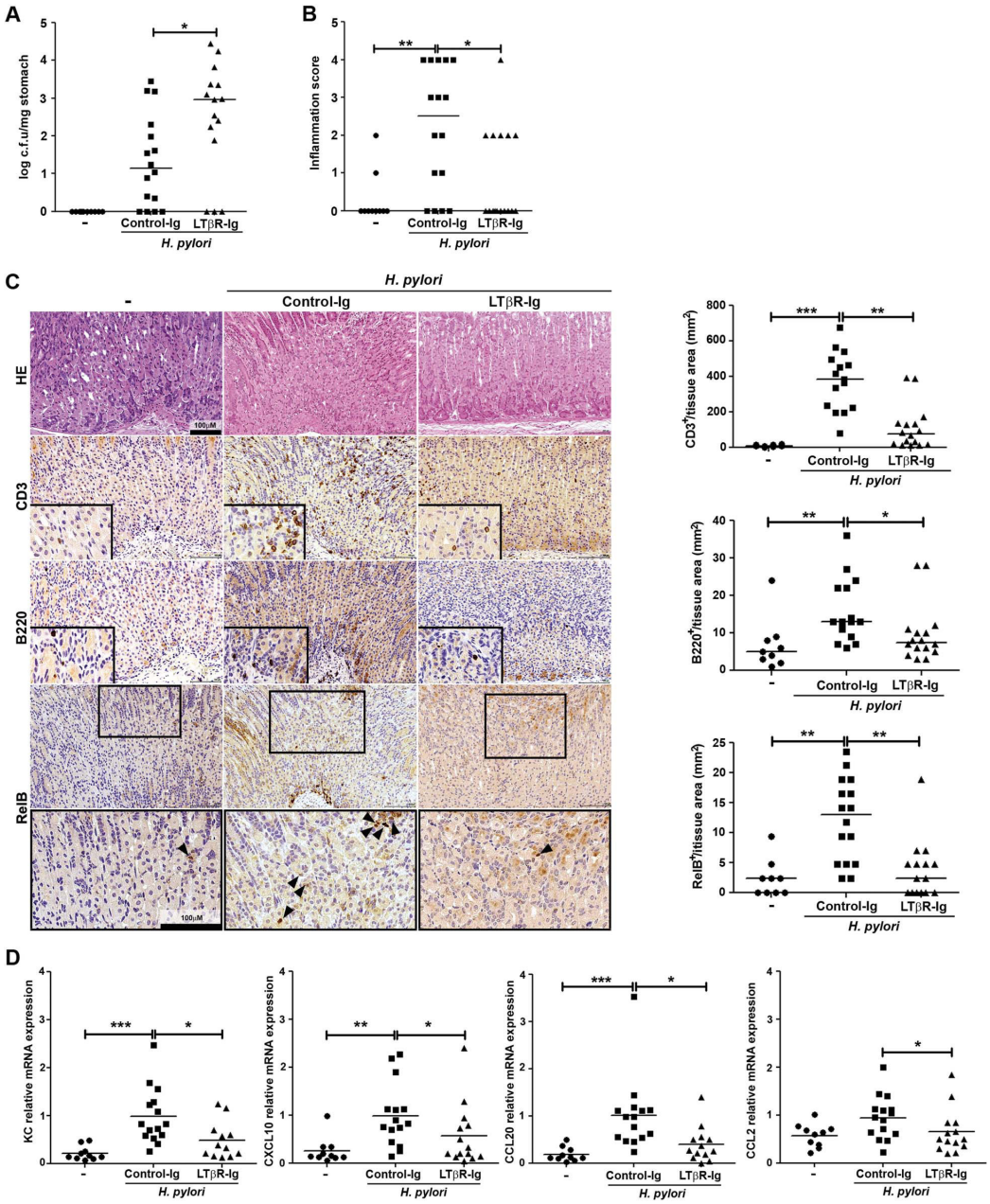

Figure 6 Blocking of lymphotoxin β receptor (LTβR) signalling during *Helicobacter pylori* infection reduces gastric inflammation. (A–D) C57BL/6 mice infected with the *H. pylori* strain PMSS1 were injected weekly with 100 μg of LTβR–Ig or the isotype control MOPC-21 (Control–Ig). Mice were sacrificed after 1-month infection. Dots represent data of individual mice pooled from two independent experiments. (A) Colony-forming units (cfu) per mg of stomach. (B) Inflammatory score. Activity and chronicity of infection was evaluated in antrum and corpus of murine stomach samples according to the updated Sydney system. (C) Murine stomach samples were stained for CD3, B220 and RelB by immunohistochemistry. Representative pictures are shown. $CD3^+$ and $B220^+$ cells and $RelB^+$ nuclei were calculated per area of tissue (mm^2). (D) Relative mRNA expression levels of KC, CXCL10, CCL20 and CCL2 in the stomach of control or *H. pylori*-infected mice treated with LTβR–Ig or MOPC-21. Ct values were normalised to GADPH. *p≤0.05, **p≤0.01, ***p≤0.001. (analysis of variance Kruskal–Wallis, Dunn's multiple comparison test.)

p100 and LTβ, have been reported to be regulated by canonical NF-κB.[33 43–45] In line, we detected enhanced expression of p100 and LTs upon *H. pylori* infection, which was reduced when activation of canonical NF-κB was blocked. However, p100 processing was still observed, indicating that p100 overexpression is insufficient to induce its processing.[46] It rather

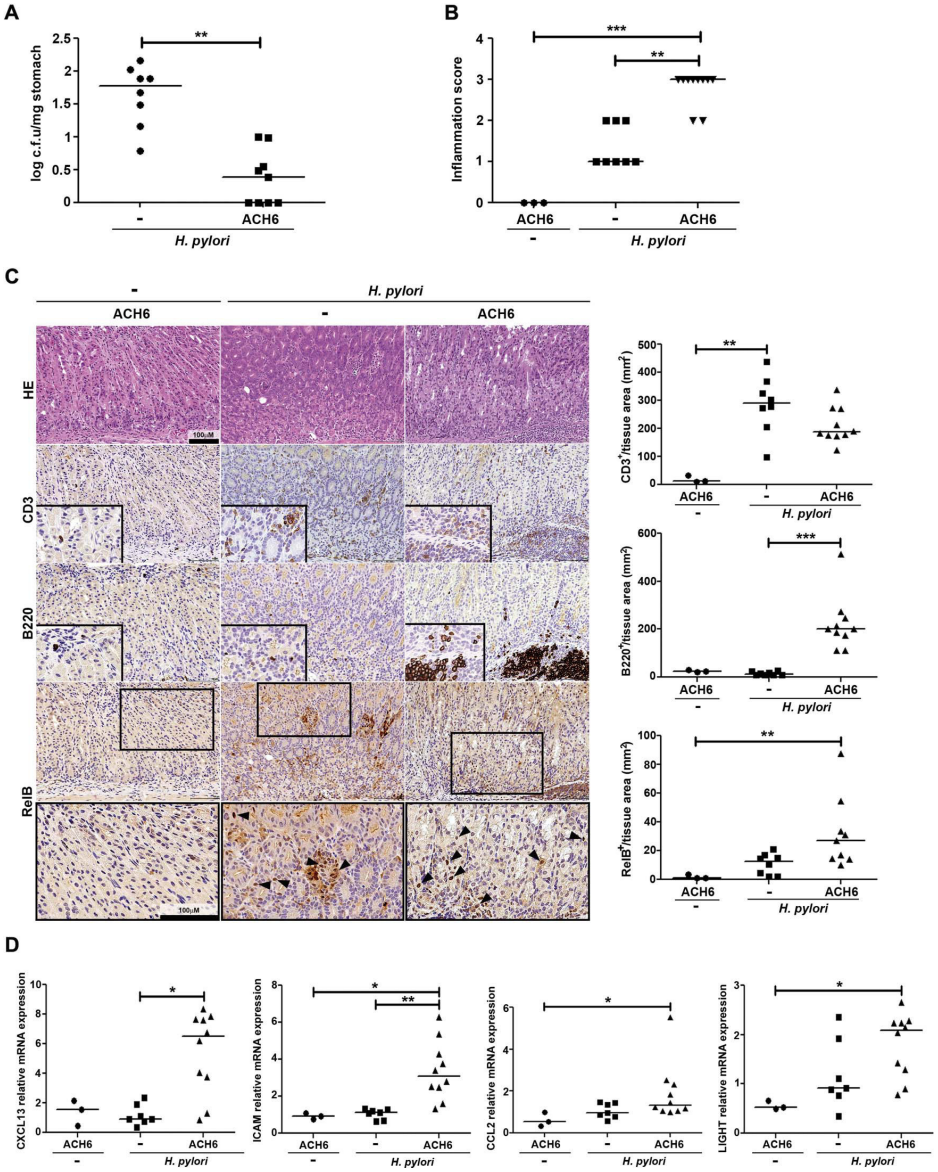

Figure 7 Agonistic activation of lymphotoxin β receptor (LTβR) signalling during *Helicobacter pylori* infection increases gastric inflammation. (A–D) C57BL/6 mice infected with the *H. pylori* strain PMSS1 were injected weekly with 50 μg of the agonist of LTβR signalling ACH6. Mice were sacrificed after 1-month infection. Horizontal bars indicate medians. (A) Colony-forming units (cfu) per mg of stomach. (B) Gastric inflammatory score evaluated according to the updated Sydney system. (C) Representative pictures of murine stomach samples stained for CD3, B220 and RelB. $CD3^+$ and $B220^+$ cells and $RelB^+$ nuclei were calculated per area of tissue (mm^2). (D) Relative mRNA expression levels of CXCL13, ICAM, CCL2 and LIGHT (homologous to **l**ymphotoxin exhibits **i**nducible expression and competes with HSV **g**lycoprotein D for binding to **h**erpes virus entry mediator, a receptor expressed on **T** lymphocytes) in stomach samples. Ct values were normalised to GADPH. *p≤0.05, **p≤0.01, ***p≤0.001. ((A) (Mann–Whitney U test); (B–D) analysis of variance Kruskal–Wallis, Dunn's multiple comparison test.)

necessitates a specific activation by LTs through LTβR upon infection. Further, p100 processing upon canonical NF-κB blockade implied another canonical NF-κB-independent, LTβR ligand to trigger this pathway, which we found to be LIGHT. In contrast, treatment with LTβR–Ig, which scavenges all LTβR ligands, fully disables alternative NF-κB signalling. Therefore, our results demonstrate a tight crosstalk between canonical and alternative pathway during *H. pylori* infection, since activation of canonical NF-κB regulates the expression of ligands important for activation of the alternative pathway.

We observed that the T4SS played a crucial role in controlling the expression of LTs and subsequent activation of LTβR signalling in vitro and in vivo, whereas the presence of CagA was dispensable. These results are in agreement with previous reports

showing that *H. pylori* CagA-deficient but T4SS-proficient strains induce NF-κB activation almost as efficiently as wild-type bacteria,[5 47] while the exact mechanism of T4SS-dependent NF-κB activation is not fully understood.[48] The presence of CagA has been linked to more severe gastric pathology in Western countries,[49] yet, our results using CagA-negative *H. pylori* isolates indicate that important inflammatory signalling cascades, such as alternative NF-κB, can still be activated and contribute to gastric inflammation in the absence of CagA.

Our in vivo experiments blocking or activating LTβR signalling in mice during *H. pylori* infection showed an important role for this pathway in the control of the inflammatory response towards the bacterium. Reduction of chemokine expression in the stomach of LTβR-treated animals confirmed LTβR inhibition at the site of infection. Depletion of FDCs and secondary lymphoid organs was observed, suggesting an additional systemic extra-gastric effect. However, our experiments using the agonist of LTβR (ACH6) refute this possibility, since no effects on FDCs or lymph nodes have been reported with this antibody,[35] but we still observed a reversed gastric phenotype (reduced bacterial load and increased gastric inflammation) compared with LTβR inhibition.

Previous studies using transgenic mouse models suggested the involvement of alternative NF-κB in gastric pathology: Knockout mice lacking the terminal ankyrin domain of NF-κB2 and constitutively expressing NF-κB2/p52 presented gastric hyperplasia in the absence of *Helicobacter* infection.[50] In line, infection experiments of *Nfkb2*$^{-/-}$ mice suggested NF-κB2-mediated signalling to be required for the development of *H. felis*-induced gastric pathology.[51] However, the specific pathways upstream of NF-κB2 remained elusive. Our in vivo studies using human pathogenic *H. pylori* reveal an essential function of LTβR signalling in gastric pathology upstream of NF-κB2.

Taken together, our data indicate that both NF-κB pathways are activated in the course of *H. pylori* infection. Our in vitro data show that activation of the canonical NF-κB signalling precedes alternative NF-κB, regulating a feed-forward loop through induction of LT expression (see online supplementary figure S7A). Ligand engagement to LTβR expressed on epithelial cells triggers p100/p52 processing and subsequent activation of the expression of chemokines important for immune cell recruitment (CXCL13, CXCL10 and CCL20). Recruitment of inflammatory cells (CD4$^+$ T cells and B cells) to the stomach, which in turn also express LTs and LIGHT, leads to a feedback loop, maintaining *H. pylori*-induced gastric inflammation (see online supplementary figure S7B). This is confirmed by our observations in human gastric tissue, where expression of LTs and target genes is linked to the severity of the lesions in the presence of *H. pylori*.

Different studies have suggested inhibition of canonical NF-κB as a therapeutic strategy to reduce *H. pylori*-triggered gastric inflammation. Natural substances as capsaicin,[52] antiulcer drugs as ecabet sodium[53] or probiotics[54] have been proven to inhibit in vitro NF-κB and IL-8 secretion in gastric epithelial cells. Moreover, inhibition of IKK2 in *Mongolian gerbils* was related to a reduced infiltration of neutrophils and mononuclear cells in the stomach, while no differences in bacterial load were detected,[55] suggesting that inhibition of canonical NF-κB was not sufficient to control the infection in this model. In light of our results showing that blocking of canonical NF-κB reduces LT expression but induces LIGHT and CXCL13 upregulation upon *H. pylori* challenge, it is tempting to speculate that inhibition of canonical NF-κB might indeed not represent the best therapeutic option to reduce gastric inflammation and pathology elicited by *H. pylori*. On the contrary, it might imply other adverse effects that have not been considered until now, such as activation of LTβR signalling through LIGHT and concomitant exacerbation of inflammation.

This, in context with the self-sustaining inflammatory alternative NF-κB signalling loop, may aggravate the deleterious inflammatory effects induced by chronic *H. pylori* infection, especially in patients presenting with a high degree of gastritis. Having observed that blocking of LTβR signalling during *H. pylori* infection in mice reduces gastric inflammation and infiltration of inflammatory cells, we propose that such strategy could be considered as a supplement after antibiotic treatment or concomitant with inhibition of canonical NF-κB signalling.

Author affiliations
[1]Institut für Medizinische Mikrobiologie, Immunologie und Hygiene, Technische Universität München, Munich, Germany
[2]German Centre for Infection Research (DZIF), partner site Munich, Munich, Germany
[3]Institut für Virologie, Technische Universität München, Helmholtz Zentrum München, Neuherberg, Germany
[4]Institut für Pathologie, Klinikum Bayreuth, Bayreuth, Germany
[5]Immunology Screen, German Mouse Clinic, Helmholtz Zentrum München, Neuherberg, Germany
[6]Institute of Molecular Cancer Research, University of Zürich, Zürich, Switzerland
[7]Department of Immunobiology, Biogen Idec, Cambridge, Massachusetts, USA
[8]Division of Chronic Inflammation and Cancer, German Cancer Research Center (DKFZ), Heidelberg, Germany

Acknowledgements The authors would like to thank Daniel Kull, Ruth Hillermann, Olga Seelbach and Andreas Wanisch for valuable technical assistance and Ivo Boneca for providing bacteria.

Contributors Study concept and design: RM-L, JZ, MG, and MH. Acquisition of data: RM-L, JZ, FA, EL-G, TA, DBE and SU. Analysis and interpretation of data: RM-L, JZ, MG and MH. Drafting of the manuscript: RM-L. Critical revision of the manuscript: RM-L, JZ, AM, MG and MH. Administrative, technical or material support: MV, JLB and AM. Study supervision: MG and MH.

Funding This work was supported by an ERC starting grant (Liver Cancer Mechanism), the Stiftung für Biomedizinische Forschung (Hofschneider Foundation), the Helmholtz foundation through a young investigator group (YIG), the SFB-TR 36 and the Graduierten Kolleg GRK-42 to MH, and the Swiss National Science foundation (310030-143609 and BSCGIO 157841/1) to AM.

Competing interests None declared.

Provenance and peer review Not commissioned; externally peer reviewed.

REFERENCES

1 Correa P. Human gastric carcinogenesis: a multistep and multifactorial process—First American Cancer Society Award Lecture on Cancer Epidemiology and Prevention. *Cancer Res* 1992;52:6735–40.
2 Lamb A, Chen LF. Role of the *Helicobacter pylori*-induced inflammatory response in the development of gastric cancer. *J Cell Biochem* 2013;114:491–7.
3 Wroblewski LE, Peek RM Jr, Wilson KT. *Helicobacter pylori* and gastric cancer: factors that modulate disease risk. *Clin Microbiol Rev* 2010;23:713–39.
4 Wiedemann T, Hofbaur S, Tegtmeyer N, *et al*. *Helicobacter pylori* CagL dependent induction of gastrin expression via a novel αvβ5-integrin-integrin linked kinase signalling complex. *Gut* 2012;61:986–96.
5 Sokolova O, Borgmann M, Rieke C, *et al*. *Helicobacter pylori* induces type 4 secretion system-dependent, but CagA-independent activation of IκBs and NF-κB/RelA at early time points. *Int J Med Microbiol* 2013;303:548–52.
6 Isomoto H, Mizuta Y, Miyazaki M, *et al*. Implication of NF-kappaB in *Helicobacter pylori*-associated gastritis. *Am J Gastroenterol* 2000;95:2768–76.
7 Keates S, Hitti YS, Upton M, *et al*. *Helicobacter pylori* infection activates NF-kappa B in gastric epithelial cells. *Gastroenterology* 1997;113:1099–109.
8 Takeshima E, Tomimori K, Takamatsu R, *et al*. *Helicobacter pylori* VacA activates NF-kappaB in T cells via the classical but not alternative pathway. *Helicobacter* 2009;14:271–9.
9 Aggarwal BB. Signalling pathways of the TNF superfamily: a double-edged sword. *Nat Rev Immunol* 2003;3:745–56.
10 Schneider K, Potter KG, Ware CF. Lymphotoxin and LIGHT signaling pathways and target genes. *Immunol Rev* 2004;202:49–66.
11 Ware CF. Network communications: lymphotoxins, LIGHT, and TNF. *Annu Rev Immunol* 2005;23:787–819.

12 Wolf MJ, Seleznik GM, Zeller N, *et al*. The unexpected role of lymphotoxin beta receptor signaling in carcinogenesis: from lymphoid tissue formation to liver and prostate cancer development. *Oncogene* 2010;29:5006–18.
13 Remouchamps C, Boutaffala L, Ganeff C, *et al*. Biology and signal transduction pathways of the Lymphotoxin-αβ/LTβR system. *Cytokine Growth Factor Rev* 2011;22:301–10.
14 Solan NJ, Miyoshi H, Carmona EM, *et al*. RelB cellular regulation and transcriptional activity are regulated by p100. *J Biol Chem* 2002;277:1405–18.
15 Coope HJ, Atkinson PG, Huhse B, *et al*. CD40 regulates the processing of NF-kappaB2 p100 to p52. *EMBO J* 2002;21:5375–85.
16 Derudder E, Dejardin E, Pritchard LL, *et al*. RelB/p50 dimers are differentially regulated by tumor necrosis factor-alpha and lymphotoxin-beta receptor activation: critical roles for p100. *J Biol Chem* 2003;278:23278–84.
17 Ansel KM, Ngo VN, Hyman PL, *et al*. A chemokine-driven positive feedback loop organizes lymphoid follicles. *Nature* 2000;406:309–14.
18 Cook KW, Letley DP, Ingram RJ, *et al*. CCL20/CCR6-mediated migration of regulatory T cells to the *Helicobacter pylori*-infected human gastric mucosa. *Gut* 2014;63:1550–9.
19 Galamb O, Györffy B, Sipos F, *et al*. *Helicobacter pylori* and antrum erosion-specific gene expression patterns: the discriminative role of CXCL13 and VCAM1 transcripts. *Helicobacter* 2008;13:112–26.
20 Nakashima Y, Isomoto H, Matsushima K, *et al*. Enhanced expression of CXCL13 in human *Helicobacter pylori*-associated gastritis. *Dig Dis Sci* 2011;56:2887–94.
21 Yoshida A, Isomoto H, Hisatsune J, *et al*. Enhanced expression of CCL20 in human *Helicobacter pylori*-associated gastritis. *Clin Immunol* 2009;130:290–7.
22 Ammirante M, Luo JL, Grivennikov S, *et al*. B-cell-derived lymphotoxin promotes castration-resistant prostate cancer. *Nature* 2010;464:302–5.
23 Or YY, Chung GT, To KF, *et al*. Identification of a novel 12p13.3 amplicon in nasopharyngeal carcinoma. *J Pathol* 2010;220:97–107.
24 Hehlgans T, Stoelcker B, Stopfer P, *et al*. Lymphotoxin-beta receptor immune interaction promotes tumor growth by inducing angiogenesis. *Cancer Res* 2002;62:4034–40.
25 Haybaeck J, Zeller N, Wolf MJ, *et al*. A lymphotoxin-driven pathway to hepatocellular carcinoma. *Cancer Cell* 2009;16:295–308.
26 Hütz K, Mejías-Luque R, Farsakova K, *et al*. The stem cell factor SOX2 regulates the tumorigenic potential in human gastric cancer cells. *Carcinogenesis* 2014;35:942–50.
27 Xiang Z, Censini S, Bayeli PF, *et al*. Analysis of expression of CagA and VacA virulence factors in 43 strains of *Helicobacter pylori* reveals that clinical isolates can be divided into two major types and that CagA is not necessary for expression of the vacuolating cytotoxin. *Infect Immun* 1995;63:94–8.
28 Lee A, O'Rourke J, De Ungria MC, *et al*. A standardized mouse model of *Helicobacter pylori* infection: introducing the Sydney strain. *Gastroenterology* 1997;112:1386–97.
29 Haas R, Meyer TF, van Putten JP. Aflagellated mutants of *Helicobacter pylori* generated by genetic transformation of naturally competent strains using transposon shuttle mutagenesis. *Mol Microbiol* 1993;8:753–60.
30 Arnold IC, Lee JY, Amieva MR, *et al*. Tolerance rather than immunity protects from *Helicobacter pylori*-induced gastric preneoplasia. *Gastroenterology* 2011;140:199–209.
31 Van de Bovenkamp JH, Mahdavi J, Korteland-Van Male AM, *et al*. The MUC5AC glycoprotein is the primary receptor for *Helicobacter pylori* in the human stomach. *Helicobacter* 2003;8:521–32.
32 Ansari SA, Devi S, Tenguria S, *et al*. *Helicobacter pylori* protein HP0986 (TieA) interacts with mouse TNFR1 and triggers proinflammatory and proapoptotic signaling pathways in cultured macrophage cells (RAW 264.7). *Cytokine* 2014;68:110–17.
33 Subrata LS, Voon DC, Yeoh GC, *et al*. TNF-inducible expression of lymphotoxin-β in hepatic cells: an essential role for NF-κB and Ets1 transcription factors. *Cytokine* 2012;60:498–504.
34 Viala J, Chaput C, Boneca IG, *et al*. Nod1 responds to peptidoglycan delivered by the *Helicobacter pylori* cag pathogenicity island. *Nat Immunol* 2004;5:1166–74.
35 Lukashev M, LePage D, Wilson C, *et al*. Targeting the lymphotoxin-beta receptor with agonist antibodies as a potential cancer therapy. *Cancer Res* 2006;66:9617–24.
36 Drayton DL, Liao S, Mounzer RH, *et al*. Lymphoid organ development: from ontogeny to neogenesis. *Nat Immunol* 2006;7:344–53.
37 Genta RM, Hamner HW, Graham DY. Gastric lymphoid follicles in *Helicobacter pylori* infection: frequency, distribution, and response to triple therapy. *Hum Pathol* 1993;24:577–83.
38 Kobayashi M, Mitoma J, Nakamura N, *et al*. Induction of peripheral lymph node addressin in human gastric mucosa infected by *Helicobacter pylori*. *Proc Natl Acad Sci USA* 2004;101:17807–12.
39 Shomer NH, Fox JG, Juedes AE, *et al*. Helicobacter-induced chronic active lymphoid aggregates have characteristics of tertiary lymphoid tissue. *Infect Immun* 2003;71:3572–7.
40 Maeda S, Yoshida H, Ogura K, *et al*. H. pylori activates NF-kappaB through a signaling pathway involving IkappaB kinases, NF-kappaB-inducing kinase, TRAF2, and TRAF6 in gastric cancer cells. *Gastroenterology* 2000;119:97–108.
41 Neumann M, Foryst-Ludwig A, Klar S, *et al*. The PAK1 autoregulatory domain is required for interaction with NIK in *Helicobacter pylori*-induced NF-kappaB activation. *Biol Chem* 2006;387:79–86.
42 Ohmae T, Hirata Y, Maeda S, *et al*. *Helicobacter pylori* activates NF-kappaB via the alternative pathway in B lymphocytes. *J Immunol* 2005;175:7162–9.
43 de Wit H, Dokter WH, Koopmans SB, *et al*. Regulation of p100 (NFKB2) expression in human monocytes in response to inflammatory mediators and lymphokines. *Leukemia* 1998;12:363–70.
44 Kuprash DV, Osipovich OA, Pokholok DK, *et al*. Functional analysis of the lymphotoxin-beta promoter. Sequence requirements for PMA activation. *J Immunol* 1996;156:2465–72.
45 Voon DC, Subrata LS, Karimi M, *et al*. TNF and phorbol esters induce lymphotoxin-beta expression through distinct pathways involving Ets and NF-kappa B family members. *J Immunol* 2004;172:4332–41.
46 Xiao G, Harhaj EW, Sun SC. NF-κB-inducing kinase regulates the processing of NF-κB2 p100. *Mol Cell* 2001;7:401–9.
47 Schweitzer K, Sokolova O, Bozko PM, *et al*. *Helicobacter pylori* induces NF-kappaB independent of CagA. *EMBO Rep* 2010;11:10–11; author reply 1–2.
48 Backert S, Naumann M. What a disorder: proinflammatory signaling pathways induced by *Helicobacter pylori*. *Trends Microbiol* 2010;18:479–86.
49 Shiota S, Suzuki R, Yamaoka Y. The significance of virulence factors in *Helicobacter pylori*. *J Dig Dis* 2013;14:341–9.
50 Ishikawa H, Carrasco D, Claudio E, *et al*. Gastric hyperplasia and increased proliferative responses of lymphocytes in mice lacking the COOH-terminal ankyrin domain of NF-kappaB2. *J Exp Med* 1997;186:999–1014.
51 Burkitt MD, Williams JM, Duckworth CA, *et al*. Signaling mediated by the NF-κB sub-units NF-κB1, NF-κB2 and c-Rel differentially regulate Helicobacter felis-induced gastric carcinogenesis in C57BL/6 mice. *Oncogene* 2013;32:5563–73.
52 Lee IO, Lee KH, Pyo JH, *et al*. Anti-inflammatory effect of capsaicin in *Helicobacter pylori*-infected gastric epithelial cells. *Helicobacter* 2007;12:510–17.
53 Kim JM, Kim JS, Jung HC, *et al*. Inhibition of *Helicobacter pylori*-induced nuclear factor-kappa B activation and interleukin-8 gene expression by ecabet sodium in gastric epithelial cells. *Helicobacter* 2003;8:542–53.
54 Yang YJ, Chuang CC, Yang HB, *et al*. Lactobacillus acidophilus ameliorates *H. pylori*-induced gastric inflammation by inactivating the Smad7 and NFκB pathways. *BMC Microbiol* 2012;12:38.
55 Yanai A, Maeda S, Shibata W, *et al*. Activation of IkappaB kinase and NF-kappaB is essential for *Helicobacter pylori*-induced chronic gastritis in Mongolian gerbils. *Infect Immun* 2008;76:781–7.

Supplementary Figure Legends

Supplementary Figure 1. LTβR signaling is activated in *H. pylori*-induced gastritis and gastric tumors.

(A) Whiskers (minimum to maximum) box plots show relative mRNA levels of LTα, LTβ, CD40L, TWEAK, BAFF in healthy human gastric mucosa and *H. pylori*-induced gastritis. Data from 12 (LTα and LTβ) or 6 (CD40L, TWEAK, BAFF) tissue samples of each condition are shown. Significances were calculated using Student's t test. ***p≤0.001. (B) Negative (DapB) and positive controls (+, Pol2A and ++, UBC) used for LTβR *in situ* hybridization. (C) T cells (CD3), B cells (CD20) and macrophages (CD68) detected by immunohistochemistry in normal gastric mucosa, mild, moderate and severe gastritis as well as in tumor-associated gastritis. Representative images are shown. (D) Representative images of LTβ expression in human normal gastric mucosa, mild, moderate and severe gastritis as well as in early gastric adenocarcinoma biopsy samples, detected by immunohistochemistry. Thick arrows indicate expression of LTβ in epithelial cells. Thin arrows show expression of LTβ in immune cells. (Scale bar: 100μm). (E) Quantification of $LT\beta^+$ cells in intestinal-type and diffuse-type tumors. (F) $RelB^+$ and $p52^+$ cells in human normal gastric mucosa, mild, moderate and severe gastritis as well as in early gastric adenocarcinoma biopsy samples (n=10, each). *p≤0.05, **p≤0.01, ***p≤0.001. One-way ANOVA with Bonferroni's multiple comparison test

Supplementary Figure 2. *H. pylori* activates LTβR signaling.

(A) LTβR expression on the surface of MKN45, KATOIII and St3051 GC cells detected by flow cytometry. HepG2 and HEK293 cells were used as positive and negative control, respectively. One representative experiment is shown. (B) p100/p52 basal protein expression levels in GC cell lines analyzed by western blot. β-actin served as loading control. (C) LTβR, TNFR1, TNFα, LTα, LTβ and LIGHT mRNA basal expression levels in gastric cancer cell lines. HepG2 or cells treated with the agonist of LTβR signaling BS-1 (0.5 μg/ml) were used as positive controls. Results (mean ± S.D.) of two independent experiments performed in duplicates are shown. (D) p-p65 and p65 basal protein expression levels in gastric cancer

cell lines analyzed by western blot. β-actin served as loading control. (E) St3051 cells were infected with *H. pylori* G27 at different MOI and p100 processing to p52 was detected by western blot. BS-1 (0.5 μg/ml) was used as a positive control. β-actin served as loading control. One representative blot of three independent experiments is shown. (F) MKN45 and St3051 cell were infected with *H. pylori* G27 strain at the indicated MOI and p-p65 and p65 levels were analyzed by western blot. β-actin was used as loading control. One representative blot from three independent experiments is shown. (G) p100 and p52 levels in MKN45 and St3051 cells detected by western blot after infection with *H. pylori* G27 at MOI 10 for different time points. BS-1 (0.5 μg/ml) was used as a positive control. β-actin served as loading control. (H) Gastric cancer cells MKN45 and St3051 were infected with *H. pylori* G27 at MOI 10 for 12 hours. The mRNA expression levels of LTβR were analyzed by real time PCR. Ct values were normalized to GADPH. Results (mean ± S.D.) of three independent experiments are presented as fold induction. Significances were calculated using One-way ANOVA with Bonferroni's multiple comparison test. (I) St3051 cells were infected with *H. pylori* G27 at MOI 10 for 12 hours. The mRNA expression levels of CXCL13, CXCL10, CCL20 and A20 were analyzed by real time PCR. Ct values were normalized to GADPH. BS-1 (0.5 μg/ml) was used as a positive control. Results (mean ± S.D.) from three independent experiments are presented as fold induction. Control cells were compared to *H. pylori*-infected cells and significances were calculated using Student's t-test. *p≤0.05, **p≤0.01, ***p≤0.001.

Supplementary Figure 3. Activation of LTβR signaling is induced by secreted LT in response to *H. pylori* infection.

(A) MKN45 cells were infected with G27 *H. pylori* strain for 3 hours and lysates were immunoprecipitated with anti-LTβR or anti-CagA antibodies. Irrelevant rabbit IgG were used as control. Immunoprecipitates were subjected to western blot for detection of *H. pylori* proteins. (B) MKN45 cells were incubated LTβR-Ig one hour prior to *H. pylori* infection. LTβ mRNA levels were measured after 12 hours infection. Values were normalized to GADPH.

Results (mean ± S.D.) of three independent experiments are shown. p values were calculated using One-way ANOVA with Bonferroni's multiple comparison test. (C) LTα, LTβ, A20 and LIGHT mRNA expression levels in MKN45 cells after stimulation with 10ng/ml of TNFα for 12h. Values were normalized to GADPH. Results (mean ± S.D.) of three independent experiments are shown. p values were calculated using Student's t-test. *p≤0.05. (D) MKN45 and St3051 cells were incubated with the inhibitor of human IκB kinase 2 (IKK2) TPCA-1 to block canonical NF-κB signaling. Cells were stimulated with 50ng/ml of TNFα or the LTβR agonist BS-1 (0.5µg/ml) where indicated. Cell lysates were obtained after 12h infection with the *H. pylori* strain G27 and levels of p-p65 and p65 were assessed by western blot. β-actin was used as a loading control. One representative blot and quantification from three independent experiments is shown. (E) St3051 cells were incubated with TPCA-1 1h prior to infection with the *H. pylori* strain G27 (MOI 10). Cell lysates were obtained after 12h infection and levels of p100/p52 were assessed by western blot. β-actin served as loading control. One representative blot of three independent experiments is shown. (F) TWEAK mRNA expression in MKN45 cells after inhibition of canonical NF-κB using TPCA-1. Values were normalized to GADPH. Results from three independent experiments are shown (mean ± S.D.).

Supplementary Figure 4. Activation of non-canonical NF-κB is independent of CagA.

(A) LIGHT mRNA expression in MKN45 and St3051 cells infected for 12 hours with the *H. pylori* strain G27 and the isogenic CagA and CagE mutants. Values were normalized to GADPH. Results from three independent experiments are shown (mean ± S.D.) (B) p100 processing to p52 detected by western blot in St3051 cells infected for 12 hours with *H. pylori* G27, the isogenic mutant strains G27*ΔCagA*, G27*ΔCagE*, G27*ΔBabA*, G27*ΔSabA*, G27*ΔVacA*, G27*ΔgGT*, G27*ΔUreA/B* or the SS1 and PMSS1 wild type strains at MOI of 10. β-actin was used as a loading control. (C) p100 processing to p52 detected by western blot in MKN45 cells infected with *H. pylori* G27 or the isogenic mutant strains G27*ΔCagA*, G27*ΔCagE*, G27*ΔCagF*, G27*ΔCagI* at MOI of 10. β-actin was used as a loading control. (D)

Expression of CagA and isocitrate dehydrogenase (ICD), used as a housekeeping gene, detected by PCR in different *H. pylori* clinical isolates. (E) p100 processing to p52 detected by western blot in MKN45 cells infected with *H. pylori* P12 or the peptidoglycan mutant P12*slt*. Quantification of three independent experiments is shown.

Supplementary Figure 5. Blocking LTβR during *H. pylori* infection reduces gastric inflammation.

(A) Time schedule of LTβR-Ig treatment. C57BL/6 mice were injected with 100µg of LTβR-Ig or the isotype control MOPC-21 at the indicated time points ( ). At day 0, 2 and 5, mice were infected with a 10^9 orogastric dose of the *H. pylori* strain PMSS1. Mice were sacrificed at day 36 for analyses. (B) Immunohistochemical staining of FDC-M1 or CD21/35 in cryosections of spleens to detect follicular dendritic cells from MOPC-21 or LTβR-Ig-treated mice, infected with *H. pylori* PMSS1. (C) Representative pictures of CD4 T cells and macrophages (F4/80) detected in gastric tissue samples of control, MOPC-21 and LTβR-Ig-treated mice infected with *H. pylori* PMSS1. (Scale bar 100µm).

Supplementary Figure 6. Agonistic activation of LTβR-signaling during *H. pylori* infection increases gastric inflammation.

(A) Representative pictures of CD4 T cells and macrophages (F4/80) detected in gastric tissue samples of control, *H. pylori* PMSS1-infected and ACH6-treated and PMSS1-infected mice. (Scale bar 100µm). (B) B220 positive cells calculated per area of tissue (mm^2) in untreated and ACH6-treated control mice. Significances were calculated using Student's t-test. *p≤0.05. (C) Relative mRNA expression levels of KC and CCL20 in the stomach of control, *H. pylori*-infected mice and *H. pylori*-infected mice and treated with ACH6. Ct values were normalized to GADPH. Statistical significance was calculated by using One-way ANOVA Kruskal-Wallis with Dunn's multiple comparison test. *p≤0.05, **p≤0.01.

Supplementary Figure 7. Representative model of the alternative NF-κB activation via LTβR-activation upon *H. pylori* infection.

(A) *H. pylori* type IV secretion system-mediated activation of canonical NF-κB induces the expression of LTα and LTβ and low levels of LIGHT in gastric epithelial cells. Secreted $LT\alpha_1\beta_2$ and LIGHT bind to LTβR expressed on the gastric epithelium leading to activation of alternative NF-κB and up-regulation of chemokines such as CXCL13, CCL17, CCL20 or CXCL10 in cis and in trans. These chemokines contribute to the recruitment of B and T cells and macrophages to the stomach, which once activated in turn secrete LTs (Chiang et al., 2009) and possibly also LIGHT, enhancing LTβR-activation and chemokine secretion resulting in a feed-forward loop driving gastric inflammation. Treatment with LTβR-Ig increases bacterial load, while decreasing gastric inflammation and inflammatory chemokine expression. Conversely, agonistic activation of LTβR by ACH6 reduces *H. pylori* colonization, but increases gastric inflammation as well as chemokine expression. (B) Inhibition of canoncical NF-κB during *H. pylori* infection enhances the expression of LIGHT and strongly reduces LTβ expression. Under these conditions, LIGHT can signal through LTβR activating the expression of target chemokines such as CXCL13, leading to a positive feed-forward loop sustaining gastric inflammation.

Figure S1

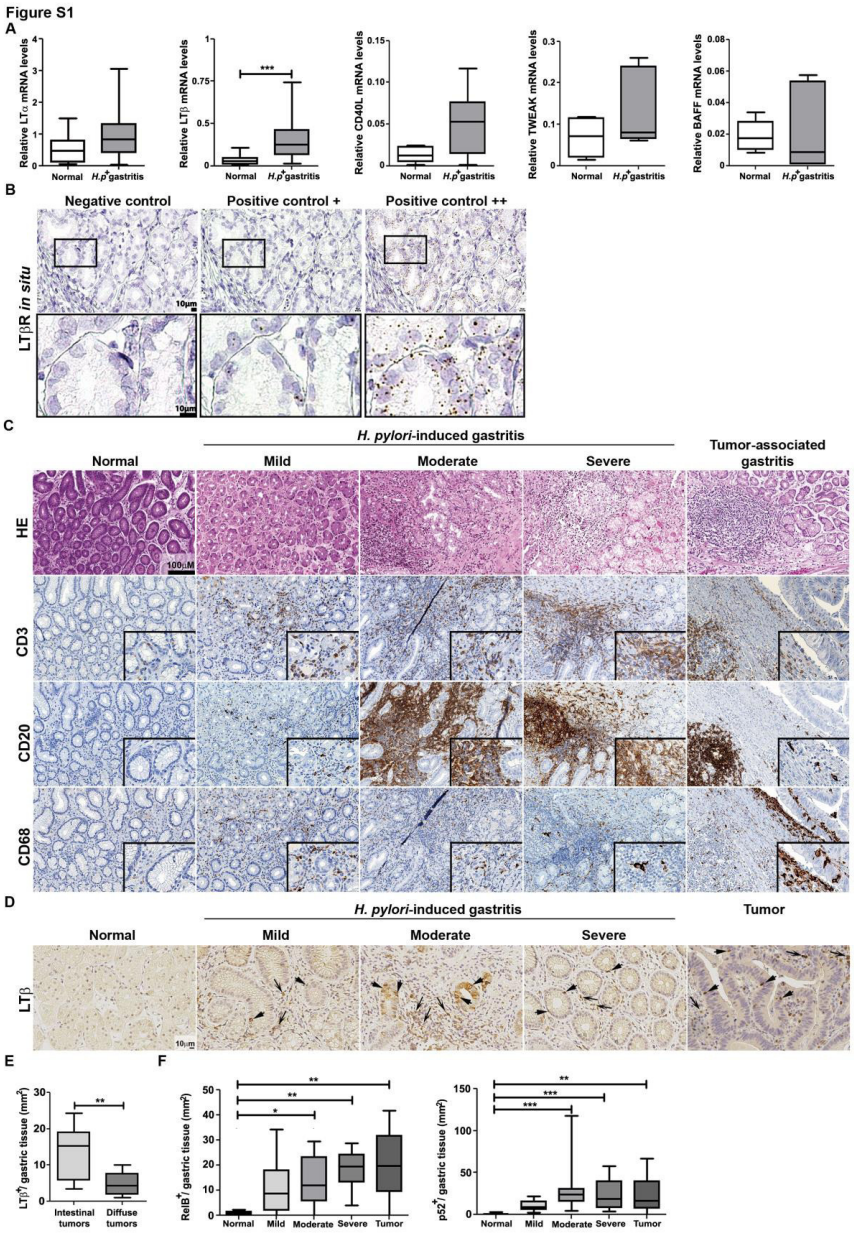
A
Relative LTα mRNA levels
Relative LTβ mRNA levels
Relative CD40L mRNA levels
Relative TWEAK mRNA levels
Relative BAFF mRNA levels
Normal
H.p+gastritis
***
B
Negative control
Positive control +
Positive control ++
LTβR in situ
10μm
C
H. pylori-induced gastritis
Normal
Mild
Moderate
Severe
Tumor-associated gastritis
HE
CD3
CD20
CD68
100μM
D
H. pylori-induced gastritis
Tumor
LTβ
E
LTβ+/ gastric tissue (mm2)
Intestinal tumors
Diffuse tumors
F
RelB+/ gastric tissue (mm2)
p52+/ gastric tissue (mm2)
Tumor

Figure S2

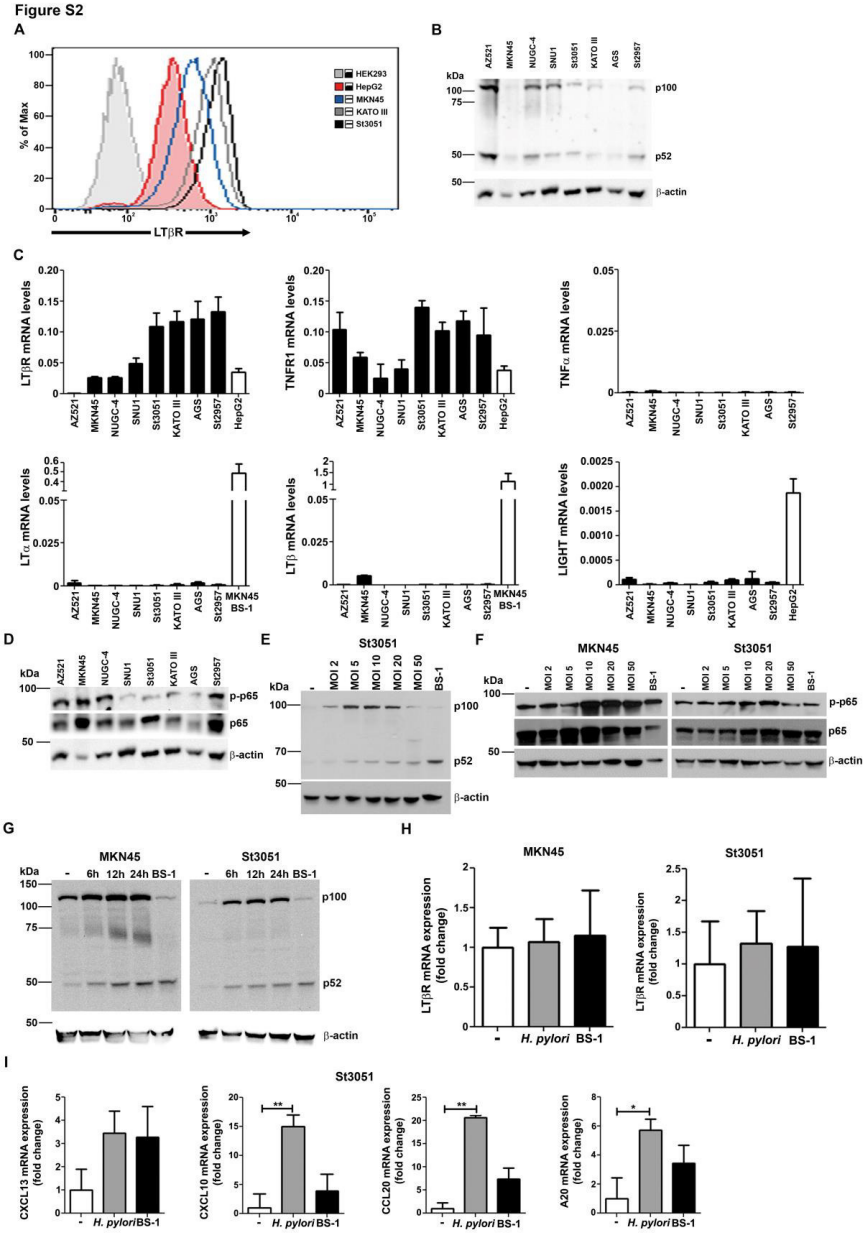
A
HEK293
HepG2
MKN45
KATO III
St3051
% of Max
LTβR
B
AZ521
MKN45
NUGC-4
SNU1
St3051
KATO III
AGS
St2957
kDa
p100
p52
β-actin
C
LTβR mRNA levels
TNFR1 mRNA levels
TNFα mRNA levels
LTα mRNA levels
LTβ mRNA levels
LIGHT mRNA levels
HepG2
MKN45 BS-1
D
p-p65
p65
β-actin
E
St3051
MOI 2
MOI 5
MOI 10
MOI 20
MOI 50
BS-1
F
MKN45
St3051
G
6h
12h
24h
H
LTβR mRNA expression (fold change)
H. pylori
I
CXCL13 mRNA expression (fold change)
CXCL10 mRNA expression (fold change)
CCL20 mRNA expression (fold change)
A20 mRNA expression (fold change)

Figure S3

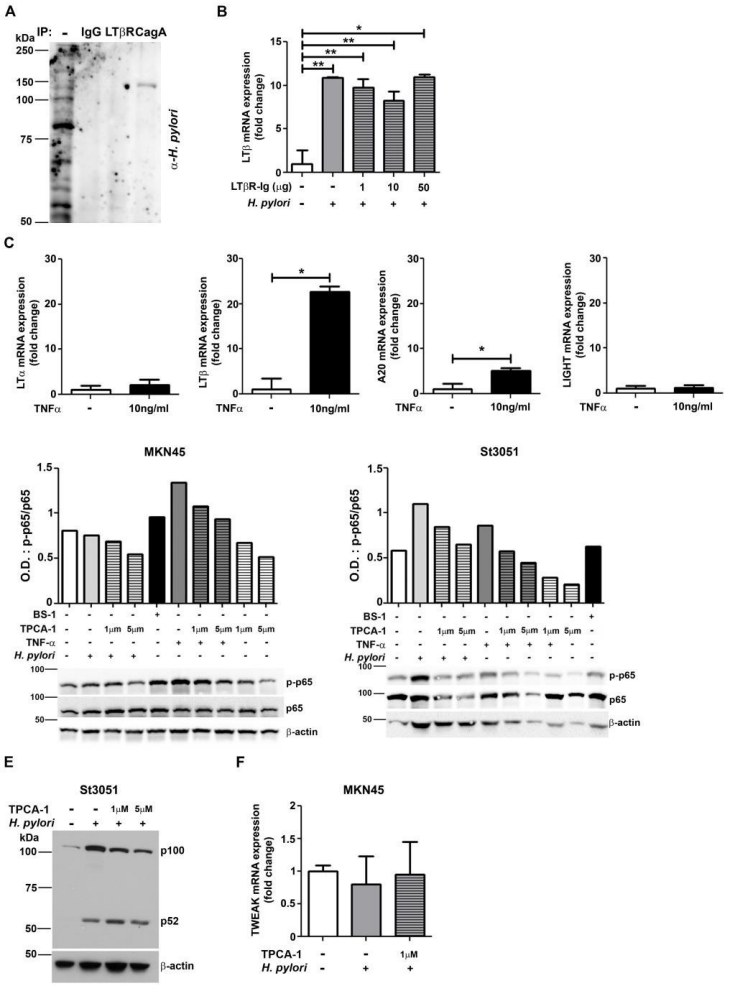

Figure S4

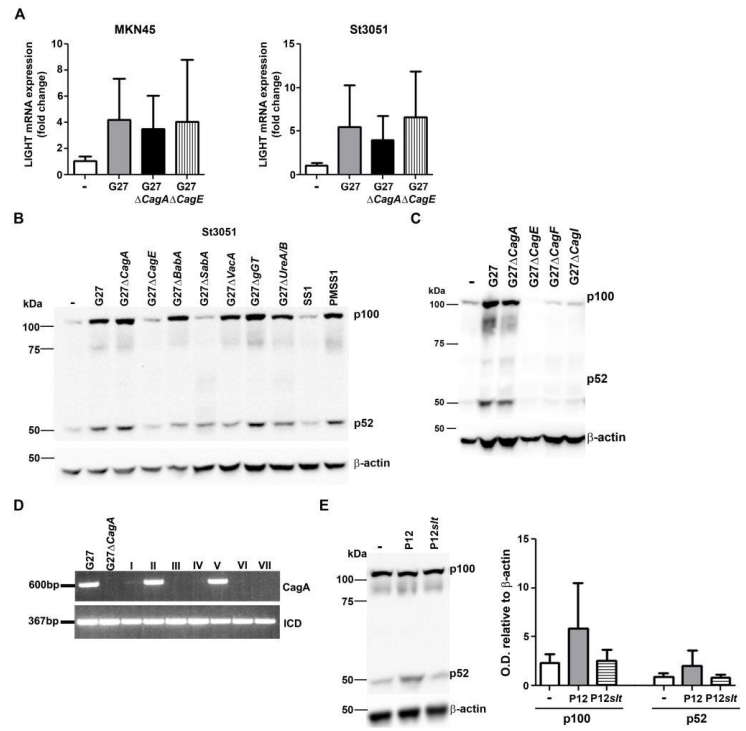

Figure S5

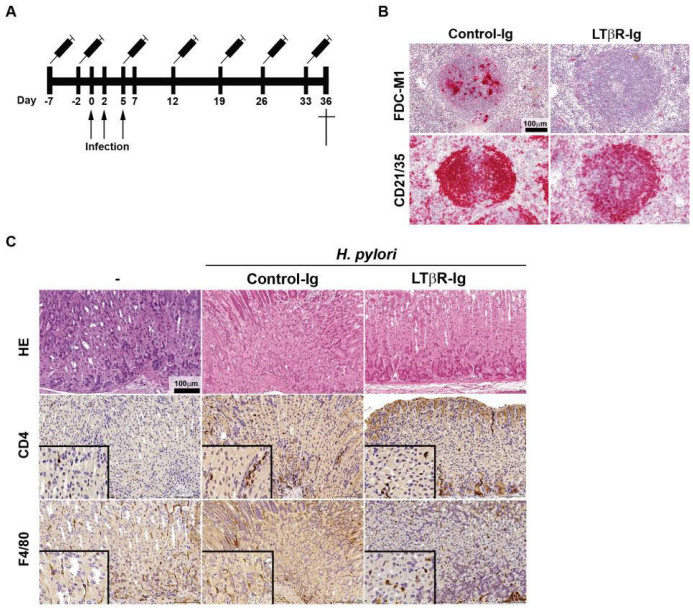

Figure S6

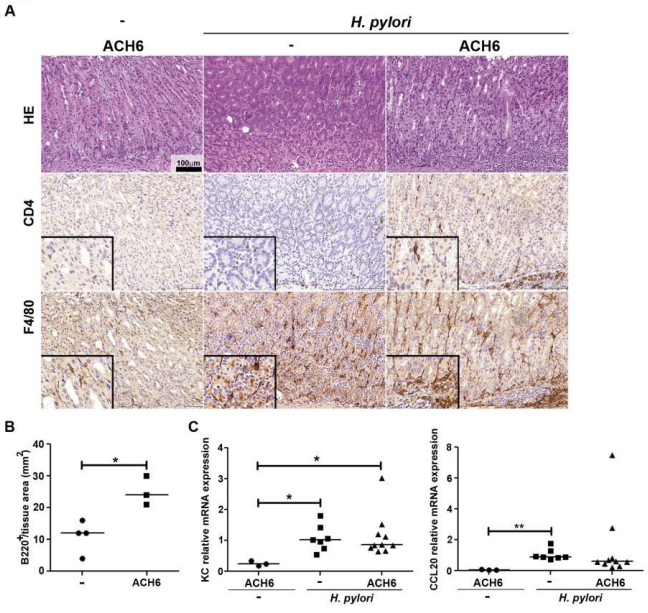

Figure S7

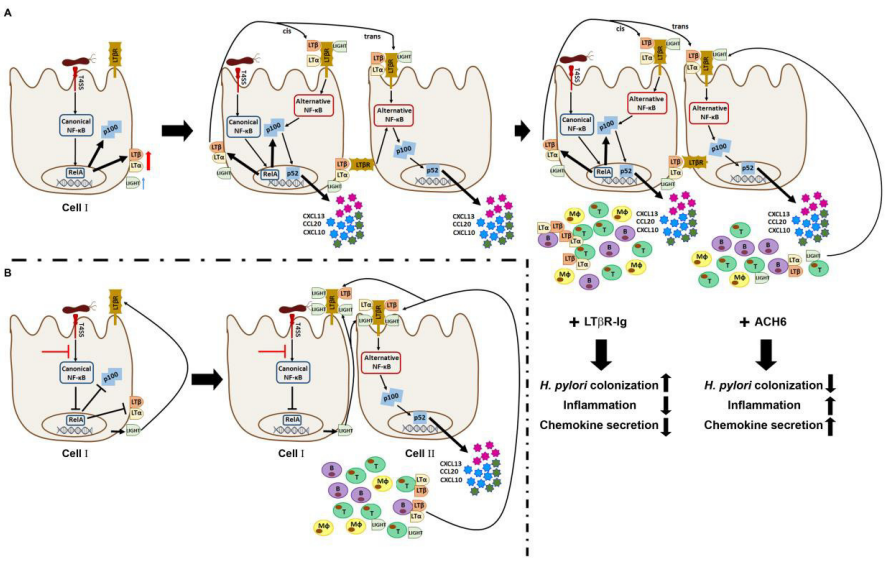
A
B
Cell I
Cell II
cis
trans
Canonical NF-κB
Alternative NF-κB
RelA
p52
p100
CXCL13
CCL20
CXCL10
+ LTβR-Ig
+ ACH6
H. pylori colonization
Inflammation
Chemokine secretion

2. MANUSCRIPT IN PROGRESS

2.1 *Helicobacter pylori* and its secreted immunomodulator VacA protect against food allergy

authors: Andreas Kyburz, Sabine Urban, Aleksandra Djekic, Stefan Floess, Jochen Huehn, Timothy L. Cover and Anne Müller

contribution: I helped with the mice studies and contributed to figure 4.

***Helicobacter pylori* and its secreted immunomodulator VacA protect against food allergy**

Andreas Kyburz[1], Sabine Urban[1], Aleksandra Djekic[1], Stefan Floess[2], Jochen Huehn[2], Timothy L. Cover[3] and Anne Müller[1]

[1]Institute of Molecular Cancer Research, University of Zürich, Zürich, Switzerland

[2]Department Experimental Immunology, Helmholtz Center for Infection Research, Braunschweig, Germany

[3]Vanderbilt University Medical Center and Veterans Affairs Tennessee Valley Healthcare System, Nashville, Tennessee

For correspondence: Anne Müller, Institute of Molecular Cancer Research, Univ. of Zürich, Winterthurerstr. 190, 8057 Zürich, Switzerland; mueller@imcr.uzh.ch; phone: ++41 44 635 3474; fax: ++41 44 635 3484

Running title: *H. pylori* protects against food allergy

Word count: 4648 words not including figure legends

Summary

Background

Food allergy is an increasingly common health problem in Western populations. Epidemiological studies have suggested both positive and negative associations between food allergy and infection with the gastric bacterium *Helicobacter pylori*.

Objective

The objective of this work was to investigate whether experimental infection with *H. pylori*, or prophylactic treatment with *H. pylori*-derived immunomodulatory molecules, affects the onset and severity of food allergy, either positively or negatively.

Methods

We infected neonatal mice with *H. pylori* or treated animals with *H. pylori* components (bacterial lysate or the immunomodulator VacA) and subsequently subjected them to one of three different protocols for food allergy induction, using either ovalbumin or peanut extract as allergens for sensitization and challenge. Readouts included anaphylaxis scoring, quantification of allergen-specific serum IgE and IgG1 and of the mast cell protease MCPT1, as well as splenic T-helper-2 cell-derived cytokine production. Mesenteric lymph node $CD4^+FoxP3^+$ regulatory T-cells were subjected to DNA methylation analyses of the Treg-specific demethylated region (TSDR) within the *FOXP3* locus.

Results

Mice that had been infected with *H. pylori* or treated with *H. pylori*-derived immunomodulators were protected against anaphylaxis induced by allergen sensitization and challenge, irrespective of the allergen used. Most of the immunologic assays confirmed a protective effect of *H. pylori*.

$CD4^+FoxP3^+$ T-cells from protected mice exhibited a stable Treg phenotype characterized by *FOXP3* TSDR demethylation.

Conclusions and Clinical Relevance

H. pylori confers protection against ovalbumin and peanut allergy and affects the epigenome of T-cells, thereby promoting stable Treg differentiation and functionality. Prophylactic treatment with *H. pylori*-derived immunomodulators appears to be a promising strategy for food allergy prevention.

Key words: anaphylaxis, bacterial immunomodulators, epigenetics, food allergy

Introduction

Food allergy is an increasingly common condition in Western countries as well as Asia, affecting ~6-8 % of children and ~4 % of adults [1, 2]. It is caused by inappropriate T-cell-driven immune responses to harmless food components of milk, eggs, peanuts, tree nuts, seafood, shellfish, soy, wheat (the "big eight") and other foods. Food allergy often co-occurs with other atopic diseases such as allergic rhinitis and conjunctivitis, eczema and allergic asthma and is believed to result mechanistically from the breakdown of the T-cell suppressive mechanisms conferred by oral immune tolerance. Symptoms of food allergy usually occur with a fast onset (from seconds to one hour) and include rashes, hives, swelling and itching of parts or the whole face, wheezing, diarrhea, nausea and, in severe cases, anaphylaxis. The mainstay of treatment is the strict avoidance of food allergens; accidental intake requires epinephrine injections in severe and anti-histamines and steroids in mild cases. The benefits of allergen immunotherapy for food allergies are currently unclear and the procedures are thus not (yet) recommended.

The hygiene [3] and disappearing microbiota [4] hypotheses postulate that the reduced exposure to environmental and pathogenic microbes early in life and/or the loss of ancestral indigenous microbes colonizing various niches of the human body contribute to an increased allergy risk. Both hypotheses have served to explain the dramatic increase of the prevalence of food allergy in Western countries. The paradigmatic example of a microbe that is increasingly lost from human populations is *H. pylori*. Chronic infection with this gastric colonizer on the one hand represents an important risk factor for the development of gastritis, ulcers and gastric cancer [5, 6] but on the other hand appears to confer protection against esophageal disorders such as

gastro-esophageal reflux disease and esophageal cancer, as well as asthma, allergy and inflammatory bowel diseases [7, 8]. Whereas the inverse association of *H. pylori* with allergic asthma, rhinitis and eczema is well supported by large epidemiological studies and meta-analyses [9-12], the effects of *H. pylori* positivity on the risk of developing food allergy are controversial. Few reports are available and the existing studies suffer from small sample sizes, heterogeneous populations and non-standardized methodologies [13]. Several studies have found a positive association of *H. pylori*, especially of strains harboring the virulence factor CagA, with food allergy in children [14, 15] or adults [16]. Other studies have found no association [17], or a negative association [12]. The latter study reported both a decreased sero-prevalence of *H. pylori* in food allergy patients relative to controls (33% vs. 40% as determined by urea breath test and serology) as well as a reduced production of allergic mediators (such as eosinophilic cationic protein and mast cell tryptase) in *H. pylori*-positive relative to *H. pylori*-negative food allergy patients [12]. Mechanistically, positive associations with food allergy were explained by a breakdown of the epithelial barrier to food allergens due to the chronic inflammation of the *H. pylori*-infected gastric mucosa, whereas negative associations were attributed to the immunomodulatory activity of *H. pylori* on the activation and polarization of T-cell responses.

We have previously examined the role of *H. pylori* in various experimental models of allergic asthma and have consistently detected a strong protective effect, especially of neonatal exposure to the bacteria, on the development of allergic asthma in response to various allergens [18-20]. Given the controversial results from observational studies in humans with food allergy, the strongly increasing prevalence of food allergy in children and adults, and the robust effects observed in our allergic asthma models, we asked whether experimental *H. pylori* infection would

alleviate the clinical and immunological symptoms of food allergy induced by two different common food allergens. We used recombinant ovalbumin and peanut extract, administered via various routes, to trigger anaphylaxis symptoms. When administered intraperitoneally for the purpose of allergen challenge, peanut extract was superior to ovalbumin in inducing swelling and edema of the mucosal surfaces of the face, as well as a variety of systemic parameters related to Th2, B- and mast cell activity. *H. pylori* infection and *H. pylori* extract treatment, and also the administration of several doses of purified VacA, alleviated all clinical symptoms of food allergy in the three examined models and reduced Th2 cytokine production, mast cell protease secretion, and allergen-specific serum IgG1 levels. The same treatments could be shown to promote Treg stability by demethylating the TSDR of the *FOXP3* locus in regulatory T-cells (Tregs) from mesenteric lymph nodes. Our results thus suggest that *H. pylori* down-modulates immune responses to common food allergens by affecting the epigenome of Tregs and promoting their stable lineage differentiation, thereby conferring long-lasting protection against food allergy.

Methods

Animal experimentation

C57BL/6 mice were purchased from Janvier and included in experiments at 5-7 weeks of age. For the induction of ovalbumin (OVA)-induced food allergy, mice were sensitized twice i.p. with 50 µg OVA (Sigma A5503-5G) emulsified in aluminum hydroxide (Alum Imject, Thermo Scientific 77161) on day 0 and 14, followed by challenge via oral gavage on days 28, 29, 30 and 31 with 60 mg OVA. Symptoms were scored after each of the first three challenges; mice were sacrificed by CO_2 inhalation 30-45 min after the last challenge and blood and tissue samples were collected. For the induction of peanut extract (PE)-induced food allergy, mice were sensitized orally once a week for four weeks with 2 mg PE adjuvanted with 20 µg cholera toxin (List Biologicals 101B) followed by either four oral challenges on four consecutive days with 10 mg PE (in this model, symptoms were scored after the first three challenges) or two i.p. challenges (with a two-day break) with 1 mg PE (in that case, symptoms were scored after the first challenge). Scoring was done for 40 min beginning right after challenge, with scores indicating the following: 0, no sign of reaction; 1, repetitive scratching and rubbing around the nose/mouth and head, ear canal digging with hind legs; 2, decreased activity with an increased respiratory rate, pilar erecti and/or puffing around the eyes and/or mouth; 3, labored respiration and cyanosis around the mouth and tail and/or periods of motionless for more than 1 min; lying prone on stomach; 4, slight or no activity after prodding/whisker stimuli or tremors and convulsion; 5, death. In the oral challenge models, cumulative scores were calculated by adding up three individual scores per mouse. The processing and analysis of animal tissues is described below; MCPT1 in serum was quantified by ELISA (88-7503-88, eBioscience) according to the manufacturer's instructions. All

animal experimentation was reviewed and approved by the Zurich Cantonal Veterinary Office (license 170/2014 to A.M.). The *H. pylori* strain PMSS1 was cultured as previously described [21]; mice were infected by oral gavage on day 6 and 7 after birth with 10^7 to 10^8 bacteria. For the production of *H. pylori* extract, bacterial cultures were pelleted, washed with PBS, and subjected to three freeze-thaw cycles and homogenization using a pressure cell homogenizer (Stansted SPCH-18). The homogenate was centrifuged at 3000x g, the resulting supernatant was sterile filtered, and the protein concentration was determined by BCA Protein Assay Kit (Thermo Scientific 23227). S1m1 type VacA was purified from *H. pylori* strain 60190 as described previously [22]. The dosage of extract and VacA was adjusted to the age of the mice and the application mode: extract i.p. 5-100 µg, extract p.o. 50-200 µg, VacA i.p. 5-20 µg. Mice were treated with VacA or extract once a week. For the production of peanut extract, partially defatted peanut flour (Golden Peanut Company) was extracted overnight in 10x PBS, solid parts were removed by centrifugation, and extract was concentrated using Amicon Ultracel 3K centrifugal filters (Merck Millipore UFC900324). The final protein concentration was determined by BCA Protein Assay Kit (Thermo Scientific 23227).

Allergen-specific ELISAs

For OVA-specific IgG1 ELISA, high affinity plates were coated with 10 µg OVA in carbonate-bicarbonate coating buffer (pH 9.6) overnight at 4° C. After washing and blocking with 2 % BSA in PBS, serum samples were diluted in 1 % BSA/PBS and added for 2 hours at 37°C. After further washing, the plates were incubated for 1 h at 37°C with HRP-coupled anti-mouse IgG1 (eBioscience 18-4015-82). Wells were washed again before adding HRP substrate and measuring

absorbance in a Spectromax plate reader. OVA-specific IgE was measured using the same procedure as described for IgG1, except that HRP-coupled anti-mouse IgE (GeneTex GTX77227) was used for detection. For PE-specific IgE ELISA, high affinity plates were coated with 500 µg PE overnight as described above. After washing and blocking with 5 % gelatine in PBS at 37°C for 1 hour, serum samples diluted in 2 % BSA/PBS were added to the plate for 2 hours at 37°C. After further washing, the plates were incubated with anti-mouse IgE-biotin (BD Biosciences 553419) and washed before avidin-HRP (Thermo Scientific 21130) was added. Wells were washed again before addition of HRP substrate and absorbance detection in a plate reader.

Re-stimulation of splenocytes and cytokine ELISAs

Spleens were pushed through a 40 µm cell strainer and washed with PBS prior to red blood cell lysis. Splenocytes were seeded into 96 well plates in RPMI 1640 medium (Gibco 21875-034 plus FCS and Penicillin-Streptomycin) supplemented with 200 µg/ml PE or OVA. After 4 days in culture, supernatants were collected and stored at -20°C until cytokines were quantified by IL-5 (88-7054-88) and IL-13 (88-7137-88) ELISA according to the manufacturer's instructions (eBioscience).

TSDR methylation analysis

Total mesenteric lymph node cells of male C57BL/6 mice were isolated by means of collagenase type IV (Sigma C5138) digestion and pushing through a cell strainer. After fixation, permeabilization and washing, the cells were stained with anti-mouse CD4-FITC (Biolegend 100510) and Foxp3-APC antibodies (eBioscience 17-5773-82). $CD4^+Foxp3^+$ and $CD4^+Foxp3^-$ cells were sorted on a FACS Aria. Genomic DNA was isolated from sorted cell subsets using the

NucleoSpin® Tissue kit (Macherey-Nagel). An additional step was added to the manufacturer's protocol to remove formaldehyde-induced crosslinking. Briefly, Chelex-100 beads (Biorad) were added after the lysis step and incubated at 95°C for 15 min in a shaker. Chelex-100 beads were spun down and the supernatant was transferred to a fresh tube. After addition of an adjusted amount of 100 % ethanol the following purification steps were performed according to the manufacturer's protocol. Genomic DNA was converted with bisulfite using the EZ DNA Methylation Kit (Zymo Research) according to the manufacturer's instructions. The Treg-specific demethylated region (TSDR) was amplified by PCR and analyzed by pyrosequencing on a PSQ96MA (Qiagen) as described recently [23]. Primers for sequencing were (in 5' to 3' direction), S1: CCATACAAAACCCAAATTC, S2: ACCCAAATAAAATAATATAAATACT, S3: ATCTACCCCACAAATTT, S4: AACCAAATTTTTCTACCATT), which cover CpG motifs 3-12 of the TSDR core region.

Statistical analysis

GraphPad Prism 6 was for all statistical analyses. In all graphs each symbol represents an individual animal and horizontal lines indicate medians. To evaluate statistically significant differences between experimental groups an unpaired, nonparametric Mann-Whitney test was applied throughout. Stars are used to indicate the level of significance according to the p-value: * $p<0.05$, ** $p<0.01$, *** $p<0.001$, **** $p<0.0001$.

Results

Live *H. pylori* infection or treatment with *H. pylori* whole cell extract efficiently alleviates symptoms in an ovalbumin-induced food allergy model

To assess whether infection with *H. pylori* or treatment with whole cell extract protects against allergic responses to ingested ovalbumin, we either infected neonatal mice with live *H. pylori* on days 6 and 7 after birth or intragastrically administered weekly doses of whole cell extract from day 7 onwards. As adults, mice were subjected to intraperitoneal ovalbumin (OVA, adjuvanted with alum) sensitization followed by intragastric OVA challenges (see schematic in Figure 1A). Mice were scored for anaphylactic symptoms such as scratching around the nose, mouth and ears, decreased activity and increased respiratory rate and puffy eyes for 40 min after each challenge. At the study endpoint, serum levels of OVA-specific IgE and IgG1 antibodies, serum levels of mast cell protease 1 (MCPT1), and the splenic production of the Th2 cytokines IL-5 and IL-13 were quantified by ELISA. Mice that had been sensitized and challenged with OVA (positive controls) developed mild to moderate anaphylactic symptoms accompanied by high serum titers of OVA-specific IgE and IgG1 and elevated levels of MCPT1, a systemic marker of mast cell degranulation (Figure 1B-D, suppl. Figure 1A,B). The re-stimulation of splenic single cell preparations with OVA revealed a clearly elevated production of IL-5 and IL-13 relative to control groups that had not been sensitized (but challenged) or had never been exposed to OVA (Figure 1E,F). In contrast, mice that were infected with *H. pylori* or had received *H. pylori* whole cell extract were assigned significantly lower anaphylaxis scores, exhibited reduced serum levels of OVA-specific IgG1, and produced lower amounts of splenic Th2 cytokines upon re-stimulation

(Figure 1B-F); the assessment of serum IgE and MCPT-1 levels confirmed these trends for the extract treatment, but not for the live infection (suppl. Figure 1A,B). Overall, the results indicate that *H. pylori* infection and extract treatment efficiently reduce anaphylaxis symptoms and most other hallmarks of ovalbumin-specific allergy; the effects on anaphylaxis scores in particular, the most relevant readout from a clinical perspective, are strong and robust.

Food allergy symptoms induced by peanut extract are reduced by *H. pylori* infection and treatment with *H. pylori* extract or the *H. pylori* immunomodulator VacA

We next sought to determine if these results could be corroborated in additional models of food allergy. As proteins contained in peanuts are among the most common food allergens in Western societies, we opted for peanut-specific sensitization and challenge. Mice received four intragastric weekly doses of cholera toxin-adjuvanted peanut extract (PE) for the purpose of sensitization, followed by intragastric challenge with PE on four consecutive days beginning one week after the last sensitization (Figure 2A). Neonatally infected mice and mice treated with either *H. pylori* extract or the purified *H. pylori* immunomodulator VacA were sensitized and challenged alongside a group of positive controls that received no intervention whatsoever. The food allergy symptoms elicited by intragastric sensitization and challenge with peanut extract were relatively mild and comparable to symptoms induced with OVA (Figure 2B-D). Similar to the OVA model, *H. pylori* infection and extract treatment, and also regular treatment with the purified immunomodulator VacA, effectively reduced the anaphylaxis scores, but failed to affect peanut-specific serum IgE levels (Figure 2B,C). MCPT serum levels were reduced by all three interventions (Figure 2D). In summary, we observe in two complementary food allergy models

that *H. pylori* and its immunomodulator VacA reduce clinically relevant symptoms of food allergy and modulate immunologic correlates of the disease.

Severe anaphylaxis induced by peanut extract is alleviated by *H. pylori*

Both above described models of food allergy produce relatively mild symptoms. Mice rarely develop systemic symptoms such as decreased activity or effects on respiration rates. To mimic more severe anaphylactic reactions, which can be life-threatening in peanut-allergic children, we devised a model that produced significantly higher anaphylaxis scores, accompanied by higher serum MCPT levels and stronger cytokine production by restimulated splenocytes relative to the other two models. In this model, mice are sensitized orally by four CT-adjuvanted doses of peanut extract followed by two intraperitoneal challenges with the same extract (Figure 3A). Most mice of the positive control group were assigned anaphylaxis scores of three (defined as labored respiration and cyanosis around the mouth and tail and/or periods of motionless for more than 1 min, lying prone on stomach) and four (slight or no activity after prodding/whisker stimuli or tremors and convulsion; Figure 3B,C) already after the first challenge dose. Anaphylaxis scores were reduced by all interventions (live neonatal infection, extract administered either i.p. or orally, and VacA, Figure 3B, suppl. Figure 2A). Lower scores were accompanied by somewhat reduced cytokine production (Figure 3D,E) and MCPT and IgE levels measured in serum (suppl. Figure 2A,B). In summary, the severe anaphylaxis induced by the intraperitoneal administration of allergen to sensitized mice can be measurably reduced by prior infection with *H. pylori*, or the regular exposure to *H. pylori* extract or VacA.

***H. pylori* infection, as well as extract and VacA treatment induce demethylation of the Treg-specific demethylated region (TSDR) in FoxP3$^+$ Tregs**

Tregs have been implicated in asthma protection in *H. pylori*-infected mice and are numerically and functionally different in naïve and infected animals [18-20]. To assess whether the interventions shown here to confer food allergy protection affect the differentiation and stability of Tregs, we set out to quantify the methylation status of CpG motifs (Figure 4A) localized within a region of the *FOXP3* locus termed TSDR because of its selective demethylation in lineage-committed (stable) Tregs [24, 25]. Tregs from pooled mesenteric lymph nodes of 6-8 male mice per group were FACS-sorted based on their CD4 and FoxP3 expression, and subjected to genomic DNA extraction, bisulfite conversion and TSDR-specific pyrosequencing. CD4$^+$ FoxP3$^-$ T-cells were sorted and analyzed in parallel. FoxP3$^-$ T-cells exhibited a more or less complete methylation of the TSDR, with on average 96 % methylated CpG motifs (Figure 4B and data not shown); their methylation did not change upon intervention (data not shown). In contrast, FoxP3$^+$ T-cells showed differences in their methylation status: whereas FoxP3$^+$ T-cells that had been harvested from naive mice showed methylation levels varying between 25-50 % depending on the experiment, this level decreased to 10 % upon extract treatment, 10-17 % upon live infection and down to 1 % upon VacA treatment (Figure 4B). As reported previously [24, 25], the CpG motifs within the TSDR showed very consistent methylation patterns within one sample, indicating an all-or-nothing mechanism of demethylation that encompasses the entire locus (not all regions could be analyzed in all samples though, Figure 4B). We conclude from these data that epigenetic marks leading to stable expression of FoxP3, and to the definitive lineage commitment of Tregs,

reflect the suppressive effects of *H. pylori*-specific treatments on food allergy in the models described above.

Discussion

Although food allergy represents an important human disorder of increasing prevalence in most parts of the world and *H. pylori* is known to be protective against allergies with respiratory tract manifestations [10, 18-20, 26, 27], little experimental or epidemiological evidence is available that addresses a possible inverse correlation, or protective effect, of *H. pylori* in food allergy. One of the reasons for this lack of data probably lies in the fact that no universally accepted food allergy model exists that would faithfully reflect all or most aspects of the human condition. We have adapted and optimized three complementary food allergy models, using various routes of sensitization and challenge and two different common food allergens, to investigate in a comprehensive manner whether the presence of *H. pylori* affects clinically relevant food allergy symptoms, in either a beneficial or detrimental way. We found no evidence whatsoever for a promoting role of *H. pylori* in food allergy, as had been suggested in two observational studies in humans [14, 15]. In contrast, live *H. pylori* infection conferred a clearly detectable protection against anaphylactic symptoms; the effects on clinical symptoms were associated with protective effects on systemic parameters of food allergy, such as mast cell protease levels in serum and allergen-specific IgG1 levels. Although robust and consistent in the three models, the effects of *H. pylori* on food allergy were not as impressive as its beneficial effects in models of allergic asthma in which neonatal exposure to the bacteria essentially reduces parameters of airway inflammation, airway hyper-responsiveness and goblet cell metaplasia to almost background levels [18-20]. The stronger effects in the asthma models may have to do with the so-called “gut-lung axis”, the idea of a special connection between the mucosal immune systems of the two organs that has been put forward to explain the effects of (deliberate or pathogenic alterations

of) the gut microbiota on lung diseases [28]. We were able to link the protection against the airway hyper-reactivity, inflammation, eosinophilia and excessive mucus production that are hallmarks of allergic asthma to the strong suppressive activity of *H. pylori*-induced Tregs [19, 20]. Here, we present a possible epigenetic correlate of the suppressive/protective activity of Tregs in allergy, as these cells- coming from an *H. pylori*-infected host- exhibit an epigenetic signature at their *FOXP3* locus that is consistent with stable expression of FoxP3 and stable lineage differentiation and functionality [24, 25]. We have shown in earlier work that the induction of Tregs depends on the *H. pylori* virulence factor and immunomodulator VacA; VacA mutants fail to induce suppressive Tregs and to confer asthma protection, and VacA alone, administered in purified form, recapitulates many of the beneficial effects of live infection [22, 29]. *H. pylori* VacA mutants fail to colonize persistently and at wild type levels, and rather are cleared effectively by an overshooting T-helper-1 response. The immunomodulatory effects of VacA were confirmed in the food allergy models presented here, and were reflected in the epigenetic signature of Tregs isolated from VacA-treated mice. In conclusion, *H. pylori* possesses strong immunomodulatory properties, mediated at least in part by the VacA protein, that allow it to modulate T-cell responses directed at the infection itself, as well as at conspicuous food and environmental antigens. These properties are evident not only locally in the gastric mucosa, but systemically, and strongly affect the individual carrier's allergy risk.

Acknowledgements

This work was funded by the Swiss National Science Foundation (grants BSCGIO_157841/1 and SNF 310030-143609 to A.M.), the National Institutes of Health (AI039657 and CA116087) and the Department of Veterans Affairs.

Author contributions

AK and AM contributed to study concept and design. AK conducted all animal experiments with help from SU and AD. AK, SF, JH performed analyses and interpretation of data. TLC provided critical materials. All authors critically revised the manuscript for accuracy. AK and AM wrote the paper.

Conflicts of interest

The authors declare that they have no conflicts of interest.

References

1. Branum AM, Lukacs SL. Food allergy among children in the United States. *Pediatrics* 2009; **124**:1549-55.
2. Sicherer SH, Sampson HA. Food allergy: Epidemiology, pathogenesis, diagnosis, and treatment. *The Journal of allergy and clinical immunology* 2014; **133**:291-307; quiz 8.
3. Strachan DP. Hay fever, hygiene, and household size. *Bmj* 1989; **299**:1259-60.
4. Blaser MJ, Falkow S. What are the consequences of the disappearing human microbiota? *Nat Rev Microbiol* 2009; **7**:887-94.
5. Parsonnet J, Friedman GD, Vandersteen DP*, et al.* Helicobacter pylori infection and the risk of gastric carcinoma. *The New England journal of medicine* 1991; **325**:1127-31.
6. Huang JQ, Zheng GF, Sumanac K*, et al.* Meta-analysis of the relationship between cagA seropositivity and gastric cancer. *Gastroenterology* 2003; **125**:1636-44.
7. Kyburz A, Muller A. The Gastrointestinal Tract Microbiota and Allergic Diseases. *Dig Dis* 2016; **34**:230-43.
8. Koch KN, Muller A. Helicobacter pylori activates the TLR2/NLRP3/caspase-1/IL-18 axis to induce regulatory T-cells, establish persistent infection and promote tolerance to allergens. *Gut Microbes* 2015; **6**:382-7.
9. Wang Q, Yu C, Sun Y. The association between asthma and Helicobacter pylori: a meta-analysis. *Helicobacter* 2013; **18**:41-53.
10. Chen Y, Blaser MJ. Helicobacter pylori colonization is inversely associated with childhood asthma. *J Infect Dis* 2008; **198**:553-60.
11. Luther J, Dave M, Higgins PD*, et al.* Association between Helicobacter pylori infection and inflammatory bowel disease: a meta-analysis and systematic review of the literature. *Inflamm Bowel Dis* 2010; **16**:1077-84.
12. Konturek PC, Rienecker H, Hahn EG*, et al.* Helicobacter pylori as a protective factor against food allergy. *Med Sci Monit* 2008; **14**:CR452-8.
13. Ma ZF, Majid NA, Yamaoka Y*, et al.* Food Allergy and Helicobacter pylori Infection: A Systematic Review. *Front Microbiol* 2016; **7**:368.
14. Corrado G, Luzzi I, Lucarelli S*, et al.* Positive association between Helicobacter pylori infection and food allergy in children. *Scand J Gastroenterol* 1998; **33**:1135-9.
15. Corrado G, Luzzi I, Pacchiarotti C*, et al.* Helicobacter pylori seropositivity in children with atopic dermatitis as sole manifestation of food allergy. *Pediatr Allergy Immunol* 2000; **11**:101-5.
16. Figura N, Perrone A, Gennari C*, et al.* CagA-positive Helicobacter pylori infection may increase the risk of food allergy development. *J Physiol Pharmacol* 1999; **50**:827-31.
17. Kolho KL, Haapaniemi A, Haahtela T*, et al.* Helicobacter pylori and specific immunoglobulin e antibodies to food allergens in children. *J Pediatr Gastr Nutr* 2005; **40**:180-3.
18. Koch KN, Hartung ML, Urban S*, et al.* Helicobacter urease-induced activation of the TLR2/NLRP3/IL-18 axis protects against asthma. *J Clin Invest* 2015; **125**:3297-302.
19. Arnold IC, Dehzad N, Reuter S*, et al.* Helicobacter pylori infection prevents allergic asthma in mouse models through the induction of regulatory T cells. *J Clin Invest* 2011; **121**:3088-93.

20. Oertli M, Sundquist M, Hitzler I*, et al.* DC-derived IL-18 drives Treg differentiation, murine Helicobacter pylori-specific immune tolerance, and asthma protection. *J Clin Invest* 2012; **122**:1082-96.
21. Arnold IC, Lee JY, Amieva MR*, et al.* Tolerance rather than immunity protects from Helicobacter pylori-induced gastric preneoplasia. *Gastroenterology* 2011; **140**:199-209.
22. Engler DB, Reuter S, van Wijck Y*, et al.* Effective treatment of allergic airway inflammation with Helicobacter pylori immunomodulators requires BATF3-dependent dendritic cells and IL-10. *Proc Natl Acad Sci U S A* 2014; **111**:11810-5.
23. Yang BH, Hagemann S, Mamareli P*, et al.* Foxp3(+) T cells expressing ROR gamma t represent a stable regulatory T-cell effector lineage with enhanced suppressive capacity during intestinal inflammation. *Mucosal immunology* 2016; **9**:444-57.
24. Toker A, Engelbert D, Garg G*, et al.* Active demethylation of the Foxp3 locus leads to the generation of stable regulatory T cells within the thymus. *J Immunol* 2013; **190**:3180-8.
25. Polansky JK, Kretschmer K, Freyer J*, et al.* DNA methylation controls Foxp3 gene expression. *Eur J Immunol* 2008; **38**:1654-63.
26. Blaser MJ, Chen Y, Reibman J. Does Helicobacter pylori protect against asthma and allergy? *Gut* 2008; **57**:561-7.
27. Reibman J, Marmor M, Filner J*, et al.* Asthma is inversely associated with Helicobacter pylori status in an urban population. *PLoS One* 2008; **3**:e4060.
28. Budden KF, Gellatly SL, Wood DL*, et al.* Emerging pathogenic links between microbiota and the gut-lung axis. *Nat Rev Microbiol* 2016.
29. Oertli M, Noben M, Engler DB*, et al.* Helicobacter pylori gamma-glutamyl transpeptidase and vacuolating cytotoxin promote gastric persistence and immune tolerance. *Proc Natl Acad Sci U S A* 2013; **110**:3047-52

Figure legends

Figure 1. OVA- induced food allergy is ameliorated by neonatal *H. pylori* infection or weekly extract treatment. (A) Schematic of OVA-induced food allergy and *H. pylori* interventions. Mice were sensitized twice intraperitoneally (i.p.) with 50 μg of alum-adjuvanted OVA and orally challenged four weeks later on four consecutive days with 60 mg OVA (s/c; positive controls). Negative control animals were challenged but not sensitized, or neither sensitized nor challenged. One group of mice was neonatally infected on day 6 and 7 after birth with the *H. pylori* strain PMSS1 (inf), and another group was treated weekly by oral gavage with 100-200 μg (adjusted to body weight) whole cell *H. pylori* extract starting on day 6 or 7 after birth (extr p.o.). (B) Cumulative anaphylaxis score assigned upon challenge (sum of three scores). s/c, sensitization and challenge. (C) Representative pictures showing mice with a score of 1 (repetitive scratching around nose and head, and hind-leg-ear-digging) and a score of 2 (puffing around eyes, pilar erecti, decreased activity). (D) Serum OVA-specific IgG1, as determined by ELISA. (E,F) Cytokine production, as determined by IL-5 and IL-13 ELISA, of splenocytes that had been re-stimulated *in vitro* with OVA for four days. In B,D,E and F, each symbol represents one mouse. Graphs show pooled data from 5 (B), 4 (D) and 2 (E,F) experiments. Horizontal lines indicate medians; an unpaired Mann-Whitney U test was used for calculation of p-values. * $p<0.05$, ** $p<0.01$, *** $p<0.001$, **** $p<0.0001$.

Figure 2. Amelioration of allergic symptoms in an oral challenge peanut allergy model upon *H. pylori* specific treatments. (A) Schematic of PE-induced food allergy and *H. pylori* interventions. Mice were sensitized four times by oral gavage (p.o.) with 2 mg of peanut-extract (PE) adjuvanted

with 20 μg cholera toxin (CT), followed four weeks later by oral challenges on four consecutive days with 60 mg OVA (positive controls). Negative control animals were challenged but not sensitized, or neither sensitized nor challenged. One group of mice was neonatally infected on day 6 and 7 after birth with the *H. pylori* strain PMSS1 (inf), and another group was treated weekly by oral gavage with 100-200 μg (adjusted to body weight) whole cell *H. pylori* extract starting on day 6 or 7 after birth (extr p.o.). A final group received once-weekly increasing doses (adjusted to body weight) of 5-20 μg purified VacA (VacA i.p.) starting on day 6 or 7 after birth. (B) Cumulative anaphylaxis score assigned upon challenge (sum of three scores). (C,D) Serum PE-specific IgE and MCPT1 levels, as determined by ELISA. In B-D, each symbol represents one mouse. Graphs show pooled data from 4 (B), 3 (C) and 2 (D) experiments. Horizontal lines indicate medians; an unpaired Mann-Whitney U test was used for calculation of p-values. ** $p<0.01$, **** $p<0.0001$.

Figure 3. Systemically induced peanut food allergy is reduced upon neonatal *H. pylori* infection or weekly treatment with extract or VacA. (A) Schematic of PE-induced food allergy and *H. pylori* interventions. Mice were sensitized four times by oral gavage (p.o.) with 2 mg of peanut-extract (PE) adjuvanted with 20 μg cholera toxin (CT), followed one week later by two i.p. challenges (with a two day interval) with 1 mg OVA (positive controls). Negative control animals were challenged but not sensitized, or neither sensitized nor challenged. One group of mice was neonatally infected on day 6 and 7 after birth with the *H. pylori* strain PMSS1 (inf), and another group was treated weekly by oral gavage or i.p. with whole cell *H. pylori* extract starting on day 6 or 7 after birth (extr p.o./i.p.). A final group received weekly increasing doses (adjusted to body

weight) of 5-20 μg purified VacA (VacA i.p.) starting on day 6 or 7 after birth. (B) Anaphylaxis score assigned at first challenge. (C) Representative pictures showing mice with a score of 3 (lying prone on stomach for more than one minute). (D,E) Cytokine production, as determined by IL-5 and IL-13 ELISA, of splenocytes that had been re-stimulated *in vitro* with PE for four days. In B,D, and E, each symbol represents one mouse. Graphs show pooled data from 8 (B) and 5 (D,E) experiments. Horizontal lines indicate medians; an unpaired Mann-Whitney U test was used for calculation of p-values. * $p<0.05$, **** $p<0.0001$.

Figure 4. Decreased methylation of the Treg-specific-demethylated-region (TSDR) upon *H. pylori*-specific treatment. (A) Schematic overview of the *FOXP3* locus with the TSDR upstream of the TSS (retrieved using BLAST). The CG-containing region is marked in blue and CG motifs covered by pyrosequencing are marked in bold red. (B) Methylation pattern of 10 CG dinucleotides within the TSDR, of FACS-sorted MLN-derived $CD4^+Foxp3^+$ and $CD4^+FoxP3^-$ T-cells. Animals were treated as indicated. The methylation status of the individual CGs is color-coded (left panel). White cells indicate sequences that failed to yield interpretable results due to technical problems.

Figures

Figure 1

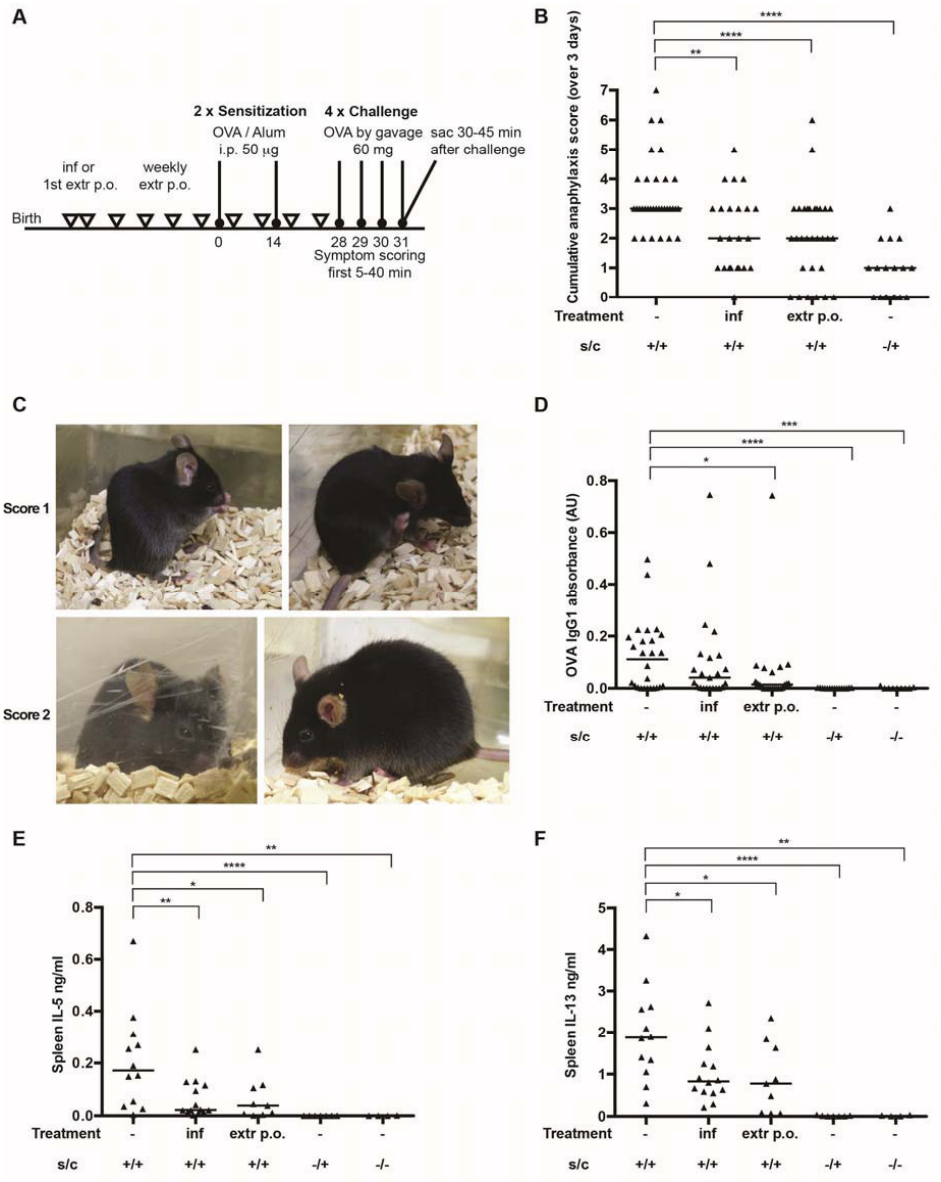

Figure 2

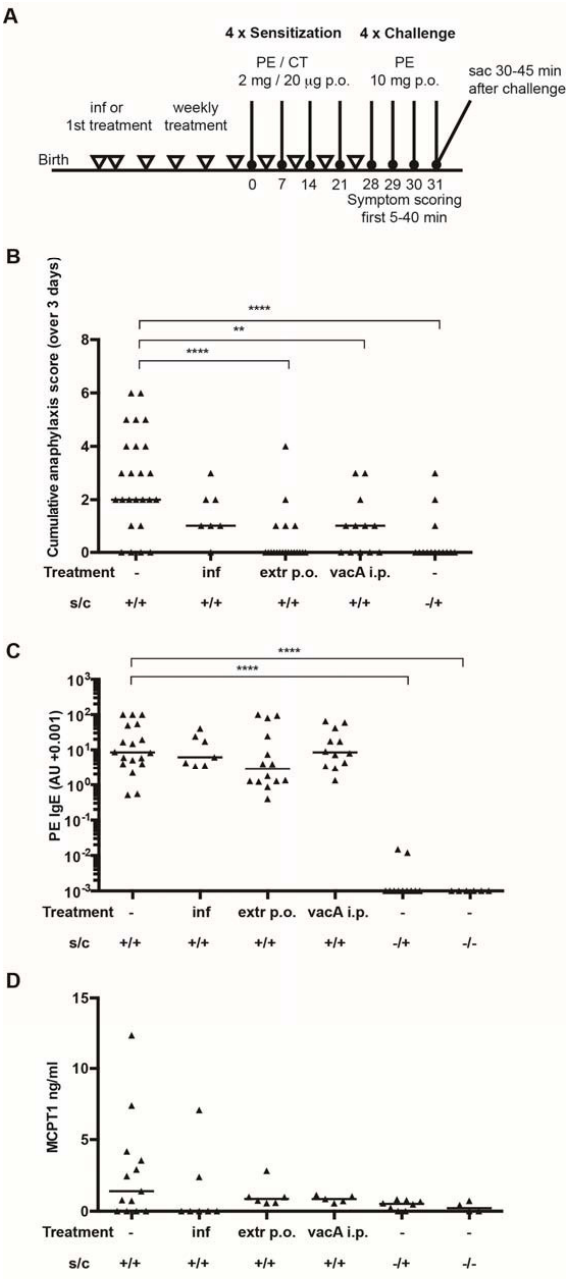
A
4 x Sensitization
4 x Challenge
PE / CT
2 mg / 20 µg p.o.
PE
10 mg p.o.
sac 30-45 min
after challenge
inf or
1st treatment
weekly
treatment
Birth
0 7 14 21 28 29 30 31
Symptom scoring
first 5-40 min
B
Cumulative anaphylaxis score (over 3 days)
****
**
****
Treatment - inf extr p.o. vacA i.p. -
s/c +/+ +/+ +/+ +/+ -/+
C
PE IgE (AU +0.001)
****
****
Treatment - inf extr p.o. vacA i.p. - -
s/c +/+ +/+ +/+ +/+ -/+ -/-
D
MCPT1 ng/ml
Treatment - inf extr p.o. vacA i.p. - -
s/c +/+ +/+ +/+ +/+ -/+ -/-

Figure 3

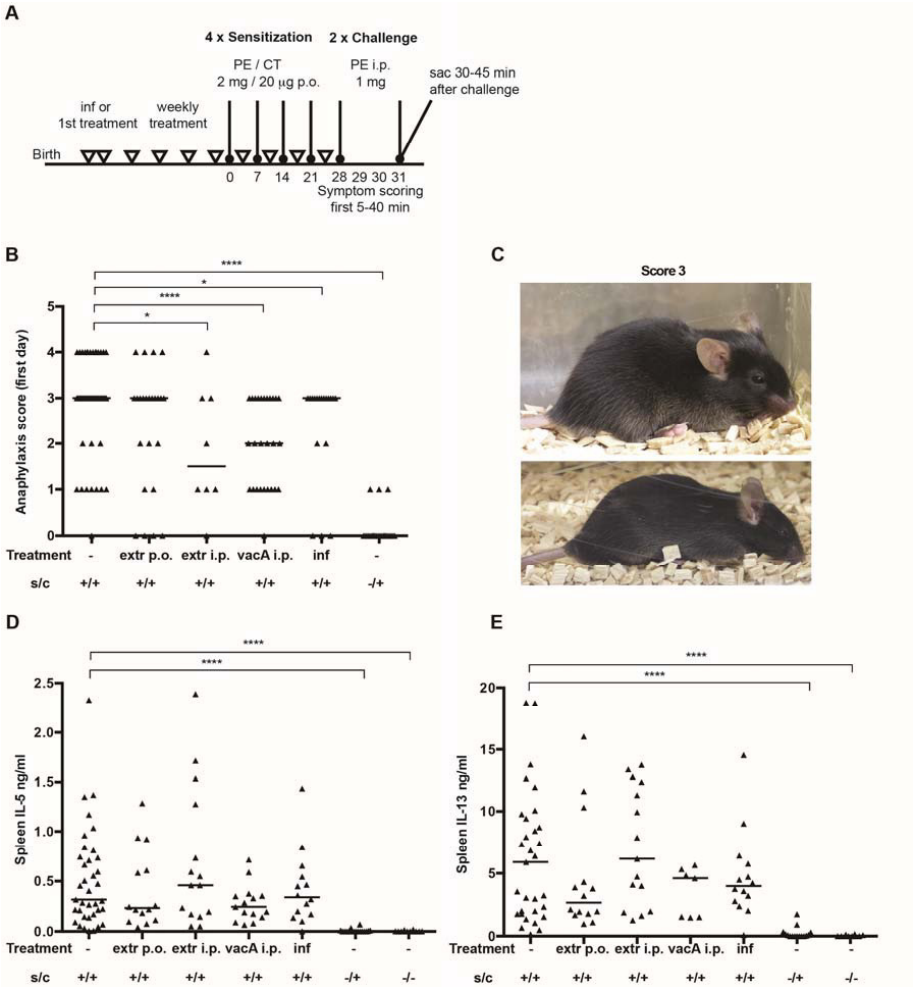
A
4 x Sensitization
2 x Challenge
PE / CT
2 mg / 20 µg p.o.
PE i.p.
1 mg
sac 30-45 min
after challenge
inf or
1st treatment
weekly
treatment
Birth
0 7 14 21 28 29 30 31
Symptom scoring
first 5-40 min
B
Anaphylaxis score (first day)
Treatment - extr p.o. extr i.p. vacA i.p. inf -
s/c +/+ +/+ +/+ +/+ +/+ -/+
C
Score 3
D
Spleen IL-5 ng/ml
Treatment - extr p.o. extr i.p. vacA i.p. inf - -
s/c +/+ +/+ +/+ +/+ +/+ -/+ -/-
E
Spleen IL-13 ng/ml
Treatment - extr p.o. extr i.p. vacA i.p. inf - -
s/c +/+ +/+ +/+ +/+ +/+ -/+ -/-

Figure 4

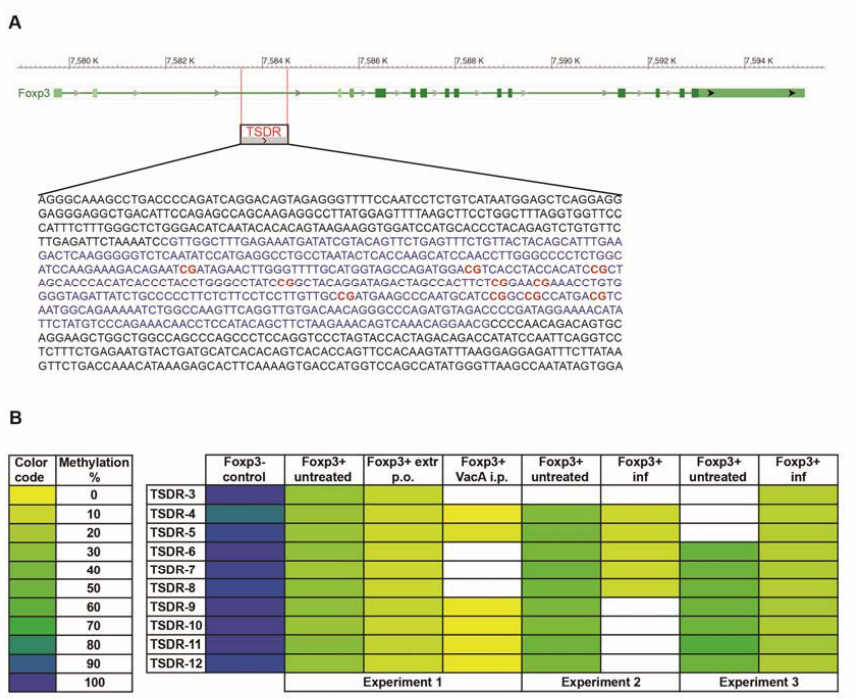
A
7,580 K
7,582 K
7,584 K
7,586 K
7,588 K
7,590 K
7,592 K
7,594 K
Foxp3
TSDR
AGGGCAAAGCCTGACCCCAGATCAGGACAGTAGAGGGTTTTCCAATCCTCTGTCATAATGGAGCTCAGGAGG
GAGGGAGGCTGACATTCCAGAGCCAGCAAGAGGCCTTATGGAGTTTTAAGCTTCCTGGCTTTAGGTGGTTCC
CATTTCTTTGGGCTCTGGGACATCAATACACACAGTAAGAAGGTGGATCCATGCACCCTACAGAGTCTGTGTTC
TTGAGATTCTAAAATCCGTTGGCTTTGAGAAATGATATCGTACAGTTCTGAGTTTCTGTTACTACAGCATTTGAA
GACTCAAGGGGGTCTCAATATCCATGAGGCCTGCCTAATACTCACCAAGCATCCAACCTTGGGCCCCTCTGGC
ATCCAAGAAAGACAGAATCGATAGAACTTGGGTTTTGCATGGTAGCCAGATGGACGTCACCTACCACATCCGCT
AGCACCCACATCACCCTACCTGGGCCTATCCGGCTACAGGATAGACTAGCCACTTCTCGGAACGAAACCTGTG
GGGTAGATTATCTGCCCCCTTCTCTTCCTCCTTGTTGCCGATGAAGCCCAATGCATCCGGCCGCCATGACGTC
AATGGCAGAAAAATCTGGCCAAGTTCAGGTTGTGACAACAGGGCCCAGATGTAGACCCCGATAGGAAAACATA
TTCTATGTCCCAGAAACAACCTCCATACAGCTTCTAAGAAACAGTCAAACAGGAACGCCCCAACAGACAGTGC
AGGAAGCTGGCTGGCCAGCCCAGCCCTCCAGGTCCCTAGTACCACTAGACAGACCATATCCAATTCAGGTCC
TCTTTCTGAGAATGTACTGATGCATCACACAGTCACACCAGTTCCACAAGTATTTAAGGAGGAGATTTCTTATAA
GTTCTGACCAAACATAAAGAGCACTTCAAAAGTGACCATGGTCCAGCCATATGGGTTAAGCCAATATAGTGGA
B
Color code
Methylation %
0
10
20
30
40
50
60
70
80
90
100
Foxp3-control
Foxp3+ untreated
Foxp3+ extr p.o.
Foxp3+ VacA i.p.
Foxp3+ untreated
Foxp3+ inf
Foxp3+ untreated
Foxp3+ inf
TSDR-3
TSDR-4
TSDR-5
TSDR-6
TSDR-7
TSDR-8
TSDR-9
TSDR-10
TSDR-11
TSDR-12
Experiment 1
Experiment 2
Experiment 3

Supplemental Figures

Suppl. Figure 1

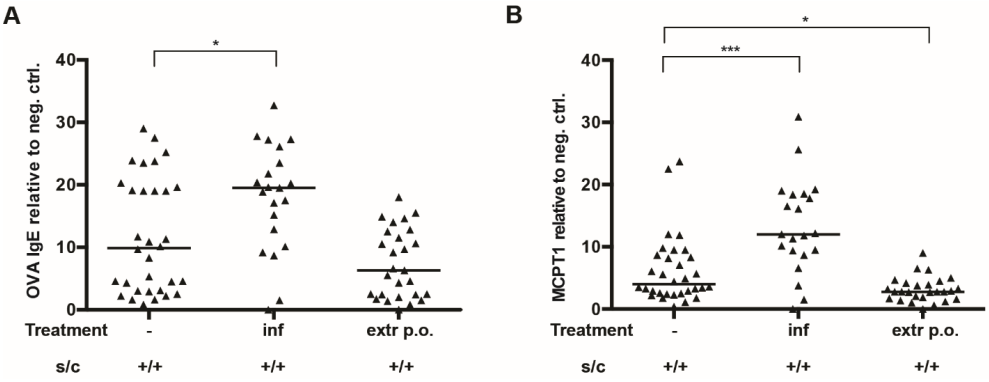

Suppl. Figure 1. OVA-specific IgE and mast cell protease (MCPT) 1 levels are reduced upon *H. pylori* extract treatment in an OVA-induced food allergy model. Mice were sensitized, challenged and treated as described in Figure 1. *(A)* OVA-specific IgE levels in serum, as determined by ELISA, of animals that were sensitized and challenged (s/c) with OVA and infected or not with *H. pylori*. Additional mice received regular doses of *H. pylori* extract by oral gavage (p.o.). All values were normalized to the average negative control (challenged, but not sensitized mice) IgE level. *(B)* Mast cell protease 1 (MCPT1) concentration in serum, as measured by ELISA, of the mice shown in A, normalized to the average negative control value. In A and B, each symbol represents one mouse. Graphs show pooled data from 5 (in A) and 4 (in B) experiments. Horizontal lines indicate medians; an unpaired Mann-Whitney U test was used for calculation of p-values. * $p<0.05$, *** $p<0.001$.

Suppl. Figure 2

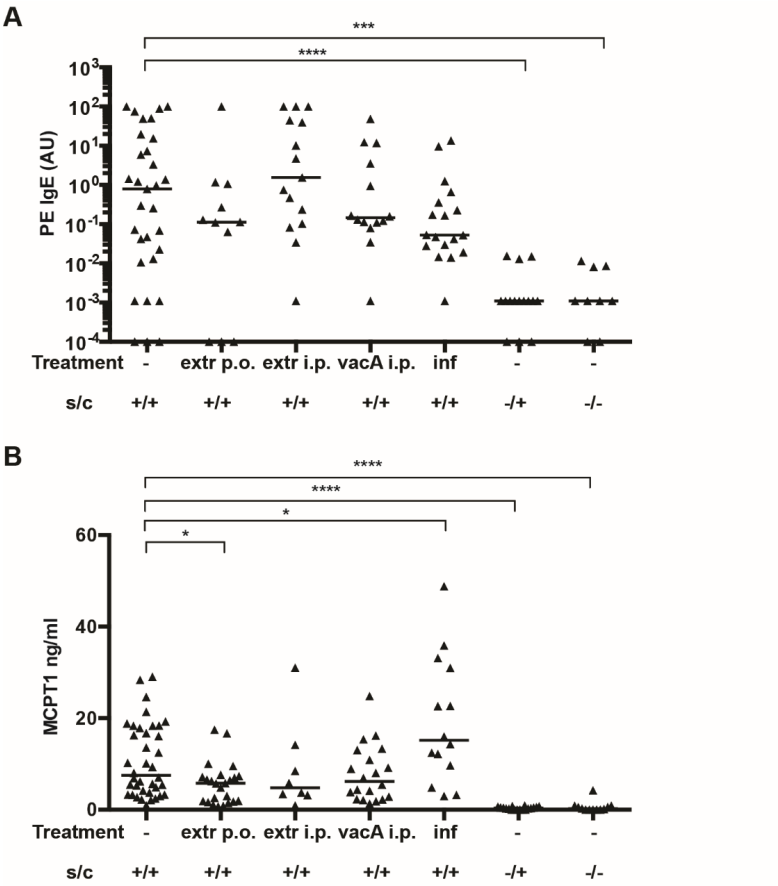

Suppl. Figure 2. PE-specific IgE and mast cell protease 1 levels are partially reduced upon *H. pylori* extract treatment or infection. Mice were sensitized, challenged and treated as described in Figure 3. *(A)* PE-specific OVA-specific IgE levels in serum, as determined by ELISA, of animals that were sensitized and challenged (s/c) with PE and infected or not with *H. pylori*. Additional mice received regular doses of *H. pylori* extract by oral gavage (p.o.) or i.p., or were treated i.p. with VacA. *(B)* In A and B, each symbol represents one mouse. Graphs show pooled data from 5 (in A) and 6 (in B) experiments. Horizontal lines indicate medians; an unpaired Mann-Whitney U test was used for calculation of p-values. * $p<0.05$, *** $p<0.001$.